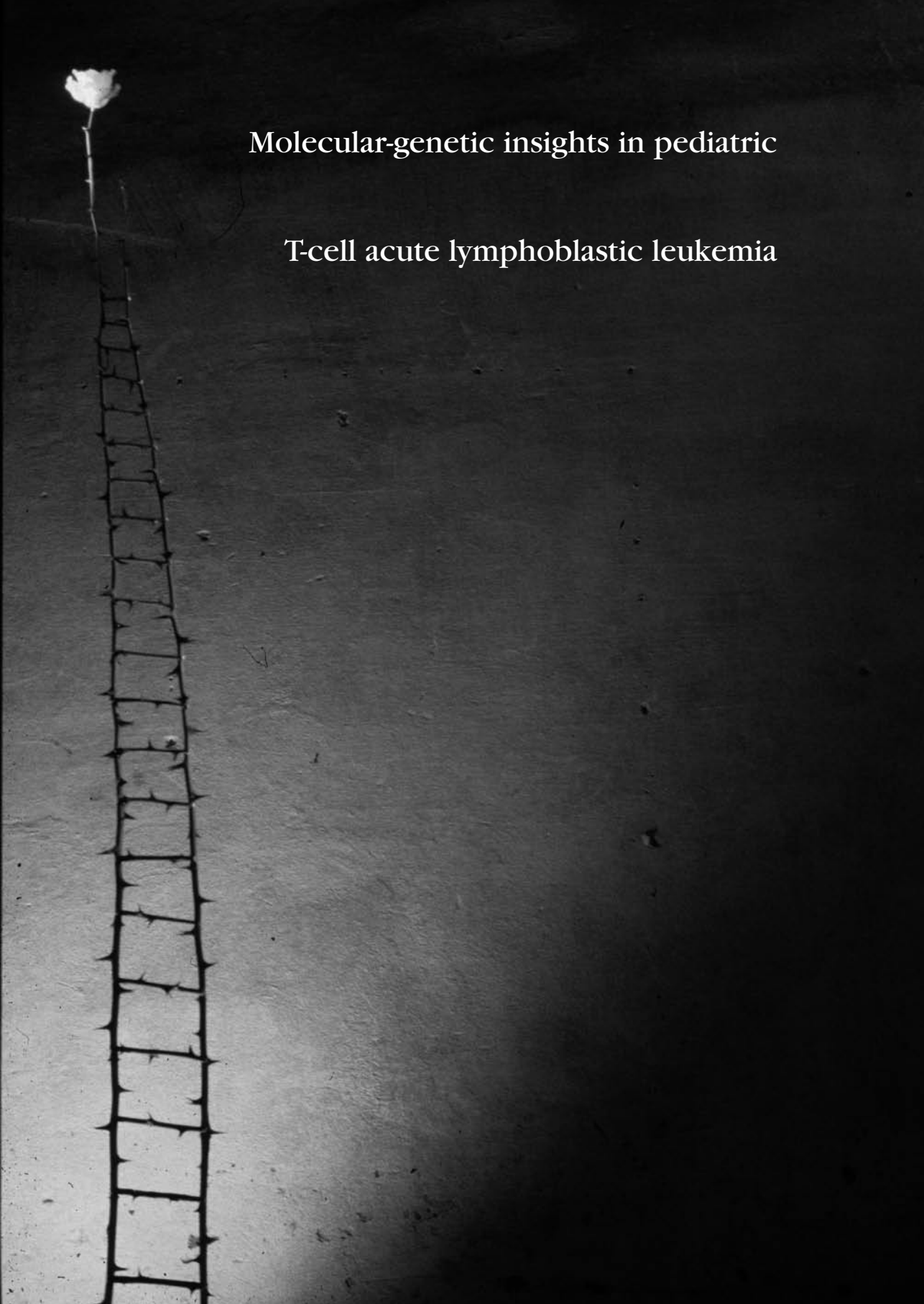

Molecular-genetic insights in pediatric T-cell acute lymphoblastic leukemia

The studies described in this thesis were financially supported by a grant from the Sophia Foundation for Medical Research (SSWO grant 404).

Financial support for the print and reproduction of this thesis was kindly provided by the Pediatric Oncology Foundation Rotterdam (KOCR), Agilent Technologies, ServiceXS, MRC Holland, Genzyme, Mundipharma and GlaxoSmithKline.

ISBN 978-90-8559-370-0
Layout: Optima Grafische Communicatie, Rotterdam. (www.ogc.nl)
Cover: “Rinascita” by Marcello Chiarenza
Chapter Cover: “La scala del paradiso” by Marcello Chiarenza
Printed by Optima Grafische Communicatie, Rotterdam.

Molecular-genetic insights in pediatric T-cell acute lymphoblastic leukemia

Moleculair genetische inzichten in T-cel acute lymfatische leukemie bij kinderen

Proefschrift

Ter verkrijging van de graad van doctor
aan de Erasmus Universiteit Rotterdam

op gezag van de Rector Magnificus
Prof. dr. S.W.J. Lamberts

en volgens besluit van het College voor Promoties

De openbare verdediging zal plaatsvinden op 17 april 2008 om 13:30 uur

door

Pieter Van Vlierberghe

geboren te Antwerpen

PROMOTIECOMMISSIE

Promotor:	Prof. dr. R. Pieters
Overige leden:	Prof. dr. J.J.M. van Dongen
	Prof. dr. F. Grosveld
	Prof. dr. B. Löwenberg
Copromotoren:	Dr. J.P.P. Meijerink
	Dr. H.B. Beverloo

Voor Liesbeth
Luna en Ella

CONTENTS

Chapter 1	General introduction.	9
Chapter 2	Molecular-genetic insights in pediatric T-ALL.	23
Chapter 3	The cryptic chromosomal deletion, del(11)(p12p13), as a new activation mechanism of *LMO2* in pediatric T-cell acute lymphoblastic leukemia.	63
Chapter 4	Mono- or biallelic *LMO2* expression in relation to genomic *LMO2* rearrangements and T-cell immunophenotype in pediatric T-ALL.	89
Chapter 5	The recurrent *SET-NUP214* fusion as a new *HOXA* activation mechanism in pediatric T-cell acute lymphoblastic leukemia.	99
Chapter 6	Duplication of the *MYB* oncogene in T-cell acute lymphoblastic leukemia.	125
Chapter 7	Additional genetic lesions in *TLX3* positive pediatric T-cell acute lymphoblastic leukemia.	135
Chapter 8	Leukemia associated *NF1* inactivation in pediatric T-ALL and AML patients lacking evidence for neurofibromatosis.	155
Chapter 9	A new recurrent 9q34 duplication in pediatric T-cell acute lymphoblastic Leukemia.	171
Chapter 10	Activating *FLT3* mutations in CD4+/CD8- pediatric T-cell acute lymphoblastic leukemias.	193
Chapter 11	Summary, general discussion and perspectives.	199
Chapter 12	Nederlandstalige samenvatting.	213
About the author		225
List of publications		227
Curriculum vitae		229
Dankwoord		231
Color figures		239

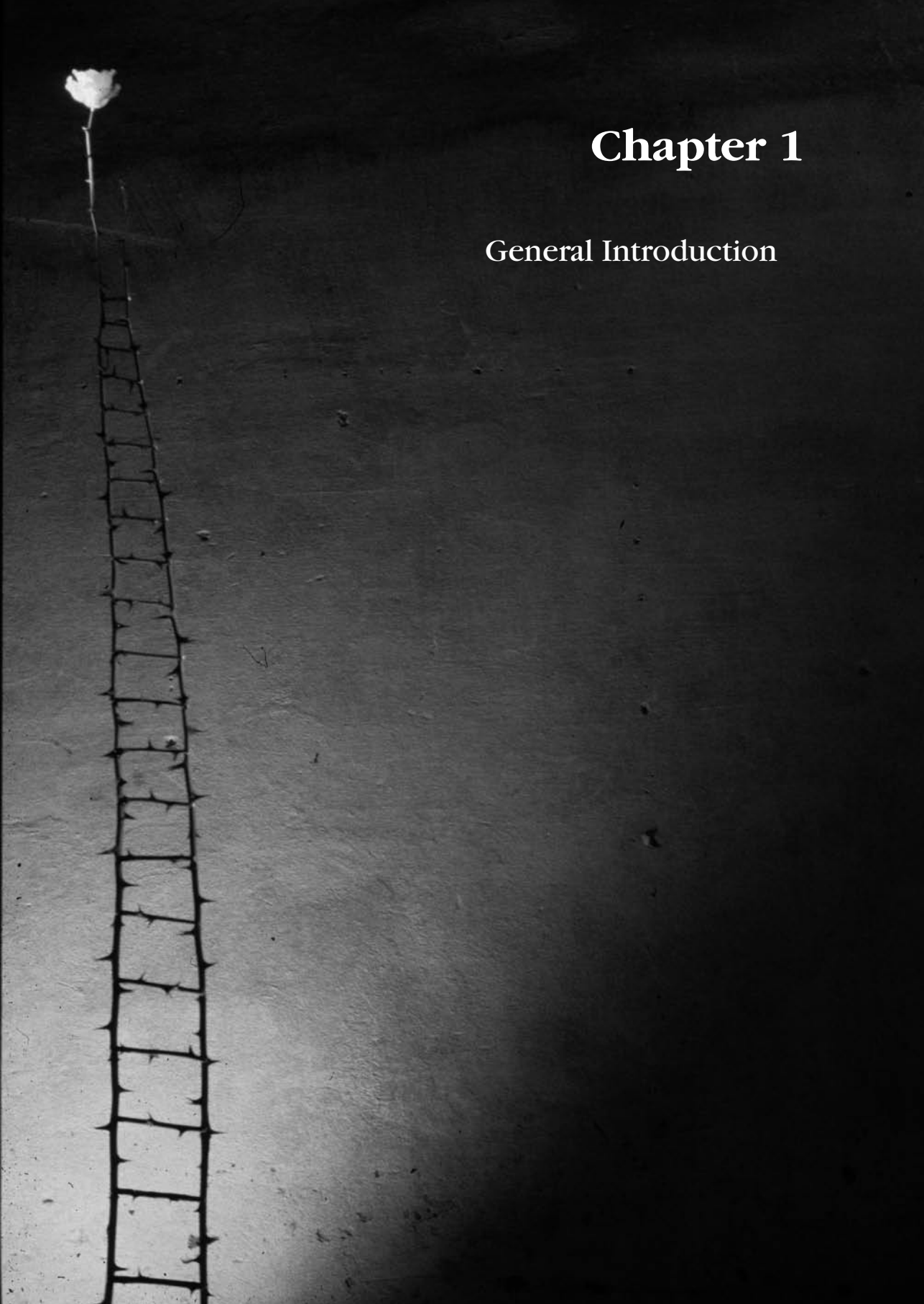

Chapter 1

General Introduction

LEUKEMIA

A historical perspective

In 1845, 3 independent pathologists, Bennett, Craigie and Virchow, described leukemia as a lethal disease characterized by abnormal high levels of blood cells[1-3]. Although many textbooks assign the discovery of this disease to either one of them, actually the French physicians Alfred Velpeau and Alfred Francois Donné made the first clinical and microscopic descriptions of this disease in 1827 and 1844, respectively[4,5]. Nevertheless, it was the German pathologist Rudolf Virchow who provided this condition in 1847 with its rightful name, leukemia (derived from the greek words *leukos* and *heima*, meaning white blood)[1]. Indeed, leukemia is a cancer of the blood, characterized by uncontrolled accumulation of immature white blood cells.

Pathogenesis of leukemia

The formation of blood cells (hematopoiesis) is a balanced process of proliferation, differentiation and cell survival that mainly occurs in the bone marrow. In case of leukemia, uncontrolled expansion of immature malignant cells will harm the maintenance of a healthy blood cell population, and results in anemia (red blood cell deficiency), internal bleeding (platelets deficiency) and increased risk for infections (normal white blood cell deficiency). Further malignant expansion will drive the leukemic cells into the peripheral blood circulation and eventually lead to organ infiltration including spleen, liver and kidney. Without treatment, leukemia is a lethal disease.

Types of leukemia

All different types of blood cells are derived from a common ancestor, the hematopoietic stem cell (HSC), which only comprises about 0.01-0.05% of the total bone marrow population. These self-renewing and pluripotent HSCs can differentiate either into lymphoid or myeloid committed stem cells. The lymphoid stem cells will eventually differentiate into B- or T-lymphocytes, whereas myeloid cells will differentiate towards monocytes, macrophages and granulocytes (neutrophils, eosinophils and basophils), or towards megakaryocytes, platelets and erythrocytes. Based upon their cell of origin, leukemias are divided into lymphoid and myeloid leukemia. Lymphoid leukemias are further subdivided into T- and B-lineage leukemias, whereas the several subgroups of myeloid leukemia depend on the myeloid cell of origin. Finally, both lymphoid and myeloid leukemias can be further subdivided into acute and chronic leukemias. Acute leukemias are characterized by rapid progression and accumulation of immature malignant cells. They mostly occur in children and young adults and can be fatal within weeks or months without immediate treatment.

Chronic leukemias develop more slowly and involve more mature blood cells. They mainly occur in older people and immediate treatment is not required as therapy is often postponed to ensure maximum treatment efficiency.

Childhood acute lymphoblastic leukemia (ALL)

In general, leukemia is the most common form of childhood cancer, representing about 30 percent of all cancers in children. Acute lymphoblastic leukemia (ALL) is the most prevalent type, accounting for approximately 80-85% of childhood leukemias, whereas acute myeloid leukemia (AML) represents about 15-20%[6,7]. About 120 children with ALL and 20 children with AML are diagnosed yearly in the Netherlands. The peak incidence of childhood ALL is situated between 3 and 5 years of age.

T-CELL ACUTE LYMPHOBLASTIC LEUKEMIA (T-ALL)

T-ALL is an aggressive malignancy of thymocytes that mainly develops in children but can also affect adults[8]. Pediatric T-ALL accounts for about 15 percent of ALL cases and has been associated with an inferior outcome compared to pediatric B-ALL. Current T-ALL treatment schedules, mainly consisting of multi-agent combination chemotherapy, provide overall event-free survival rates of about 75% in children, whereas in adults these survival rates only reach 30 to 40%. In addition, T-ALL patients tend to relapse earlier compared to B-lineage ALL[7,8].

On the immunophenotypic level, leukemic cells from T-ALL patients are typically positive for cytoplasmatic CD3 and surface CD7, and show variable expression of other T-cell-associated antigens like CD2, surface CD3, CD4, CD5, CD8 and CD1a[9-11]. In addition, a number of very immature T-ALL cases also show aberrant expression of myeloid-associated antigens including CD13 and CD33. The expression of these antigens does not seem to have any impact on treatment outcome[12-14].

Genetic rearrangements identified in leukemic cells of T-ALL patients often involve the T-cell receptor genes (TCR), *TCR*α/δ or *TCR*β. During normal T-cell development, maturating T-cells rearrange their TCR genes in order to generate a wide variety of different TCR chains[15,16]. These gene rearrangement processes are highly vulnerable to recombination errors, thereby creating TCR-associated translocations. These translocations result in oncogene activation due to juxtaposition of a TCR enhancer element in the proximity of a T-cell specific proto-oncogene[8,17-19]. TCR-mediated translocations occur in about 35% of T-ALL patients and this percentage is still growing given the regular identification of novel TCR translocations.

Extensive research on the genetics of T-ALL during the last years has elucidated a large number of other, non TCR-mediated, genetic lesions in T-ALL, including other

chromosomal translocations, inversions, cryptic deletions, duplications, amplifications and mutations[8,17-19]. The main mutational target in T-ALL is *NOTCH1*, mutated in more than 50% of patients[20]. An in-depth overview of T-ALL genetics is provided in chapter 2.

GENETICS

Conventional cytogenetics and fluorescent in situ hybridization (FISH)

Cytogenetics, which studies chromosomes and chromosomal abnormalities, has evolved intensively during the past decades. At first, conventional karyotyping, based upon chromosome banding, allowed the identification of a large number of structural chromosomal abnormalities in a wide variety of malignancies. One of the first observations was the association of an additional copy of chromosome 21 with Down's syndrome[21]. In terms of hematology research, the identification of the Philadelphia chromosome in 1973 became a milestone in the understanding of leukemia genetics[22]. However, the limited resolution of conventional chromosome analysis triggered the search for new genetic techniques that could detect more cryptic rearrangements that are easily missed by conventional cytogenetics.

Fluorescent in situ hybridization (FISH) is a technique that may enable the verification of the rearrangement status of specific chromosomal regions. It makes use of specific probes, covering particular chromosomal loci, which are hybridized on cells. This technique became a valuable addition to conventional karyotyping and allowed detection of specific chromosomal translocations, inversions, deletion or amplifications[23,24]. However, this analysis depends on the availability of adequately working FISH probes in the genomic region of interest and is only capable of investigating a few genomic regions simultaneously[23,24].

Comparative genome hybridization (CGH) and array-CGH

General principle

Comparative genome hybridization (CGH) is a method developed for the comparison of copy number changes (i.e. amplification and/or deletions) between tumor DNA versus normal reference DNA. Differential labeling of both DNAs using a different fluorescent label, for example Cy3 and Cy5, and hybridization on methaphase spreads from a normal individual allows for the measurement of the fluorescent ratio along each chromosome. This way, genomic regions of relative gain and loss can be visualized in the tumor DNA sample[25,26]. This technique has been shown to be a valuable tool for the identification of new genomic imbalances in a number of

hematological malignancies[27,28]. However, the limited resolution of about 5-10 Mb has remained the major drawback for this genome comparison technique.

On April 14, 2003, the Human Genome Project was completed[29], providing great opportunities for the improvement of CGH resolution. This publicly accessible genome project, which claimed the identification of nearly the complete human genome, provided large-insert clone libraries of bacterial artificial chromosomes (BAC-clones) that were assembled into overlapping contigs by sequencing[30,31]. This know-how could be used to replace the methaphase chromosome slides with arrays containing BAC-clones precisely mapped onto the human genome and spotted robotically onto glass slides. Therefore, the resolution was no longer limited to 5-10 Mb, but depended on the size and the number of sequences present on the array. The experiments that used this type of technology were first reported in 1997 as matrix-CGH[32] and in 1998 as array-CGH[33], the term that is currently used for this genome-wide copy number screening assay. Similar to conventional CGH, the fluorescent ratios are measured for each clone and plotted relative to the clone's position along the genome.

Depending on the DNA sequences used for the construction of the arrays, different array-CGH platforms have been introduced in the past. BAC array-CGH platforms used large-insert BAC clones containing human DNA inserts of about 50-200 kb. Due to the relative long DNA sequences present on each spot, this type of arrays produced high signal-to-noise ratio's and were considered as the most reliable array-CGH platform in the first years after the introduction of this novel method[34,35]. However, in recent years, array technology has progressed rapidly and there has been a significant trend towards increased numbers of spots and shorter DNA hybridization targets. Especially the introduction of oligonucleotide arrays[36,37] provided enormous opportunities to further increase the resolution of array-CGH analyses. A number of commercial platforms have used advanced printing technologies to reliably spot up to 244,000 probe sets on a single glass slide, and it is expected that within a couple of years this number of spots will be increased further. These developments will further increase array-CGH resolution up until a couple of thousand base pairs. In addition, this will provide opportunities for high-throughput array-CGH analysis in which multiple samples can be analyzed on a single glass slide with a reasonable resolution, further reducing the price for a single experiment. In the last couple of years, numerous reports have shown that array-CGH is a reliable tool for the detection of new genetic deletions and/or amplifications in different hematological malignancies[38-41].

Approximately at the same time as array-CGH was implemented successfully in a large number of laboratories, the possibility of using Single Nucleotide Polymorphism (SNP) chips for the assessment of DNA copy number alterations was discovered[42].

Although these SNP arrays were originally developed for the detection of specific base compositions present at a particular SNP locus, the intensity information of these arrays can be used to determine the copy number of specific genomic loci. In contrast to array-CGH, in which 2 DNA samples are co-hybridized, SNP arrays are hybridized with a single DNA sample. An important advantage of this technology is the ability to detect uniparental disomy (UPD), a phenomenon in which 2 copies of a chromosome, or part of a chromosome, originate from a single parent through duplication and replacement of the other copy[43-46]. Using SNP array analysis, genomic regions that show UPD are visualized by successive homozygous SNPs in combination with 2 copies of that specific genomic locus. Therefore, UPD remains undetected using array-CGH technology. Recently, SNP array platforms have been used successfully to identify numerous novel genetic lesions and chromosomal regions of UPD in different hematological malignancies, including ALL[47-49].

Large-scale copy number variation in the human genome

Besides the clear benefits of array-CGH technology in terms of disease related genetic research, the introduction of this genome-wide screening technique also had great impact on our understanding and knowledge of genomic variation between healthy individuals. Before the array-CGH era, variation in the human genome was thought to be mainly present at the single nucleotide level through the occurrence of SNPs. However, this idea was challenged in 2004 by two independent studies that analyzed the genomes of healthy individuals using array-CGH and found that more than 100 genomic regions differed between individuals with respect to the number of copies present of a specific DNA fragment[50,51]. These copy number variants (CNV) are currently defined as DNA segments, longer than 1 kb, with a variable copy number compared to a reference genome. After the first landmark studies on the occurrence of CNVs in humans, the knowledge on structural variation has improved rapidly, mainly through large-scale projects that used high-density oligonucleotide or SNP arrays to map structural variation in different populations[52]. Currently, a number of publicly available databases try to collect CNV data from different human variation studies. For example, the Database of Genomic Variants (http://projects.tcag.ca/variation) currently assembled 6482 CNV entries from 40 different published studies.

It is clear that studies on the variation in the human genome are extremely important with regard to the use of array-CGH for the linkage of specific copy number alterations to a particular disease phenotype. Indeed, the identification of specific genomic regions of gain or loss in patients with a certain malignancy could originate from the genetic variation between the two individuals tested, rather than being disease related. Therefore, it is mandatory that array-CGH studies that identify new

genetic aberrations, confirm that these specific abnormalities are acquired genetic events, for example by analyzing the patients' remission material.

OUTLINE OF THIS THESIS

T-ALL is an aggressive T-cell malignancy with an inferior treatment outcome compared to B-lineage ALL. Intensive T-ALL research efforts during the last years lead to the identification of multiple genetic abnormalities that cooperate in the malignant transformation of thymocytes. Currently and in contrast to B-lineage ALL, genetic abnormalities are clinically not used for therapy stratification. Further progress on the treatment of T-ALL will require further genetic characterization, which will provide us with a better understanding of the pathogenesis of T-ALL and hopefully will lead to improved treatment schedules. As the general scope of this thesis, we performed genome-wide copy number analysis using array-CGH for the identification of novel genomic rearrangements in T-ALL that possibly relate to treatment outcome, i.e. prognostic factors, or provide further insight in the pathogenesis of T-cell leukemia.

In **Chapter 2** we provide a review on the genetics of T-ALL. In the first part, we discuss the different genetic abnormalities and their respective target genes that are currently associated with T-cell leukemia and propose a new classification of these genetic defects into 'Type A' and 'Type B' abnormalities. Mutations that occur in a mutually exclusive manner and probably delineate specific T-ALL subtypes are denoted as type A mutations, whereas other mutational events that are shared by various subtypes and may synergize with type A mutations during T-cell pathogenesis are denoted as type B mutations. These type B mutations affect genes that normally play a role in cell cycle regulation, self-renewal and T-cell commitment, (pre)TCR signaling, T-cell differentiation or lead to the aberrant activation of tyrosine kinases. In the second part, we provide an overview of genome-wide copy number analysis on 107 genetically well-characterized T-ALL patients. We discuss all recurrent genomic lesions together with their potential genes of interest in relation to the major genetic subgroups in T-ALL.

Chapter 3 describes the identification of a cryptic deletion, del(11)(p12p13), as a new mechanism of *LMO2* activation in pediatric T-ALL. Detailed molecular-cytogenetic analysis revealed that this deletion activates the *LMO2* oncogene in most of the del(11)(p12p13)-positive T-ALL patients, mainly through deletion of negative regulatory sequences upstream of *LMO2*. The relation to other recurrent cytogenetic abnormalities, the immunophenotypic characteristics and clinical outcome of T-ALL cases with this new cryptic abnormality is discussed.

This negative regulatory region of *LMO2* is a relatively small domain comprised by a region of approximately 3000 base pairs. We assumed that our initial screening for cryptic *LMO2* deletions using FISH may have been unsuccessful to detect relatively small deletions upstream of *LMO2* including this negative regulatory element. **Chapter 4** describes the development of an *LMO2* specific MLPA assay to detect even smaller deletions upstream of the *LMO2* oncogene. Using this approach, we identified one additional T-ALL case with an *LMO2* deletion that remained undetected in our previous FISH analysis. In this chapter, we also investigate the relation between mono- or biallelic *LMO2* expression and the presence of specific *LMO2* rearrangements in T-ALL.

Elevated expression of *HOXA* genes is a hallmark of a specific T-ALL subgroup that includes *MLL*-rearranged, *CALM-AF10* translocated and inv(7)(p15q34) positive cases. In **Chapter 5**, we combined gene expression profiling and array-CGH analysis to detect a new and recurrent molecular cytogenetic abnormality in T-ALL patients that co-clustered with well-defined *HOXA*-activated T-ALL samples. We describe the cloning of the recurrent *SET-NUP214* fusion product in these samples, and identify the mechanism by which SET-NUP214 can activate the *HOXA* gene cluster as potential leukemogenic event in T-ALL.

In collaboration with the research group of Dr. Jan Cools (Leuven, Belgium), we identified a duplication of the MYB oncogene by means of array-CGH, which is described in **Chapter 6**. Screening of our pediatric T-ALL cohort by quantitative PCR analysis revealed that this *MYB* duplication was present in about 8% of pediatric T-ALL cases. A role for *MYB* duplications in the pathogenesis of human T-ALL is investigated through specific down regulation of *MYB* expression. MYB is evaluated as a potential new therapeutic target in human T-ALL by studying the potential synergism between MYB down regulation and inhibition of NOTCH1, the main mutational target in T-ALL[20].

In **Chapter 7**, we specifically focus on *TLX3* rearranged pediatric T-ALL patients and use array-CGH to identify new chromosomal imbalances that may provide further insight in the development of *TLX3* mediated T-cell leukemia. All genomic lesions are discussed in relation to potential target genes and known genetic aberrations, including *NOTCH1* mutations, *NUP214-ABL1* amplifications and mono-/biallelic *CDKN2A/CDKN2B* deletions.

Another part of the research focused on leukemia associated *NF1* inactivation in pediatric T-ALL patients that lack evidence for neurofibromatosis. Neurofibromatosis type 1 (NF1) is an autosomal dominant genetic disorder caused by mutations in the *NF1* gene. NF1 patients have a higher risk to develop juvenile myelomonocytic leukemia (JMML) and acute myeloid leukemia (AML). In **chapter 8**, we identify somatic *NF1* microdeletions as a cryptic genetic abnormality in T-ALL patients that did not

have any clinical evidence of NF1. Subsequent mutation analysis was performed to identify potential mutations in the remaining *NF1* allele, and to confirm a role for *NF1* as a bona fide tumor-suppressor gene in T-ALL. In addition, we investigated if *NF1* microdeletions were exclusively present in T-ALL or represented a general leukemogenic mechanism also present in other types of leukemia, including AML and B-lineage ALL.

In T-ALL, a number of genetic defects are only detected in a limited percentage of leukemic cells, indicating that they probably reflect a progression marker, rather than an initiating leukemogenic event. In **chapter 9** and **chapter 10**, we describe examples of such genetic abnormalities that only occur in a subclone of the leukemic T-ALL population. **Chapter 9** illustrates the identification of a new and recurrent 9q34 duplication present in 33 percent of pediatric T-ALL samples. This duplication was studied in relation to other 9q34 abnormalities in T-ALL, including *NUP214-ABL1* amplifications and activational mutations in *NOTCH1*. This chapter demonstrates that the 9q34 region is genetically unstable in T-ALL. In **chapter 10**, we show that *FLT3* mutations in pediatric T-ALL are rare, and mainly occur in immature T-ALL cases as a subclonal event.

In **chapter 11**, we provide a summary and general conclusions on the work presented in this thesis and speculate on future directions in T-cell leukemia research. **Chapter 12** contains a brief summary of this thesis in Dutch.

REFERENCES

1. Virchow R. Weisses Blut. Floriep's Notizen. 1845;36:151-157.
2. Craigie D. Case of disease of the spleen, in which death took place in consequence of the presence of purulent matter in the blood. Edinb Med Surg J. 1845;64:400-413.
3. Bennet J. Case of hypertrophy of the spleen and liver, in which death took place from suppuration of the blood. Edinb Med Surg J. 1845;64:413-423.
4. Donne A. Cours de Microscopie Complementaire des Etudes Medicales, Anatomie Microscopique et Physiologie des Fluides. Paris: Bailliere. 1844:132-136.
5. Velpeau A. Sur la resorption du pus ets ur l'alteration dus sang dans les maladies. Rev Med. 1827;2:218-234.
6. Pui CH, Relling MV, Downing JR. Acute lymphoblastic leukemia. N Engl J Med. 2004;350:1535-1548.
7. Pui CH, Evans WE. Treatment of acute lymphoblastic leukemia. N Engl J Med. 2006;354:166-178.
8. Grabher C, von Boehmer H, Look AT. Notch 1 activation in the molecular pathogenesis of T-cell acute lymphoblastic leukaemia. Nat Rev Cancer. 2006;6:347-359.
9. Brouet JC, Seligmann M. The immunological classification of acute lymphoblastic leukemias. Cancer. 1978;42:817-827.
10. Bene MC, Castoldi G, Knapp W, et al. Proposals for the immunological classification of acute leukemias. European Group for the Immunological Characterization of Leukemias (EGIL). Leukemia. 1995;9:1783-1786.
11. Campana D, van Dongen JJ, Mehta A, et al. Stages of T-cell receptor protein expression in T-cell acute lymphoblastic leukemia. Blood. 1991;77:1546-1554.
12. Pui CH, Behm FG, Singh B, et al. Myeloid-associated antigen expression lacks prognostic value in childhood acute lymphoblastic leukemia treated with intensive multiagent chemotherapy. Blood. 1990;75:198-202.
13. Pui CH, Rubnitz JE, Hancock ML, et al. Reappraisal of the clinical and biologic significance of myeloid-associated antigen expression in childhood acute lymphoblastic leukemia. J Clin Oncol. 1998;16:3768-3773.
14. van Grotel M, Meijerink JP, van Wering ER, et al. Prognostic significance of molecular-cytogenetic abnormalities in pediatric T-ALL is not explained by immunophenotypic differences. 2007.
15. Hoffmann R, Melchers F. A genomic view of lymphocyte development. Curr Opin Immunol. 2003;15:239-245.
16. Aifantis I, Mandal M, Sawai K, Ferrando A, Vilimas T. Regulation of T-cell progenitor survival and cell-cycle entry by the pre-T-cell receptor. Immunol Rev. 2006;209:159-169.
17. Armstrong SA, Look AT. Molecular genetics of acute lymphoblastic leukemia. J Clin Oncol. 2005;23:6306-6315.
18. Graux C, Cools J, Michaux L, Vandenberghe P, Hagemeijer A. Cytogenetics and molecular genetics of T-cell acute lymphoblastic leukemia: from thymocyte to lymphoblast. Leukemia. 2006.
19. De Keersmaecker K, Marynen P, Cools J. Genetic insights in the pathogenesis of T-cell acute lymphoblastic leukemia. Haematologica. 2005;90:1116-1127.

20. Weng AP, Ferrando AA, Lee W, et al. Activating mutations of NOTCH1 in human T-cell acute lymphoblastic leukemia. Science. 2004;306:269-271.

21. Jacobs PA, Baikie AG, Court Brown WM, Strong JA. The somatic chromosomes in mongolism. Lancet. 1959;1:710.

22. Rowley JD. Letter: A new consistent chromosomal abnormality in chronic myelogenous leukaemia identified by quinacrine fluorescence and Giemsa staining. Nature. 1973;243:290-293.

23. Trask B, Pinkel D. Fluorescence in situ hybridization with DNA probes. Methods Cell Biol. 1990;33:383-400.

24. Trask BJ. Fluorescence in situ hybridization: applications in cytogenetics and gene mapping. Trends Genet. 1991;7:149-154.

25. Kallioniemi OP, Kallioniemi A, Sudar D, et al. Comparative genomic hybridization: a rapid new method for detecting and mapping DNA amplification in tumors. Semin Cancer Biol. 1993;4:41-46.

26. Kallioniemi A, Kallioniemi OP, Sudar D, et al. Comparative genomic hybridization for molecular cytogenetic analysis of solid tumors. Science. 1992;258:818-821.

27. Kim MH, Stewart J, Devlin C, Kim YT, Boyd E, Connor M. The application of comparative genomic hybridization as an additional tool in the chromosome analysis of acute myeloid leukemia and myelodysplastic syndromes. Cancer Genet Cytogenet. 2001;126:26-33.

28. Jarosova M, Holzerova M, Jedlickova K, et al. Importance of using comparative genomic hybridization to mprove detection of chromosomal changes in childhood acute lymphoblastic leukemia. Cancer Genet Cytogenet. 2000;123:114-122.

29. Nature Human Genome Collection. Nature. 2006;S1.

30. Cheung VG, Nowak N, Jang W, et al. Integration of cytogenetic landmarks into the draft sequence of the human genome. Nature. 2001;409:953-958.

31. Bentley DR, Deloukas P, Dunham A, et al. The physical maps for sequencing human chromosomes 1, 6, 9, 10, 13, 20 and X. Nature. 2001;409:942-943.

32. Solinas-Toldo S, Lampel S, Stilgenbauer S, et al. Matrix-based comparative genomic hybridization: biochips to screen for genomic imbalances. Genes Chromosomes Cancer. 1997;20:399-407.

33. Pinkel D, Segraves R, Sudar D, et al. High resolution analysis of DNA copy number variation using comparative genomic hybridization to microarrays. Nat Genet. 1998;20:207-211.

34. Ishkanian AS, Malloff CA, Watson SK, et al. A tiling resolution DNA microarray with complete coverage of the human genome. Nat Genet. 2004;36:299-303.

35. Fiegler H, Redon R, Andrews D, et al. Accurate and reliable high-throughput detection of copy number variation in the human genome. Genome Res. 2006;16:1566-1574.

36. Carvalho B, Ouwerkerk E, Meijer GA, Ylstra B. High resolution microarray comparative genomic hybridisation analysis using spotted oligonucleotides. J Clin Pathol. 2004;57:644-646.

37. Lucito R, Healy J, Alexander J, et al. Representational oligonucleotide microarray analysis: a high-resolution method to detect genome copy number variation. Genome Res. 2003;13:2291-2305.

38. Schwaenen C, Nessling M, Wessendorf S, et al. Automated array-based genomic profiling in chronic lymphocytic leukemia: development of a clinical tool and discovery of recurrent genomic alterations. Proc Natl Acad Sci U S A. 2004;101:1039-1044.

39. Rucker FG, Bullinger L, Schwaenen C, et al. Disclosure of candidate genes in acute myeloid leukemia with complex karyotypes using microarray-based molecular characterization. J Clin Oncol. 2006;24:3887-3894.

40. Baldus CD, Liyanarachchi S, Mrozek K, et al. Acute myeloid leukemia with complex karyotypes and abnormal chromosome 21: Amplification discloses overexpression of APP, ETS2, and ERG genes. Proc Natl Acad Sci U S A. 2004;101:3915-3920.

41. Graux C, Cools J, Melotte C, et al. Fusion of NUP214 to ABL1 on amplified episomes in T-cell acute lymphoblastic leukemia. Nat Genet. 2004;36:1084-1089.

42. Nannya Y, Sanada M, Nakazaki K, et al. A robust algorithm for copy number detection using high-density oligonucleotide single nucleotide polymorphism genotyping arrays. Cancer Res. 2005;65:6071-6079.

43. Raghavan M, Lillington DM, Skoulakis S, et al. Genome-wide single nucleotide polymorphism analysis reveals frequent partial uniparental disomy due to somatic recombination in acute myeloid leukemias. Cancer Res. 2005;65:375-378.

44. Fitzgibbon J, Smith LL, Raghavan M, et al. Association between acquired uniparental disomy and homozygous gene mutation in acute myeloid leukemias. Cancer Res. 2005;65:9152-9154.

45. Flotho C, Steinemann D, Mullighan CG, et al. Genome-wide single-nucleotide polymorphism analysis in juvenile myelomonocytic leukemia identifies uniparental disomy surrounding the NF1 locus in cases associated with neurofibromatosis but not in cases with mutant RAS or PTPN11. Oncogene. 2007.

46. Wouters BJ, Sanders MA, Lugthart S, et al. Segmental uniparental disomy as a recurrent mechanism for homozygous CEBPA mutations in acute myeloid leukemia. Leukemia. 2007.

47. Pfeifer D, Pantic M, Skatulla I, et al. Genome-wide analysis of DNA copy number changes and LOH in CLL using high-density SNP arrays. Blood. 2007;109:1202-1210.

48. Mullighan CG, Goorha S, Radtke I, et al. Genome-wide analysis of genetic alterations in acute lymphoblastic leukaemia. Nature. 2007;446:758-764.

49. Kawamata N, Ogawa S, Zimmermann M, et al. Molecular allelokaryotyping of pediatric acute lymphoblastic leukemias by high resolution single nucleotide polymorphism oligonucleotide genomic microarray. 2007.

50. Iafrate AJ, Feuk L, Rivera MN, et al. Detection of large-scale variation in the human genome. Nature genetics. 2004;36:949-951.

51. Sebat J, Lakshmi B, Troge J, et al. Large-scale copy number polymorphism in the human genome. Science (New York, NY. 2004;305:525-528.

52. Redon R, Ishikawa S, Fitch KR, et al. Global variation in copy number in the human genome. Nature. 2006;444:444-454.

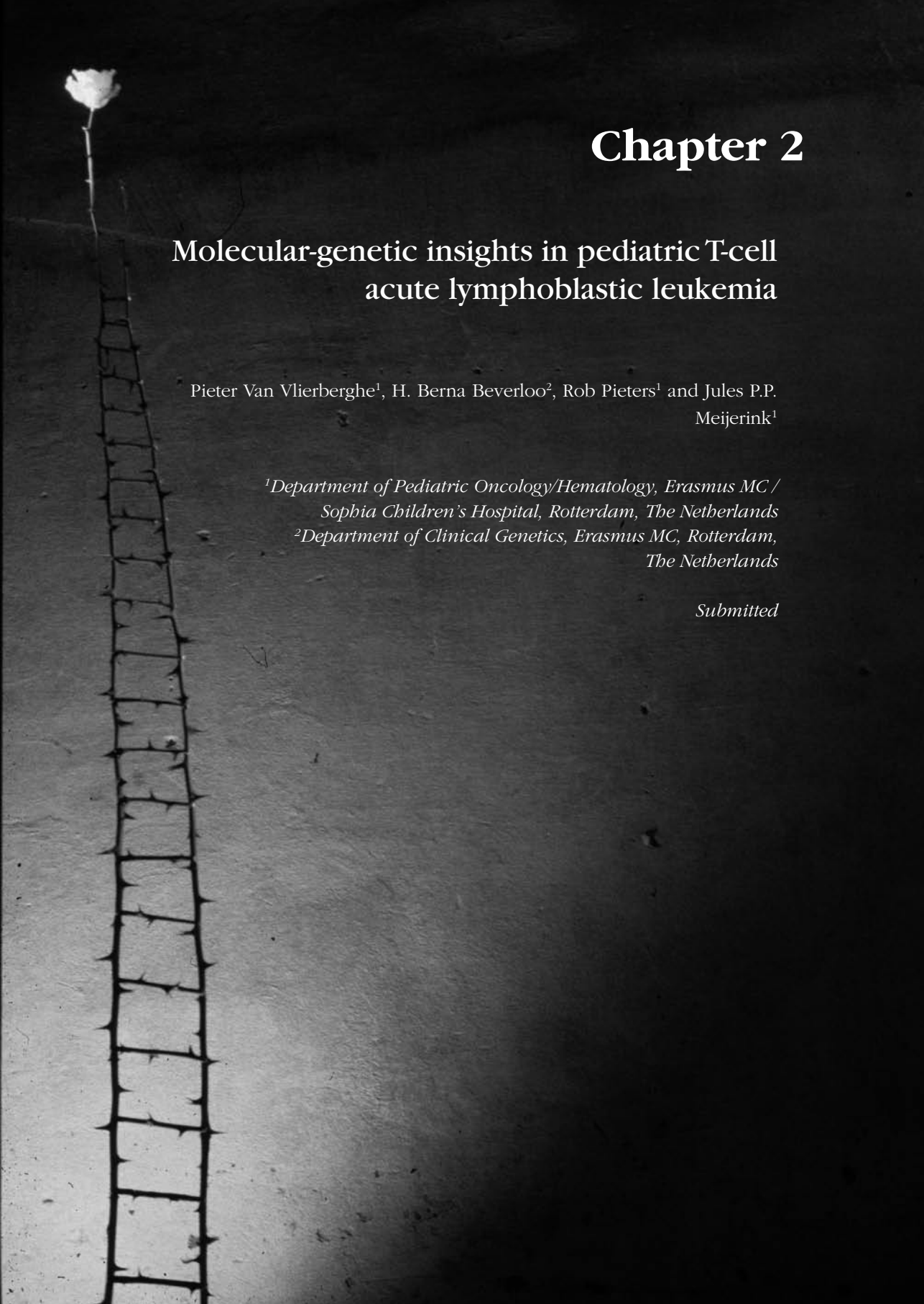

Chapter 2

Molecular-genetic insights in pediatric T-cell acute lymphoblastic leukemia

Pieter Van Vlierberghe[1], H. Berna Beverloo[2], Rob Pieters[1] and Jules P.P. Meijerink[1]

[1]Department of Pediatric Oncology/Hematology, Erasmus MC / Sophia Children's Hospital, Rotterdam, The Netherlands
[2]Department of Clinical Genetics, Erasmus MC, Rotterdam, The Netherlands

Submitted

ABSTRACT

Pediatric T-cell ALL is an aggressive malignancy of thymocytes that accounts for about 15 percent of ALL cases and for which treatment outcome remains inferior compared to B-lineage acute leukemias. In T-ALL, leukemic transformation of maturating thymocytes is caused by a multistep pathogenesis involving numerous genetic abnormalities that drive normal T-cells into uncontrolled cell growth and clonal expansion. In this review, we provide an overview of the current knowledge on onco- and tumor suppressor genes in T-ALL and suggest a classification of these genetic defects into type A and type B abnormalities. Type A abnormalities occur in a mutually exclusive manner and may delineate distinct molecular-cytogenetic T-ALL subgroups, whereas type B abnormalities are found in all major T-ALL subgroups and may synergize with these type A mutations during T-cell pathogenesis. In addition, we review our genome-wide copy number data on 107 T-ALL patients and discuss all recurrent genomic lesions in T-ALL together with their potential genes of interest and possible link towards leukemogenesis.

INTRODUCTION

T-cell acute lymphoblastic leukemia (T-ALL) is an aggressive malignancy of thymocytes that is diagnosed in children, adolescents and adults. Although this neoplastic disorder originates in the thymus, it metastasises throughout the body and is rapidly fatal without therapy. Current treatment, mainly consisting of multi-agent combination chemotherapy, provides an overall survival rate of ~70% in children, whereas in adults the long-term survival rate only reach 30 to 40%[1].

Leukemic transformation of immature thymocytes is caused by a multistep pathogenesis involving numerous genetic abnormalities that drive normal T-cells into uncontrolled cell growth and clonal expansion. A wide variety of genetic events affecting cellular processes like the cell cycle, differentiation and survival have thus far been identified in T-ALL and result in developmental arrest in nearly all stages of T-cell maturation in the thymus. In normal T-cell development, lymphoid progenitor cells migrate from the bone marrow towards the thymus, where mature T-cell receptor (TCR) αβ or γδ positive T-cells develop from a common $CD4^-CD8^-$ double negative progenitor cells (reviewed in[2-4] and figure 1).

Many of the genes that are involved in chromosomal rearrangements in T-ALL become activated due to disturbances in the rearrangement process of the T-cell receptor genes (TCR). Other genes become activated or inactivated due to the presence of specific point- or insertion/deletion mutations, or are affected by somatic copy number variations, i.e. amplifications and/or deletions. Many of these genes normally play important roles in T-cell commitment and differentiation or control important checkpoints in T-cell development that warrant for the selection of proper antigen specificity[5]. In this review, we provide an overview of the current literature on onco- and tumor suppressor genes in T-ALL. We have distinguished between mutations that occur in a mutually exclusive manner, probably delineating specific T-ALL subtypes (denoted as “type A” mutations), and other mutational events that are shared by various of the subtypes and that may synergize with type A mutations during T-cell pathogenesis (denoted as “type B’ mutations). These type B mutations affect genes that normally play a role in cell cycle regulation, self-renewal and T-cell commitment, (pre)TCR signaling, T-cell differentiation or lead to the aberrant activation of tyrosine kinases.

Recently, a number of studies showed that large-scale genome wide screening using microarray-based comparative genomic hybridisation (array-CGH) or single nucleotide polymorphism (SNP) arrays are valuable tools for the identification of novel genetic aberrations that are associated with specific types of leukemia[6-10]. In this review, we present our genome-wide copy number analyses on 107 genetically well-characterized T-ALL patients. All recurrent genomic lesions in the various T-ALL

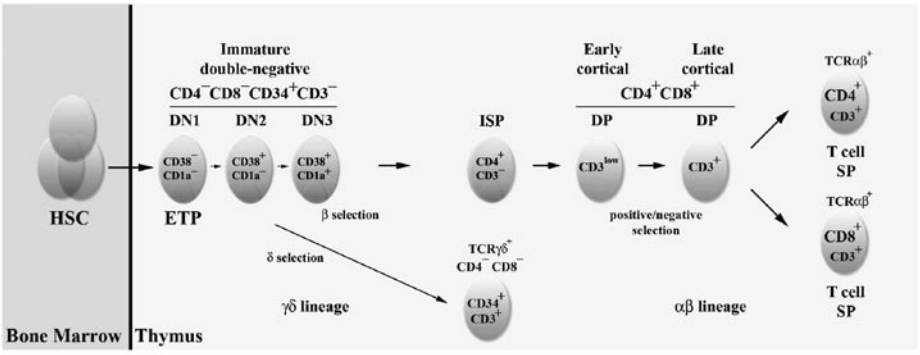

Figure 1. Schematic representation of normal T-cell development.
The earliest phases of T-cell development can be subdivided according to the expression of CD38 and CD1a membrane markers while still lacking expression of either CD4 and/or CD8, i.e. the double-negative (DN) stages. It is believed that T-cells that express CD34, but lack CD38 and CD1a expression (DN1: CD38-, CD1a-) are not yet committed to the T-cell lineage and may still be able to differentiate towards B cells, dendritic cells or natural killer cells[165]. Commitment to the T lineage is characterized by upregulation of CD38 (DN2: CD38+, CD1a) and CD1a (DN3: CD38+, CD1a+) expression and depends on signals from the thymic microenvironment like IL7 and c-KIT ligand[166]. During the early double negative stages, T-cell progenitors start to rearrange their *TCR* β, γ and δ loci by V(D)J recombination at similar time points, whereas *TCR* α rearrangements occur at later stage of pre T-cell maturation[167]. This V(D)J recombination process, in which joining of diversity segments (D) to joining segments (J) is followed by the fusion of variable segments (V) V to already joined DJ elements warrants almost unlimited diversity of the TCR chains towards antigens[168]. At this point, the choice between the αβ or γδ lineage takes place. Next, the selected TCR β chains associates with pTα and CD3 on the cell surface to form the pre-T-cell receptor (pre-TCR) complex (DN3). Although this complex lacks CD4 and CD8, it is capable of initiating T-cell signaling, leading to clonal expansion and proliferation[169]. After a *TCR*α gene rearrangement, a mature αβTCR will be expressed on the surface of the developing T-cell. These T-cells will be educated by positive and negative selection at the double positive stages (DP; $CD4^+/CD8^+$) which is crucial to distinguish between self and foreign antigens[4]. Finally, these $CD4^+/CD8^+$ thymocytes will undergo transition towards single positive ($CD4^+$ or $CD8^+$) mature T-cells.

subgroups will be discussed including potential genes of interest and their possible leukemogenic role.

1. Type A abnormalities delineate specific subgroups in T-ALL

Over the last years, great progress has been made in unravelling molecular-genetic abnormalities in T-ALL, including chromosomal translocations, deletions, amplifications, duplications and mutations[11-14]. A number of these genetic events occur in a mutually exclusive manner, and it is believed that they delineate distinct molecular-cytogenetic T-ALL subgroups. These abnormalities include defects that result in

Table 1. Overview type A and B abnormalities in T-ALL

	Genetic T-ALL subgroups				
	TAL/LMO	**TLX1**	**TLX3**	**HOXA**	**MYB**
	TAL1	***TLX1***	***TLX3***	***HOXA***	***MYB***
Type A	***TAL2***			***CALM-AF10***	
abnormalities	***LMO1***			***MLL***	
T cell differentiation	***LMO2***			***SET-NUP214***	
	bHLHB1				

	Type B1 Cell cycle	**Type B2 *NOTCH***	**Type B3 (pre)TCR**	**Type B4 differentiation**	**Type B5 Other kinases**
	CDKN2A	***NOTCH1***	***LCK***	***MYB duplication***	***ABL1***
Type B	***CDKN2B***	***FBXW7***	***RAS***		***JAK2***
abnormalities	***CYCLIND2***		***PTEN***		***FLT3***
			Calcineurin		

	Type B1 Cell cycle	**Type B2 *NOTCH***	**Type B3 (pre)TCR**	**Type B4 differentiation**	**Type B5 Other kinases**
	ATM	***FBXW7***	***NFKB1***	***MYB***	***none***
Type B	***RB1***	***cMYC***	***TCF1***		
abnormalities	***p27KIP***	***CTCF***	***SYK***		
array-CGH		***NFKB1***	***PTEN***		
			NF1		

ectopic expression of *TAL1*, *TAL2*, *LMO1*, *LMO2*, *LYL1*, *TLX1*, *TLX3, MYB* and *HOXA* genes, or generate specific fusion products including *CALM-AF10, MLL-ENL* and *SET-NUP214*[9,11-21]. These genetic defects mainly function by facilitating differentiation arrest at specific stages of T-cell development and will be further denoted in this review as 'type A' mutations. Various micro-array studies led to the establishment of specific expression profiles for several of these 'type A' subgroups[17,20,22]. These studies pointed to overlapping expression profiles for subgroups with *TAL1*, *TAL2*, *LMO1* and *LMO2* abnormalities. These genes normally participate in the same transcriptional complex (see below), and may together form the *TAL/LMO* subgroup. Also, *CALM-AF10*, *MLL*-rearrangements, inversion 7 positive patients and *SET-NUP214* positive T-ALL patients share a similar expression profile that is characterized by the activation of the cluster of *HOXA* genes[17,20]. T-ALL cases with these abnormalities are now recognized as the *HOXA* subgroup. Other type A mutations including *TLX1*, *TLX3,* and MYB have each been shown to have a unique gene expression profile[15,17,20,22] (table 1).

Deregulation of the *TAL/LMO* transcription complex: the *TAL/LMO* subgroup

Basic helix-loop-helix (bHLH) transcription factors share a 60 amino acid HLH motif that includes a dimerization domain and a DNA binding domain for specific E-box sites[23]. Class A bHLH proteins like E2A (E12/E47) and HEB control the expression of various genes that are involved in V(D)J recombination of the *TCR* genes. *E2A* knockout mice develop aggressive T-cell lymphomas[24], indicating that disruption of E2A/HEB function may represent an important mechanism in human T-ALL. However, genetic rearrangements in human T-ALL directly affecting *E2A* or *HEB* have not been described.

Another class of bHLH proteins, i.e. class B type of bHLH proteins, include **TAL1**, **TAL2, LYL1**, and **bHLHB1**. These proteins function as transcriptional co-factors that form complexes with E2A/HEB[23]. *TAL2* is not expressed during normal T-cell development, whereas *LYL1* and *TAL1* expression in mice are restricted to the earliest double-negative stages of T-cell maturation[25]. Class B bHLH members are predominantly targeted by chromosomal rearrangements in T-ALL mostly due to miss rearrangements of the *TCR*α/δ or *TCR*β loci. Consequently, the aberrant juxtaposition of these genes in the vicinity of TCR enhancers may result in their ectopic expression. *TAL1* activation in childhood T-ALL results from the t(1;14)(p32;q11) or variant t(1;7)(p32;q35) or from a small interstitial deletion placing the protein coding domains of the *TAL1* gene under the control of the promoter region of the *SIL* gene[26]. *TAL2* and *bHLHB1* can also be activated by the rare translocations t(7;9)(q34;q32)[21] and t(14;21)(q11;q22)[27], respectively.

For function, bHLH family members also bind to members of the LIM-domain only (LMO) gene family. Class B bHLH and LMO proteins participate in a single transcription complex that inhibits E2A function[28-32]. The LIM domain only genes ***LMO1*** and ***LMO2*** are also frequently targeted in T-ALL by chromosomal translocations t(11;14)(p13;q11), t(7;11)(q35;p13), t(11;14)(p15;q11) or t(7;11)(q35;p15), leading to high activation of *LMO1* or *LMO2*[33]. Recently, we identified an interstitial deletion, i.e. the del(11)(p12p13), that functions as an alternative mechanism for *LMO2* activation in T-ALL. This intra-chromosomal deletion leads to the loss of a negative regulatory domain directly upstream of the *LMO2* gene and results in elevated *LMO2* expression[9]. Loss of this negative regulatory domain has now also been suggested to drive ectopic *LMO2* expression in *LMO2* translocations[34]. *LMO1* is not expressed during T-cell development, whereas *LMO2* expression, like *TAL1* and *LYL1* expression, is confined to the most immature T-cell development stages in mice[25]. Inhibition of an E2A enforced cell proliferation block may represent the most predominant function for the *TAL/LMO* transcription complex and could explain synergy of *bHLH* and *LMO* genes in T-cell pathogenesis[29].

The *TLX1* T-ALL subgroup

TLX1 is a class II homeobox gene that is normally involved in spleen development but is not expressed during normal T-cell development. In about 5% of pediatric T-ALL cases, *TLX1* is activated through the translocations t(7;10)(q34;q24) or t(10;14)(q24;q11) in which *TCR*α/δ or *TCR*β regulatory sequences drive *TLX1* expression[35]. *TLX1* positive T-ALL cases share a highly similar gene expression profile that shows arrest at the early cortical, CD1-positive thymocyte stage[22]. This differentiation arrest was recently confirmed by a study in which retroviral *TLX1* expression in differentiating murine and human thymocytes caused a block in T cell differentiation prior to the DP thymocyte stage[36]. *TLX1* positive T-ALL has been associated with a favorable outcome, possibly due to a low expression of anti-apoptotic proteins characteristic for this early cortical differentiation stage[22] or a high expression of genes involved in cell growth and proliferation[22,37]. In addition, this subset has also been associated with elevated expression levels of the glucocorticoid receptor[22] that may explain the enhanced sensitivity towards dexamethasone[38]. Murine studies confirmed that overexpression of *TLX1* in bone marrow cells induced T-cell leukemia after a long latency period, indicating that additional genetic hits are required for T-cell leukemogenesis[39].

TLX1 expression has occasionally been reported in T-ALL cases in the absence of *TLX1* rearrangements, indicating that alternative mechanisms like promoter demethylation or trans-activating mechanism may be responsible for this aberrant gene expression[40]. However, the current controversy on *TLX1* expression in the absence of genetic rearrangements may be due to differences in the sensitivity of *TLX1* expression quantification methods. We found a strict correlation between *TLX1* expression and the presence of *TLX1* rearrangements[41]. Also in a recent study, high *TLX1* expression was associated with genomic rearrangements at the *TLX1* locus and a good prognosis, whereas low *TLX1* expression was observed in a heterogeneous T-ALL subgroup frequently characterized by other type A abnormalities without prognostic relevance[42].

The *TLX3* T-ALL subgroup

Ectopic expression of *TLX3*, another class II homeobox gene, is present in about 20% of childhood T-ALL patients[43]. *TLX3* expression is mostly due to the cryptic translocation t(5;14)(q35;q32), juxtaposing *TLX3* to *BCL11B*, a gene expressed during T-cell maturation[19]. Like *TLX1*, *TLX3* is not expressed during normal T-cell development. A number of alternative *TLX3* translocations have been described, including t(5;14)(q32;q11)[44], involving the *TCR*α/δ locus, and t(5;7)(q35;q21), involving the *CDK6* gene[45]. *TLX3* positive T-ALL has been associated with poor outcome in some studies, but this effect was not confirmed in other studies[41,46,47], possibly due to differences

in treatment protocols or differences in additional cooperating genetic aberrations. *TLX3* positive T-ALL patients are recognized as a single cluster in gene expression profiling studies[17,22]. However, the link towards T-cell differentiation is inconclusive. Some *TLX3* positive cases are restricted to the γδ lineage, while others have an immature immunophenotype[41]. However, these patients never show a mature immunophenotype from the αβ lineage[41].

The *HOXA* T-ALL subgroup

In a previous micro-array study[17], 3 different molecular-cytogenetic abnormalities tightly clustered into a T-ALL subgroup sharing an expression profile that was characterized by elevated expression levels of members of the ***HOXA*** gene cluster. This subgroup of patients was characterized by *CALM-AF10* translocations, *MLL*-rearrangements or inversions on chromosome 7, i.e. the inv(7)(p15q35)[17].

The chromosomal inversion **inv(7)(p15q35)** has been observed in about 3% of T-ALL cases[17,48]. This inversion results in the relocation of the ***HOXA*** gene cluster in the vicinity of the *TCR*β locus enhancer, possibly boosting expression of the entire *HOXA* gene cluster. These cases show a mature immunophenotype that can originate from both αβ or γδ lineage[17,18].

The ***CALM-AF10*** fusion gene is caused by a recurrent translocation, t(10;11)(p13;q14), which is found in both T-ALL and AML patients[49]. This observation is in line with murine studies in which retroviral *CALM-AF10* expression induced leukemias showing both myeloid and lymphoid characteristics[50]. The *CALM-AF10* fusion is detected in about 10% of childhood T-ALL and has been associated with poor prognosis[41,51]. All of these patients have an immature or γδ-positive T-cell immunophenotype[51]. *HOXA* gene activation by *CALM-AF10* depends on the recruitment of the histone H3 methyltransferase hDOT1L by the AF10 motion[52]. hDOT1L was shown to be a crucial factor for cellular transformation that prevents nuclear export of CALM-AF10 and activates *HOXA5* expression through specific histone H3 methylation on residue K79[52].

Rearrangements of the ***MLL*** gene, situated on chromosome 11q23, are frequently identified in infant ALL and AML[53]. *MLL* fusions are only detected in a small subset (<1%) of pediatric T-ALL[54] and are associated with maturation arrest at a γδ-positive differentiation stage[55]. The expression profile of *MLL* rearranged T-ALL also shows activation of the *HOXA* cluster of genes like *CALM-AF10* positive cases[55,56]. Like *CALM-AF10*, both *MLL-AF10*[57] and *MLL-ENL*[58] also interacts with the H3K79 methyltransferase hDOT1L resulting in the activation of the *HOXA* cluster.

In a recent study, we combined gene expression profiling and array-CGH analysis to identify 5 T-ALL cases with an *HOXA* gene signature that lacked *MLL*-rearrangements, *CALM-AF10* translocations and the inv(7)(p15q35). In 3 out of these 5 pediatric T-ALL

cases, a new recurrent deletion, the del(9)(q34.11q34.13), was identified resulting in a conserved **SET-NUP214** fusion product[20]. A similar fusion product was previously described for a single acute undifferentiated leukemia patient having a reciprocal translocation t(9;9)(q34;q34)[59] and more recently in a single case of AML[60]. SET-NUP214 functions as a transcription co-factor that binds in the promoter regions of specific *HOXA* genes, i.e. *HOXA9* and *HOXA10*, where it interacts with CRM1 and the H3K79 methyltransferase hDOT1L. Methylation of the histone H3 backbone is accompanied by histone H3 acetylation in the promoter regions of all *HOXA* gene members as identified in the *SET-NUP214* positive cell line LOUCY. This possibly results in an "open state" chromatin structure that allows binding of other transcription regulators and eventually leads to the activation of the entire *HOXA* gene cluster. In our study[20], 2 additional T-ALL cases with a *HOXA* gene signature that lack any of the *HOXA* related rearrangements, as mentioned, above were identified, indicating that other *HOXA* activating mechanisms await identification in T-ALL.

From a therapeutic point of view, the recruitment of hDOT1L by SET-NUP214 is of particular interest since this methyltransferase has previously been implicated in *HOXA* activation by *CALM-AF10, MLL-AF10* and *MLL-ENL* mediated leukemias (see above). Since hDOT1L seems to be the common factor in the leukemogenic *HOXA* activation for these different fusion genes, further research could focus on the potential of hDOT1L as a therapeutic target in the treatment of *SET-NUP214, MLL-AF10, MLL-ENL* and *CALM-AF10* mediated leukemias.

The *MYB* T-ALL subgroup

The t(6;7)(q23;q34) was recently identified as a novel recurrent translocation in T-ALL that results in the activation of the ***MYB*** oncogene through rearrangement with the *TCR*β locus[15]. This *MYB* translocation was predominantly identified in very young children and may define a new and unique T-ALL subgroup based upon gene expression profiling. At this point, it is unclear at which stage of T-cell development these *MYB* translocated cases become arrested[15].

2. Shared genetic abnormalities among T-ALL subgroups: Type B abnormalities.

Various genetic abnormalities that have been identified in T-ALL are found in all major T-ALL subgroups. These abnormalities will be denoted as type B abnormalities, and affect genes that are involved in cell cycle (type B1 mutations), self-renewal (type B2 mutations), TCR signaling pathway (type B3 mutations), T-cell differentiation

(type B4 mutations) or lead to the activation of tyrosine kinases (type B5 mutations) (table 1).

Genetic abnormalities affecting the cell cycle (type B1 mutations)

The cell cycle is a tightly regulated process, in which a number of checkpoints control the coordination between cell growth, cell division and differentiation (as reviewed in[61]). Major regulators of the cell cycle are summarized in figure 2.

Homozygous or heterozygous inactivation of the genomic ***CDKN2A*** and ***CDKN2B*** loci, that are located in tandem at chromosome 9p21, is the most frequent genetic abnormality identified in T-ALL[62]. In up to 90% of cases, the *CDKN2A/2B* loci are inactivated through cryptic deletions, promoter hypermethylation, inactivating mutations or (post)-transcriptional modifications[63-65]. The *CDKN2A* and *CDKN2B* loci encode for **p16** and **p15**, respectively, and act as inhibitors of the cyclinD/cyclin-dependent kinase CDK4 proteins (INK4). The *CDKN2A* locus also encodes for the alternative **p14ARF** product which is a negative regulator of HDM2 as part of the p53-regulatory circuitry. Therefore, deletion of *CDKN2A* and *CDKN2B* not only promotes uncontrolled cell cycle entry, but also disables the p53-controlled cell cycle checkpoint and apoptosis machinery. *CDKN2A* and *CDKN2B* deletions are not restricted to T-cell leukemia but reflect a general mechanism in cancer.

Apart from inactivation of cell cycle regulators, overexpression of cyclins may similarly promote uncontrolled cell cycle entry. In the translocation, t(7;12)(q34;p13), as identified in a number of childhood T-ALL cases, the ***cyclin D2*** gene is positioned in the vincinity of the *TCR*β locus resulting in ectopic *cyclin D2* levels[66]. Since some of these patients also demonstrated homozygous loss of *CDKN2A/CDKN2B* of cell cycle may synergize on multiple levels in the leukemic conversion of a cell.

Activation of the *NOTCH1* pathway (type B2 mutations)

NOTCH1 is a transmembrane receptor that plays a major role in normal hematopoiesis as an early transcription factor and regulates self-renewal of stem-cells and lineage commitment of lymphoid progenitor cells towards T-cell development[67]. Inactivation of NOTCH1 signaling in lymphoid progenitor cells in mice results in almost exclusive B-cell development at the expense of T-cells[68-70]. In the reciprocal setting, constitutive activation of NOTCH1 inhibits B-cell development and promotes extrathymic T-cell development[71,72].

NOTCH1 is synthesized as a single precursor protein (pre-NOTCH) which requires a proteolytic cleavage step resulting in an extracellular subunit that dimerizes to the transmembrane/intracellular subunit of NOTCH1. Upon binding of ligands, NOTCH1 undergoes several successive proteolytic cleavages leading to the release of intracellular NOTCH (ICN)[68]. ICN is transported to the nucleus where it mediates

the expression of various target genes including *HES1*, *HEY1*, *cMYC*, *PTCRα*, *DEL-TEX1*[14,73-75] and members of the NFκB pathway[76]. At the protein level, activation of NOTCH1 can cause phosphorylation of multiple signaling proteins in the mTOR pathway, indicating that NOTCH1 may also regulate the activity of the mTOR pathway[77] .

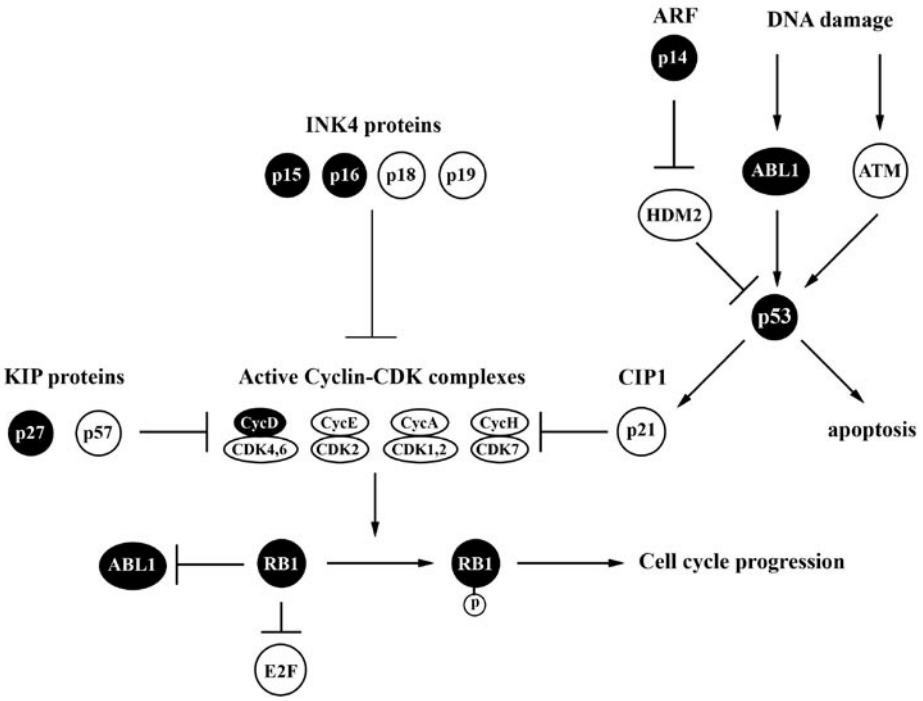

Figure 2. Schematic representation of the human cell cycle.

Mitogenic signals will initiate and activate the interaction between cyclins and cyclin-dependent kinases (CDK). These cyclin-CDK complexes cause phosphorylation of RB1 after which RB1 is unable to bind and repress the E2F transcription factors[113] and the ABL1 tyrosine kinase[170]. Initiation of E2F will relieve the G0/G1 cell cycle arrest, whereas release of ABL1 will restore the its ability to react at DNA damage in the cell[170,171]. The INK4 proteins, p15, p16, p18 and p19, the KIP proteins, p27 and p57, and the CIP1/p21 protein, all inhibit the activity of these cyclin-CDK complexes and therefore keep the cells in an inactive state. Upon detection of cellular DNA damage, activation of ATM will cooperate with activated ABL1 tyrosine kinase in upregulating expression of the *p53* tumor suppressor gene[110,172]. Next, p53 will initiate transcriptional activation of *CDKN1A*, which encodes p21. This CDK inhibitor will cause cell cycle arrest allowing DNA repair or apoptosis in case of irreversible DNA damage. The activity of p53 is regulated by HDM2, which mediates its degradation, whereas the ARF protein, p14, inhibits HDM2 activity[112].

Proteins that are targeted by genetic defects and therefore have potential roles in the development of T-ALL are depicted in black. This overview is based upon the Kyoto Encyclopedia of Genes and Genomes (Kegg Pathway database).

A specific role for ***NOTCH1*** in human T-ALL was previously postulated due to its involvement in the rare chromosomal translocation, t(7;9)(q34;q34.3), coupling the intracellular part of *NOTCH1* to the T-cell receptor-β locus[78]. Activating *NOTCH1* mutations have now been identified in more than 50% of T-ALL samples resulting in constitutive NOTCH signaling[79]. ***NOTCH1*** mutations affect the heterodimerization (HD) domain and the C-terminal PEST domain. It was postulated that point mutations in the HD domain enhance the accessibility for proteolytic cleavage by gamma-secretase leading to ligand independent cleavage of NOTCH1 and release of ICN. Truncating mutations, as predominantly identified in the PEST domain, result in the removal of so-called Cdc phosphodegron domains (CPDs), which are normally involved in the degradation of ICN by the proteasome-complex. PEST domain mutations therefore lead to the stabilization of ICN. One of the proteins that binds to CPDs, thereby priming ICN for degradation, is the F-box protein FBXW7. FBXW7 is an E3-ubiquitin ligase that also regulates the half-life of other proteins including CyclinE, cMYC and cJUN. About 20% of T-ALL patients harbor mutations in both the HD and PEST domain of NOTCH1[79]. In one study, the presence of activating *NOTCH1* mutations has been associated with a favorable early treatment response[80].

Great interest exists in the inhibition of NOTCH1 signaling by gamma-secretase inhibitors (GSIs) as a potential therapeutic strategy in T-ALL. These small molecules interfere with the proteolytic cleavage of the receptor, inhibiting the release of ICN to the nucleus. GSIs induce growth arrest in some T-ALL cell lines and cause prolonged cell cycle arrest and apoptosis in primary T-ALL cells[79,81]. Unfortunately, a clinical trial using GSI-based therapies in T-ALL has thus far been unsuccessful due to limited toxicity on leukemic blasts *in vivo* and the emergence of serious side effects like severe gastrointestinal toxicity[82-84].

In a number of T-ALL cell lines, sustained ICN levels were detected upon GSI treatment, indicating that these cell lines posses a mechanism of GSI resistance[79]. In addition, some T-ALL patients show activation of the NOTCH1 pathway in the absence of NOTCH1 mutations. From these data it was hypothesized that other mechanisms for NOTCH1 activation/stabilization should exist in human T-ALL. Indeed, some of the GSI resistant T-cell lines demonstrated inactivating mutations in ***FBXW7***[85-88]. Heterozygous *FBXW7* point mutations were also identified in 8-30% of T-ALL patients, and can occur in combination with *NOTCH1* HD mutations. In that case, *FBXW7* inactivation may complement the weak transcriptional activation of *NOTCH1* HD mutations[87]. In contrast, *FBXW7* mutations have not been observed in combination with PEST mutations[85-88], indicating that *NOTCH1* PEST mutations may relieve the mutational pressure of the *FBXW7* gene[87]. *FBXW7* mutations render FBXW7 inactive to prime target proteins including NOTCH1 for proteosomal degradation. *FBXW7* mutations therefore represent an alternative mechanism for NOTCH1

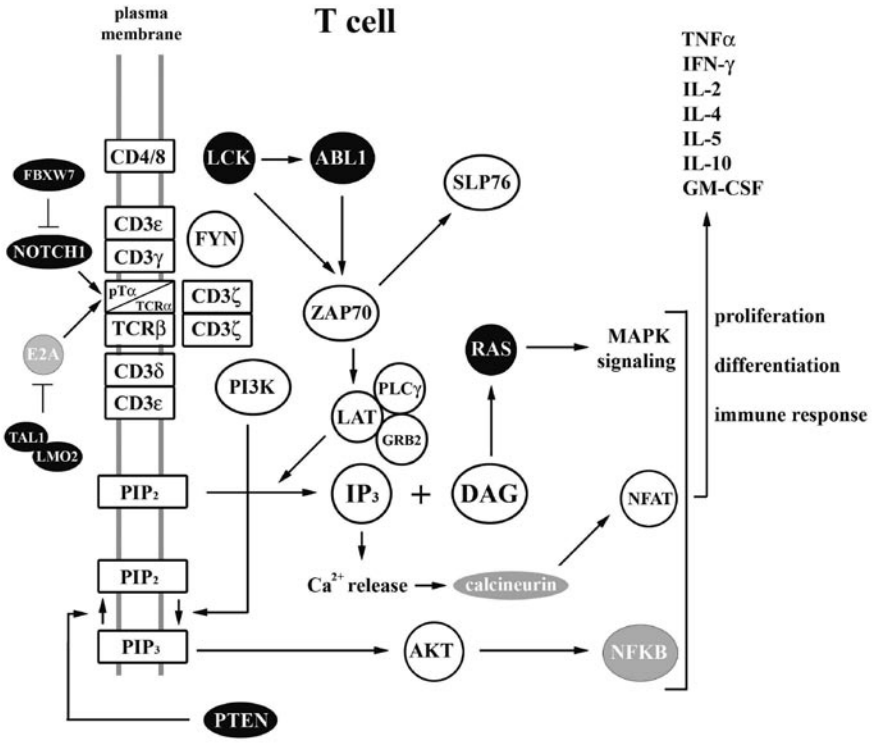

Figure 3. Schematic representation of the (pre)-T-Cell Receptor signaling pathway.
After antigen stimulating of the TCR-CD3 complex, the SCR proteins, LCK and FYN, are activated. These tyrosine kinases catalyze phosphorylation of tyrosine residues in the immunoreceptor tyrosine based activation motifs (ITAM) of the TCR-CD3 complex leading to recruitment of ZAP70 and PI3K[173]. Besides direct activation through LCK, ZAP70 can also be triggered indirectly by ABL1[104,105]. Activated ZAP70 subsequently phosphorylates SLP76 and LAT, after which LAT interacts with PLCγ1 to hydrolyse PIP_2 into DAG and IP_3[174]. IP_3 induces the release of intracellular Ca^{2+}, which initiates calcineurin phosphatase activity. Active calcineurin dephosphorylates NFAT resulting in the translocation of NFAT to the nucleus[175]. Activated DAG will interact with PKC (not shown) to activate RAS, which will lead to ERK (not shown) activation and increased MAPK signaling[176]. PI3K is the other kinase (besides ZAP70) that is recruited through the TCR-CD3 complex. PI3K induces phosphorylation of PIP_2 to PIP_3, which cause activation of AKT and eventually lead to activation of the NFKB pathway[177]. PTEN has the exact opposite function of PI3K as it dephosphorylates PIP_3 into PIP_2[178]. Finally, nuclear NFAT will cooperate with activated RAS/MAPK and NFKB signaling to trigger the activation of multiple transcription factors, which will eventually lead to T-cell proliferation, differentiation, or the induction of a T-cell immune response.
Proteins that are targeted by genetic defects and therefore have potential roles in the development of T-ALL are depicted in black. Since the NFKB pathway is deregulated indirectly (through NOTCH1[76] or TAL1[179]) in T-ALL, it is depicted in grey. Proteins that are targeted by genetic defects and therefore have potential roles in the development of T-ALL are depicted in black. Interplay between pathways that are deregulated in T-ALL pathogenesis is shown on the left panel of the figure. Both NOTCH1 and E2A regulate the expression of the *preTCRα* gene. The NOTCH pathway can be activated through *NOTCH1* or *FBXW7* mutations, whereas E2A is inhibited through TAL or LMO activation. This overview is based upon the Kyoto Encyclopedia of Genes and Genomes (Kegg Pathway database).

activation in T-ALL. The combined presence of *FBXW7* and *NOTCH1* mutations has been associated with good treatment response in T-ALL patients[86].

Subclonal duplications of the chromosomal region 9q34, which includes *NOTCH1*, are present in about 30% of pediatric T-ALL patients[8]. Although there is no clear relationship between the presence of *NOTCH1* mutations and this 9q34 abnormality, duplication of this genomic region could induce subtle changes in *NOTCH1* gene expression levels and contribute to global *NOTCH1* activation in T-ALL.

Genetic defects in the (pre)TCR signaling pathway (type B3 mutations)

In normal T-cell development, various checkpoints warrant for a proper selection of T-cells with high affinity for foreign antigens without specificity for self-antigens (reviewed in[89]). One such important checkpoint is the β-selection which depends on signals generated through a primitive TCR complex, i.e. the preTCR complex. This complex consists of a rearranged TCRβ-chain, a surrogate TCRα chain called pre-Tα (pTα) and CD3 accessory molecules. Signals generated through this complex lead to the activation of a cascade of signaling molecules and eventually lead to the downstream activation of the RAS-MAPK pathway, the PI3K-AKT pathway, the PLCγ-calcineurin-NFAT pathway and others (reviewed in[90,91]; figure 3). Multiple components of the (pre)TCR signaling pathway are targeted by either mutations or chromosomal rearrangements in T-ALL indicating that the (pre)TCR pathway or downstream components play an important role in T-cell leukemogenesis.

LCK is a member of the SRC family of tyrosine kinases which is highly expressed in T-cells and plays a central role in the initiating events of (pre)TCR signaling[92] (figure 3). In a few T-ALL cases, a translocation, t(1;7)(p34;q34), has been described causing ectopic *LCK* expression through rearrangement with the *TCR*β locus[93].

The **RAS** protein is involved in the transmission of TCR signaling from the membrane receptor molecules to the ERK protein. However, RAS is also involved in a variety of other signal transduction pathways and is commonly mutated in a wide variety of malignancies[94]. In T-ALL, activating *RAS* mutations have been identified in 4-10% of cases[95-97]. T-ALL patients with activated RAS could potentially benefit from additional treatment with RAS inhibitors like farnesylthiosalicylic acid.

The **PTEN** phosphatase has been identified as an important regulator of downstream (pre)TCR signaling, that directly opposes the activity of the phosphor-inosital-3 kinase (PI3K). PTEN dephosphorylates PIP_3 into PIP_2 thereby functioning as a negative regulator of the AKT pathway (figure 3). Independent from activation following (pre)TCR stimulation, PTEN is negatively regulated by NOTCH1[98]. Homozygous PTEN inactivation through frameshift and non-sense mutations have been found in 17% of primary T-ALL patient samples[98], and revert the sensitivity of T-ALL cell lines for GSI treatment. Inactivation of PTEN was associated with activation of the PI3K-

AKT pathway resulting in enhanced cell size, glucose uptake and proliferation[98]. Since *PTEN* mutations were also identified in relapse samples while being absent at diagnsosis, *PTEN* inactivation could represent a progression marker rather than an initiating event in T-ALL. Albeit providing resistance for NOTCH1 inhibition by GSIs, PTEN mutant T-cell lines were still sensitive for AKT inhibition, providing a rational for combined NOTCH1- and PI3K-AKT- directed therapeutic approaches in human T-ALL.

Calcineurin is a phosphatase, with an important role in (pre)TCR signaling. (Pre)TCR activation results in a calcium-dependent activation of the phosphatase 2A (PP2A/calcineurin) leading to dephosphorylation and nuclear translocation of the transcription factor NFAT. Sustained calcineurin activity has been identified in mouse models of T-cell leukemia induced by TEL-JAK2 or ICN. Interestingly, this sustained calcineurin activity was rapidly lost when cells were maintained in culture, and it was concluded that specific signals from the tumor microenvironment are required to maintain calcineurin activation. Treatment of TEL-JAK2 or ICN leukemic mice with calcineurin inhibitors restored normal hematopoiesis and induced apoptosis of leukemic cells[99]. Although these preclinical data provide a rationale to use calcineurin inhibitors as a new therapeutic strategy in T-ALL, detailed studies on primary samples are required to clarify which molecular subtypes have sustained calcineurin activity.

Additional deregulation of T-cell differentiation (type B4 mutations)

Apart from *MYB* translocations, a second type of genomic abnormality involving the ***MYB*** locus was recently identified, ie. duplications of the *MYB* oncogene, present in about 8% of T-ALL cases[15,100]. For reasons that are poorly understood, *MYB* duplications in contrast to *MYB* translocations do not represent a unique T-ALL entity, as *MYB* duplications were identified in T-ALL patients with different type A mutations[15,100]. Interestingly, functional analyses revealed that *MYB* expression is required to block differentiation in *MYB* duplicated T-ALL cell lines[100]. Since *MYB* duplications occur in combination with other genetic rearrangements that contribute to T-cell differentiation arrest (*TAL/LMO*, *TLX1*, *TLX3, HOXA)*, different genetic aberrations can cooperate in the complete deregulation of T-cell maturation in T-ALL. Combined inhibition of MYB and NOTCH1 showed strong effects on cell proliferation and viability of T-ALL cell lines, indicating that MYB could act as a novel target for therapy in T-ALL[100].

Activation of other tyrosine kinases (type B5 mutations)

In T-ALL, ***ABL1*** is involved in various molecular-cytogenetic abnormalities including the episomal ***NUP214-ABL1*** amplification that is identified in about 6% of cases,

and results in the formation of a variable number of *ABL1* gene copies[16]. Other variant *ABL1* aberrations with a very low incidence have been identified in T-ALL, including the gene fusions ***ETV6-ABL1***, ***EML1-ABL1*** and ***BCR-ABL1***[101,102]. For most T-ALL patient samples, *NUP214-ABL1* is only detected in a limited percentage of leukemic cells, indicating that it may represent a relatively late genetic event in T-ALL that probably reflects a progression marker. The various *ABL1* fusion products are constitutively phosphorylated and lead to an aberrant tyrosine kinase activation and excessive proliferation. This constitutive ABL1 activation can be reverted by imatinib, a tyrosine kinase inhibitor, and these patients may therefore benefit from additional imatinib treatment[103]. Apart from a role in the DNA damage response pathway, ABL1 also acts in the (pre)TCR signaling cascade[104,105] (figure 3). Therefore, genetic *ABL1* rearrangements could also lead to the deregulation of (pre)TCR signaling in T-ALL.

JAK2 encodes for the Janus tyrosine kinase 2, which is involved in cytokine signaling. The ***ETV6-JAK2*** fusion gene was identified in a t(9;12)(p24;p13) positive T-ALL patient, resulting in constitutive tyrosine kinase activity[106]. The leukemogenic role of this fusion protein was subsequently shown in an ETV6-JAK2 mouse model, which developed T-cell leukemias with high penetrance[107].

Activating mutations in the ***FLT3*** gene are the most common genetic aberration in AML. Internal tandem duplications in the juxtamembrane domain or point mutations in the activation loop of the tyrosine kinase domain lead to a constitutive activated state of the FLT3 tyrosine kinase. In T-ALL, *FLT3* mutations are rare and, in some patients, only present in leukemic subclones[108,109] indicating that *FLT3* mutations may represent a T-ALL progression marker rather than an initiating event.

3. Genome-wide copy number analysis of 107 pediatric T-ALL patients in relation to T-ALL subgroups

During the last years, large-scale genome-wide screening techniques including array-CGH and SNP-arrays have evolved rapidly in terms of quality and resolution. Recent studies, mainly focusing on B-ALL patients, confirmed that such a SNP-array based, high resolution genomic screening approach provides valuable information on new genes that may play important roles during the pathogenesis of leukemia[6,7,10]. Array-CGH analysis of T-ALL patients have proved successful over the last years, and led to the identification of various new abnormalities including the del(11)(p12p13) leading to *LMO2* activation[9] and the del(9)(q34.11q34.13) resulting in the *SET-NUP214* fusion gene[20] that are part of *TAL/LMO* and *HOXA* subgroups, respectively. Also, other abnormalities have been identified that are shared by various T-ALL subgroups including the duplication of *MYB*[15,100] and duplication of 9q34[8].

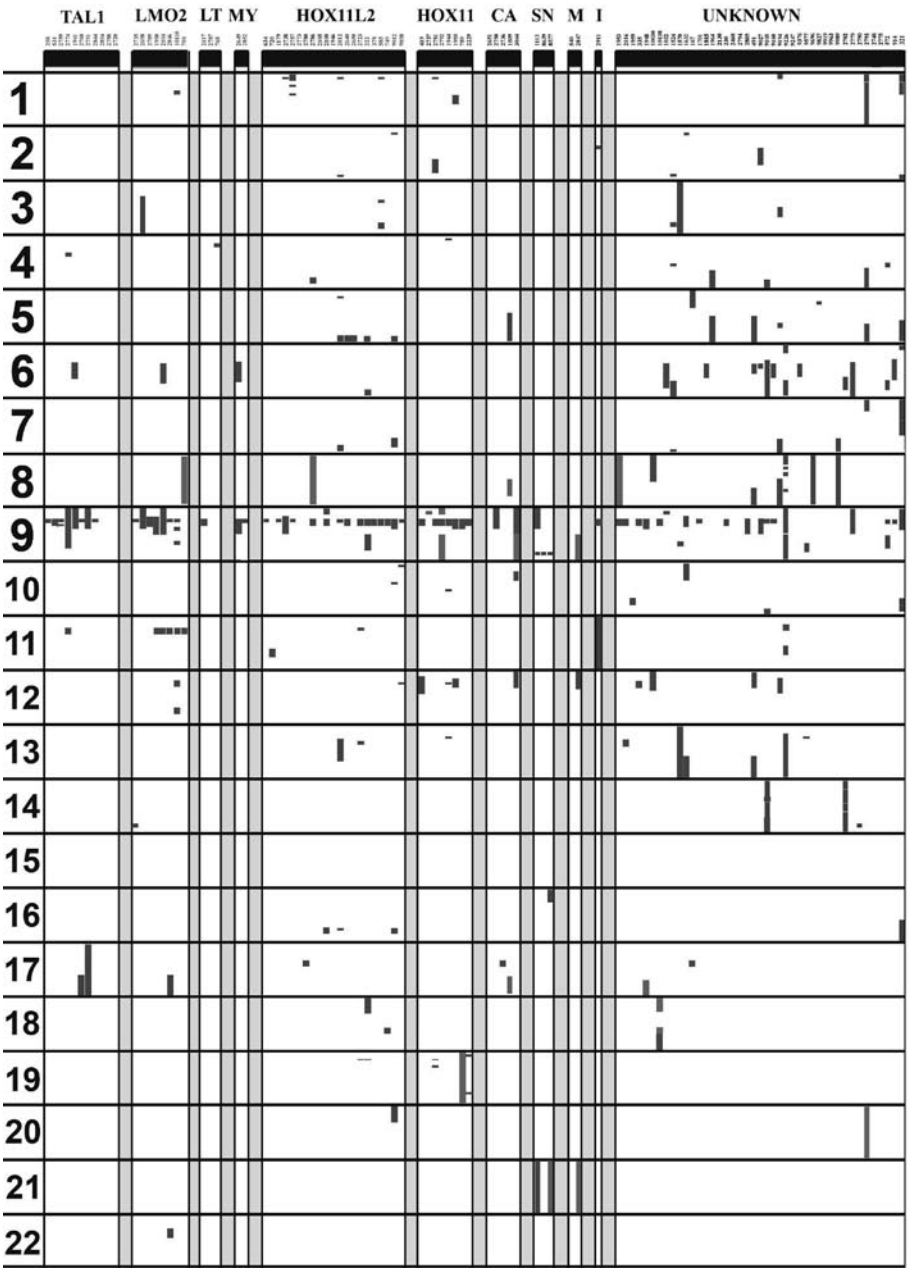

Figure 4. Genome-wide copy number analysis of 107 pediatric T-ALL patients in relation to T-ALL subgroups.

Overview of array-CGH data on 107 genetically well-characterized T-ALL patients including *TAL1* (n=11), *LMO2* (n=8), *LMO1/TAL2* (n=3), *MYC* (n=2), *TLX3* (n=21), *TLX1* (n=8), *CALM-AF10* (n=5), *SET-NUP214* (n=3), *MLL* (n=2), inv(7) (n=1) and unknown (=43) cases. Deletions are visualized in red, whereas amplifications are shown in blue.

Table 2. Novel recurrent genetic lesions in pediatric T-ALL

Chromosome Band	Gain Loss	Start (Mb)	End (Mb)	Size (Mb)	Cases # (%)	Subgroup(s)	Gene(s) in region
1p36.31	Loss	5.95	7.21	1.26	7 (7)	TLX1/TLX3/Unkn	***HES2, HES3,CDH5, CAMTA1 and TNFRFS25***
1p31.3-1p34.2	Gain	39.40	64.01	24.61	2 (2)	Unkn	> 100 genes
2p23.3-2p24.1	Loss	20.50	24.50	4.00	2 (2)	TLX3/Unkn	***NCOA1***
2q37.1	Loss	233.30	234.45	1.15	3 (3)	TLX3/Unkn	10 genes
3q13.32-3q21.2	Loss	119.90	126.40	6.50	2 (2)	LMO2/ TLX3	***miR-198***
3q26.2-3q26.31	Loss	172.10	176.40	4.30	3 (3)	LMO2/ TLX3/Unkn	***miR-569***
4q23-4q24	Loss	100.25	103.90	3.65	2 (2)	Unkn	***NFKB1***
4q26-4qter	Gain	148.73	180.90	32.17	3 (3)	Unkn	>100 genes, ***miR-578***
5q35.2-5qter	Loss	172.60	180.90	8.30	5 (5)	TLX3	> 50 genes, ***miR-340***
5q31.1-5q31.1	Loss	132.40	134.85	2.45	6 (6)	Unkn/ CA	16 genes including ***TCF7***
6q14.1-6q15	Loss	76.50	88.40	11.90	12 (11)	Unkn/ TAL1/ LMO2/MYC	> 30 genes
6q16.1-6q22.1	Loss	94.10	114.20	20.10	7 (7)	Unkn/ TAL1/ LMO2/MYC	> 50 genes
6q22.1-6q24.4	Gain	113.74	149.11	35.37	3 (3)	Unkn	> 100 genes, including ***MYB***
7q34-7q36.3	L/G	141.81	158.82	17.01	2 (2)	TLX3/ Unkn	Unbalanced *TCR*β rearrangements
8p12-8pter	Loss	0	45.20	45.20	2 (2)	Unkn	> 100 genes

Table 2. Novel recurrent genetic lesions in pediatric T-ALL							
8q23.3-8q24.24	Gain	112.70	141.70	29.00	8 (7)	LMO2 /TLX3/ CA/ Unkn	> 100 genes, including ***cMYC***
9p22.3-9p24.1	Loss	7.50	13.90	6.40	12 (11)	TAL1/LMO2/CA SET-NUP214/Unkn	6 genes including ***PTPRD***
9p13.2-9p13.3	Loss	34.60	37.80	3.20	12 (11)	TAL1/LMO2/CA SET-NUP214/Unkn cMYC/TLX3	40 genes, including ***PAX5***
9q21.13-9q21.13	Loss	77.50	79.20	1.70	4 (4)	TAL1/TLX3/Unkn	7 genes
9q22.1-9q22.31	Gain	89.80	94.10	4.30	5 (5)	TLX1/CA/MLL/ Unkn	26 genes including ***SYK***
10q23.2-10q23.31	Loss	89.30	91.80	2.50	2 (2)	Unkn	23 genes including ***PTEN*** and ***miR-107***
11p13-11p13	Loss	32.00	33.50	1.50	2 (2)	TLX3/Unkn	10 genes including ***WT1***
11q14.1-11q22.3	Loss	83.67	107.67	24.00	2 (2)	TLX3/Unkn	< 100 genes, breakpoint in the ***ATM*** gene
12p13.1-12p13.2	Loss	12.50	13.10	0.60	11 (10)	LMO2/TLX3/TLX1 CA/MLL/Unkn	12 genes including ***CDKN1B***, ***miR-613*** and ***miR-614***
13q14.2-13q14.2	Loss	47.80	48.00	0.20	3 (3)	TLX1/Unkn	*RB1*
13q14.3-13q14.3	Loss	49.45	50.35	0.90	4 (4)	TLX3/Unkn	***miR-15/16a***
13q21.2-13qter	Gain	58.78	114.14	55.36	3 (3)	Unkn	> 100 genes, ***miRNA-17/92*** **cluster**
14q32.2-14q32.2	Loss	95.45	100.21	4.76	2 (2)	LMO2/Unkn	6 genes including ***BCL11B***

Table 2. Novel recurrent genetic lesions in pediatric T-ALL							
16q22.1-16q22.1	Loss	66.20	66.60	0.40	4 (4)	TLX3/Unkn	***CTCF***
17q23.1-17qter	Gain	59.77	78.77	19.0	5 (5)	TAL1/LMO2/CA	> 100 genes, ***miR-634 miR-635, miR-636,***
						Unkn	***miR-338, miR-657 and miR-548d***
17q11.2-17q11.2	Loss	26.20	27.40	1.20	3 (3)	TLX3/CA/Unkn	***NF1***
19p13.2-19p13.2	loss	10.75	11.90	1.15	3 (3)	TLX3/TLX1	33 genes, ***miR-199a***
20	gain	0	26.70	26.70	2 (2)	TLX3/Unkn	> 100 genes
21	gain	0	46.94	46.94	2 (2)	MLL/SET-NUP214	> 100 genes

Here, we will review our array-CGH data for 107 molecular-cytogenetically well-characterized pediatric T-ALL samples. The patient cohort consisted of samples from various T-ALL subgroups, including ***TAL/LMO*** (n=24; *TAL1* (n=11), *LMO2* (n=8), *LMO1/TAL2* (n=3), *MYC* (n=2)), ***TLX3*** (n=21), ***TLX1*** (n=8), ***HOXA*** (n=11; *CALM-AF10* (n=5), *SET-NUP214* (n=3), *MLL* (n=2) and inv(7) (n=1)). The remaining 43 patient samples lack rearrangements at any of these loci and are denoted as "unknown" cases. Recurrent genetic lesions, as observed in this patient cohort and different from those already discussed in the previous part, will be discussed with their potential genes of interest (summarized in Figure 4, Table 1 and 2). Most of the genetic abnormalities that were identified as a single case observation are not further discussed in detail.

Type B1 mutations: Deregulation of cell cycle

ATM induces a cell cycle arrest following cellular DNA damage (figure 2)[110], and genetic variants of the ATM gene have been associated with susceptibility to T-ALL[111]. In one *TLX3* and one unknown T-ALL patient, we identified a cryptic deletion on chromosome 11, del(11)(q14.1q22.3), for which the breakpoints were situated in the *ATM* gene. Therefore, rearrangements of the *ATM* gene could contribute to the deregulation of the cell cycle and response to DNA damage in T-ALL.

The ***RB1*** gene plays a crucial role in the progression through the cell cycle. Mitogenic signals that generate active cyclin-CDK complexes lead to phosphorylation of RB1 and consequently cell cycle progression (figure 2)[112-114]. In two T-ALL patients (TLX3 and unknown), large deletions of the long arm of chromosome 13, covering *RB1*, were identified. In addition, two other T-ALL cases (*TLX1* and unknown) harbored cryptic interstitial deletions targeting the *RB1* gene. Therefore, *RB1* is a potential target gene on chromosome 13 and RB1 inactivation may contribute to cell cycle deregulation in T-ALL.

p27/KIP1 is an inhibitor of cyclin-CDK complexes that functions as an important negative regulator of cell cycle. Loss of *p27/KIP1* could contribute to uncontrolled cell cycle activity. Deletions on the short arm of chromosome 12 are frequently detected in a wide range of hematological malignancies. A recent genome-wide copy number analysis showed 12p deletions in about 25% of B-ALL cases and suggested the *TEL* gene as the main target of this genomic abnormality[6]. In our T-ALL cohort, 12p deletions were identified in about 10% of cases of various T-ALL subgroups, including *LMO2* (n=1), *TLX3* (n=1), *TLX1* (n=3), *CALM-AF10* (n=1), *MLL* (n=1) and unknown (n=4). However, the minimal deleted region, which was about 600 kb in size, included the *CDKN1B* gene (encoding p27/KIP1), but not the *TEL* gene.

Type B2 mutations: Deregulation of the *NOTCH1* pathway

Apart from point mutations in the *FBXW7* gene, as described above, we identified a heterozygous and cryptic deletion on the long arm of chromosome 4, del(4)(q31.3q32.1), of about 2.5 Mb in size that included the *FBXW7* gene in a single *TLX3* T-ALL case.

Amplifications of the complete or part of the **chromosome 8** occurred in about 8% of T-ALL patients. This genetic defect was present in *LMO2* (n=1), *TLX3* (n=1), *CALM-AF10* (n=1) and unknown (n=5) patients, indicating that there is no link to a specific genetic subtype. Since *TCR*-mediated *cMYC* translocations have been described in T-ALL and *cMYC* has been shown to represent an important downstream target of activated NOTCH1[115,116], ***cMYC,*** which is present in the minimal amplified region, could be the potential target gene of these chromosome 8 amplifications. However, this genomic region contains too many genes to make a valid prediction of potential oncogene(s).

Cryptic deletions on chromosomal band **16q22.1** were identified in *TLX3* (n=3) and unknown (n=1) T-ALL cases. In AML, this genomic region is recurrently targeted by cytogenetic abnormalities including an inversion, inv(16)(p13q22), a translocation, t(16;16)(p13q22) and a deletion, del(16)(q22)[117]. The inv(16) and t(16;16) both result in a *CBFB-MYH11* fusion gene, which is associated with a more favorable prognosis[118]. In contrast, the deletion del(16)(q22) does not provide a favorable outcome and it remains to be elucidated whether *CBFB* is targeted in the 16q deletions in AML[119]. In the T-ALL patients, the minimal deleted region on 16q22.1 contained 21 genes but lacked the *CBFB* gene. One interesting candidate gene in this genomic region is ***CTCF***, which is a conserved transcriptional repressor of the *MYC* oncogene[120]. Therefore, inactivation of *CTCF* could represent an alternative mechanism for *MYC* activation in T-ALL.

Type B3 mutations: Deregulation of the (pre)TCR pathway

The **NFkB** pathway is an important regulator of cell survival and cell cycle, and deregulation of this pathway has been implicated in a variety of human cancers[121]. T-cell transformation by human T-cell leukemia virus type I involves deregulation of NF-kB signaling[122]. The NFkB pathway is one of the key transcriptional factors activated by (pre)TCR engagement, and is important for proliferation, differentiation, and survival of T-cells (figure 3)[123]. T-cell specific overexpression of *v-Rel*, a viral NFKB pathway component, leads to the development of T-cell tumors in mice[124]. Also, NFkB can synergize with transgenic Notch3 to induce T-cell lymphoma[125-127]. Recently, ***NFKB2*** was identified as one of the downstream target genes of NOTCH1, and inhibition of the *NFkB* pathway efficiently restricted tumor growth both in vitro and in vivo[128].

In our array-CGH screen, we identified a recurrent deletion on chromosome 4, ie. del(4)(q23q24), in 2 unknown T-ALL cases. The minimal deleted region was approximately 3 Mb in size and contained the ***NFKB1*** gene. These data, in combination with the previously established link between T-ALL and NFkB, provide a rational for a future mutational screening of *NFKB1* and other components of the NFkB pathway, in T-ALL.

Terminal or interstitial deletions of all or part of the long arm of chromosome 5 were present in 5 unknown T-ALL cases and a single *CALM-AF10* case. Similar deletions have been observed in about 15% of human myelodysplastic syndrome (MDS) that progressed into secondary AML[129,130], in which loss of the ***CTNNA1*** tumor suppressor gene was suggested as the prime target of these deletions[131]. The minimal deleted area of the 5q deletions in our T-ALL cohort did not comprise the *CTNNA1* gene, providing evidence for the presence of another tumor suppressor gene in this area. One of the candidate genes may be the ***TCF1/TCF7*** gene, which is a T-cell-specific transcription factor that regulates *CD3*α gene expression[132]. Therefore, *TCF1/TCF7* inactivation could potentially deregulate TCR signaling and thymocyte differentiation. In mice, *TCF1/TCF7* inactivation leads to a block in the double-positive stage of T-cell differentiation[133].

Complete **9q amplifications** were identified in 4 T-ALL patients (*TLX1, CALM-AF10, MLL* and unknown), whereas one other patient (unknown) showed a small region of **amplification** at **9q22.1-9q22.31**. This minimal amplified region contained 26 genes and included the spleen tyrosine kinase **SYK**. This protein kinase is homologous to ZAP70 and is activated upon TCR stimulation[134]. Therefore, constitutive SYK activation may lead to the constitutive activation of downstream (pre)TCR signaling cascade.

A recurrent deletion at chromosome 10, del(10)(q23.2q23.31), was identified in 2 unknown T-ALL cases and included the ***PTEN*** tumor suppressor gene[135]. The role of mutated PTEN in T-ALL has been described above.

NF1 is a negative regulator of the RAS signaling pathway[136] and therefore NF1 inactivation could act as an alternative RAS activation mechanism. We identified *NF1* micro deletions on chromosome 17 in a *TLX3* and an unknown T-ALL patient without clinical evidence for neurofibromatosis. Both patients showed truncation mutations on the remaining *NF1* allele, confirming potential NF1 inactivation as an alternative RAS activation mechanism in these T-ALL cases[137].

Loss/gain of microRNA clusters

MicroRNAs are a recently discovered class of small (~22nt) endogenously expressed translational-repressor RNAs that play key roles in many cellular pathways. Several lines of evidence suggest that microRNAs may play important roles in the pathogenesis

of human cancer[138]. Moreover, it has been suggested that for different cancer types, microRNA expression profiling can distinguish between tumor samples and their corresponding tissue of origin[139]. In our genome wide copy number analysis in T-ALL, a number of genomic deletions and/or amplifications were identified that contain known microRNA clusters. Therefore, deregulated expression of specific microRNAs could potentially contribute to development of T-cell leukemia.

As discussed in the first part of this review, deletions of the short arm of chromosome 9 are frequently detected in T-ALL. Although there is great variation between these 9p deletions, both in size as well as copy number, the main target of this deletion is thought to be the ***INK/ARF*** locus. However, this genomic region also harbors the microRNAs ***mir-491*** and ***mir-31***. Deletions of 12p that cover the ***CDKN1B*** gene were identified in about 10% of cases. Moreover, the minimal deleted area also covers the microRNAs ***miR-613*** and ***miR-614***. It would be interesting to investigate if these microRNAs are expressed during normal T-cell development, and whether alterations in their expression levels could contribute to T-ALL pathogenesis.

Deletions on chromosome 13 may target the *RB1* gene. Two other T-ALL patients (one TLX3, one unknown) defined a chromosome 13 minimal deleted region containing the ***miR-15/miR-16a*** cluster. Similar deletions were recently identified in B-ALL, indicating that these genetic defects could have a general role in the pathogenesis of ALL[6]. In CLL, inactivation of this *miR-15/miR-16a* cluster leads to BCL2 activation, providing enhanced cell survival[140]. Therefore, it would be interesting to investigate whether in T-ALL (and B-lineage ALL), BCL2 is a target of this microRNA cluster.

Large 13q amplifications were observed in 3 unknown T-ALL patients and included the miRNA cluster ***miR-17-92***, consisting of 6 different microRNAs, and the single microRNAs, ***miR-622*** and ***miR-623***. The *miR-17-92* cluster is located in a genomic region frequently amplified in human B-cell lymphomas. Enforced expression of the *miR-17-92* cluster acts together with *cMYC* to accelerate B-cell lymphoma in mice[141]. Given the clear role of *cMYC* in T-ALL (see above), over expression of the *miRNA-17-92* cluster could synergize with *cMYC* activation in the development of T-cell leukemia.

Other recurrent abnormalities in which deregulated miRNA expression could potentially contribute to T-ALL development include the deletions del(3)(q13.32q21.2) (***miR-198***), del(3)(q26.2q26.31) (***miR-569***), del(5)(q35.3) (***miR-340***), del(10)(q23.2q23.31) (***miR-107***), del(19)(p13.2p13.2) (***miR-199a***) and the amplifications, amp(4)(q26qter) (***miR-578***), amp(17)(q23.1qter) (***miR-634, miR-635, miR-636, miR-338, miR-657*** and ***miR-548d***) (table 2).

Other recurrent copy number aberrations in T-ALL

Recurrent deletions on the short arm of **chromosome 1** were identified in *TLX3* (n=4), *TLX1* (n=1) and unknown (n=2) T-ALL cases with a commonly deleted region surrounding chromosomal band 1p36. Similar 1p36 deletions were previously identified in about 30% of human neuroblastomas[142], 25% of colorectal cancer patients[143], and a variety of hematological malignancies including AML[144], CML[145] and non-Hodgkin's lymphoma[146]. In neuroblastoma and colorectal cancer, reduced expression levels of the ***CAMTA1*** gene correlated with adverse outcome, suggesting that *CAMTA1* could act as the 1p36-specifc tumor suppressor gene in these malignancies[142,143]. Another interesting target gene in this genomic region is the chromodomain helicase DNA binding domain 5 (***CHD5***) gene, which is a tumor suppressor that controls proliferation and apoptosis via the $p19^{Arf}$/p53 pathway[147]. Other potential target genes within this genomic region include ***HES2*** and ***HES3***, both of which are highly similar to *HES1,* a bHLH transcriptional repressor and known *NOTCH1* target gene[148], and ***TNFRSF25***. *TNFRSF25* is a member of the TNF-receptor family which controls lymphocyte proliferation and apoptosis[149]. Two unknown T-ALL patients showed **chromosome 1 amplification** in combination with a terminal 1p34.2 deletion next to the amplified region. In both patients, the genomic breakpoints of this deletion were situated in the ***MACF1*** gene, a cytoskeletal linker protein.

At **Chromosome 2**, the cryptic deletion, **del(2)(p23.3p24.1)**, was identified in a *TLX3* and unknown T-ALL patient. This genomic region contained the ***NCOA1*** gene which is a transcriptional coactivator highly homologous to *NCOA2* and *NCOA3*. Both *NCOA2* and *NCOA3* are involved in chromosomal rearrangements in AML, i.e. the inv(8)(p11q13)[150] and the t(8;20)(p11;q13)[151].

In an *LMO2* rearranged T-ALL patient, the complete long arm of **chromosome 3** was deleted, whereas a *TLX3* positive case showed 2 smaller 3q deletions, ie. **del(3)(q13.32q21.2)** and **del(3)(q26.2q26.31).** A third T-ALL patient (unknown) only had a del(3)(q26.2q26.31). We suggest that especially the common deleted 3q26.2-q26.31 area may contain an important tumor suppressor gene. The *EVII* gene that is situated on 3q26 and frequently targeted by chromosomal 3q rearrangements in AML was not present in the minimal deletion region for 3q deletions in T-ALL.

Amplifications of the long arm of **chromosome 4** were identified in 3 unknown T-ALL patients. The common amplified region for the 3 T-ALL patients is about 32Mb in size, ranging from 4q26 until 4qter.

Our array-CGH analysis revealed small terminal **5q35 deletions** that were exclusively detected in *TLX3* rearranged cases (n=5). In 3 out of these 5 cases, the deletion starts just downstream of *TLX3*, whereas the other 2 deletions started downstream of *NKX2-5*. Whether or not these deletions occur in combination with *TLX3* transloca-

tions or that they may aberrantly activate the *TLX3* gene due to the loss of a potential negative regulating element in the 5q35 region remains to be determined.

Deletions of the long arm of **chromosome 6** are known recurrent aberrations in T-ALL for which the target gene(s) remain(s) to be identified[152]. In our large-scale copy number analysis, 6q deletions (n=13) were identified in different T-ALL subgroups (TAL1 (n=1), LMO2 (n=1), cMYC (n=1)) but especially in the unknown patients (n=10). Strikingly, no 6q deletions in any of the *HOX* rearranged (including *TLX1*, *TLX3*, *HOXA*) T-ALL cases were identified, indicating that this potential tumor suppressor gene on 6q does not cooperate with *TLX1*, *TLX3* or *HOXA* oncogenes in the malignant transformation of thymocytes. In addition, the search for potential tumor suppressor genes on 6q could be hampered by the fact that 2 different minimal deleted areas seem to be present, at 6q14 and at 6q16-q21, respectively. Both domains contain multiple potential tumor suppressor genes. Large **6q amplifications** were identified in 3 unknown T-ALL cases. The minimal amplified region included the ***MYB*** oncogene. Since *MYB* duplications were recently identified in T-ALL[15,100], *MYB* is a likely target of these large 6q amplifications in T-ALL. Nevertheless, upregulation of other genes in this genomic region could also contribute to T-cell leukemogenesis.

Recurrent amplifications/deletions at **chromosome 7** were present in or near the *TCR*β locus at 7q35 and therefore probably reflect unbalanced *TCR*β translocations or rearrangements of the normal *TCR*β gene.

As discussed in the first part of this review, **9p deletions** are frequently detected in T-ALL with the *CDKN2A/CDKN2B* locus as the principle target. In our array-CGH screening, we identified one T-ALL patient with a different 9p deletion, **del(9)(p22.3p24.1)**, which included the protein tyrosine phosphatase receptor type D (*PTPRD*) gene. ***PTPRD*** has been suggested as a potential tumor suppressor gene in lung carcinoma, cutaneous squamous cell carcinomas and neuroblastoma due to recurrent homozygous *PTPRD* deletions[153-156]. Although this particular deletion was only present in a single T-ALL case, 11 other T-ALL patients showed larger 9p deletions including both the *PTPRD* and the *CDKN2A/CDKN2B* locus. Similarly, one T-ALL patient showed a 9p deletion, **del(9)(p13.2p13.3)** that included the ***PAX5*** gene, which was recently shown to be recurrently deleted in B-ALL[6]. Larger 9p deletions including both *PAX5* and the *CDKN2A/CDKN2B* locus were present in 11 other T-ALL patients. Four T-ALL patients showed variable **9q deletions** with a minimal deleted region surrounding the chromosomal region **9q21.13** that covered 7 genes that have previously not been associated with malignant transformation.

A recurrent deletion, **del(11)(p13p14.1)**, was identified in a *TLX3* and an unknown T-ALL case that included the ***WT1*** gene. In one patient, we demonstrated that the remaining *WT1* gene was also lost due to the presence of a smaller del(11)

(p13p13) deletion on the second chromosome 11, suggesting that *WT1* may represent the prime target of these deletions. This was further strengthened by the presence of a non-sense mutation in the remaining *WT1* allele of the second patient leading to truncation of WT1. WT1 is a transcription factor involved in normal cellular development and cell survival and was initially discovered as a tumor suppressor in Wilms' Tumor[157]. There is some controversy on the exact role of *WT1* since there are reports suggesting both an oncogene[158] as well as a tumor suppressor role[159] for WT1 in acute leukemias.

Large **13q amplifications** were identified in 3 unknown T-ALL patients. Trisomy 13 is a recurrent chromosomal abnormality in a small subset of acute leukemias. Previously, *FLT1* and *RB1* have been suggested as potential target genes for trisomy 13 in acute leukemia, but these genes were not present in the common amplified region in our T-ALL cases. Although specific miRNAs could be the target of these amplifications (see above), the common amplified region contains a large portion of genes which also could contribute to malignant transformation.

Two T-ALL patients (*LMO2* and unknown) showed a similar deletion, **del(14)(q32.2)**, on **chromosome 14**. ***BCL11B***, which is involved in the pathogenesis of T-ALL through an inv(14)(q11q32)[160], could be the potential target of this deletion.

Besides the *NF1* microdeletions, which were recently described in T-ALL, B-ALL and AML[6,138], the main genetic lesions on chromosome 17 were large **17q amplifications**, which were detected in *TAL1* (n=2), *LMO2* (n=1), *CALM-AF10* (n=1) and unknown (n=1) T-ALL cases. The 17q gain is the most common chromosomal abberation in neuroblastoma, and is associated with a poor outcome[161,162]. The target genes for these 17q amplifications in neuroblastoma remain to be elucidated, but the general idea is that increased dosage of a number of genes may confer a growth advantage to the tumour cells. Similarly, given the large common amplified region in T-ALL, the oncogene(s) that contribute to T-ALL pathogenesis remain to be elucidated.

A recurrent deletion, **del(19)(p13.2p13.2)**, was identified in *TLX3* (n=2) and *TLX1* (n=1) T-ALL patients. The minimal deleted region is about 1.2 Mb in size, but none of the genes situated in this chromosomal region have been previously linked to any form of cancer.

Finally, **amplification** of the complete or short arm of **chromosome 20** was identified in a *TLX3* and unknown T-ALL patients, whereas **trisomy 21** was observed in an *MLL* and *SET-NUP214* positive case. Down's syndrome has been associated with an increased risk of developing acute leukemia[163]. However, it remains unclear which genes on chromosome 21 truly contribute to the leukemic transformation process.

4. CONCLUSIONS

T-ALL is an aggressive T-cell malignancy with an inferior treatment outcome compared to B-lineage ALL. Currently and in contrast to B-lineage ALL, genetic abnormalities are clinically not used for therapy stratification. However, upon reviewing the genetics of T-ALL, it becomes clear that different combinations of a large variety of genetic defects may lead to common types of T-cell ALL. Despite the diversity in genetic rearrangements, the biological processes that are targeted seem conserved throughout all T-ALL cases, i.e. T-cell differentiation, T-cell receptor signaling and cell cycling. The cooperative deregulation of all these processes will lead to the transformation of a normal thymocyte into a leukemic T-cell.

Gene expression profiling and array CGH contributed to the classification of T-ALL patients into unique subgroups. Type A genetic abnormalities that determine the T-ALL subgroups are mutually exclusive and are thought to cause arrest at a specific stage of normal T-cell differentiation. Type B genetic abnormalities, in contrast, are shared by several T-ALL subgroups and target cellular processes including the cell cycle, the *NOTCH1* pathway and TCR signaling.

Although great improvement has been made in the elucidation of novel genetic defects that contribute to T-ALL pathogenesis, numerous questions remain unanswered. Which pathways are used in T-ALL cells that are independent of activated NOTCH1 signaling? Or alternatively, which other mechanisms, besides *NOTCH1* and *FBXW7* mutations, are present in T-ALL to activate the NOTCH1 pathway. Therefore, it would be interesting to screen a large cohort of T-ALL samples, and determine the exact percentage of patients that have sustained protein levels of activated ICN, irrespective of their *NOTCH1* activation mechanism. In a recent mouse study, over expression of β-catenin as one of the key players in the WNT-signaling cascade induced T-cell leukemias that did not depend on NOTCH1 signaling[164]. Therefore, the WNT signaling cascade may act as an attractive target in T-ALL patients that do not depend on activated NOTCH1 signaling.

For *TAL/LMO* driven T-cell leukemias, E2A and NOTCH1, which execute opposite functions during the β-selection checkpoint of normal T-cell development, seem to represent the most predominant oncogenic targets. Aberrant expression of *TAL/LMO* family members will induce E2A inhibition, whereas activation of the NOTCH1 pathway may enforce a pre-TCR dependent relieve of cell cycle arrest and enable proliferation. So for these types of T-ALL patients, inactivation of E2A and activation of NOTCH1, in combination with a functional (pre)-TCR complex, could reflect essential processes that synergize in the pathogenesis of T-ALL.

In contrast to the data present on the role of *TAL/LMO* family members in T-ALL, the oncogenic mechanism behind *HOX* driven T-cell leukemias remains largely

unknown. Especially the molecular mechanisms by which deregulated *TLX1*, *TLX3* or *HOXA* expression interfere with normal T-cell differentiation remains to be elucidated. In our molecular-genetic characterization studies in pediatric T-ALL, we observed that activating tyrosine kinase mutations, mainly targeting crucial components of the (pre)-TCR signaling complex, exclusively occurred in *HOX* driven T-ALL cases and not in *TAL/LMO* rearranged cases. Therefore, it remains unclear whether *TAL/LMO* driven T-ALL truly needs activational tyrosine kinase mutations, or whether the synergy between *TAL/LMO* activation and *NOTCH1* mutations is sufficient for leukemic transformation. In contrast, 6q deletions were completely absent in any of the *HOX* rearranged T-ALL cases, suggesting that 6q specific tumor suppressor genes fail to cooperate with *HOX* mediated leukemogenesis.

In conclusion, this review on molecular-cytogenetic research in T-ALL shows that T-cell leukemia is not a single disease entity, but rather reflects a genetically diverse malignancy that targets the same cell of origin. Therefore, specific treatment modalities in which chemotherapy is combined with additional treatment based on the genetic T-ALL subtype, could lead to further treatment progress in T-cell leukemia. In addition, genome wide copy number screening is a valuable tool for the identification of new chromosomal imbalances in T-ALL and could provide further insight in the pathogenesis of T-cell leukemia. Indeed, the identification of *FBXW7* and *PTEN* deletions in our copy number screening nicely illustrates that detection of new genomic deletions/amplifications, even at low frequency, can reveal new and important genes with a broader role in T-ALL. Therefore, the new copy number changes in T-ALL described in this review offer great new challenges for the identification of new target genes that may play a role in the pathogenesis of T-ALL and may serve as new therapeutic targets.

REFERENCES

1. Pui CH, Evans WE. Treatment of acute lymphoblastic leukemia. The New England journal of medicine. 2006;354:166-178.
2. Hoffmann R, Melchers F. A genomic view of lymphocyte development. Curr Opin Immunol. 2003;15:239-245.
3. Aifantis I, Mandal M, Sawai K, Ferrando A, Vilimas T. Regulation of T-cell progenitor survival and cell-cycle entry by the pre-T-cell receptor. Immunol Rev. 2006;209:159-169.
4. Saito T, Watanabe N. Positive and negative thymocyte selection. Crit Rev Immunol. 1998;18:359-370.
5. Murre C. Intertwining proteins in thymocyte development and cancer. Nat Immunol. 2000;1:97-98.
6. Mullighan CG, Goorha S, Radtke I, et al. Genome-wide analysis of genetic alterations in acute lymphoblastic leukaemia. Nature. 2007;446:758-764.
7. Kuiper RP, Schoenmakers EF, van Reijmersdal SV, et al. High-resolution genomic profiling of childhood ALL reveals novel recurrent genetic lesions affecting pathways involved in lymphocyte differentiation and cell cycle progression. Leukemia. 2007;21:1258-1266.
8. van Vlierberghe P, Meijerink JP, Lee C, et al. A new recurrent 9q34 duplication in pediatric T-cell acute lymphoblastic leukemia. Leukemia. 2006;20:1245-1253.
9. Van Vlierberghe P, van Grotel M, Beverloo HB, et al. The cryptic chromosomal deletion del(11)(p12p13) as a new activation mechanism of LMO2 in pediatric T-cell acute lymphoblastic leukemia. Blood. 2006;108:3520-3529.
10. Kawamata N, Ogawa S, Zimmermann M, et al. Molecular allelokaryotyping of pediatric acute lymphoblastic leukemias by high resolution single nucleotide polymorphism oligonucleotide genomic microarray. 2007.
11. Armstrong SA, Look AT. Molecular genetics of acute lymphoblastic leukemia. J Clin Oncol. 2005;23:6306-6315.
12. De Keersmaecker K, Marynen P, Cools J. Genetic insights in the pathogenesis of T-cell acute lymphoblastic leukemia. Haematologica. 2005;90:1116-1127.
13. Graux C, Cools J, Michaux L, Vandenberghe P, Hagemeijer A. Cytogenetics and molecular genetics of T-cell acute lymphoblastic leukemia: from thymocyte to lymphoblast. Leukemia. 2006;20:1496-1510.
14. Grabher C, von Boehmer H, Look AT. Notch 1 activation in the molecular pathogenesis of T-cell acute lymphoblastic leukaemia. Nat Rev Cancer. 2006;6:347-359.
15. Clappier E, Cuccuini W, Kalota A, et al. The C-MYB locus is involved in chromosomal translocation and genomic duplications in human T-cell acute leukemia (T-ALL) - the translocation defining a new T-ALL subtype in very young children. Blood. 2007.
16. Graux C, Cools J, Melotte C, et al. Fusion of NUP214 to ABL1 on amplified episomes in T-cell acute lymphoblastic leukemia. Nat Genet. 2004;36:1084-1089.
17. Soulier J, Clappier E, Cayuela JM, et al. HOXA genes are included in genetic and biologic networks defining human acute T-cell leukemia (T-ALL). Blood. 2005;106:274-286.
18. Speleman F, Cauwelier B, Dastugue N, et al. A new recurrent inversion, inv(7)(p15q34), leads to transcriptional activation of HOXA10 and HOXA11 in a subset of T-cell acute lymphoblastic leukemias. Leukemia. 2005;19:358-366.

19. Bernard OA, Busson-LeConiat M, Ballerini P, et al. A new recurrent and specific cryptic translocation, t(5;14)(q35;q32), is associated with expression of the Hox11L2 gene in T acute lymphoblastic leukemia. Leukemia. 2001;15:1495-1504.

20. Van Vlierberghe P, Tchinda J, van Grotel M, et al. The recurrent SET-NUP214 fusion as a new HOXA activation mechanism in pediatric T-cell acute lymphoblastic leukemia. PLoS Medicine. 2007.

21. Xia Y, Brown L, Yang CY, et al. TAL2, a helix-loop-helix gene activated by the (7;9)(q34;q32) translocation in human T-cell leukemia. Proc Natl Acad Sci U S A. 1991;88:11416-11420.

22. Ferrando AA, Neuberg DS, Staunton J, et al. Gene expression signatures define novel oncogenic pathways in T cell acute lymphoblastic leukemia. Cancer Cell. 2002;1:75-87.

23. Jones S. An overview of the basic helix-loop-helix proteins. Genome Biol. 2004;5:226.

24. Yan W, Young AZ, Soares VC, Kelley R, Benezra R, Zhuang Y. High incidence of T-cell tumors in E2A-null mice and E2A/Id1 double-knockout mice. Mol Cell Biol. 1997;17:7317-7327.

25. Ferrando AA, Herblot S, Palomero T, et al. Biallelic transcriptional activation of oncogenic transcription factors in T-cell acute lymphoblastic leukemia. Blood. 2004;103:1909-1911.

26. Baer R. TAL1, TAL2 and LYL1: a family of basic helix-loop-helix proteins implicated in T cell acute leukaemia. Semin Cancer Biol. 1993;4:341-347.

27. Wang J, Jani-Sait SN, Escalon EA, et al. The t(14;21)(q11.2;q22) chromosomal translocation associated with T-cell acute lymphoblastic leukemia activates the BHLHB1 gene. Proc Natl Acad Sci U S A. 2000;97:3497-3502.

28. Valge-Archer VE, Osada H, Warren AJ, et al. The LIM protein RBTN2 and the basic helix-loop-helix protein TAL1 are present in a complex in erythroid cells. Proc Natl Acad Sci U S A. 1994;91:8617-8621.

29. Chervinsky DS, Zhao XF, Lam DH, Ellsworth M, Gross KW, Aplan PD. Disordered T-cell development and T-cell malignancies in SCL LMO1 double-transgenic mice: parallels with E2A-deficient mice. Mol Cell Biol. 1999;19:5025-5035.

30. Herblot S, Steff AM, Hugo P, Aplan PD, Hoang T. SCL and LMO1 alter thymocyte differentiation: inhibition of E2A-HEB function and pre-T alpha chain expression. Nat Immunol. 2000;1:138-144.

31. O'Neil J, Shank J, Cusson N, Murre C, Kelliher M. TAL1/SCL induces leukemia by inhibiting the transcriptional activity of E47/HEB. Cancer Cell. 2004;5:587-596.

32. Bain G, Engel I, Robanus Maandag EC, et al. E2A deficiency leads to abnormalities in alphabeta T-cell development and to rapid development of T-cell lymphomas. Mol Cell Biol. 1997;17:4782-4791.

33. Sanchez-Garcia I, Rabbitts TH. LIM domain proteins in leukaemia and development. Semin Cancer Biol. 1993;4:349-358.

34. Dik WA, Nadel B, Przybylski GK, et al. Different chromosomal breakpoints impact the level of LMO2 expression in T-ALL. Blood. 2007;110:388-392.

35. Hatano M, Roberts CW, Minden M, Crist WM, Korsmeyer SJ. Deregulation of a homeobox gene, HOX11, by the t(10;14) in T cell leukemia. Science. 1991;253:79-82.

36. Owens BM, Hawley TS, Spain LM, Kerkel KA, Hawley RG. TLX1/HOX11-mediated disruption of primary thymocyte differentiation prior to the CD4+CD8+ double-positive stage. Br J Haematol. 2006;132:216-229.

37. Ferrando AA, Neuberg DS, Dodge RK, et al. Prognostic importance of TLX1 (HOX11) oncogene expression in adults with T-cell acute lymphoblastic leukaemia. Lancet. 2004;363:535-536.

38. Wuchter C, Ruppert V, Schrappe M, Dorken B, Ludwig WD, Karawajew L. In vitro susceptibility to dexamethasone- and doxorubicin-induced apoptotic cell death in context of maturation stage, responsiveness to interleukin 7, and early cytoreduction in vivo in childhood T-cell acute lymphoblastic leukemia. Blood. 2002;99:4109-4115.

39. Hawley RG, Fong AZ, Reis MD, Zhang N, Lu M, Hawley TS. Transforming function of the HOX11/TCL3 homeobox gene. Cancer Res. 1997;57:337-345.

40. Watt PM, Kumar R, Kees UR. Promoter demethylation accompanies reactivation of the HOX11 proto-oncogene in leukemia. Genes Chromosomes Cancer. 2000;29:371-377.

41. van Grotel M, Meijerink JP, Beverloo HB, et al. The outcome of molecular-cytogenetic subgroups in pediatric T-cell acute lymphoblastic leukemia: a retrospective study of patients treated according to DCOG or COALL protocols. Haematologica. 2006;91:1212-1221.

42. Bergeron J, Clappier E, Radford I, et al. Prognostic and oncogenic relevance of TLX1/HOX11 expression level in T-ALLs. Blood. 2007.

43. Mauvieux L, Leymarie V, Helias C, et al. High incidence of Hox11L2 expression in children with T-ALL. Leukemia. 2002;16:2417-2422.

44. Hansen-Hagge TE, Schafer M, Kiyoi H, et al. Disruption of the RanBP17/Hox11L2 region by recombination with the TCRdelta locus in acute lymphoblastic leukemias with t(5;14)(q34;q11). Leukemia. 2002;16:2205-2212.

45. Su XY, Busson M, Della Valle V, et al. Various types of rearrangements target TLX3 locus in T-cell acute lymphoblastic leukemia. Genes Chromosomes Cancer. 2004;41:243-249.

46. Ballerini P, Blaise A, Busson-Le Coniat M, et al. HOX11L2 expression defines a clinical subtype of pediatric T-ALL associated with poor prognosis. Blood. 2002;100:991-997.

47. Cave H, Suciu S, Preudhomme C, et al. Clinical significance of HOX11L2 expression linked to t(5;14)(q35;q32), of HOX11 expression, and of SIL-TAL fusion in childhood T-cell malignancies: results of EORTC studies 58881 and 58951. Blood. 2004;103:442-450.

48. Cauwelier B, Cave H, Gervais C, et al. Clinical, cytogenetic and molecular characteristics of 14 T-ALL patients carrying the TCRbeta-HOXA rearrangement: a study of the Groupe Francophone de Cytogenetique Hematologique. Leukemia. 2007;21:121-128.

49. Bohlander SK, Muschinsky V, Schrader K, et al. Molecular analysis of the CALM/AF10 fusion: identical rearrangements in acute myeloid leukemia, acute lymphoblastic leukemia and malignant lymphoma patients. Leukemia. 2000;14:93-99.

50. Deshpande AJ, Cusan M, Rawat VP, et al. Acute myeloid leukemia is propagated by a leukemic stem cell with lymphoid characteristics in a mouse model of CALM/AF10-positive leukemia. Cancer Cell. 2006;10:363-374.

51. Asnafi V, Radford-Weiss I, Dastugue N, et al. CALM-AF10 is a common fusion transcript in T-ALL and is specific to the TCRgammadelta lineage. Blood. 2003;102:1000-1006.

52. Okada Y, Jiang Q, Lemieux M, Jeannotte L, Su L, Zhang Y. Leukaemic transformation by CALM-AF10 involves upregulation of Hoxa5 by hDOT1L. Nat Cell Biol. 2006;8:1017-1024.

53. Armstrong SA, Staunton JE, Silverman LB, et al. MLL translocations specify a distinct gene expression profile that distinguishes a unique leukemia. Nat Genet. 2002;30:41-47.

54. Rubnitz JE, Behm FG, Curcio-Brint AM, et al. Molecular analysis of t(11;19) breakpoints in childhood acute leukemias. Blood. 1996;87:4804-4808.

55. Ferrando AA, Armstrong SA, Neuberg DS, et al. Gene expression signatures in MLL-rearranged T-lineage and B-precursor acute leukemias: dominance of HOX dysregulation. Blood. 2003;102:262-268.

56. Dik WA, Brahim W, Braun C, et al. CALM-AF10+ T-ALL expression profiles are characterized by overexpression of HOXA and BMI1 oncogenes. Leukemia. 2005;19:1948-1957.

57. Okada Y, Feng Q, Lin Y, et al. hDOT1L links histone methylation to leukemogenesis. Cell. 2005;121:167-178.

58. Mueller D, Bach C, Zeisig D, et al. A role for the MLL fusion partner ENL in transcriptional elongation and chromatin modification. 2007.

59. von Lindern M, Breems D, van Baal S, Adriaansen H, Grosveld G. Characterization of the translocation breakpoint sequences of two DEK-CAN fusion genes present in t(6;9) acute myeloid leukemia and a SET-CAN fusion gene found in a case of acute undifferentiated leukemia. Genes, chromosomes & cancer. 1992;5:227-234.

60. Rosati R, La Starza R, Barba G, et al. Cryptic chromosome 9q34 deletion generates TAF-Ialpha/CAN and TAF-Ibeta/CAN fusion transcripts in acute myeloid leukemia. Haematologica. 2007;92:232-235.

61. Nurse P. A long twentieth century of the cell cycle and beyond. Cell. 2000;100:71-78.

62. Cayuela JM, Madani A, Sanhes L, Stern MH, Sigaux F. Multiple tumor-suppressor gene 1 inactivation is the most frequent genetic alteration in T-cell acute lymphoblastic leukemia. Blood. 1996;87:2180-2186.

63. Merlo A, Herman JG, Mao L, et al. 5' CpG island methylation is associated with transcriptional silencing of the tumour suppressor p16/CDKN2/MTS1 in human cancers. Nat Med. 1995;1:686-692.

64. Herman JG, Jen J, Merlo A, Baylin SB. Hypermethylation-associated inactivation indicates a tumor suppressor role for p15INK4B. Cancer Res. 1996;56:722-727.

65. Okamoto A, Demetrick DJ, Spillare EA, et al. Mutations and altered expression of p16INK4 in human cancer. Proc Natl Acad Sci U S A. 1994;91:11045-11049.

66. Clappier E, Cuccuini W, Cayuela JM, et al. Cyclin D2 dysregulation by chromosomal translocations to TCR loci in T-cell acute lymphoblastic leukemias. Leukemia. 2006;20:82-86.

67. Sambandam A, Maillard I, Zediak VP, et al. Notch signaling controls the generation and differentiation of early T lineage progenitors. Nat Immunol. 2005;6:663-670.

68. Radtke F, Wilson A, MacDonald HR. Notch signaling in T- and B-cell development. Curr Opin Immunol. 2004;16:174-179.

69. Wilson A, MacDonald HR, Radtke F. Notch 1-deficient common lymphoid precursors adopt a B cell fate in the thymus. J Exp Med. 2001;194:1003-1012.

70. Radtke F, Ferrero I, Wilson A, Lees R, Aguet M, MacDonald HR. Notch1 deficiency dissociates the intrathymic development of dendritic cells and T cells. J Exp Med. 2000;191:1085-1094.

71. Pui JC, Allman D, Xu L, et al. Notch1 expression in early lymphopoiesis influences B versus T lineage determination. Immunity. 1999;11:299-308.

72. Schmitt TM, Zuniga-Pflucker JC. Induction of T cell development from hematopoietic progenitor cells by delta-like-1 in vitro. Immunity. 2002;17:749-756.

73. Sharma VM, Calvo JA, Draheim KM, et al. Notch1 contributes to mouse T-cell leukemia by directly inducing the expression of c-myc. Mol Cell Biol. 2006;26:8022-8031.

74. Weng AP, Millholland JM, Yashiro-Ohtani Y, et al. c-Myc is an important direct target of Notch1 in T-cell acute lymphoblastic leukemia/lymphoma. Genes Dev. 2006;20:2096-2109.

75. Palomero T, Lim WK, Odom DT, et al. NOTCH1 directly regulates c-MYC and activates a feed-forward-loop transcriptional network promoting leukemic cell growth. Proc Natl Acad Sci U S A. 2006;103:18261-18266.

76. Vilimas T, Mascarenhas J, Palomero T, et al. Targeting the NF-kappaB signaling pathway in Notch1-induced T-cell leukemia. Nat Med. 2007;13:70-77.

77. Chan SM, Weng AP, Tibshirani R, Aster JC, Utz PJ. Notch signals positively regulate activity of the mTOR pathway in T cell acute lymphoblastic leukemia. Blood. 2007.

78. Ellisen LW, Bird J, West DC, et al. TAN-1, the human homolog of the Drosophila notch gene, is broken by chromosomal translocations in T lymphoblastic neoplasms. Cell. 1991;66:649-661.

79. Weng AP, Ferrando AA, Lee W, et al. Activating mutations of NOTCH1 in human T cell acute lymphoblastic leukemia. Science. 2004;306:269-271.

80. Breit S, Stanulla M, Flohr T, et al. Activating NOTCH1 mutations predict favorable early treatment response and long-term outcome in childhood precursor T-cell lymphoblastic leukemia. Blood. 2006;108:1151-1157.

81. Lewis HD, Leveridge M, Strack PR, et al. Apoptosis in T cell acute lymphoblastic leukemia cells after cell cycle arrest induced by pharmacological inhibition of notch signaling. Chem Biol. 2007;14:209-219.

82. Milano J, McKay J, Dagenais C, et al. Modulation of notch processing by gamma-secretase inhibitors causes intestinal goblet cell metaplasia and induction of genes known to specify gut secretory lineage differentiation. Toxicol Sci. 2004;82:341-358.

83. van Es JH, van Gijn ME, Riccio O, et al. Notch/gamma-secretase inhibition turns proliferative cells in intestinal crypts and adenomas into goblet cells. Nature. 2005;435:959-963.

84. DeAngelo DJ. A phase I clinical trial of the notch inhibitor MK-0752 in patients with T-cell acute lymphoblastic leukemia (T-ALL) and other leukemias. Journal of Clinical Oncology. 2006;2006 ASCO Annual Meeting Proceedings Part I:6585.

85. Maser RS, Choudhury B, Campbell PJ, et al. Chromosomally unstable mouse tumours have genomic alterations similar to diverse human cancers. Nature. 2007.

86. Malyukova A, Dohda T, von der Lehr N, et al. The Tumor Suppressor Gene hCDC4 Is Frequently Mutated in Human T-Cell Acute Lymphoblastic Leukemia with Functional Consequences for Notch Signaling. Cancer Res. 2007;67:5611-5616.

87. Thompson BJ, Buonamici S, Sulis ML, et al. The SCFFBW7 ubiquitin ligase complex as a tumor suppressor in T cell leukemia. J Exp Med. 2007.

88. O'Neil J, Grim J, Strack P, et al. FBW7 mutations in leukemic cells mediate NOTCH pathway activation and resistance to {gamma}-secretase inhibitors. J Exp Med. 2007.

89. Kruisbeek AM, Haks MC, Carleton M, Michie AM, Zuniga-Pflucker JC, Wiest DL. Branching out to gain control: how the pre-TCR is linked to multiple functions. Immunology today. 2000;21:637-644.

90. Germain RN, Stefanova I. The dynamics of T cell receptor signaling: complex orchestration and the key roles of tempo and cooperation. Annual review of immunology. 1999;17:467-522.

91. Samelson LE, Donovan JA, Isakov N, Ota Y, Wange RL. Signal transduction mediated by the T-cell antigen receptor. Annals of the New York Academy of Sciences. 1995;766:157-172.

92. Palacios EH, Weiss A. Function of the Src-family kinases, Lck and Fyn, in T-cell development and activation. Oncogene. 2004;23:7990-8000.

93. Tycko B, Smith SD, Sklar J. Chromosomal translocations joining LCK and TCRB loci in human T cell leukemia. J Exp Med. 1991;174:867-873.

94. Campbell SL, Khosravi-Far R, Rossman KL, Clark GJ, Der CJ. Increasing complexity of Ras signaling. Oncogene. 1998;17:1395-1413.

95. Kawamura M, Ohnishi H, Guo SX, et al. Alterations of the p53, p21, p16, p15 and RAS genes in childhood T-cell acute lymphoblastic leukemia. Leuk Res. 1999;23:115-126

96. Yokota S, Nakao M, Horiike S, et al. Mutational analysis of the N-ras gene in acute lymphoblastic leukemia: a study of 125 Japanese pediatric cases. Int J Hematol. 1998;67:379-387.

97. von Lintig FC, Huvar I, Law P, Diccianni MB, Yu AL, Boss GR. Ras activation in normal white blood cells and childhood acute lymphoblastic leukemia. Clin Cancer Res. 2000;6:1804-1810.

98. Palomero T, Sulis ML, Cortina M, et al. Mutational loss of PTEN induces resistance to NOTCH1 inhibition in T-cell leukemia. Nature medicine. 2007;13:1203-1210.

99. Medyouf H, Alcalde H, Berthier C, et al. Targeting calcineurin activation as a therapeutic strategy for T-cell acute lymphoblastic leukemia. Nat Med. 2007;13:736-741.

100. Lahortiga I, De Keersmaecker K, Van Vlierberghe P, et al. Duplication of the MYB oncogene in T cell acute lymphoblastic leukemia. Nat Genet. 2007;39:593-595.

101. Van Limbergen H, Beverloo HB, van Drunen E, et al. Molecular cytogenetic and clinical findings in ETV6/ABL1-positive leukemia. Genes Chromosomes Cancer. 2001;30:274-282.

102. De Keersmaecker K, Graux C, Odero MD, et al. Fusion of EML1 to ABL1 in T-cell acute lymphoblastic leukemia with cryptic t(9;14)(q34;q32). Blood. 2005;105:4849-4852.

103. Capdeville R, Buchdunger E, Zimmermann J, Matter A. Glivec (STI571, imatinib), a rationally developed, targeted anticancer drug. Nat Rev Drug Discov. 2002;1:493-502.

104. Wange RL. TCR signaling: another Abl-bodied kinase joins the cascade. Curr Biol. 2004;14:R562-564.

105. Zipfel PA, Zhang W, Quiroz M, Pendergast AM. Requirement for Abl kinases in T cell receptor signaling. Curr Biol. 2004;14:1222-1231.

106. Lacronique V, Boureux A, Valle VD, et al. A TEL-JAK2 fusion protein with constitutive kinase activity in human leukemia. Science. 1997;278:1309-1312.

107. Carron C, Cormier F, Janin A, et al. TEL-JAK2 transgenic mice develop T-cell leukemia. Blood. 2000;95:3891-3899.

108. Paietta E, Ferrando AA, Neuberg D, et al. Activating FLT3 mutations in CD117/KIT(+) T-cell acute lymphoblastic leukemias. Blood. 2004;104:558-560.

109. Van Vlierberghe P, Meijerink JP, Stam RW, et al. Activating FLT3 mutations in CD4+/CD8- pediatric T-cell acute lymphoblastic leukemias. Blood. 2005;106:4414-4415.

110. Shafman T, Khanna KK, Kedar P, et al. Interaction between ATM protein and c-Abl in response to DNA damage. Nature. 1997;387:520-523.

111. Meier M, den Boer ML, Hall AG, et al. Relation between genetic variants of the ataxia telangiectasia-mutated (ATM) gene, drug resistance, clinical outcome and predisposition to childhood T-lineage acute lymphoblastic leukaemia. Leukemia. 2005;19:1887-1895.

112. Sherr CJ, Weber JD. The ARF/p53 pathway. Curr Opin Genet Dev. 2000;10:94-99.

113. Sherr CJ, McCormick F. The RB and p53 pathways in cancer. Cancer Cell. 2002;2:103-112.

114. Sherr CJ. The INK4a/ARF network in tumour suppression. Nat Rev Mol Cell Biol. 2001;2:731-737.

115. Palomero T, Lim WK, Odom DT, et al. NOTCH1 directly regulates c-MYC and activates a feed-forward-loop transcriptional network promoting leukemic cell growth. Proceedings of the National Academy of Sciences of the United States of America. 2006;103:18261-18266.

116. Weng AP, Millholland JM, Yashiro-Ohtani Y, et al. c-Myc is an important direct target of Notch1 in T-cell acute lymphoblastic leukemia/lymphoma. Genes & development. 2006;20:2096-2109.

117. Betts DR, Rohatiner AZ, Evans ML, Rassam SM, Lister TA, Gibbons B. Abnormalities of chromosome 16q in myeloid malignancy: 14 new cases and a review of the literature. Leukemia. 1992;6:1250-1256.

118. Plantier I, Lai JL, Wattel E, Bauters F, Fenaux P. Inv(16) may be one of the only 'favorable' factors in acute myeloid leukemia: a report on 19 cases with prolonged follow-up. Leukemia research. 1994;18:885-888.

119. Betts DR, Ammann RA, Hirt A, et al. The prognostic significance of cytogenetic aberrations in childhood acute myeloid leukaemia. A study of the Swiss Paediatric Oncology Group (SPOG). European journal of haematology. 2007;78:468-476.

120. Filippova GN, Fagerlie S, Klenova EM, et al. An exceptionally conserved transcriptional repressor, CTCF, employs different combinations of zinc fingers to bind diverged promoter sequences of avian and mammalian c-myc oncogenes. Molecular and cellular biology. 1996;16:2802-2813.

121. Karin M. Nuclear factor-kappaB in cancer development and progression. Nature. 2006;441:431-436.

122. Portis T, Harding JC, Ratner L. The contribution of NF-kappa B activity to spontaneous proliferation and resistance to apoptosis in human T-cell leukemia virus type 1 Tax-induced tumors. Blood. 2001;98:1200-1208.

123. Hayden MS, Ghosh S. Signaling to NF-kappaB. Genes Dev. 2004;18:2195-2224.

124. Carrasco D, Rizzo CA, Dorfman K, Bravo R. The v-rel oncogene promotes malignant T-cell leukemia/lymphoma in transgenic mice. Embo J. 1996;15:3640-3650.

125. Bellavia D, Campese AF, Alesse E, et al. Constitutive activation of NF-kappaB and T-cell leukemia/lymphoma in Notch3 transgenic mice. Embo J. 2000;19:3337-3348.

126. Mandal M, Borowski C, Palomero T, et al. The BCL2A1 gene as a pre-T cell receptor-induced regulator of thymocyte survival. J Exp Med. 2005;201:603-614.

127. Vacca A, Felli MP, Palermo R, et al. Notch3 and pre-TCR interaction unveils distinct NF-kappaB pathways in T-cell development and leukemia. Embo J. 2006;25:1000-1008.

128. Vilimas T, Mascarenhas J, Palomero T, et al. Targeting the NF-kappaB signaling pathway in Notch1-induced T-cell leukemia. Nature medicine. 2007;13:70-77.

129. Sole F, Espinet B, Sanz GF, et al. Incidence, characterization and prognostic significance of chromosomal abnormalities in 640 patients with primary myelodysplastic syndromes. Grupo Cooperativo Espanol de Citogenetica Hematologica. Br J Haematol. 2000;108:346-356.

130. Heim S, Mitelman F. Chromosome abnormalities in the myelodysplastic syndromes. Clin Haematol. 1986;15:1003-1021.

131. Liu TX, Becker MW, Jelinek J, et al. Chromosome 5q deletion and epigenetic suppression of the gene encoding alpha-catenin (CTNNA1) in myeloid cell transformation. Nat Med. 2007;13:78-83.

132. van de Wetering M, Oosterwegel M, Holstege F, et al. The human T cell transcription factor-1 gene. Structure, localization, and promoter characterization. J Biol Chem. 1992;267:8530-8536.

133. Verbeek S, Izon D, Hofhuis F, et al. An HMG-box-containing T-cell factor required for thymocyte differentiation. Nature. 1995;374:70-74.

134. Palacios EH, Weiss A. Distinct roles for Syk and ZAP-70 during early thymocyte development. The Journal of experimental medicine. 2007;204:1703-1715.

135. Sansal I, Sellers WR. The biology and clinical relevance of the PTEN tumor suppressor pathway. J Clin Oncol. 2004;22:2954-2963.

136. McCormick F. Ras signaling and NF1. Curr Opin Genet Dev. 1995;5:51-55.

137. Balgobind B, Van Vlierberghe P, van den Ouweland A, et al. Leukemia associated NF1 inactivation in pediatric T-ALL and AML patients lacking evidence for neurofibromatosis. Blood. 2007.

138. Calin GA, Croce CM. MicroRNA-cancer connection: the beginning of a new tale. Cancer Res. 2006;66:7390-7394.

139. Lu J, Getz G, Miska EA, et al. MicroRNA expression profiles classify human cancers. Nature. 2005;435:834-838.

140. Cimmino A, Calin GA, Fabbri M, et al. miR-15 and miR-16 induce apoptosis by targeting BCL2. Proc Natl Acad Sci U S A. 2005;102:13944-13949.

141. He L, Thomson JM, Hemann MT, et al. A microRNA polycistron as a potential human oncogene. Nature. 2005;435:828-833.

142. Henrich KO, Fischer M, Mertens D, et al. Reduced expression of CAMTA1 correlates with adverse outcome in neuroblastoma patients. Clinical cancer research. 2006;12:131-138.

143. Kim MY, Yim SH, Kwon MS, et al. Recurrent genomic alterations with impact on survival in colorectal cancer identified by genome-wide array comparative genomic hybridization. Gastroenterology. 2006;131:1913-1924.

144. Mori N, Morosetti R, Mizoguchi H, Koeffler HP. Progression of myelodysplastic syndrome: allelic loss on chromosomal arm 1p. British journal of haematology. 2003;122:226-230.

145. Mori N, Morosetti R, Spira S, et al. Chromosome band 1p36 contains a putative tumor suppressor gene important in the evolution of chronic myelocytic leukemia. Blood. 1998;92:3405-3409.

146. Melendez B, Cuadros M, Robledo M, et al. Coincidental LOH regions in mouse and humans: evidence for novel tumor suppressor loci at 9q22-q34 in non-Hodgkin's lymphomas. Leukemia research. 2003;27:627-633.

147. Bagchi A, Papazoglu C, Wu Y, et al. CHD5 is a tumor suppressor at human 1p36. Cell. 2007;128:459-475.

148. Fischer A, Gessler M. Delta-Notch--and then? Protein interactions and proposed modes of repression by Hes and Hey bHLH factors. Nucleic acids research. 2007;35:4583-4596.

149. Chinnaiyan AM, O'Rourke K, Yu GL, et al. Signal transduction by DR3, a death domain-containing receptor related to TNFR-1 and CD95. Science (New York, NY. 1996;274:990-992.

150. Carapeti M, Aguiar RC, Watmore AE, Goldman JM, Cross NC. Consistent fusion of MOZ and TIF2 in AML with inv(8)(p11q13). Cancer genetics and cytogenetics. 1999;113:70-72.

151. Esteyries S, Perot C, Adelaide J, et al. NCOA3, a new fusion partner for MOZ/MYST3 in M5 acute myeloid leukemia. 2007.

152. Sinclair PB, Sorour A, Martineau M, et al. A fluorescence in situ hybridization map of 6q deletions in acute lymphocytic leukemia: identification and analysis of a candidate tumor suppressor gene. Cancer Res. 2004;64:4089-4098.

153. Stallings RL, Nair P, Maris JM, et al. High-resolution analysis of chromosomal breakpoints and genomic instability identifies PTPRD as a candidate tumor suppressor gene in neuroblastoma. Cancer research. 2006;66:3673-3680.

154. Nagayama K, Kohno T, Sato M, Arai Y, Minna JD, Yokota J. Homozygous deletion scanning of the lung cancer genome at a 100-kb resolution. Genes, chromosomes & cancer. 2007;46:1000-1010.

155. Purdie KJ, Lambert SR, Teh MT, et al. Allelic imbalances and microdeletions affecting the PTPRD gene in cutaneous squamous cell carcinomas detected using single nucleotide polymorphism microarray analysis. Genes, chromosomes & cancer. 2007;46:661-669.

156. Sato M, Takahashi K, Nagayama K, et al. Identification of chromosome arm 9p as the most frequent target of homozygous deletions in lung cancer. Genes, chromosomes & cancer. 2005;44:405-414.

157. Little M, Wells C. A clinical overview of WT1 gene mutations. Hum Mutat. 1997;9:209-225.

158. Chiusa L, Francia di Celle P, Campisi P, Ceretto C, Marmont F, Pich A. Prognostic value of quantitative analysis of WT1 gene transcripts in adult acute lymphoblastic leukemia. Haematologica. 2006;91:270-271.

159. King-Underwood L, Pritchard-Jones K. Wilms' tumor (WT1) gene mutations occur mainly in acute myeloid leukemia and may confer drug resistance. Blood. 1998;91:2961-2968.

160. Przybylski GK, Dik WA, Wanzeck J, et al. Disruption of the BCL11B gene through inv(14)(q11.2q32.31) results in the expression of BCL11B-TRDC fusion transcripts and is associated with the absence of wild-type BCL11B transcripts in T-ALL. Leukemia. 2005;19:201-208.

161. Janoueix-Lerosey I, Penther D, Thioux M, et al. Molecular analysis of chromosome arm 17q gain in neuroblastoma. Genes, chromosomes & cancer. 2000;28:276-284.

162. Bown N, Cotterill S, Lastowska M, et al. Gain of chromosome arm 17q and adverse outcome in patients with neuroblastoma. The New England journal of medicine. 1999;340:1954-1961.

163. Robison LL, Neglia JP. Epidemiology of Down syndrome and childhood acute leukemia. Progress in clinical and biological research. 1987;246:19-32.

164. Guo Z, Dose M, Kovalovsky D, et al. {beta}-Catenin stabilization stalls the transition from double-positive to single-positive stage and predisposes thymocytes to malignant transformation. Blood. 2007;109:5463-5472.

165. Ardavin C, Wu L, Li CL, Shortman K. Thymic dendritic cells and T cells develop simultaneously in the thymus from a common precursor population. Nature. 1993;362:761-763.

166. Plum J, De Smedt M, Leclercq G, Verhasselt B, Vandekerckhove B. Interleukin-7 is a critical growth factor in early human T-cell development. Blood. 1996;88:4239-4245.

167. Willerford DM, Swat W, Alt FW. Developmental regulation of V(D)J recombination and lymphocyte differentiation. Curr Opin Genet Dev. 1996;6:603-609.

168. von Boehmer H. Shaping the T cell repertoire. J Immunol. 2005;175:7067-7068.

169. von Boehmer H. Unique features of the pre-T-cell receptor alpha-chain: not just a surrogate. Nat Rev Immunol. 2005;5:571-577.

170. Nagano K, Itagaki C, Izumi T, et al. Rb plays a role in survival of Abl-dependent human tumor cells as a downstream effector of Abl tyrosine kinase. Oncogene. 2006;25:493-502.

171. Wang JY. Regulation of cell death by the Abl tyrosine kinase. Oncogene. 2000;19:5643-5650.

172. Whang YE, Tran C, Henderson C, et al. c-Abl is required for development and optimal cell proliferation in the context of p53 deficiency. Proc Natl Acad Sci U S A. 2000;97:5486-5491.

173. Latour S, Veillette A. Proximal protein tyrosine kinases in immunoreceptor signaling. Curr Opin Immunol. 2001;13:299-306.

174. Zhang W, Sloan-Lancaster J, Kitchen J, Trible RP, Samelson LE. LAT: the ZAP-70 tyrosine kinase substrate that links T cell receptor to cellular activation. Cell. 1998;92:83-92.

175. Wang CR, Hashimoto K, Kubo S, et al. T cell receptor-mediated signaling events in CD4+CD8+ thymocytes undergoing thymic selection: requirement of calcineurin activation for thymic positive selection but not negative selection. J Exp Med. 1995;181:927-941.

176. Teixeira C, Stang SL, Zheng Y, Beswick NS, Stone JC. Integration of DAG signaling systems mediated by PKC-dependent phosphorylation of RasGRP3. Blood. 2003;102:1414-1420.

177. Carrera AC, Rodriguez-Borlado L, Martinez-Alonso C, Merida I. T cell receptor-associated alpha-phosphatidylinositol 3-kinase becomes activated by T cell receptor cross-linking and requires pp56lck. J Biol Chem. 1994;269:19435-19440.

178. Wang X, Gjorloff-Wingren A, Saxena M, Pathan N, Reed JC, Mustelin T. The tumor suppressor PTEN regulates T cell survival and antigen receptor signaling by acting as a phosphatidylinositol 3-phosphatase. J Immunol. 2000;164:1934-1939.

179. Chang PY, Draheim K, Kelliher MA, Miyamoto S. NFKB1 is a direct target of the TAL1 oncoprotein in human T leukemia cells. Cancer Res. 2006;66:6008-6013.

Chapter 3

The cryptic chromosomal deletion, del(11)(p12p13), as a new activation mechanism of *LMO2* in pediatric T-cell acute lymphoblastic leukemia

Pieter Van Vlierberghe[1], Martine van Grotel[1], H. Berna Beverloo[2], Charles Lee[3], Tryggvi Helgason[1], Jessica Buijs-Gladdines[1], Monique Passier[1], Elisabeth R. van Wering[4], Anjo J.P. Veerman[4,5], Willem A. Kamps[4,6], Jules P.P. Meijerink[1] and Rob Pieters[1]

[1]Department of Pediatric Oncology/Hematology, Erasmus MC / Sophia Children's Hospital,
[2]Department of Clinical Genetics, Erasmus MC, Rotterdam, The Netherlands
[3]Department of Pathology, Brigham and Women's Hospital, Harvard Medical School, Boston, MA 02115, USA
[4]Dutch Childhood Oncology Group (DCOG), The Hague, The Netherlands
[5]Department of Pediatric Oncology/Hematology, VU University MC, Amsterdam, the Netherlands
[6]Department of Pediatric Oncology, Beatrix Children's Hospital, University MC Groningen, the Netherlands

Blood 2006; 108(10):3520-9

ABSTRACT

To identify new cytogenetic abnormalities associated with leukemogenesis or disease outcome, T-ALL patient samples were analyzed by means of the array-comparative genome hybridization technique (array-CGH). Here, we report the identification of a new recurrent and cryptic deletion on chromosome 11, i.e. the del(11)(p12p13), in about 4% (6/138) of pediatric T-ALL patients. Detailed molecular-cytogenetic analysis revealed that this deletion activates the *LMO2* oncogene in 4 out of 6 del(11)(p12p13) positive T-ALL patients, alike patients with an *LMO2* translocation (9/138). The *LMO2* activation mechanism of this deletion is loss of a negative regulatory region upstream of *LMO2*, causing activation of the proximal *LMO2* promoter. *LMO2* rearrangements, including this del(11)(p12p13) and t(11;14)(p13;q11) or t(7;11)(q35;p13), were found in the absence of other recurrent cytogenetic abnormalities involving *TLX3*, *TLX1*, *CALM-AF10*, *TAL1*, *MLL* or *MYC*. *LMO2* abnormalities represent about 9% (13/138) of pediatric T-ALL cases and are more frequent in pediatric T-ALL than appreciated up till now.

INTRODUCTION

T-cell acute lymphoblastic leukemia (T-ALL) is a high-risk malignancy of thymocytes, and accounts for 10-15% of pediatric ALL cases. T-ALL often presents with a high tumor-mass that is accompanied by a rapid progression of disease. About 30% of T-ALL cases relapse within the first years during or following treatment and eventually die[1].

Genetic analyses of T-ALL have elucidated an enormous heterogeneity in genetic abnormalities including chromosomal translocations, deletions, amplifications and mutations[2]. These abnormalities result in the aberrant expression of transcription factors like the basic Helix-Loop-Helix (bHLH) genes *MYC*, *TAL1(SCL)*, *TAL2*, *LYL1*, or *bHLHB1*, genes involved in transcriptional regulation like the Cysteine rich LIM-domain-only genes *LMO1* or *LMO2* or the Krüppel-like zinc-finger gene *BCL11B*. It can also affect genes that are involved in embryonic development like the homeodomain genes *TLX1/TLX1*, *TLX3/TLX3*, or members of the *HOXA* cluster as well as signalling molecules like the tyrosine kinase *ABL1*[3-6](reviewed in[7,8]). Other translocations lead to the formation of specific fusion products and include *CALM-AF10*[9] or *MLL* rearrangements. Mutational mechanisms may also enhance gene activity as, for example, activating mutations in the *NOTCH1* gene were recently identified in about 50% of human T-ALL[10].

LMO2 encodes a protein that participates in the transcription factor complex, which includes E2A, TAL1, GATA1 and LDB1 in erythroid cells[11,12]. Within this transcription complex, LMO2 mediates the protein-protein interactions by recruiting LDB1, whereas TAL1, GATA1 and E2A regulate the binding to specific DNA target sites[13]. This complex regulates the expression of several genes in various cellular backgrounds including *C-KIT*[14], *EKLF*[15] and *RALDH*[16]. In normal T-cell development, *LMO2* is expressed in immature CD4/CD8 double-negative thymocytes, and is down-regulated during T-cell maturation[17,18]. In various mouse models, ectopic expression of *LMO2* leads to clonal expansion of T-cells, eventually leading to T-ALL development. *LMO2*-mediated leukemogenesis seems restricted to the T-cell, as transgenic mice with constitutive expression of *LMO2* in all tissues develop malignancies involving the T-lineage only[19-22]. The long latency of leukemia in these mice suggests that T-ALL development requires secondary mutations in addition to the activation of *LMO2*[22,23].

LMO2 driven oncogenesis in humans was suggested by its frequent involvement in the chromosomal translocations t(11;14)(p13;q11) and t(7;11)(q35;p13) in T-ALL, in which the *TCR*α/δ or *TCR*β locus is fused to *LMO2*[24,25]. Direct prove came from the retroviral IL2Rγc gene therapy trial for X-linked severe combined immunodeficiency

(X-SCID) patients, in which 2 patients developed T-ALL after retroviral insertions in the *LMO2* gene[26,27].

In this study, we report the identification of a new recurrent and cryptic deletion, i.e. the del(11)(p12p13), in about 4% (6/138) of pediatric T-ALL patients. Detailed molecular-cytogenetic analysis revealed that this deletion activates the *LMO2* oncogene in 4 out of 6 of these del(11)(p12p13) positive T-ALL patients, mainly through deletion of negative regulatory sequences upstream of *LMO2*. The relation to other recurrent cytogenetic abnormalities, the immunophenotypic characteristics and clinical outcome of this new cryptic abnormality in pediatric T-ALL is discussed.

MATERIALS & METHODS

Patient samples

Viably frozen diagnostic bone marrow or peripheral blood samples from 64 pediatric T-ALL patients and clinical and immunophenotypic data were provided by the Dutch Childhood Oncology Group (DCOG). Patients were considered positive as more than 25 percent of total cells were positive for a specific immunophenotypic marker. A second pediatric T-ALL cohort (n=74) was obtained from the German Co-operative study group for childhood acute lymphoblastic leukemia (COALL). The patients' parents or their legal guardians provided informed consent to use leftover material for research purposes. Leukemic cells were isolated and enriched from these samples as previously described[28]. All resulting samples contained ≥90% leukemic cells, as determined morphologically by May-Grünwald-Giemsa (Merck, Darmstadt, Germany)-stained cytospins. Viably frozen T-ALL cells were used for DNA and RNA extraction, and a minimum of 5×10^6 leukemic cells were lysed in Trizol reagent (Gibco BRL, Life Technologies, Breda, The Netherlands) and stored at -80°C. A total of 25×10^3 leukemic cells was used for cytospin slides for fluorescence *in-situ* hybridization (FISH) and stored at -20°C. For the preparation of metaphase slides, a minimum of 5×10^6 leukemic cells were cultured for 72 hr in serum free medium (JRH Biosciences, Kansas, USA) in the presence of IL7 (10ng/ml) and IL2 (10ng/ml), and harvested according to standard cytogenetic techniques.

Genomic DNA isolation, RNA extraction and cDNA synthesis

Genomic DNA and total cellular RNA were isolated according to the manufacturers' protocol, with minor modifications. An additional phenol-chloroform extraction was performed and the DNA was precipitated with isopropanol along with 1 µl (20µg/ml) glycogen (Roche, Almere, The Netherlands). After precipitation, RNA pellets were dissolved in 20µl RNAse-free TE-buffer (10mM Tris-HCl, 1mM EDTA, pH=8.0). The RNA concentration was quantified spectrophotometrically. Following a denaturation

step of 5 min at 70°C, 1µg of RNA was reverse transcribed to single-stranded cDNA using a mix of random hexamers (2.5µM) and oligodT primers (20nM). The RT reaction was performed in a total volume of 25µl containing 0.2mM of each dNTP (Amersham Pharmacia BioTech, Piscataway, NJ, USA), 200U Moloney murine leukemia virus reverse transcriptase (M-MLV RT) (Promega, Madison, WI, USA) and 25U RNAsin (Promega). Conditions for the RT reaction were 37°C for 30', 42°C for 15', and 94°C for 5'. The cDNA was diluted to a final concentration of 8ng/µl and stored at -80°C.

BAC array-comparative genomic hybridization (BAC array-CGH)

BAC array-CGH analysis was performed using a dye-swap experimental design to minimize false positive results. Patient genomic DNA (2µg) and male/female reference DNA (2µg) (Promega) were fragmented by sonification (VibraCell Model VC130, Sonics & Materials, Newtown, CT, USA). DNA fragmentation was verified by agarose gel electrophoresis. Individual reference and experimental samples were then purified using the QIAQuick PCR clean-upkit (Qiagen, Valencia, CA, USA). Labeling reactions with Cy5-dUTP and Cy3-dUTP (PerkinElmer, Wellesley, MA, USA) were performed with 5µg of purified restricted DNA using the Bioprime labeling kit (Invitrogen, Paisley, UK) according to the manufacturer's instructions. The patient and reference DNA were combined, denatured, and applied to the 1Mb GenomeChip™ V1.2 Human BAC arrays (2,632 BAC clones spotted on a single array; Spectral Genomics, Houston, TX, USA) according to the manufacturer's protocol. Hybridization and washing procedures were performed as recommended, and the slides were scanned on a GenePix 4000B Microarray Scanner (Axon Instruments, Union City, CA, USA). Cy3 and Cy5 fluorescent intensities at each DNA spot were quantified using GenePix Pro 4.0 Microarray Image Analysis Software, and the data were subsequently imported into SpectralWare software (www.spectralgenomics.com). Using this software, background intensities were subtracted and initial fluorescent ratios were log2 transformed. The ratios for each clone were subsequently plotted into chromosome-ideograms. At this stage, known large-scale copy number polymorphisms were not considered disease-related[29].

Oligo array-CGH

Oligo array-CGH analysis was performed, as previously described[30], on the human genome CGH Microarray 44A (Agilent Technologies, Palo Alto, USA), which consists of ~40,000 60-mer oligonucleotide probes that span both coding and non-coding sequences with an average spatial resolution of ~35Kb. Briefly, 10µg of genomic reference or patient DNA was digested with AluI (20U) and RsaI (20U) (Invitrogen) overnight at 37°C. Verification of DNA fragmentation, purification and Cy-3 or Cy-5

labeling was as described above. Experimental and reference targets for each hybridization were pooled and mixed with 50µg of human Cot-1 DNA (Invitrogen), 100µg of yeast tRNA (Invitrogen), and 1× hybridization control targets (SP310, Operon Technologies, Alameda, CA, USA) in a final volume of 500µl *in-situ* hybridization buffer (Agilent Technologies). The hybridization mixtures was denatured at 95°C for 3', pre-incubated at 37°C for 30', and hybridized to the array in a microarray hybridization chamber (Agilent Technologies) for 14-18h at 65°C in a rotating oven (Robbins Scientific, Mountain View, CA, USA) at 20rpm. The array slides were washed in 0.5× SSC/0.005% Triton X-102 at room temperature for 5', followed by 5' at 37°C in 0.1× SSC/0.005% Triton X-102. Slides were dried and scanned using a 2565AA DNA microarray scanner (Agilent Technologies). Microarray images were analyzed using feature extraction software (version 8.1, Agilent Technologies) and the data were subsequently imported into array-CGH analytics software v3.1.28 (Agilent Technologies).

FISH-procedure

BACs were obtained from BAC/PAC Resource Center (Children's Hospital, Oakland, USA). BAC DNA was isolated using DNA MiniPrep plasmid kit (Promega) and labeled with biotin-16-dUTP/digoxigenin-11-dUTP (Roche) by nick translation[31]. BAC clones RP11-646J21, RP11-98C11 and RP11-603J2 were used for the characterization of the telomeric breakpoints of the del(11)(p12p13), whereas the centromeric breakpoints were localized using RP11-36H11, RP11-769M16, and RP11-465C16. LMO2 translocations were identified using a split-FISH procedure with the LMO2 flanking BAC clones RP11-646J21 and RP11-90F13. FISH analysis was performed on freshly prepared interphase and metaphase slides from methanol/acetic acid cell suspensions or cytospins stored at –20°C. Slides were pretreated by an RNase and pepsin treatment, fixed with acid-free formaldehyde and denatured at 72°C. Probes were denatured (4' 72°C in 70% formamide/2x SSC) in the presence of a 100-fold excess of human Cot-1 DNA (Gibco BRL). Following pre-annealing at 37°C for 30', biotinylated probes were hybridized overnight at 37°C, and visualized by fluorescein avidin (Vector Laboratories, Burlingame, VT, USA) and biotinylated anti-avidin D sandwich detection (affinity purified; Vector Laboratories). The digoxigenin hybridization signal was detected using anti-digoxigenin-rhodamine (Boehringer Mannheim) and donkey anti-sheep-Texas Red (Jackson ImmunoResearch Laboratories, Westgrove, PA, USA). Cells were counterstained with DAPI/Vectashield mounting medium. Fluorescence signals were visualized on a Zeiss Axioplan II fluorescence microscope (Zeiss, Sliedrecht, The Netherlands) equipped with double and triple bandpass filters for simultaneous visualization of rhodamine-TR/FITC/DAPI. *TAL1*-, *TLX3*-, *TLX1*- and *MLL*- chromosomal rearrangements or the *SIL-TAL1* deletion were

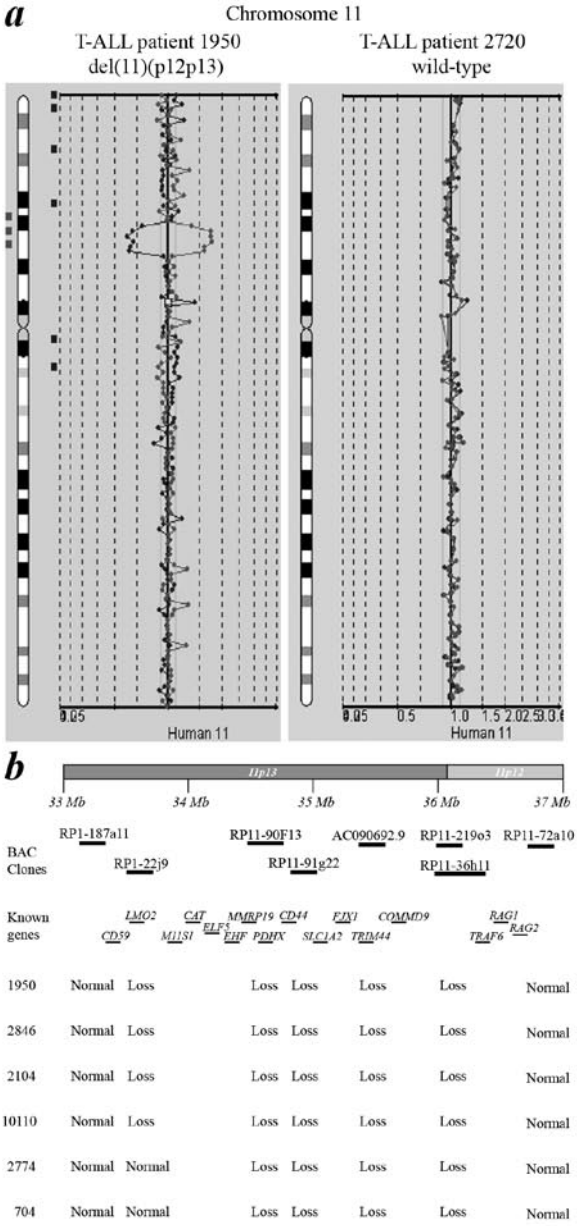

Figure 1. New recurrent deletion, del(11)(p12p13), in pediatric T-ALL.
(a) Chromosome 11 ideogram and corresponding BAC array-CGH plot of test DNA:control DNA ratios (blue tracing) versus the dye-swap experiment (red tracing) for T-ALL patients 1950 (left panel) and 2720 (right panel). **(b)** Overview of BAC array-CGH results for the 11p12-11p13 region for the 4 DCOG and the 2 COALL T-ALL patients with del(11)(p12p13). The BAC clones present on the DNA array and located on chromosome bands 11p12-11p13 are shown. Specific genes located in this region are indicated. Depicted genome positions are based on the UCSC Genome Browser at http://genome.ucsc.edu/.

determined using FISH kits (DakoCytomation, Glostrup, Denmark)[32], hybridized and scored as described by the manufacturer. The CALM-AF10 chromosomal rearrangement was detected using FISH as previously described[32].

Genomic and cDNA PCR

The genomic breakpoint in T-ALL patient 1950 was determined by long-range PCR using forward primer 5' GATGCCTTCCCTCATGTA 3' (intron 1 *RAG2*) and reverse primer 5' CGCAGTGCCTAGAACAGT 3' (intron 1 *LMO2*). PCR reactions were performed using 200ng of genomic DNA (200ng/µl), 10pmol primers, 10nmol of dNTPs, 4mM $MgCl_2$, 1.25U of ampli*Taq* gold (Applied Biosystems, Foster City, CA, USA) in 10x PCR buffer II (Applied Biosystems) in a total volume of 50µl. After the initial denaturation at 94°C for 10', PCR was performed for 15 cycles of 95°C for 15", 60°C for 1' and 68°C for 3' followed by 15 cycles consisting of 95°C for 15", 60°C for 1' and 68°C for 3' (+10s/cycle).

To identify the *RAG2-LMO2* fusion gene in T-ALL patient 1950, cDNA PCR (RT-PCR) was performed in the presence of forward primer 5' GTGGGCAGTCAGTGAATC 3' (exon 1 *RAG2*) and reverse primer 5' TGCAAGTTCAGGTTGAAA 3' (exon 2 *LMO2*). RT-PCR reactions were as described above in a total volume of 50µl. Following initial denaturation at 95°C for 10', reactions were amplified for 39 cycles of 95°C for 15" and 60°C for 1'.

Ligation-mediated PCR

Ligation-mediated PCR (LM-PCR) was performed as previously described[33]. Briefly, 1 µg of patient (2846) and control DNA (2720) was digested with blunt-end restriction enzymes (*Eco*RV, *Dra*I, *Pvu*II and *Stu*I) and 50 µM of an adaptor was ligated to both ends of the restriction fragments. The ligation products were subjected to two rounds of PCR with nested adaptor-specific primers AP1 (5' GCT AGA TAC GAC TCA GTA TAG 3') and AP2 (5' TAT AGG CGC ACG AAC G 3') and nested *LMO2*-intron 1-specific primers *LMO2*F (5' CAG CCA CAT GGG TAG AAC 3') amd *LMO2*Fnested (5' TGG CAT TAG GGT ATG GAA 3'). The band that differed in size from the expected band in the control patient, lacking the del(11)(p12p13), was excised from the gel and purified using the QIAquick gel extraction kit (Qiagen, Hilden, Germany) and subjected to direct nucleotide sequencing.

Quantitative real-time RT-PCR (RQ-PCR)

Expression levels of *LMO2*, *TAL1, TLX1* and *TLX3* transcripts and the *CALM-AF10* fusion product were quantified relative to the expression level of the endogenous housekeeping gene glyceraldehyde-3-phosphate dehydrogenase (*GAPDH*) using real-time RT-PCR in an ABI 7700 sequence detection system (Applied Biosystems) as

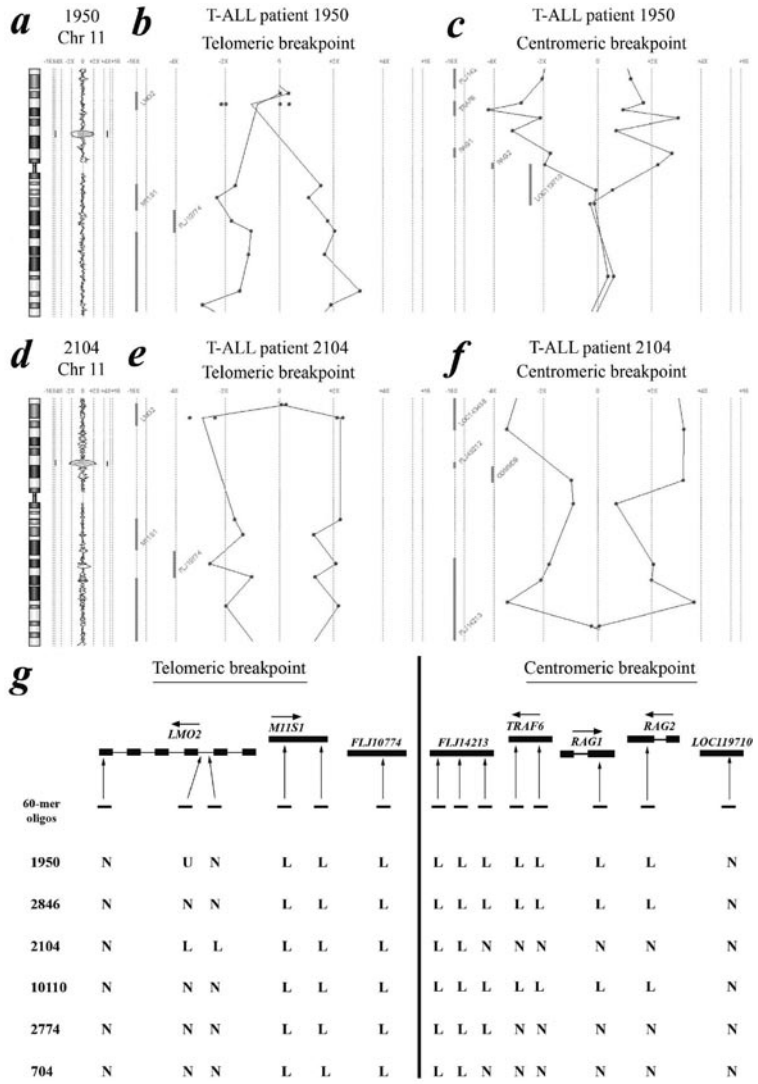

Figure 2. Molecular characterization of deletion, del(11)(p12p13), in 6 pediatric T-ALL patients.

Chromosome 11 ideogram and corresponding oligo array-CGH plot of test DNA:control DNA ratios (blue tracing) versus the dye-swap experiment (red tracing) for T-ALL patient 1950 **(a)** and patient 2104 **(d)**. Hybridization signals in the absence of amplifications or deletions scatter around the "zero"line, indicating equal hybridization for patient and reference DNA. Hybridization signals around the –2X or +2X lines represent loss of the corresponding region in the patient DNA. Detailed analysis of the telomeric breakpoints in patients 1950 **(b)** and 2104 **(e)** and the centromeric breakpoints in patients 1950 **(c)** and 2104 **(f)** of the deletion, del(11)(p12p13). **(g)** Overview of oligo array-CGH results in the potential breakpoint regions for 4 DCOG and the 2 COALL T-ALL patients with del(11)(p12p13). The 60-mer oligos present on the DNA array and located in the telomeric and centromeric breakpoint regions, as well as the specific genes located in this region with their transcription direction, are shown. Abbreviations: N; normal, L; loss, U; non-informative.

described previously[28,34]. The expression levels relative to the *GAPDH* housekeeping gene were calculated following the equation:

Relative expression level as percentage of GAPDH expression = $2^{-\Delta Ct}$ x 100%, whereby $\Delta Ct = Ct_{target} - Ct_{GAPDH}$ Primer and probe combinations were designed using Oligo 6.22 software (Molecular Biology Insight, Cascade, CO, USA), and were purchased from Eurogentec (Seraing, Belgium). Primers and probe had melting temperatures of 65-66.5°C and 73-75°C respectively, and performed with 95% efficiency or higher as determined from slopes of standard curves. This allows direct normalization of the target reaction to *GAPDH* expression levels at the Ct-level[34]. Primers and probe for the detection of the house-keeping gene *GAPDH* have been described previously[28]. For the detection of total *LMO2* transcripts derived from the *LMO2* distal promoter (upstream of exon 1), *RAG2-LMO2* fusion transcripts and transcripts derived from the *LMO2* proximal promoter (exon 3), the forward primer 5'-TTG GGG ACC GCT ACT T-3' and reverse primer 5'-ATG TCC TGT TCG CAC ACT-3' were used in combination with the probe 5'-(FAM)-AAG CTC TGC CGG AGA GAC TAT CT-3'. For the detection of distal *LMO2* transcripts and/or *RAG2-LMO2* fusion transcripts, forward primer 5'-TCA ACC TGA ACT TGC AGT AG-3' and reverse primer 5'-TCT CTC GGG AAG GTC TAT TT-3' were used in combination with the probe 5'-(FAM)-AAC CAG AGA CAG AGG GAA GCT G-3. For *CALM-AF10*, 5' and 3' *CALM-AF10* fusion transcripts were detected in separate reactions using the *CALM-AF10* forward primer 5'-TTA ACT GGG GGA TCT AAC TG-3' in combination with the 5' fusion transcript reverse primer 5'-GCT GCT TTG CTT TCT CTT C-3 or the 3' fusion transcript reverse primer 5'-CCC TCT GAC CCT CTA GCT TC-3' both in combination with the common *CALM-AF10* probe 5'-(FAM)-CTT GGA ATG CGG CAA CAA TG-(TAMRA)-3'. For detection of *TLX1* expression levels, the forward primer 5'-CTC ACT GGC CTC ACC TT-3' and reverse primer 5'-CTG TGC CAG GCT CTT CT-3' were used in combination with the probe 5'-(FAM)-CCT TCA CAC GCC TGC AGA TC-(TAMRA)-3'. For detection of *TLX3* expression levels, forward primer 5'-TCT GCG AGC TGG AAA A-3' and reverse primer 5'-GAT GGA GTC GTT GAG GC-3' were used in combination with probe 5'-(FAM)-CCA AAA CCG GAG GAC CAA GT-(TAMRA)-3'. For the detection of *TAL1* transcripts, the forward primer 5'-TGC CTT CCC TAT GTT CAC-3' and reverse primer 5'-AAG ATA CGC CGC ACA AC-3' were used in combination with probe 5'-(FAM)-CCT TCC CCC TAT GAG ATG GAG A-(TAMRA)-3'. The *SIL-TAL1* primers (ENF601, ENR664) and probe (ENP641) for the detection of a *SIL-TAL1* deletion were used as recommended by the Europe Against Cancer Program[32].

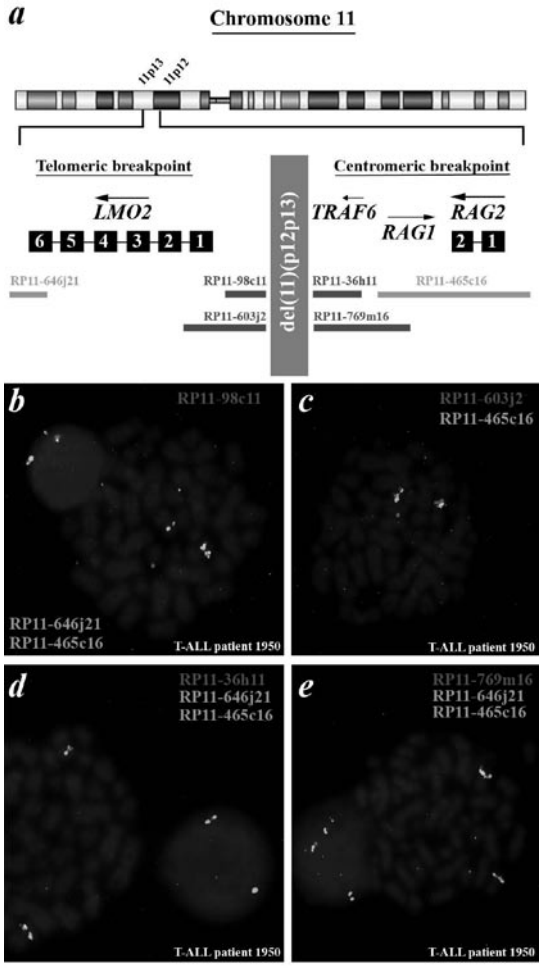

Figure 3. FISH analysis confirms the presence of del(11)(p12p13) in T-ALL patient 1950. **(a)** Chromosome ideogram and overview of the genomic position of the BAC clones used for FISH analysis, located in the telomeric and centromeric breakpoint regions. **(b)** Dual-color FISH analysis on metaphase spreads of patient 1950 using RP11-465C16 (Green), RP11-646J21 (Green) and RP11-98C11 (Red). The wild-type allele of chromosome 11 shows 2 green and 1 red signal, whereas on the mutated allele the red signal is lost and both green signals fuse. The extrachromosomal red signal represents background. **(c)** Dual-color FISH analysis on metaphase spreads of the same patient using RP11-465C16 (Green) and RP11-603J2 (Red). The intensity of the red signal is lower compared to the wild-type allele of chromosome 11, suggesting that only part of RP11-603J2 is deleted. **(d)** Dual-color FISH analysis on metaphase spreads using RP11-465C16 (Green), RP11-646J21 (Green) and RP11-36H11 (Red). The wild-type allele of chromosome 11 shows 2 green and 1 red signal, whereas on the mutated allele the red signal is lost and both green signals fuse. **(e)** Dual-color FISH analysis on metaphase spreads using RP11-465C16 (Green), RP11-646J21 (Green) and RP11-769M16 (Red). The wild-type allele of chromosome 11 shows 2 green and 1 red signal, whereas on the mutated allele the red signal is lost and both green signals fuse.

Table 1. FISH analysis in 6 pediatric T-ALL patients with del(11)(p12p13)

	Number of hybridization signals					
	Telomeric breakpoint			Centromeric breakpoint		
Patient ID	646j21	603j2	98c11	36h11	769m16	465c16
1950	2	2 (int)	1	1	1	2
2846	2	2 (int)	1	1	1	2
2104	2	1	1	2 (int)	2 (int)	2
10110	2	2 (int)	1	1	1	2
2774	2	2	2	2 (int)	2 (int)	2
704	2	2	2	2 (int)	2 (int)	2

Int; intensity difference between the hybridization signal on the wild-type and the mutated allele.

Statistical analysis

Kaplan Meier curves were constructed in SPSS 11.0 software in a stratified analysis pair wise over strata, and *p*-values were determined using the log-rank test. An event was defined as having a relapse or being a non-responder after induction therapy. The Mann-Whitney U-test was used to analyze differences in *LMO2* expression levels between subgroups. Data were considered statistically significant if $p<0.05$.

RESULTS

New recurrent deletion del(11)(p12p13) in pediatric T-ALL

To identify new chromosomal abnormalities in pediatric T-ALL related to outcome and/or leukemogenesis, BAC array-CGH analysis was performed on a selected cohort of 30 out of 64 clinically and karyotypically well-defined diagnostic T-ALL patient samples treated according to DCOG protocols. A recurrent loss of genomic material at chromosomal band 11p12-11p13 was found in 2 out of 30 pediatric T-ALL cases (Figure 1a). Analyzing of this pediatric T-ALL cohort and an second independent cohort (n=74) treated according to the COALL97 protocol using FISH, confirmed the presence of the del(11)(p12p13) in both positive patients, but also revealed 4 additional patients with this same deletion (data not shown). BAC array-CGH analysis of these additional positive cases confirmed the presence of this del(11)(p12p13)

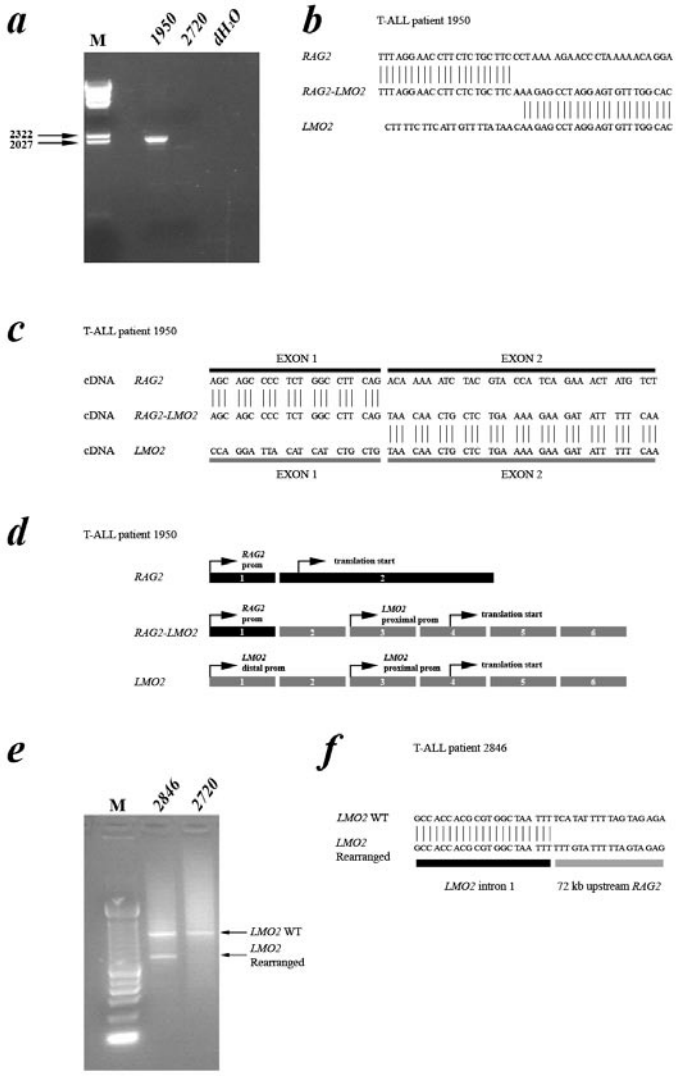

Figure 4. Molecular characterization of del(11)(p12p13) in T-ALL patients 1950 and 2846. **(a)** Long-range PCR analysis on genomic DNA of patient 1950 using primers situated in intron 1 of *RAG2* and intron 1 of *LMO2* revealed a specific band of ~2000 bp. Patient 2720 served as a negative control. **(b)** Sequence analysis confirmed the exact position of the genomic breakpoint. **(c)** PCR analysis on cDNA of this patient revealed a *RAG2-LMO2* fusion gene, in which exon 1 of *RAG2* was fused to exon 2 of *LMO2*. **(d)** Gene (exon) structure of both *RAG2* and *LMO2* shows that the translation initiation sites are situated in exon 2 and exon 4, respectively. As a consequence, translation of the *RAG2-LMO2* fusion gene will also be initiated in exon 4. **(e)** LM-PCR analysis on *Hinc*II digested genomic DNA from patient 2846 using an *LMO2* intron 1 specific primer, revealed an aberrant PCR product of ~600 bp. The expected wildtype product is ~1000 bp and is visible in both patients 2846 and 2720, which served as a negative control. **(f)** Sequence analysis confirmed that in patient 2846 the *LMO2* intron 1 sequences are fused to a genomic region upstream of *RAG2*. Abbreviation: prom; promoter.

Table 2. Immunophenotypic characteristics of *LMO2*-rearranged pediatric T-ALL patients

Patient ID	*LMO2* rearrangement	Positive cells (%)							
		CD34	CD33	CD1	CD4	CD8	cytCD3	mCD3	TCRab
1950	del(11)(p12p13)	0	0	0	85	91	90	80	pos
2846	del(11)(p12p13)	0	10	0	48	57	75	26	neg
2104	del(11)(p12p13)	0	0	0	6	1	98	45	pos
2698	t(11;14)(p13;q11)	1	8	0	42	69	93	3	neg
2789	t(11;14)(p13;q11)	1	12	25	59	73	85	12	neg
2735	t(11;14)(p13;q11)	4	1	71	90	94	82	8	neg

Pos; positive, Neg; negative, cytCD3; cytoplasmic CD3, mCD3; membrane CD3.

(Figure 1b). This deletion is therefore present in about 4% (6/138) of pediatric T-ALL patients. In 4 patients (1950, 2846, 2104 and 10110), the deleted region was flanked by the BAC clones RP1-187A11 (11p13) and RP11-72A10 (11p12), and comprised the clones RP1-22J9, RP11-90F13, RP11-91G22, AC090692.9, RP11-219O3 and RP11-36H11. In the 2 remaining cases (2774 and 704), the deleted area was smaller and flanked by the clones RP1-22J9 and RP11-72A10 (Figure 1b).

The resolution of the BAC array-CGH system as used for our analysis is approximately 1 Mb. To determine the exact telomeric and centromeric breakpoints for this del(11)(p12p13) in pediatric T-ALL, we used the oligo array-CGH system of Agilent Technologies with a resolution of approximately 35 Kb. In agreement with the BAC array-CGH data, the oligo array-CGH analysis showed identical genomic losses at 11p12-11p13 for these 6 patients albeit at higher resolution (Figure 2a-g). Detailed analysis of the telomeric breakpoints indicated that both *LMO2* probes located in intron 2, hybridized in a 1:1 ratio in patients 1950 (Figure 2b), 2846, 10110, 2774 and 704 (Figure 2g), indicating that this part of *LMO2* was retained. In all these cases, both probes situated in *M11S1* were deleted (Figure 2b, 2g). For patient 2104, the *LMO2* intron 2 probes were lost whereas the telomeric part of *LMO2* (exon 6) was retained (Figure 2e), indicating that the genomic breakpoint is probably located downstream of *LMO2* intron 2. At the centromeric breakpoint, the hybridization signals of both *RAG1* and *RAG2* probes were altered and indicated that one copy of both *RAG1* and *RAG2* genes were lost in patients 1950, 2846 and 10110, whereas they had retained the *LOC119710* locus (Figure 2c, 2g). For patient 2104 and 704, the centromeric breakpoint seemed to be situated in the *FLJ14213* gene (Figure 2f, 2g). For patient 2774, both *FLJ14213* probes were lost whereas the *TRAF6* probes hybridized normally.

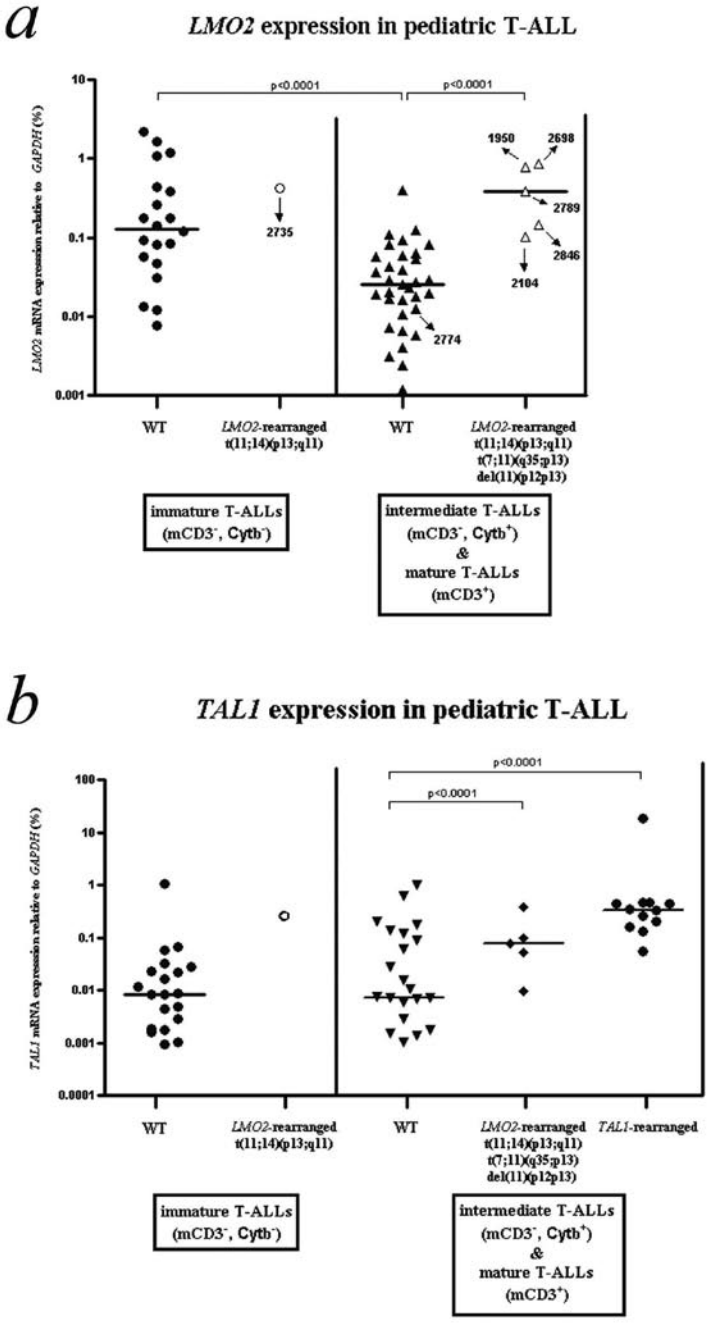

Figure 5. *LMO2* and *TAL1* expression in pediatric T-ALL.
Relative expression levels of *LMO2* **(a)** and *TAL1* **(b)** as percentage of *GAPDH* expression levels for 59 pediatric T-ALL patients (DCOG cohort). Patients were divided into 2 maturation stages according to their cytoplasmatic TCRβ (Cytβ) and membrane CD3 (mCD3) expression[35].

FISH analysis confirms array-CGH data

To confirm the BAC and oligo array-CGH data and to further characterize the exact breakpoints of this del(11)(p12p13), metaphase and interphase cells of the positive T-ALL cases were analyzed by FISH. In Figure 3a, the genomic positions of the FISH-probes are visualized. For patient 1950, FISH analysis with RP11-465C16 which covers both *RAG* genes, RP11-646J21 which covers the telomeric part of *LMO2* and RP11-98C11 which is located directly centromeric of *LMO2*, confirmed heterozygous loss of a region directly upstream of *LMO2* (Figure 3b). The RP11-603J2 probe that includes part of the *LMO2* locus was partly retained in the mutant allele (Figure 3c), indicating the telomeric breakpoint of the del(11)(p12p13) was situated in a 9 kb region surrounding exon 1 of *LMO2*. Similar analysis in this patient of the centromeric breakpoint indicated that both RP11-36H11 (Figure 3d) and RP11-769M16 (Figure 3e) were deleted, whereas at least part of RP11-465C16 was retained. This confirms that the telomeric breakpoint of the del(11)(p12p13) in this patient was located in or just flanking the *RAG* genes.

FISH analysis for the 5 other cases with del(11)(p12p13) (table 1) confirmed that this deletion also targeted *LMO2* in patients 2846, 2104 and 10110. However, for patients 2774 and 704 (table 1) both RP11-603J2 and RP11-98C11 probes showed a normal hybridization pattern, suggesting that in these cases the break had occurred upstream of *LMO2* between the *LMO2* and *M11S1* genes.

A single patient from the DCOG T-ALL cohort had a classical t(11;14)(p13;q11) by conventional cytogenetics. To determine the exact frequency of classical t(11;14)(p13;q11) or the t(7;11)(q34;p13) translocations involving *LMO2,* both the DCOG and the COALL cohorts (n=138) were analyzed by FISH using *LMO2* flanking BAC clones (data not shown). In total, 9 cases were identified that contained a translocation involving *LMO2* (9/138, 6.5%), including the patient also positive by conventional cytogenetics. Including these *LMO2* translocated patients, the frequency of *LMO2* rearrangements (t(11;14)(p13;q11), t(7;11)(q34;p13) or del(11)(p12p13)) was 9.4% (13/138) in total.

Molecular characterization of the del(11)(p12p13)

We next characterized the genomic breakpoint of the del(11)(p12p13) in T-ALL patient 1950 in more detail. Long-range PCR analysis on genomic DNA using primers situated in intron 1 of *RAG2* and intron 1 of *LMO2* revealed a specific band of ~2000bp (Figure 4a) for patient 1950 that was not present in a del(11)(p12p13) negative control (2720). Sequence analysis showed the exact positions of the genomic breakpoints in both intron regions (Figure 4b). It was expected that this deletion gives rise to a fusion of exon 1 of *RAG2* to exon 2 of *LMO2* which was confirmed at the mRNA level (Figure 4c-d). Subsequent RT-PCR failed to detect *RAG2-LMO2* fusion

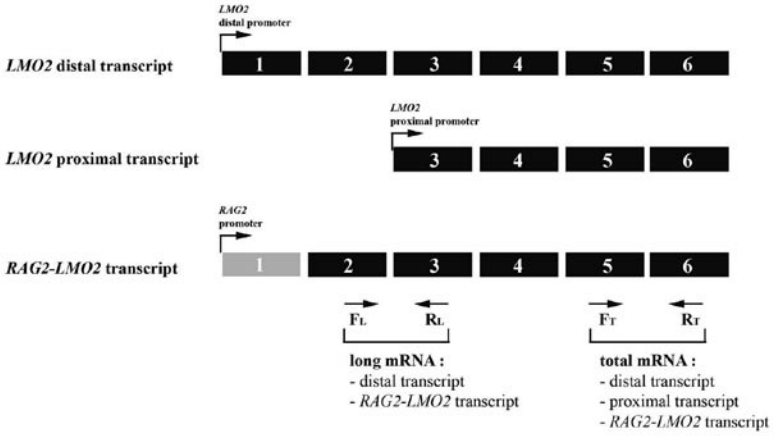

		Total *LMO2* mRNA		Long *LMO2* mRNA			
	Patient ID	dCt	expression level	dCt	expression level	%long	%prox
del(11)(p12p13)	1950	6.14	0.58577	8.52	0.05421	9.3	90.7
	2846	7.24	0.19499	10.15	0.01062	5.4	94.6
LMO2 translocation	2789	6.81	0.29974	9.11	0.03005	10.0	90.0
	2735	6.96	0.25799	9.43	0.02182	8.5	91.5

Figure 6. Elevated *LMO2* expression by activation of the *LMO2* proximal promoter.
Relative expression of long and total mRNA transcript levels of *LMO2* as measured by the RQ-PCR strategy. Long-transcripts including the *RAG2-LMO2* fusion transcript can be measured by the exon 2/3 primer combination, whereas the total amount of *LMO2* transcript was measured using an exon 5/6 primer combination. Expression of proximal promoter transcripts is calculated by subtracting the long-transcript expression from the total expression. Abbreviations: $F_{L,}$ forward primer long mRNA transcript; $R_{L,}$ reverse primer long mRNA transcript; $F_{T,}$ forward primer total mRNA transcript; $R_{T,}$ reverse primer total mRNA transcript; prox, proximal.

products in any of the remaining del(11)(p12p13) positive T-ALL patients. Therefore, we performed ligation-mediated PCR (LM-PCR) in order to determine additional genomic breakpoints. In patient 2846, LM-PCR with an *LMO2* intron 1 specific primer revealed an aberrant PCR product in addition to the expected wildtype band (Figure 4e). Sequence analysis showed that in this case *LMO2* intron 1 sequences were fused to a region located 72 kb upstream of *RAG2* (Figure 4f).

Del(11)(p12p13) correlates with a mature immunophenotype and high *LMO2* expression in T-ALL

Immunophenotypic analysis of *LMO2*-rearranged cases revealed that patients with the del(11)(p12p13) did not express CD34, CD33 or CD1 but expressed mCD3 (table 2). None of these cases expressed TCRγδ, whereas two patients expressed TCRαβ (1950 and 2104) and 2 patients were CD4/CD8 double positive (1950 and 2846)

in agreement with an immunophenotypic mature developmental stage. The *LMO2* translocated patients were immunophenotypically more immature. Two out of 3 cases expressed CD1 but none expressed mCD3 and/or the TCR. All 3 cases were CD4/CD8 double positive consistent with an early cortical developmental stage.

LMO2 mRNA expression levels of *LMO2* rearranged versus non-rearranged cases were measured using quantitative real-time RT-PCR (RQ-PCR) on 59 DCOG T-ALL patient samples for which immunophenotypic data were available. Since *LMO2* is highly expressed in T-ALL samples with an immature immunophenotype[33], we divided T-ALL samples into 2 categories: the first category included the immature double negative cases ($CD4^-/CD8^-$, mCD3-, $Cyt\beta^-$), whereas the second category comprised more mature cases with evidence for TCRβ rearrangements (Cytβ+) and/or TCR/CD3 expression[35]. For *LMO2* non-rearranged cases (WT), *LMO2* expression was significantly higher in the immature T-ALL cases compared to the immunophenotypic more advanced patients (Figure 5a, Mann-Whitney, p<0,0001). *LMO2* rearranged cases had significantly higher *LMO2* levels compared to the *LMO2* non-rearranged T-ALL patients with a comparable immunophenotype (p<0.0001). *LMO2* expression was low for patient 2774 (Figure 5a), which was in line with the observation that the deletion breakpoints did not affect the *LMO2* gene.

LMO2 rearrangements in relation to other oncogenic events in pediatric T-ALL

In order to determine the relation between *LMO2* rearrangments and other recurrent cytogenetic abnormalities in pediatric T-ALL, we screened all 13 *LMO2*-rearranged T-ALL patients for abnormalities at the *TAL1*, *TLX3*, *TLX1*, *CALM-AF10*, *MLL* and *cMYC* loci using FISH analysis and RQ-PCR (data not shown). None of the *LMO2* positive cases showed rearrangements of any of the loci mentioned above. Nevertheless, in the del(11)(p12p13) positive patient 2774 without involvement of *LMO2*, a *SIL-TAL1* interstitial deletion was identified. This indicates that del(11)(p12p13) positive T-ALL with elevated *LMO2* levels together with *LMO2* translocated T-ALL samples reflect a separate cytogenetic subgroup without detectable *TAL1*, *TLX3*, *TLX1*, *CALM-AF10*, *MLL* and *cMYC* abnormalities.

We further determined *TAL1* expression levels by RQ-PCR (Figure 5b). These analyses showed that for intermediate and mature T-ALL patients, *TAL1* is significantly higher expressed in both *LMO2*-rearranged (Figure 5b, Mann-Whitney, p<0,0001) and *TAL1*-rearranged (Figure 5b, Mann-Whitney, p<0,0001) cases, as compared to non-*LMO2/TAL1* rearranged samples.

LMO2 activation induced by enhanced activity of the *LMO2* proximal promoter

In patient 1950, the del(11)(p12p13) resulted in a *RAG2-LMO2* gene fusion in which the distal *LMO2* promoter is replaced by the *RAG2* promoter (Figure 4c). However,

in none of the remaining three del(11)(p12p13) positive patients with elevated *LMO2* levels, a comparable fusion product was detected suggesting that *RAG2-LMO2* fusion products were either expressed at very low levels or that other genomic regions were fused to *LMO2* such as found for patient 2846 (Figure 4f). We hypothesized that *LMO2* rearrangements due to the del(11)(p12p13) could result in the loss of a negative regulatory domain upstream of *LMO2*, with subsequent activation of the proximal promoter (exon 3), a situation comparable to *LMO2* translocated patients[36,37]. To elucidate which kind of *LMO2* transcripts are predominantly expressed, we developed a double RQ-PCR: one RQ-PCR can quantify *LMO2* transcripts derived from the distal *LMO2* promoter as well as *RAG2-LMO2* fusion products. The second RQ-PCR quantifies total *LMO2* transcripts derived from both the distal and proximal *LMO2* promoters as well as *RAG2-LMO2* fusion products (Figure 6). These analyses revealed that *LMO2* transcripts derived from the distal promoter or *RAG2-LMO2* fusion products in del(11)(p12p13) positive patients (1950 and 2846) only represent 5.5-9.3% of total *LMO2* transcripts (Figure 6). For both *LMO2*-translocated patients (2789 and 2735) also 8.5-10% of total *LMO2* transcripts originate from the distal promoter.

Clinical relevance of *LMO2* rearrangements in pediatric T-ALL

To study the prognostic relevance of *LMO2*-rearrangments in pediatric T-ALL, Kaplan–Meier disease-free-survival (DFS) curves were created for *LMO2*-rearranged cases versus *LMO2* wild type cases. In a stratified analysis of the combined DCOG and COALL cohorts (n=138), *LMO2*-rearrangements had borderline significance for poor outcome (log-rank, p=0.03).

DISCUSSION

LMO2 has been identified as oncogene in T-ALL due to its involvement in the translocation t(11;14)(p13;q11) or t(7;11)(q35;p13), in which the *TCR-LMO2* fusion results in a constitutive activation of the *LMO2* gene[15,16]. However, high *LMO2* expression levels have also been reported in the absence of translocations[32,38], suggesting that alternative mechanisms may exist in T-ALL resulting in the activation of *LMO2*.

Using the genome-wide array-CGH technique for the detection of genomic amplification an/or deletion areas, we identified a new recurrent deletion in pediatric T-ALL cases, i.e. the del(11)(p12p13). Screening pediatric T-ALL samples showed that this deletion is present in about 4% of pediatric T-ALL patients (6/138 cases). The genomic breakpoints are located in intron 1 of *RAG2* and intron 1 of *LMO2* for patient 1950, placing *LMO2* under the control of the *RAG2* promoter. As expected,

a *RAG2-LMO2* fusion product could be cloned. Since exon 1 of *RAG*2 does not contain a translation initiation-site and the translation initiation-site of *LMO2* is located in exon 3, this fusion product will produce normal LMO2 protein. However, *RAG2-LMO2* fusions could not be identified in any of the remaining del(11)(p12p13) positive T-ALL patients, suggesting that the localization of genomic breakpoints in these deletions are heterogeneous. This was demonstrated by the identification of the genomic breakpoint in patient 2846, in which the deletion caused fusion of a genomic region ~72 Kb upstream of the *RAG2* gene with *LMO2* intron 1 sequences. Although the exact genomic breakpoints of both other del(11)(p12p13) positive cases (2104 and 10110) remain to be identified, oligo array-CGH, FISH and RQ-PCR analyses predict involvement of *LMO2* in these cases alike patients 1950 and 2846.

Recently, it has been proposed that deletion of negative regulatory sequences, located approximately 3000 bp upstream of exon 1 of *LMO2,* could contribute to ectopic *LMO2* expression in T-cell leukemia[37]. Interestingly, this negative regulatory element was consistently removed in 4 del(11)(p12p13) positive T-ALL cases that target *LMO2*, and may therefore provide a mechanism for the enhanced *LMO2* activation in pediatric T-ALL. However, based upon the *RAG2-LMO2* fusion product that was identified in patient 1950, promoter substitution could also contribute to elevated levels of *LMO2* expression. Our RQ-PCR data supported only marginal contribution of the distal *LMO2* promoter from the remaining wildtype allele or *RAG2-LMO2* fusion products to the total *LMO2* mRNA levels in del(11)(p12p13) positive patients. Also, two *LMO2* translocated patients as analyzed by RQ-PCR demonstrated low distal *LMO2* promoter activity, confirming enhanced proximal promoter activity due to the loss of this negative regulatory domain[36,37].

Array-CGH and FISH data indicated that the deletion area for both del(11)(p12p13) positive patients 2774 and 704 is smaller compared to the other 4 del(11)(p12p13) positive patients. For both patients, the deletion seem to be located upstream of the negative regulatory region of *LMO2* as patient 2774 does not have elevated *LMO2* expression levels. These 2 cases may support the hypothesis that the minimally deleted region on chromosome 11 further contains a tumor suppressor gene that could contribute to the pathogenesis of T-ALL.

LMO2-rearranged cases of the DCOG cohort including those with the del(11)(p12p13) as well as the 3 patients with a t(11;14)(p13;q11) expressed significantly higher levels of *LMO2* than *LMO2* non-rearranged T-ALL samples with a comparable immunophenotypic development stage, i.e. the cortical or mature T-cell developmental stage. The expression was comparable to immature T-ALL patients that highly express *LMO2* as consequence of their immature developmental stage.[17,18] Nevertheless, a number of immunophenotypic more advanced T-ALL patients demonstrated high *LMO2* expression levels in the absence of currently known *LMO2* rearrangements,

yet other alternative mechanisms leading to *LMO2* activation in pediatric T-ALL may exist. *LMO2*-rearranged pediatric T-ALL samples with the del(11)(p12p13) may have a maturation stage that is more advanced in comparison to *LMO2* translocated patients. Two out of 3 cases with the del(11)(p12p13) involving the *LMO2* gene were TCRαβ positive. In contrast, none of the *LMO2* translocated patients expressed CD3 and/or TCRαβ but 2 out of these patients expressed CD1 conform an early cortical developmental stage. Whether this reflects true differences in maturation stage between patients with the del(11)(p12p13) and the *LMO2* translocated cases needs to be validated in a larger panel of patients. Similar variations in cortical and mature T-cell developmental stages were also observed for *TAL1*-rearranged T-ALL patients in the same cohort[32]. Deregulation of *LMO2* or *TAL1* may lead to a similar T-cell developmental arrest. *TAL1* and *LMO2* act in the same pentameric transcription complex, and deregulation of either of both genes may lead to the (in)activation of identical target genes.

The frequency of *LMO2* rearrangements in both cohorts combined is about 9%, and includes 4 patients with *LMO2* rearrangements due to the del(11)(p12p13) and 9 cases with a t(11;14)(p13;q11) or the t(7;11)(q35;p13). These *LMO2* abnormalities were shown to be independent of other recurrent cytogenetic abnormalities including *TAL1*, *TLX3*, *TLX1*, *CALM-AF10*, *MLL* or *cMYC*[32]. Patient 2774, which was del(11)(p12p13) positive but lacked *LMO2* activation, had an interstitial *SIL-TAL1* deletion.

Since *LMO2* and *TAL1* are frequently co-expressed in mature T-ALL cases and since no *TAL1* deletions and/or translocations were observed in the *LMO2*-rearranged cases, we determined *TAL1* mRNA expression in the 59 T-ALL samples for which *LMO2* expression data were available. These analyses confirmed that *TAL1* is significantly higher expressed in both *LMO2*- and *TAL1*-rearranged T-ALL cases, as compared to non-*LMO2/TAL1* rearranged samples. These data further suggest that for del(11)(p12p13) positive patients alternative mechanisms of *TAL1* activation besides *TAL1* deletions and translocations may exist in T-ALL or that *TAL1* may be a direct target gene for *LMO2*-driven transcription.

The presence of *LMO2*-rearrangements predicted for poor outcome in a stratified analysis of both the DCOG and COALL pediatric T-ALL cohorts. This prognostic significance has to be looked at cautiously due to the low number of patients, and a larger panel of T-ALL patients is needed to validate these findings. The presence of *LMO2* translocations did not predict for poor outcome in a previous study.[39]

In conclusion, we report the identification of a new cryptic cytogenetic abnormality, i.e. the del(11)(p12p13) in 6 pediatric T-ALL patients targeting the *LMO2* gene in 4 cases. For del(11)(p12p13) positive patients involving *LMO2*, the proximal *LMO2* promoter is highly activated due to the deletion of negative regulatory sequences upstream of *LMO2*. Abnormalities involving *LMO2*, including the del(11)(p12p13)

the t(7;11)(q35;p13) and the t(11;14)(p13;q11) are more common in pediatric T-ALL (9%) as appreciated up till now. *LMO2* abnormalities are independent from other recurrent cytogenetic abnormalities as frequently present in T-ALL.

ACKNOWLEDGEMENTS

We are greatly indebted to Dr A.W. Langerak for comments and critical discussion. We also thank Dr W. Dorlijn and R. Finch of Agilent Technologies, Dr. W. van Workum and A. Wijfjes of ServiceXS, Leiden, the Netherlands for technical support in the oligo array-CGH analysis.

REFERENCES

1. Pui CH, Relling MV, Downing JR. Acute lymphoblastic leukemia. N Engl J Med. 2004;350:1535-1548.
2. Armstrong SA, Look AT. Molecular genetics of acute lymphoblastic leukemia. J Clin Oncol. 2005;23:6306-6315.
3. Nagel S, Kaufmann M, Drexler HG, MacLeod RA. The cardiac homeobox gene NKX2-5 is deregulated by juxtaposition with BCL11B in pediatric T-ALL cell lines via a novel t(5;14)(q35.1;q32.2). Cancer Res. 2003;63:5329-5334.
4. Graux C, Cools J, Melotte C, et al. Fusion of NUP214 to ABL1 on amplified episomes in T-cell acute lymphoblastic leukemia. Nat Genet. 2004;36:1084-1089.
5. Speleman F, Cauwelier B, Dastugue N, et al. A new recurrent inversion, inv(7)(p15q34), leads to transcriptional activation of HOXA10 and HOXA11 in a subset of T-cell acute lymphoblastic leukemias. Leukemia. 2005;19:358-366.
6. Soulier J, Clappier E, Cayuela JM, et al. HOXA genes are included in genetic and biologic networks defining human acute T-cell leukemia (T-ALL). Blood. 2005;106:274-286.
7. Raimondi SC. Cytogenetics of acute leukemias. In: Pui C-H, ed. Childhood Leukemias. Cambridge: Press Syndicate of the University of Cambridge; 1999:168-196.
8. Rubnitz JE, Look AT. Molecular genetics of Acute Lymphoblastic Leukemia. In: Pui C-H, ed. Childhood Leukemiaws. Cambridge: Press Syndicate of the University of Cambridge; 1999:197-218.
9. Asnafi V, Radford-Weiss I, Dastugue N, et al. CALM-AF10 is a common fusion transcript in T-ALL and is specific to the TCRgammadelta lineage. Blood. 2003;102:1000-1006.
10. Weng AP, Ferrando AA, Lee W, et al. Activating mutations of NOTCH1 in human T cell acute lymphoblastic leukemia. Science. 2004;306:269-271.
11. Osada H, Grutz G, Axelson H, Forster A, Rabbitts TH. Association of erythroid transcription factors: complexes involving the LIM protein RBTN2 and the zinc-finger protein GATA1. Proc Natl Acad Sci U S A. 1995;92:9585-9589.
12. Wadman IA, Osada H, Grutz GG, et al. The LIM-only protein Lmo2 is a bridging molecule assembling an erythroid, DNA-binding complex which includes the TAL1, E47, GATA-1 and Ldb1/NLI proteins. Embo J. 1997;16:3145-3157.
13. Grutz GG, Bucher K, Lavenir I, Larson T, Larson R, Rabbitts TH. The oncogenic T cell LIM-protein Lmo2 forms part of a DNA-binding complex specifically in immature T cells. Embo J. 1998;17:4594-4605.
14. Vitelli L, Condorelli G, Lulli V, et al. A pentamer transcriptional complex including tal-1 and retinoblastoma protein downmodulates c-kit expression in normal erythroblasts. Mol Cell Biol. 2000;20:5330-5342.
15. Anderson KP, Crable SC, Lingrel JB. Multiple proteins binding to a GATA-E box-GATA motif regulate the erythroid Kruppel-like factor (EKLF) gene. J Biol Chem. 1998;273:14347-14354.
16. Ono Y, Fukuhara N, Yoshie O. TAL1 and LIM-only proteins synergistically induce retinaldehyde dehydrogenase 2 expression in T-cell acute lymphoblastic leukemia by acting as cofactors for GATA3. Mol Cell Biol. 1998;18:6939-6950.
17. McCormack MP, Forster A, Drynan L, Pannell R, Rabbitts TH. The LMO2 T-cell oncogene is activated via chromosomal translocations or retroviral insertion during gene therapy but has no mandatory role in normal T-cell development. Mol Cell Biol. 2003;23:9003-9013.

18. Ferrando AA, Herblot S, Palomero T, et al. Biallelic transcriptional activation of oncogenic transcription factors in T-cell acute lymphoblastic leukemia. Blood. 2004;103:1909-1911.

19. Fisch P, Boehm T, Lavenir I, et al. T-cell acute lymphoblastic lymphoma induced in transgenic mice by the RBTN1 and RBTN2 LIM-domain genes. Oncogene. 1992;7:2389-2397.

20. Neale GA, Rehg JE, Goorha RM. Ectopic expression of rhombotin-2 causes selective expansion of CD4-CD8- lymphocytes in the thymus and T-cell tumors in transgenic mice. Blood. 1995;86:3060-3071.

21. Larson RC, Osada H, Larson TA, Lavenir I, Rabbitts TH. The oncogenic LIM protein Rbtn2 causes thymic developmental aberrations that precede malignancy in transgenic mice. Oncogene. 1995;11:853-862.

22. Larson RC, Fisch P, Larson TA, et al. T cell tumours of disparate phenotype in mice transgenic for Rbtn-2. Oncogene. 1994;9:3675-3681.

23. Neale GA, Rehg JE, Goorha RM. Disruption of T-cell differentiation precedes T-cell tumor formation in LMO-2 (rhombotin-2) transgenic mice. Leukemia. 1997;11 Suppl 3:289-290.

24. McGuire EA, Hockett RD, Pollock KM, Bartholdi MF, O'Brien SJ, Korsmeyer SJ. The t(11;14)(p15;q11) in a T-cell acute lymphoblastic leukemia cell line activates multiple transcripts, including Ttg-1, a gene encoding a potential zinc finger protein. Mol Cell Biol. 1989;9:2124-2132.

25. Royer-Pokora B, Loos U, Ludwig WD. TTG-2, a new gene encoding a cysteine-rich protein with the LIM motif, is overexpressed in acute T-cell leukaemia with the t(11;14)(p13;q11). Oncogene. 1991;6:1887-1893.

26. McCormack MP, Rabbitts TH. Activation of the T-cell oncogene LMO2 after gene therapy for X-linked severe combined immunodeficiency. N Engl J Med. 2004;350:913-922.

27. Hacein-Bey-Abina S, Von Kalle C, Schmidt M, et al. LMO2-associated clonal T cell proliferation in two patients after gene therapy for SCID-X1. Science. 2003;302:415-419.

28. Stam RW, den Boer ML, Meijerink JP, et al. Differential mRNA expression of Ara-C-metabolizing enzymes explains Ara-C sensitivity in MLL gene-rearranged infant acute lymphoblastic leukemia. Blood. 2003;101:1270-1276.

29. Iafrate AJ, Feuk L, Rivera MN, et al. Detection of large-scale variation in the human genome. Nat Genet. 2004;36:949-951.

30. Barrett MT, Scheffer A, Ben-Dor A, et al. Comparative genomic hybridization using oligonucleotide microarrays and total genomic DNA. Proc Natl Acad Sci U S A. 2004;101:17765-17770.

31. Rigby PW, Dieckmann M, Rhodes C, Berg P. Labeling deoxyribonucleic acid to high specific activity in vitro by nick translation with DNA polymerase I. J Mol Biol. 1977;113:237-251.

32. van Grotel M, Meijerink JPP, Beverloo HB, Langerak AW, Buys-Gladdines J, Schneider P, Poulsen TS, Horstmann M, Kamps WA, Veerman AJ, van Wering ER, van Noesel MM, Pieters R. The outcome of molecular-cytogenetic subgroups in pediatric T-cell acute lymphoblastic leukemia: a retrospective study for patients treated according to DCOG or COALL protocols. Haematologica, 2006.

33. Przybylski GK, Dik WA, Wanzeck J, et al. Disruption of the BCL11B gene through inv(14)(q11.2q32.31) results in the expression of BCL11B-TRDC fusion transcripts and is associated with the absence of wild-type BCL11B transcripts in T-ALL. Leukemia. 2005;19:201-208.

34. Meijerink J, Mandigers C, van de Locht L, Tonnissen E, Goodsaid F, Raemaekers J. A novel method to compensate for different amplification efficiencies between patient DNA samples in quantitative real-time PCR. J Mol Diagn. 2001;3:55-61.

35. Asnafi V, Beldjord K, Boulanger E, et al. Analysis of TCR, pT alpha, and RAG-1 in T-acute lymphoblastic leukemias improves understanding of early human T-lymphoid lineage commitment. Blood. 2003;101:2693-2703.

36. Royer-Pokora B, Rogers M, Zhu TH, Schneider S, Loos U, Bolitz U. The TTG-2/RBTN2 T cell oncogene encodes two alternative transcripts from two promoters: the distal promoter is removed by most 11p13 translocations in acute T cell leukaemia's (T-ALL). Oncogene. 1995;10:1353-1360.

37. Hammond SM, Crable SC, Anderson KP. Negative regulatory elements are present in the human LMO2 oncogene and may contribute to its expression in leukemia. Leuk Res. 2005;29:89-97.

38. Ferrando AA, Neuberg DS, Staunton J, et al. Gene expression signatures define novel oncogenic pathways in T cell acute lymphoblastic leukemia. Cancer Cell. 2002;1:75-87.

39. Ferrando AA, Look AT. Gene expression profiling in T-cell acute lymphoblastic leukemia. Semin Hematol. 2003;40:274-280.

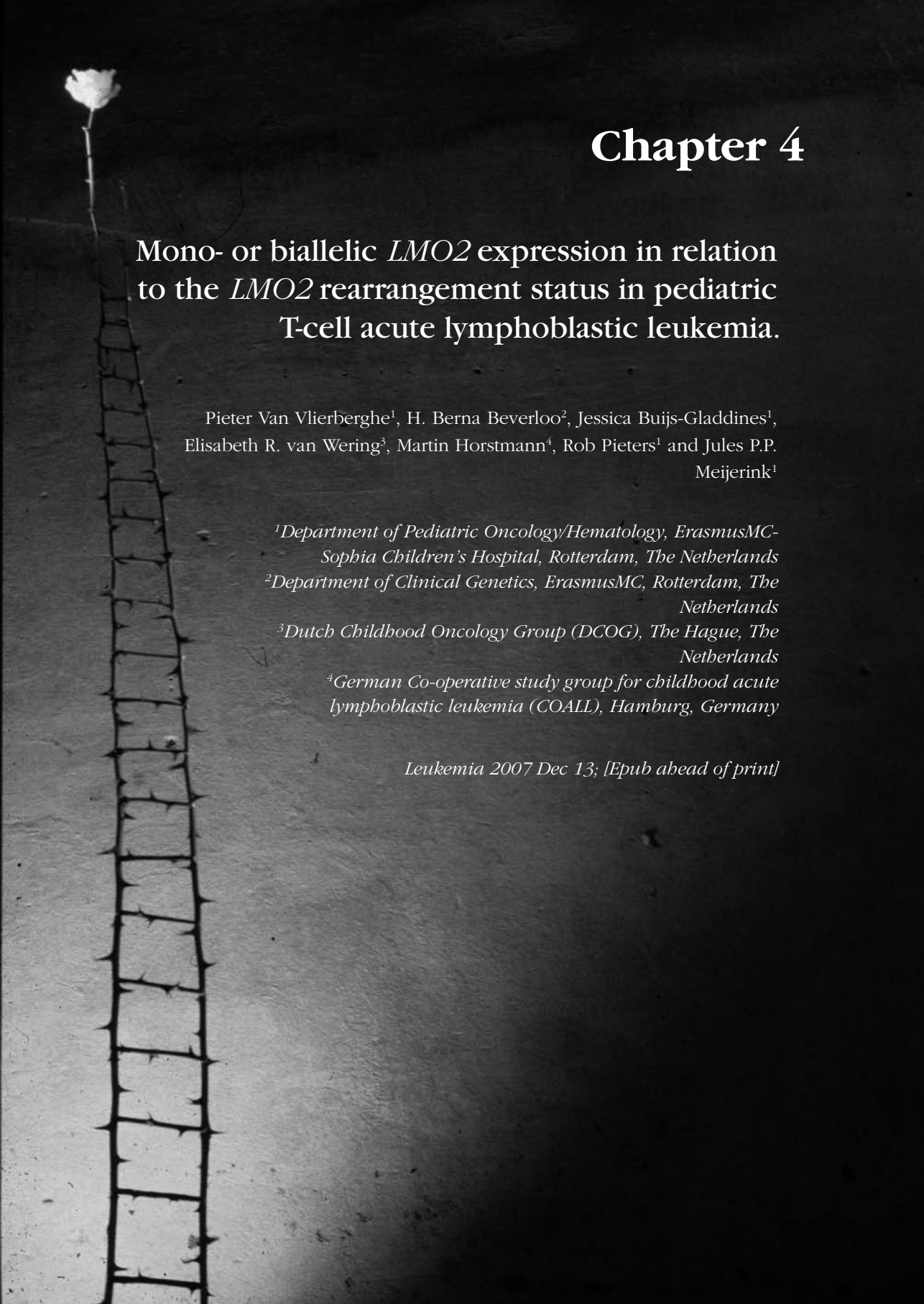

Chapter 4

Mono- or biallelic *LMO2* expression in relation to the *LMO2* rearrangement status in pediatric T-cell acute lymphoblastic leukemia.

Pieter Van Vlierberghe[1], H. Berna Beverloo[2], Jessica Buijs-Gladdines[1], Elisabeth R. van Wering[3], Martin Horstmann[4], Rob Pieters[1] and Jules P.P. Meijerink[1]

[1]Department of Pediatric Oncology/Hematology, ErasmusMC-Sophia Children's Hospital, Rotterdam, The Netherlands
[2]Department of Clinical Genetics, ErasmusMC, Rotterdam, The Netherlands
[3]Dutch Childhood Oncology Group (DCOG), The Hague, The Netherlands
[4]German Co-operative study group for childhood acute lymphoblastic leukemia (COALL), Hamburg, Germany

Leukemia 2007 Dec 13; [Epub ahead of print]

TO THE EDITOR

T-cell acute lymphoblastic leukemia (T-ALL) is an aggressive malignancy of thymocytes in which multiple genetic defects cooperate during pathogenesis resulting in uncontrolled cell growth. For T-ALL, a large variety of genetic rearrangements have been identified including chromosomal translocations, deletions, amplifications, duplications and mutations. Translocations predominantly involve aberrant rearrangements of the T-cell receptor (TCR) loci during T-cell development through illegitimate V(D)J recombination. These recombination errors ultimately result in the activation of oncogenes[1].

One such an important oncogene is *LMO2*. In the t(11;14)(p13;q11) and t(7;11)(q35;p13) translocations, the *LMO2* gene is brought in close proximity of the *TCR*α/δ or *TCR*β enhancers possibly boosting *LMO2* expression[1]. Hammond *et al*. demonstrated that deletion of a negative regulatory element (NRE) located just upstream the *LMO2* locus also activates the *LMO2* gene[2]. This alternative mechanism for *LMO2* activation also occurs in human cancer as we identified the recurrent interstitial deletion, del(11)(p12p13), in pediatric T-ALL in which loss of the NRE region is associated with *LMO2* activation[3]. It was recently proposed that for most *LMO2* translocations, *LMO2* activation is presumably caused by the loss of the NRE region during the translocation event rather than the juxtaposition of *LMO2* in the vicinity of the TCR-enhancers[4].

The NRE region is a relatively small domain comprised by a region of approximately 3000 base pairs directly upstream of the transcription initiation site of *LMO2*[2]. Our initial screening for *LMO2* translocations or cryptic *LMO2* deletions using FISH on 138 childhood T-ALL cases[3] may have been unsuccessful to detect relatively small deletions upstream of *LMO2* including this NRE region. For this reason, we developed a Multiplex Ligation Probe Amplification (MLPA) assay[5] with multiple probes located in or just flanking the NRE region to detect such smaller deletions upstream of *LMO2* (Figure 1A). Using some of our previously identified del(11)(p12p13)-positive cases[3] as positive controls, the MLPA assay confirmed the location of the telomeric breakpoints in these samples (Figure 1B). Re-screening of our cohort revealed one additional T-ALL case (#2845) with an *LMO2* deletion that had remained undetected in our previous FISH screening (Figure 1C). Oligo array-CGH analysis on patient DNA confirmed the presence of the deletion, del(11)(p13p13), which was about 400 kb in size and included part of the NRE-element and the centromeric genes *M11S1*, *NAT10* and *ABTB2* (Figure 2A). Copy number variations at this specific genomic locus have not been reported for the normal population[6]. In addition, FISH analysis using a BAC clone situated just upstream of *LMO2* (RP11-98C11) in combination with an *LMO2* telomeric BAC clone (RP11-646J21) confirmed the loss of this genomic

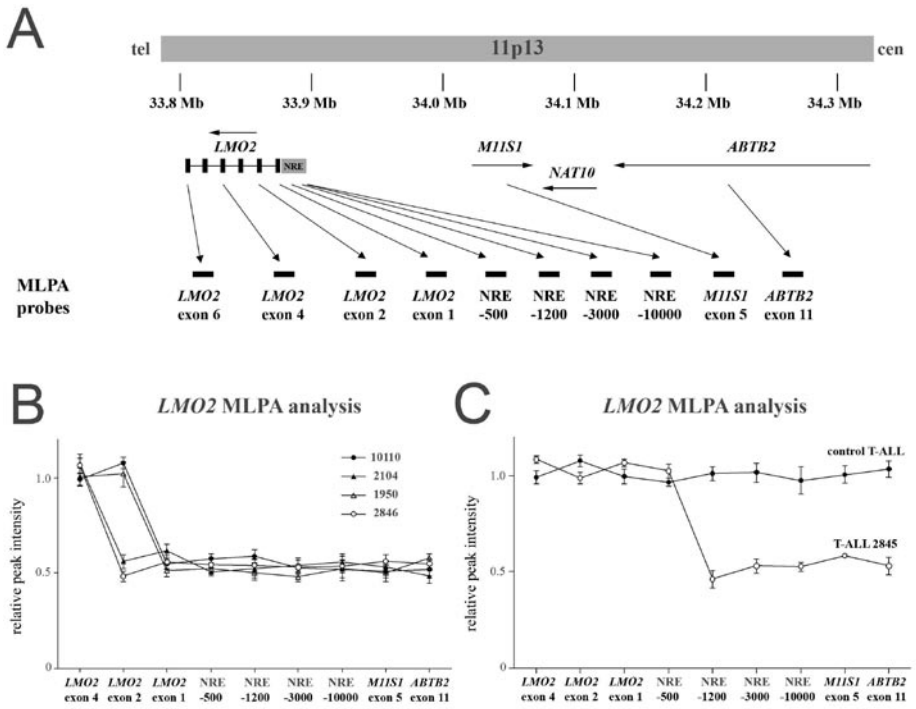

Figure 1. MLPA analysis of the *LMO2* gene in pediatric T-ALL.
(a) Overview of the localization of the MLPA probes in the genomic locus surrounding the *LMO2* gene at chromosomal band 11p13. **(b)** MLPA analysis of 4 del(11)(p12p13)-positive cases for the genomic loci described in (a). For each MLPA probe, the peak intensity, relative to the endogenous reference peak (*LMO2* exon 6), is shown for each case. When 2 copies are present for each indicated genomic region, the relative peak intensities range between 0.9 and 1.1. Peak intensities between 0.4 and 0.6 indicate a one-copy loss for that specific region. **(c)** Similar MLPA analysis on different childhood T-ALL cases revealed an additional T-ALL case (#2845) with an *LMO2* deletion, starting in between 500 and 1200 bp upstream of the *LMO2* gene.

region (Figure 2B). This indicates that smaller del(11)(p13p13) deletions compared to the del(11)(p12p13) deletions as previously described[3] occur in pediatric T-ALL (Figure 2C). Because of the differences in the deletion area among T-ALL cases, MLPA analysis could serve as a valuable additional tool to FISH screening for the proper identification of *LMO2* rearranged T-ALL cases.

To study the effect of this deletion in case #2845 in relation to *LMO2* expression, the *LMO2* mRNA expression level for this case as measured using quantitative real-time RT-PCR (RQ-PCR) was compared to the expression levels of 66 *LMO2* rearranged and non-rearranged T-ALL cases (Figure 3). As *LMO2* is normally highly expressed in early T-cell development and is repressed during later development stages[7-9], we distinguished T-ALL cases with an immature immunophenotype (IM: Cytβ^-, mCD3$^-$,

TCRαβ$^-$, TCRγδ$^-$) from those with an cytoplasmatic-beta (Cytβ) positive, intermediate (pre-αβ: Cytβ$^+$, mCD3$^-$, TCR$^-$) or mature immunophenotype (mCD3$^+$, TCRαβ$^+$ or TCRγδ$^+$)[10]. The leukemic cells from case #2845 had a mature immunophenotype and showed high *LMO2* levels comparable to levels as observed in other *LMO2* rearranged cases[3]. Pre-αβ and mature T-ALL cases without *LMO2* rearrangements significantly expressed lower *LMO2* levels (Figure 3).

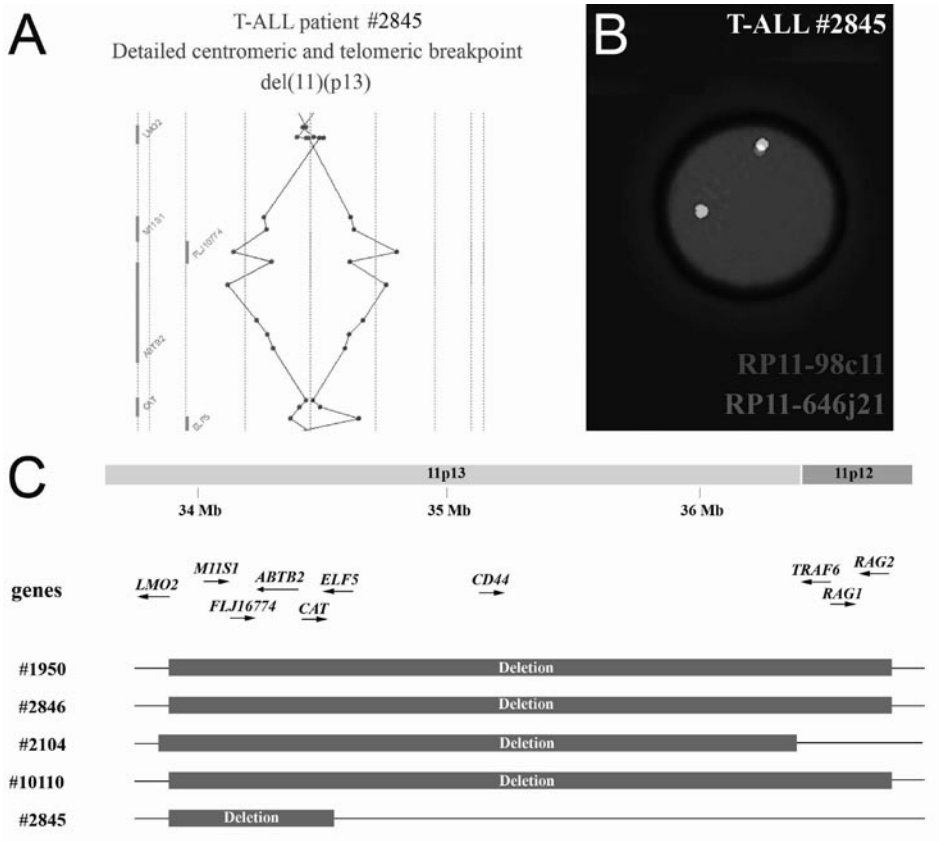

Figure 2. A novel cryptic deletion, del(11)(p13p13), targeting *LMO2* in T-ALL.
(a) Detailed overview of the centromeric and telomeric breakpoints of the del(11)(p13p13) deletion based upon oligo array-CGH micro-array results (44K oligo array, Agilent) for T-ALL case #2845. Patient DNA versus control DNA ratios are indicated in Blue whereas the reciprocal experiment is shown in red. Hybridization signals around the –2X or +2X lines represent loss of the corresponding region in the patient DNA. **(b)** FISH analysis using a BAC clone situated just upstream (RP11-98C11, Red) and downstream (RP11-646J21, Green) of *LMO2* confirming loss of a genomic region upstream of *LMO2* in case 2845. **(c)** Overview of the deletion areas for del(11)(p12p13) positive cases as previously described[3] as well as the del(11)(p13p13) of case #2845 characterized by the activation of the *LMO2* gene. RP11-98C11 is situated just upstream of *LMO2*, whereas RP11-646J21 is positioned telomeric of *LMO2*.

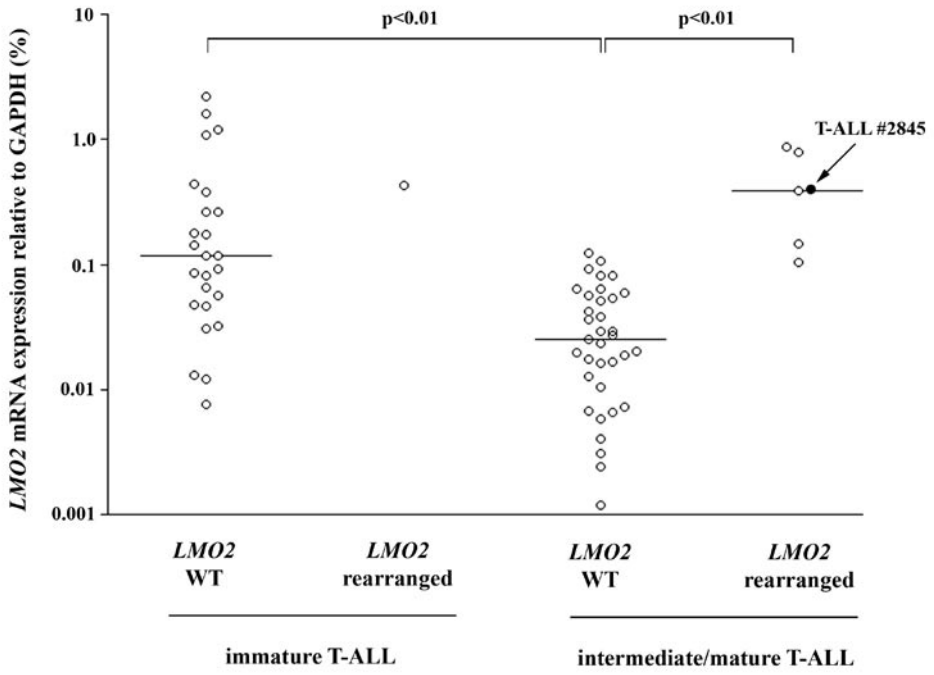

Figure 3. *LMO2* expression in *LMO2*-rearranged and non-rearranged samples in relation to T-cell development stage. Relative expression levels of *LMO2* as percentage of *GAPDH* expression levels for 67 pediatric T-ALL patients treated on DCOG protocols. Patients were classified based upon their T-cell development status: Immature cases (Cytβ$^-$, mCD3$^-$, TCRαβ$^-$, TCRγδ$^-$) versus intermediate/mature cases: pre-αβ (Cytβ$^+$, mCD3$^-$, TCRαβ$^-$, TCRγδ$^-$) and mature cases (mCD3$^+$, TCRαβ$^+$ or TCRγδ$^+$). The horizontal line indicates the median *LMO2* expression level.

About half of the immature T-ALL cases without *LMO2* rearrangements also displayed high *LMO2* levels comparable to levels as observed in *LMO2* rearranged cases. Although postulated as an oncogenic mechanism in the absence of cytogenetic rearrangements by Ferrando and coworkers (2004)[7], high *LMO2* expression levels could also be attributed to a residual characteristic of early T-cell development[7-9] rather than reflecting an oncogenic hit.

In support of this notion, 7 out of 12 IM T-ALL cases with high *LMO2* levels (above the median, Figure 3) are characterized by other recurrent abnormalities that are commonly mutually exclusive and may delineate specific subgroups in T-ALL. From these, 5 single cases had an *MLL-AF6* translocation, a *CALM-AF10* translocation, a *cMYB-TCR*β translocation, a *TAL2-TCR*β translocation or an *TLX1* rearrangement, while 2 cases had a *TLX3* rearrangement.

To further support that high *LMO2* expression in these IM T-ALL cases is a reflection of early T-cell maturation arrest rather than an oncogene activation mechanism, we investigated whether *LMO2* expression was driven from a single allele or both

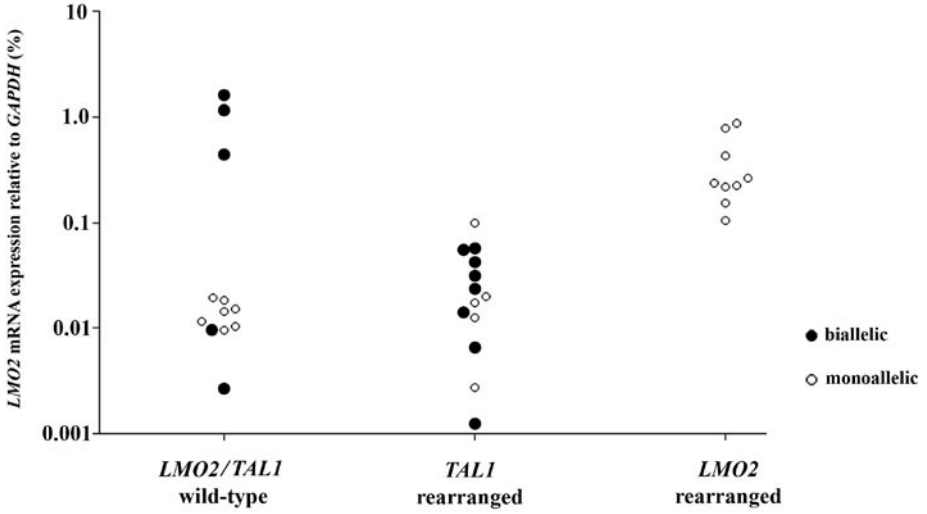

Figure 4. Mono- or biallelic *LMO2* expression in pediatric T-ALL patients.
LMO2 mRNA expression levels relative to *GAPDH* (%) for 34 selected pediatric T-ALL patients. Mono- or bi-allelic expression of the *LMO2* gene is visualized as open or filled circles, respectively.

alleles. For this, we performed allele-specific *LMO2* mRNA analysis[7] using an RT-PCR and sequencing approach on selected T-ALL cases including 27 *TAL1* rearranged cases, 14 *LMO2* rearranged cases, 1 *MLL*-rearranged case and 25 cases lacking currently known molecular-cytogenetic abnormalities. These latter cases are denoted as 'unknown' cases. Thirty-four out of these 67 samples were informative (heterozygous) at the DNA level for a single nucleotide polymorphism in the 3'UTR region of *LMO2* including 13 *TAL1* rearranged, 9 *LMO2* rearranged, and 1 *MLL* rearranged case as well as 11 unknown cases (Table 1).

All *LMO2* rearranged cases analyzed demonstrated monoallelic *LMO2* activation (Figure 4; table 1), indicating that cis-acting mechanisms (loss of the NRE and/or juxtaposition to the TCR enhancer) resulted in ectopic *LMO2* expression of the rearranged allele with no or neglectable expression of the remaining wild-type allele. A number of T-ALL cases without known *LMO2* rearrangements also expressed *LMO2* in a monoallelic manner. Although the *LMO2* expression levels in these case are relatively low, it would still be possible that they contain deletions, insertions or point-mutations in the NRE region, that have remained undetected by FISH or MLPA analysis. Most *TAL1* rearranged cases as well as about half of all *LMO2/TAL1* non-rearranged cases with lower *LMO2* levels compared to the *LMO2* rearranged cases demonstrated biallelic *LMO2* expression (Figure 4). Biallelic *LMO2* expression was also observed for the 3 *LMO2* wildtype cases with an immature phenotype (1 MLL+

Table 1. *LMO2* expression levels and genetic characteristics of 34 T-ALL cases.

ID	Genetics		LMO2 expression	Mono-/biallelic
	subgroup	rearrangement		
2793	Unknown	Unknown	0.43644	Biallelic
2847	MLL	Translocation	1.62321	Biallelic
2782	Unknown	Unknown	1.20903	Biallelic
2436	Unknown	Unknown	0.01051	Monallelic
230	Unknown	Unknown	0.00955	Monoallelic
1632	Unknown	Unknown	0.01522	Monallelic
9160	Unknown	Unknown	0.01955	Monoallelic
9696	Unknown	Unknown	0.01849	Monallelic
1032	Unknown	Unknown	0.00264	Biallelic
2805	Unknown	Unknown	0.01158	Monallelic
9027	Unknown	Unknown	0.00955	Biallelic
9376	Unknown	Unknown	0.01437	Monallelic
8815	TAL1	SIL-TAL1	0.09987	Monoallelic
9083	TAL1	SIL-TAL1	0.05399	Biallelic
2720	TAL1	Translocation	0.04265	Biallelic
1949	TAL1	SIL-TAL1	0.03254	Biallelic
9243	TAL1	SIL-TAL1	0.03216	Biallelic
3037	TAL1	SIL-TAL1	0.02325	Biallelic
258	TAL1	SIL-TAL1	0.02004	Monoallelic
1941	TAL1	SIL-TAL1	0.01757	Monoallelic
1842	TAL1	SIL-TAL1	0.01385	Biallelic
2759	TAL1	SIL-TAL1	0.01259	Monoallelic
2722	TAL1	Translocation	0.00659	Biallelic
8628	TAL1	Translocation	0.00273	Monoallelic
750	TAL1	SIL-TAL1	0.00123	Biallelic
704	LMO2	Deletion	0.26546	Monoallelic
10110	LMO2	Deletion	0.21543	Monoallelic
1950	LMO2	Deletion	0.78396	Monoallelic
2104	LMO2	Deletion	0.10322	Monoallelic
492	LMO2	Translocation	0.23423	Monoallelic
344	LMO2	Translocation	0.15513	Monoallelic
2698	LMO2	Translocation	0.86385	Monoallelic
9928	LMO2	Translocation	0.22135	Monoallelic
2735	LMO2	Translocation	0.43043	Monoallelic

case and 2 unknown cases) that had the highest *LMO2* expression levels comparable to *LMO2* rearranged cases.

In conclusion, our study confirms that MLPA analysis for the detection of deletions upstream of *LMO2* gene which includes the NRE region is a valuable tool to screen T-ALL patients for the del(11)(p12p13) mostly leading to ectopic *LMO2* expression. Furthermore, bi-allelic activation of *LMO2* in immature T-ALL cases may reflect their early T-cell development stage rather than it represents a true oncogenic mechanism.

REFERENCES

1. Graux, C., Cools, J., Michaux, L., Vandenberghe, P. & Hagemeijer, A. Cytogenetics and molecular genetics of T-cell acute lymphoblastic leukemia: from thymocyte to lymphoblast. *Leukemia* **20**, 1496-510 (2006).
2. Hammond, S. M., Crable, S. C. & Anderson, K. P. Negative regulatory elements are present in the human LMO2 oncogene and may contribute to its expression in leukemia. *Leuk Res* **29**, 89-97 (2005).
3. Van Vlierberghe, P. et al. The cryptic chromosomal deletion del(11)(p12p13) as a new activation mechanism of LMO2 in pediatric T-cell acute lymphoblastic leukemia. *Blood* **108**, 3520-9 (2006).
4. Dik, W. A. et al. Different chromosomal breakpoints impact the level of LMO2 expression in T-ALL. *Blood* **110**, 388-92 (2007).
5. Schouten, J. P. et al. Relative quantification of 40 nucleic acid sequences by multiplex ligation-dependent probe amplification. *Nucleic Acids Res* **30**, e57 (2002).
6. Redon, R. et al. Global variation in copy number in the human genome. *Nature* **444**, 444-54 (2006).
7. Ferrando, A. A. et al. Biallelic transcriptional activation of oncogenic transcription factors in T-cell acute lymphoblastic leukemia. *Blood* **103**, 1909-11 (2004).
8. Pike-Overzet, K. et al. Ectopic retroviral expression of LMO2, but not IL2Rgamma, blocks human T-cell development from CD34+ cells: implications for leukemogenesis in gene therapy. *Leukemia* **21**, 754-63 (2007).
9. Herblot, S., Steff, A. M., Hugo, P., Aplan, P. D. & Hoang, T. SCL and LMO1 alter thymocyte differentiation: inhibition of E2A-HEB function and pre-T alpha chain expression. *Nat Immunol* **1**, 138-44 (2000).
10. Asnafi, V. et al. Age-related phenotypic and oncogenic differences in T-cell acute lymphoblastic leukemias may reflect thymic atrophy. *Blood* **104**, 4173-80 (2004).

Chapter 5

The recurrent *SET-NUP214* fusion as a new *HOXA* activation mechanism in pediatric T-cell acute lymphoblastic leukemia

Pieter Van Vlierberghe[1], Martine van Grotel[1], Joëlle Tchinda[2], Charles Lee[2], H. Berna Beverloo[3], Peter J. van der Spek[4], Andrew Stubbs[4], Jan Cools[5], Kyosuke Nagata[6], Maarten Fornerod[7], Jessica Buijs-Gladdines[1], Martin Horstmann[8], Elisabeth R. van Wering[9], Jean Soulier[10], Rob Pieters[1] and Jules P.P. Meijerink[1]

[1]Department of Pediatric Oncology/Hematology, Erasmus MC / Sophia Children's Hospital, Rotterdam, The Netherlands
[2]Department of Pathology, Brigham and Women's Hospital, Harvard Medical School, Boston, USA
[3]Department of Clinical Genetics, Erasmus MC, Rotterdam, The Netherlands
[4]Department of Bioinformatics, Erasmus MC, Rotterdam, The Netherlands
[5]Department of Molecular and Developmental genetics, Flanders Interuniversity Institute for Biotechnology (VIB), University of Leuven, Leuven, Belgium
[6]Department of Infection Biology, Graduate School of Comprehensive Human Sciences and Institute of Basic Medical Sciences, University of Tsukuba, Japan
[7]Department of Tumor biology, The Netherlands Cancer Institute, Amsterdam, The Netherlands
[8]German Co-operative study group for childhood acute lymphoblastic leukemia (COALL), Hamburg, Germany
[9]Dutch Childhood Oncology Group (DCOG), The Hague, The Netherlands
[10]Hematology Laboratory, APHP, Hôpital Saint-Louis, Paris, France

Blood 2008 Feb 22; [Epub ahead of print]

ABSTRACT

T-cell acute lymphoblastic leukemia (T-ALL) is mostly characterized by specific chromosomal abnormalities, some occurring in a mutually exclusive manner possibly delineating specific T-ALL subgroups. One subgroup, including *MLL*-rearranged, *CALM-AF10* or inv(7)(p15q34) cases, is characterized by elevated expression of *HOXA* genes. Using a gene expression based clustering analysis of 67 T-ALL cases with recurrent molecular genetic abnormalities and 25 samples lacking apparent aberrations, we identified 5 new cases with elevated *HOXA* levels. Using array-CGH, a cryptic and recurrent deletion, del(9)(q34.11q34.13), was exclusively identified in 3 of these 5 cases. This deletion results in a conserved SET-NUP214 fusion product, that was also identified in the T-ALL cell line LOUCY. SET-NUP214 binds in the promoter regions of specific *HOXA* genes, where it interacts with CRM1 and DOT1L leading to the transcriptional activation of *HOXA* genes. Targeted inhibition of SET-NUP214 by siRNA abolished expression of *HOXA* genes, inhibited proliferation and induced differentiation in LOUCY but not in other T-ALL lines. We conclude that SET-NUP214 contributes to the pathogenesis of T-ALL by enforcing T-cell differentiation arrest.

INTRODUCTION

T-cell acute lymphoblastic leukemia (T-ALL) is a thymocytes malignancy, and represents about 15% of pediatric ALL cases. T-ALL often presents with a high tumour-mass, accompanied by a rapid progression of disease. Still, about 30% of T-ALL cases relapse during therapy or within the first 2 years following treatment and eventually die[1].

Over the last years, great progress has been made in unravelling the genetics of T-ALL, including chromosomal translocations (*TAL1*, *LYL1*, *LMO1*, *LMO2*, *TLX1*, *TLX3*, *MYB, Cyclin D2*), deletions (*SIL-TAL1*, del(6q), del(9)(p21), del(11)(p12p13)), amplifications (*NUP214-ABL1)*, duplications *(MYB*) and mutations (*RAS*, *NOTCH1*)[2-13]. Various of these abnormalities represent unique aberrations possibly delineating distinct T-ALL subgroups (i.e. *TAL1*, *LMO1*, *LMO2*, *TLX1*, *TLX3*, *CALM-AF10*, *MLL*, Inv(7)). Others are shared by various of these subgroups and may lead to the deregulation of cell-cycle (i.e. del(9)(p21) that includes the *CDKN2A/p15* and *CDKN2B/p16* loci)[3,4]. Some may be acquired during leukemic growth and are predominantly associated with relapse, like the episomal *NUP214-ABL1* amplification[6]. *NOTCH1* activation mutations are present in more than half of all T-ALL cases irrespective of the presence of other rearrangements[7]. It has been hypothesized that activation of *NOTCH1* represents one of the most advanced abnormalities in T-ALL that may enable for uncontrolled proliferation and/or inhibition of apoptosis possibly through upregulation of the target genes *cMYC* and *DELTEX1*[14-16].

In contrast to the wide variety of genetic abnormalities in T-ALL, initial microarray studies have revealed only 5 different expression clusters: immature/*LYL1*, *TAL1*, *TLX1*, *TLX3* and *HOXA* clusters[8,17]. One of the explanations for this phenomenon is that cases with different molecular cytogenetic defects may share a highly similar expression profile and are being recognized as one single expression cluster[8,17]. For example, cases with different abnormalities demonstrate high expression of genes of the *HOXA* cluster (*HOXA5*, *-A9*, *-A10* and *-A11*). This cluster includes patients with *CALM-AF10*[8,18] or *MLL*-rearrangements[8,19] or cases with an inversion on chromosome 7 due to the rearrangement of the *T-cell receptor-beta* (*TCR*β) locus into the *HOXA* cluster[8,10]. Elevated *HOXA* gene expression levels have also been reported in the absence of these genetic aberrations[8,20], suggesting that alternative mechanisms of *HOXA* activation may exist in T-ALL.

Previously, we have studied the incidence and prognostic relevance of recurrent molecular cytogenetic abnormalities for pediatric T-ALL[21]. Within our cohort, about half of the T-ALL patients lack currently known molecular cytogenetic abnormalities. To identify the underlying genetic defects in these patients, we used various high-resolution genomic screening strategies including microarray-based comparative

genomic hybridization (array-CGH). We recently described a new and recurrent deletion, i.e. the del(11)(p12p13), in about 4 percent of T-ALL patients[12]. This interstitial deletion leads to the loss of a negative regulatory domain upstream of *LMO2* resulting in ectopic expression of this oncogene. Array-CGH also led to the identification of a recurrent duplication of *MYB* in about 10 percent of T-ALL patients[2,9].

In this study, we combined gene expression profiling and array-CGH analysis to detect a new and recurrent molecular cytogenetic abnormality in T-ALL patients that co-clustered with 5 well-defined *HOXA*-activated T-ALL samples. We describe the cloning of a recurrent *SET-NUP214* fusion product in these samples, and identified the mechanism by which *SET-NUP214* can activate the *HOXA* gene cluster as potential leukemogenic event in T-ALL.

MATERIALS AND METHODS

Patient samples

Viably frozen diagnostic bone marrow or peripheral blood samples from 92 pediatric T-ALL patients, clinical and immunophenotypic data were provided by the German Co-operative study group for childhood Acute Lymphoblastic Leukemia (COALL) and the Dutch Childhood Oncology Group (DCOG). The patients' parents or their legal guardians provided informed consent to use leftover material for research purposes according to the declaration of Helsinki. Leukemic cells were isolated and enriched from these samples as previously described[12]. All resulting samples contained ≥90% leukemic cells, as determined morphologically by May-Grünwald-Giemsa-stained cytospins (Merck, Darmstadt, Germany). Viably frozen T-ALL cells were used for DNA and RNA extraction, and a minimum of 5×10^6 leukemic cells were lysed in Trizol reagent (Invitrogen, Life Technologies, Breda, The Netherlands) and stored at -80°C. A total of 25×10^3 leukemic cells was used to prepare cytospin slides for fluorescence *in-situ* hybridization (FISH) and stored at -20°C.

Genomic DNA isolation, RNA extraction and cDNA synthesis

Genomic DNA and total cellular RNA were isolated using Trizol (Invitrogen) according to the manufacturers' protocol, with minor modifications. An additional phenol-chloroform extraction was performed and the DNA was precipitated with isopropanol along with 1 μL (20 μg/mL) glycogen (Roche, Almere, The Netherlands). After precipitation, RNA pellets were dissolved in 20 μL RNAse-free TE-buffer (10 mM Tris-HCl, 1 mM EDTA, pH=8.0). The RNA concentration was quantified spectrophotometrically. Following a denaturation step of 5' at 70°C, 1 μg of RNA was reverse transcribed to single-stranded cDNA using a mix of random hexamers

(2.5 μM) and oligodT primers (20 nM). The RT reaction was performed in a total volume of 25 μl containing 0.2 mM of each dNTP (Amersham Pharmacia BioTech, Piscataway, NJ, USA), 200U Moloney murine leukemia virus reverse transcriptase (M-MLV RT) (Promega, Madison, WI, USA) and 25 U RNAsin (Promega). Conditions for the RT reaction were 37°C for 30', 42°C for 15', and 94°C for 5'. The cDNA was diluted to a final concentration of 8 ng/μL and stored at -80°C.

Gene expression array analysis

Integrity of total RNA was checked using the Agilent 2100 Bio-analyzer (Agilent, Santa-Clara, USA). Copy-DNA and ccRNA syntheses from total RNA, hybridization of Humane Genome U133 plus2.0 oligonucleotide microarrays (Affymetrix, Santa-Clara, USA) and washing steps were performed according to the manufacturers' protocol. Probeset intensities were extracted from CEL-files using GeneChip Operating Software (GCOS), version 1.4.0.036 (Affymetrix), and all arrays had a 3' to 5' GAPDH ratio lower than 3 fold. Probe intensities were normalized using the variance stabilization procedure (Bioconductor package VSN[22]) in the statistical data analysis environment *R,* version 2.2.0. Differentially expressed genes between T-ALL subgroups were calculated using a Wilcoxon statistical test, and corrected for multiple testing error according to the false discovery rate procedure as developed by Hochberg and Benjaminin[23] using the Bioconductor package Multtest. The fold change was calculated using the formula: $e^{(\text{median value groupA-median value groupB})}$. Supervized clustering and principal component analyses were performed using GeneMath XT 1.6.1. software (Applied Maths, Inc, Austin TX, USA).

Microarray based comparative genome hybridization (array-CGH)

Array-CGH analysis was performed, as previously described[12,24], on the human genome CGH Microarray 44A (Agilent), which consists of ~40,000 60-mer oligonucleotide probes that span both coding and non-coding sequences with an average spatial resolution of ~35kb. Briefly, 10 μg of genomic reference or patient DNA was digested overnight at 37°C with AluI (20U) and RsaI (20U) (Invitrogen). Reference and patient DNA were purified and labeled with Cy5-dUTP and Cy3-dUTP (PerkinElmer, Wellesley, MA, USA). Reference and patient DNA for each hybridization were pooled and mixed with 50 μg of human Cot-1 DNA (Invitrogen), 100 μg of yeast tRNA (Invitrogen), and 1× hybridization control targets (SP310, Operon Technologies, Alameda, CA, USA) in a final volume of 500 μL *in-situ* hybridization buffer (Agilent). The hybridization mixtures was denatured at 95°C for 3', pre-incubated at 37°C for 30', and hybridized to the array in a microarray hybridization chamber (Agilent) for 14-18h at 65°C in a rotating oven (Robbins Scientific, Mountain View, CA, USA) at 20 rpm. The array slides were washed in 0.5× SSC/0.005% Triton X-102

at room temperature for 5', followed by 5' at 37°C in 0.1× SSC/0.005% Triton X-102. Slides were dried and scanned using a 2565AA DNA microarray scanner (Agilent). Microarray images were analyzed using feature extraction software (version 8.1, Agilent) and the data were subsequently imported into array-CGH analytics software v3.1.28 (Agilent).

Fluorescent in-situ hybridization (FISH)

FISH analysis was performed on thawed cytospin slides using the LSI BCR-ABL ES translocation probe, according to the manufacturer's protocol (Vysis, IL, USA). Cells were counterstained with DAPI/Vectashield mounting medium. Fluorescence signals were visualized with a Zeiss Axioplan II fluorescence microscope (Zeiss, Sliedrecht, The Netherlands). The combined presence of a clonal del(9)(q34.11q34.13) and an episomal *NUP214-ABL1* amplification in patient #120 was determined by FISH analysis as previously described[12] using Bacterial Artificial Chromosomes (BAC) clones RP11-83J21 (covering *ABL1*) and RP11-618A20 (covering *ASS1*, located in the deleted area between *SET* and *ABL1*). BACs were obtained from BAC/PAC Resource Center (Children's Hospital, Oakland, USA).

Reverse transcriptase PCR (RT-PCR) and quantitative RT-PCR (RQ-PCR)

The *SET-NUP214* fusions were determined by RT-PCR using forward primer 5'-TTCCCGATATGGATGATG-3' (exon 7 *SET*) and reverse primer 5'-CTTTG-GGCAAGGATTTG-3' (exon 20 *NUP214*). PCR reactions were performed using 40 ng of cDNA (8 ng/µL), 10 pmol primers, 10nmol of dNTPs, 4 mM $MgCl_2$, 1.25 U of ampli*Taq* gold (Applied Biosystems, Foster City, CA, USA) in 10x PCR buffer II (Applied Biosystems) in a total volume of 50 µL. After the initial denaturation at 94°C for 10', PCR was performed for 39 cycles of 95°C for 15", 60°C for 1' and 68°C for 3'. *NUP214-ABL1* fusions were determined as previously described[6].

Expression levels of *HOXA, SET* and *SET-NUP214* transcripts were quantified relative to the expression level of the endogenous housekeeping gene glyceraldehyde-3-phosphate dehydrogenase (*GAPDH*) using RQ-PCR in an ABI 7700 sequence detection system (Applied Biosystems). The *HOXA* primers were as described previously[8]. For *SET* expression, the forward primer 5'-TTCCCGATATGGATGATG-3' (exon 7 *SET*) and the reverse primer 5'-CCCCCCAAATAAATTGAG-3' (exon 8 *SET*) were used. For *SET-NUP214* expression, the primers used were as described above.

Cell culture

T-ALL cell lines (DSMZ, Braunschweig, Germany) were cultured in RPMI-1640 medium (Invitrogen) supplemented with 10% fetal calf serum (Integro, Zaandam, The Netherlands), 100 IU/mL penicillin, 100 µg/mL streptomycin and 0.125 µg/mL

fungizone (Invitrogen) and grown as suspension cultures at 37°C in humidified air containing 5% CO_2. LOUCY and SKW3 cells (1 x 10^7) were transfected with 100 nM *SET* siRNA by electroporation in 400 µL RPMI 1640 with L-Alanyl-L-Glutamine (Invitrogen) in 4 mm electroporation cuvettes (BioRad, Hercules, CA, USA). The SET siRNA were located in exon 5 (5' GAAATCAAATGGAAATCTGGAAA) and exon 8 (5' AGGAGAAGAUGACUAAATA). To compensate for the amount of cell death induced as a consequence of the electroporation procedure, control cells were electroporated without siRNA. Electroporation was performed using an EPI 2500 gene pulser (Fischer, Heidelberg, Germany) applying a rectangle pulse of 350V for 10 ms. After incubating for 15 min at room temperature, the cells were diluted 10-fold with RPMI 1640 medium (Invitrogen) supplemented with 10% FCS (Integro), 100 IU/mL penicillin, 100 µg/mL streptomycin and 0.125 µg/mL fungizone (Invitrogen) and incubated at 37°C and 5% CO_2. Cell viability was assessed by AnnexinV/PI staining and determined by flow cytometry using a FACSCalibur (Becton Dickinson, San Jose, CA, USA). Electroporation of a FITC labeled siRNA (Eurogentec, Seraing, Belgium) and subsequent FACS analysis indicated that transfection efficiencies were >90%. Electroporation of this FITC labeled siRNA also served as negative siRNA control.

Protein extraction and Western blot analysis

Cell pellets stored at -80°C were briefly thawed and resuspended in 50 µL lysis buffer composed of 50 mM Tris buffer, 150 mM NaCl, 100 mM EDTA, 1% Triton X-100, 2 mM PMSF, 3% aprotinine (Sigma, Zwijndrecht, The Netherlands), 4 g/mL pepstatin (Sigma) and 4 µg/mL leupeptin (Sigma). Accordingly, cells were lysed for 15 min on ice. The supernatant of the lysed cells was cleared by centrifugation for 15 min at 13 000 rpm and 4°C. The protein content of the cleared lysates was determined using the BCA protein assay (Pierce Biotechnology, Inc., Rockford, USA) with different concentrations of bovine serum albumin as standards. Cell lysates containing 25 µg of protein were separated on 10% polyacrylamide gels topped with 4% stacking gels, and transferred onto nitrocellulose membranes (Schleichler & Schuell, Dassel, Germany). Western blots were probed with mouse anti-SET (provided by Dr. K. Nagata) or with mouse anti-Actin (Sigma, cat# A2547) antiserum. Anti-SET was used in different concentrations for proper detection of both SET (1:1000) and SET-NUP214 (1:250). Accordingly, the blots were labeled with peroxidase-conjugated anti-mouse IgG antibodies (DAKO, Glostrup, Denmark) and visualized using SuperSignal® West Femto chemiluminescent substrate (Pierce Biotechnology).

Immunoprecipitation (IP) and Chromatine Immunoprecipitation (ChIP)

For ChIP analysis, 20x10^6 cells were crosslinked using formaldehyde to a final concentration of 1% for 15 min at RT. Crosslinking was stopped by adding glycine to a

final concentration of 0.125 M followed by 5 min incubation at RT. Fixed cells were washed twice using ice cold 1x PBS and harvested in SDS buffer (100mM NaCl, 50mM Tris-HCl pH 8.1, 5 mM EDTA pH 8.0, 0.2% NaN_3 and protease inhibitors). After centrifugation, the pellet was resuspended in IP buffer (100 mM Tris at pH 8.6, 0.3% SDS, 1.7% Triton X-100, and 5 mM EDTA) and the cells were sonicated yielding genomic DNA fragments with a size of 500-1000 bp. After pre-clearing of the lysates with protein A beads (50% slurry protein A-Sepharose, Upstate, Charlottesville, USA), the samples were immunoprecipitated overnight at 4°C with affinity purified anti-NUP214 antibodies (provided by Dr. M. Fornerod[25]), anti-acetylated H3 (upstate, cat# 06-599) or anti-FLAG (sigma, cat# 7425). The immune complexes were recovered by adding 50 µL of protein A beads and incubated for 2 h at 4°C. Subsequently, beads were washed with low salt buffer (0.1% SDS, 1% triton X-100, 2 mM EDTA, 20 mM Tris-HCl pH 8.1, 150 mM NaCl), high salt buffer (0.1% SDS, 1% triton X-100, 2 mM EDTA, 20mM Tris-HCl pH 8.1, 500 mM NaCL), LiCl buffer (250 mM LiCl, 1 mM EDTA, 0.5% NP-40, 10 mM Tris-HCL pH 8.0, 0.2% NaN_3) and 1x TE buffer (10 mM Tris-HCL pH 8.0, 1 mM EDTA). The immune complexes were eluted from the beads by adding elution buffer (1% SDS, 0.1M $NaHCO_3$) for 15 min at RT. Cross links were reversed by overnight incubation at 65°C. The eluted material was phenol/chloroform-extracted and ethanol-precipitated. The immunoprecipitated DNA was quantified by RQ-PCR using *HOXA* specific promoter primers as previously described[26].

For immunoprecipitation analysis, cells were washed twice using ice cold 1x PBS and lysed in a single detergent lysis buffer (142,5 mM KCl, 5 mM $MgCl_2$, 10 mM HEPES pH 7.0, 1 mM EDTA, 1% NP-40 and protease inhibitors). After pre-clearing of the lysates with protein A beads (Upstate), samples were immunoprecipitated overnight at 4°C with rabbit anti-NUP214, rabbit anti-PP32 (gift from Dr. J. Brody), mouse anti-SET, rabbit anti-CRM1 (gift from Dr. M. Yoshida), rabbit anti-hDOT1L (gift from Dr. Yi Zhang). The immune complexes were recovered by adding 50 µL of protein A beads and incubated for 2 h at 4°C. Subsequently, beads were washed twice by single detergent lysis buffer and twice by single detergent lysis buffer without NP-40. The pellets were resuspended in loading buffer, boiled for 5 min and western blot analysis was performed as described above.

RESULTS

Gene expression profiling of pediatric T-ALL subgroups

We have used gene expression profiling data to cluster 92 T-ALL patients: 67 patients with known cytogenetic abnormalities and 25 patients without recurrent aberrations (from this point denoted as unknown cases). For the 67 T-ALL patients having one of

the major molecular cytogenetic abnormalities (i.e. *TAL1* (n=24), *LMO2* (n=9), *HOXA* (n=5), *TLX1/TLX1* (n=7), and *TLX3/TLX3* (n=22)), differentially expressed probesets were calculated from Affymetrix U133plus2.0 data based upon a Wilcoxon analysis and corrected for multiple testing for each probeset. Significant and differentially expressed probesets were obtained for the *TAL1*, *TLX1* and *TLX3* subgroups (Figure 1A). No significant probesets were obtained for the *HOXA* subgroup or the *LMO2* subgroup (Figure 1A). As *TAL1* and *LMO2* both participate in the same transcriptional complex[27], activation of these genes may both lead to a highly similar expression profile. Combined analysis of *TAL1* and *LMO2* rearranged cases revealed significant and differentially expressed probesets that, as expected, almost entirely overlapped with the gene signature obtained for the *TAL1*-subgroup only.

Next, we tried to cluster all 92 T-ALL cases. Cluster analysis was performed based upon the top 25, 50 or 100 most significant probesets for the *TAL1*, *TAL1/LMO2*, *TLX1* and *TLX3* subgroups combined with 15 *HOXA* probesets identified by Soulier *et al* (2005)[8] (Figure 1A-B). Cluster and principal component analyses (PCA) led to a stable clustering of unknown T-ALL cases with specific molecular cytogenetic subgroups (Figure 1B-C): 1 patient clustered with *TLX3* rearranged cases, and this patient uniquely highly expressed the *TLX3* homologous gene *TLX1L1* (data not shown). Nineteen unknown cases tightly clustered with *TAL1* or *LMO2* rearranged cases. FISH analysis (not shown) revealed *TAL1* and/or *LMO2* homologous rearrangements to the *TCR*β or *TCR*αδ loci in 5 out of these 19 patients (i.e. *TAL2* (1 case); *LMO1* (1 case); *TAL2/LMO1* (1 case); *cMYC* (2 cases)) in line with karyotypic data. Another 5 unknown T-ALL samples formed a separate cluster with the 5 *HOXA*-type T-ALL cases (Figure 1B-C), and will be denoted as *HOXA*-like samples.

New recurrent deletion, del(9)(q34.11q34.13), in *HOXA*-like T-ALL samples

To identify new chromosomal abnormalities in the 5 *HOXA*-like cases, we screened these patients using oligonucleotide array-CGH. A one-copy loss of an approximately 3 Mb region involving chromosomal band 9q34.11-9q34.13 was identified in 3 out of 5 *HOXA*-like patients (cases #126, #125 and #120, Figure 2A-C). Detailed analysis of the centromeric breakpoints in these 3 patients revealed a breakpoint within or in the vicinity of the *SET* gene. The *PKN3* gene just telomeric to *SET* was consistently lost in all 3 patients (Figure 2A-C). The telomeric breakpoint seemed located in the *NUP214/CAN* gene in 2 patients (#125 and #126, Figure 2A-C) whereas the telomeric breakpoint of patient #120 was situated in the *ABL1* oncogene (Figure 2B-C).

The presence of the del(9)(q34.11q34.13) in patients #125 and #126 was confirmed by FISH using the LSI *BCR-ABL* ES translocation probe resulting in a single copy loss of the *ABL1* gene (Figure 2D). Strikingly, FISH analysis on patient #120 also revealed an identical mono-allelic loss of *ABL1* in all leukemic cells. However, an episomal

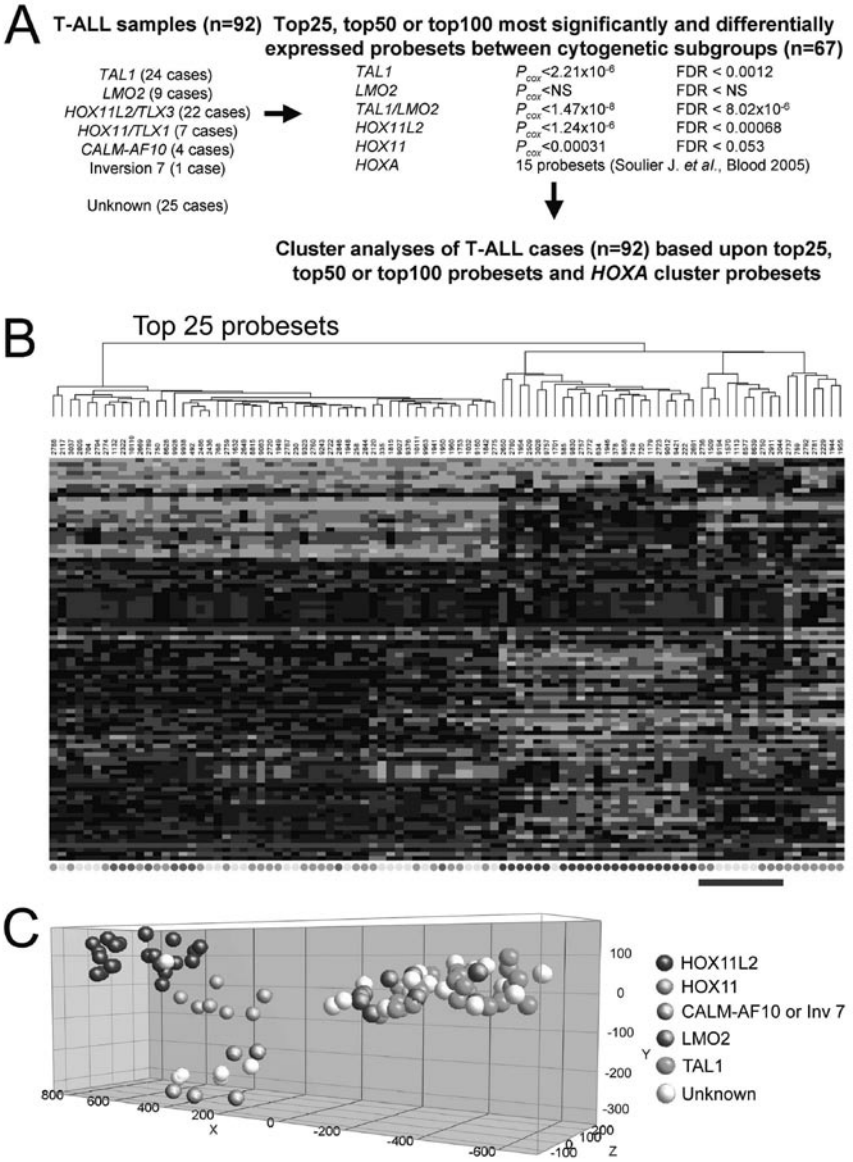

Figure 1. Gene expression profiles of 92 T-ALL patients.
(a) Differentially expressed genes among the major molecular cytogenetic T-ALL subgroups (*TAL1*, *LMO2*, *HOXA*, *TLX1*, and *TLX3, n=67*). The significance level (Wilcoxon *p*-value) and FDR corrected *p*-value for the top100 gene in each T-ALL subgroup is indicated. *TAL1*, *TLX1* and *TLX3* subgroups show significant differentially expressed probesets. (b) Cluster analysis of 92 T-ALL patients (67 known, 25 unknown) based upon the top25 most significant probesets for the *TAL1*, *TAL1/LMO2*, *TLX1* and *TLX3* subgroups combined with 15 *HOXA* probesets as previously described[8]. (c) Principal component analyses shows clustering of the unknown T-ALL cases along the molecular cytogenetic known cases: 1 *TLX3*-like, 19 *TAL1/LMO2*-like and 5 *HOXA*-like patients.

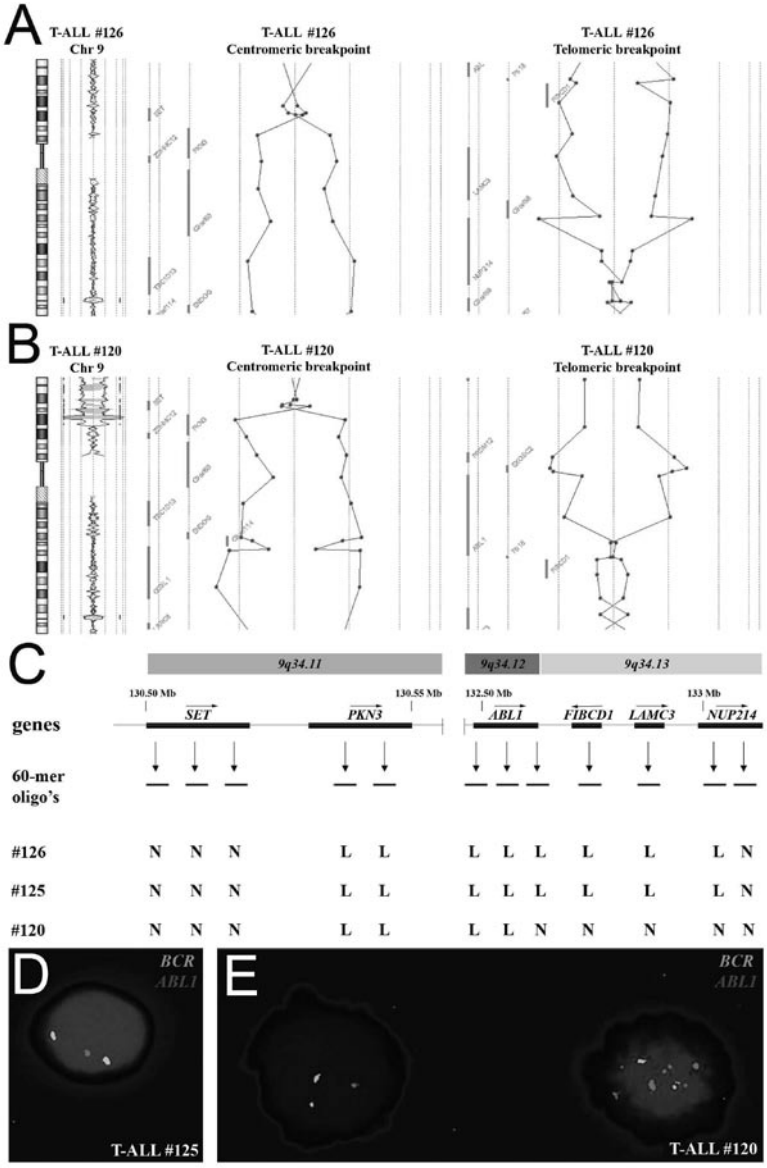

Figure 2. Submicroscopic del(9)(q34.11q34.13) in T-ALL.

(a) Chromosome 9 ideogram and corresponding oligo array-CGH plots of test DNA:control DNA ratios (blue tracing) versus the dye-swap experiment (red tracing) for patient #126. Detailed analyses of the centromeric and telomeric breakpoints show involvement of *SET* and *NUP214*. **(b)** Similar array-CGH plot for patient #120. Centromeric and telomeric breakpoints show involvement of *SET* and *ABL1*. **(c)** Overview of oligo array-CGH results in the potential breakpoint regions for 3 T-ALL patients with del(9)(q34.11q34.13). The 60-mer oligonucleotide probes present on the array-CGH slide and located in the telomeric and centromeric breakpoint regions, as well as the specific genes located in this region with their transcription direction, are shown. Dual-color FISH analysis of patient #125 **(d)** and #120 **(e)** using the LSI *BCR-ABL* ES translocation probe.

NUP214-ABL1 amplification[6] was detected in a leukemic subclone comprising ~5% of the total leukemic cell population (Figure 2E). Subsequent FISH analysis confirmed that the episomal *NUP214-ABL1* amplification as well as the del(9)(q34.11q34.13) were both present in this subclone (data not shown). The combined presence of a clonal del(9)(q34.11q34.13) in combination with an episomal *NUP214-ABL1* amplification in a leukemic subclone in this patient explains why the telomeric breakpoint of the del(9)(q34.11q34.13) seemed situated in the *ABL1* gene according to the array-CGH data. Additional FISH screening of the remaining 87 T-ALL patients did not reveal other patients with this same deletion.

SET-NUP214 fusion in del(9)(q34.11q34.13)-positive patients

Subsequent RT-PCR analysis to amplify a potential *SET-NUP214* fusion product using a *SET* forward primer (exon 7) in combination with a *NUP214* reverse primer (exon 20) revealed an *SET-NUP214* fusion product in all 3 del(9)(q34.11q34.13)-positive T-ALL patients that we also identified in the T-ALL cell line LOUCY[28] (Figure 3A). A similar *SET-NUP214* fusion product due to the reciprocal chromosomal translocation t(9;9)(q34;q34) has been described previously for a patient with an acute undifferentiated leukemia (AUL) by Von Lindern *et al* (1992)[29]. Material of this AUL patient was still available, and RT-PCR analysis revealed a *SET-NUP214* fusion product in this patient (Figure 3A). Sequence analyses of the *SET-NUP214* PCR products confirmed that these 3 T-ALL cases, the AUL patient[29] as well as the cell line LOUCY all had an identical fusion product fusing *SET* at exon 7 with the *NUP214* gene at exon 18 (Figure 3B). Additional oligonucleotide array-CGH analysis further confirmed that the *SET-NUP214* fusion in the cell line LOUCY was indeed due to the presence of a del(9)(q34.11q34.13). This deletion was not present in the AUL patient, confirming that the *SET-NUP214* fusion was the result of a balanced t(9;9)(q34;q34) in this patient[29].

RT-PCR analysis also confirmed an episomal *NUP214-ABL1* fusion product present in patient #120, as well as in control patient material with an episomal *NUP214-ABL1* amplification (Figure 3A, patient #88). Sequence analysis confirmed an in-frame fusion of *NUP214* exon 31 to exon 2 of *ABL1* for patient #120.

As expected, the presence of a SET-NUP214 fusion protein was detected by western blotting in LOUCY (Figure 3C), but was absent in other T-ALL cell lines lacking the del(9)(q34.11q34.13). For all patients described, the breakpoints are situated in the acidic tail of SET and the coiled-coil domain of NUP214, generating an in-frame fusion protein with a molecular weight of approximately 155 kDa (Figure 3D).

Clinical and genetic patient characteristics (i.e. *NOTCH1* mutation status and additional aberrations detected by array-CGH) of the *SET-NUP214* positive T-ALL cases and the cell line LOUCY are summarized in table 1.

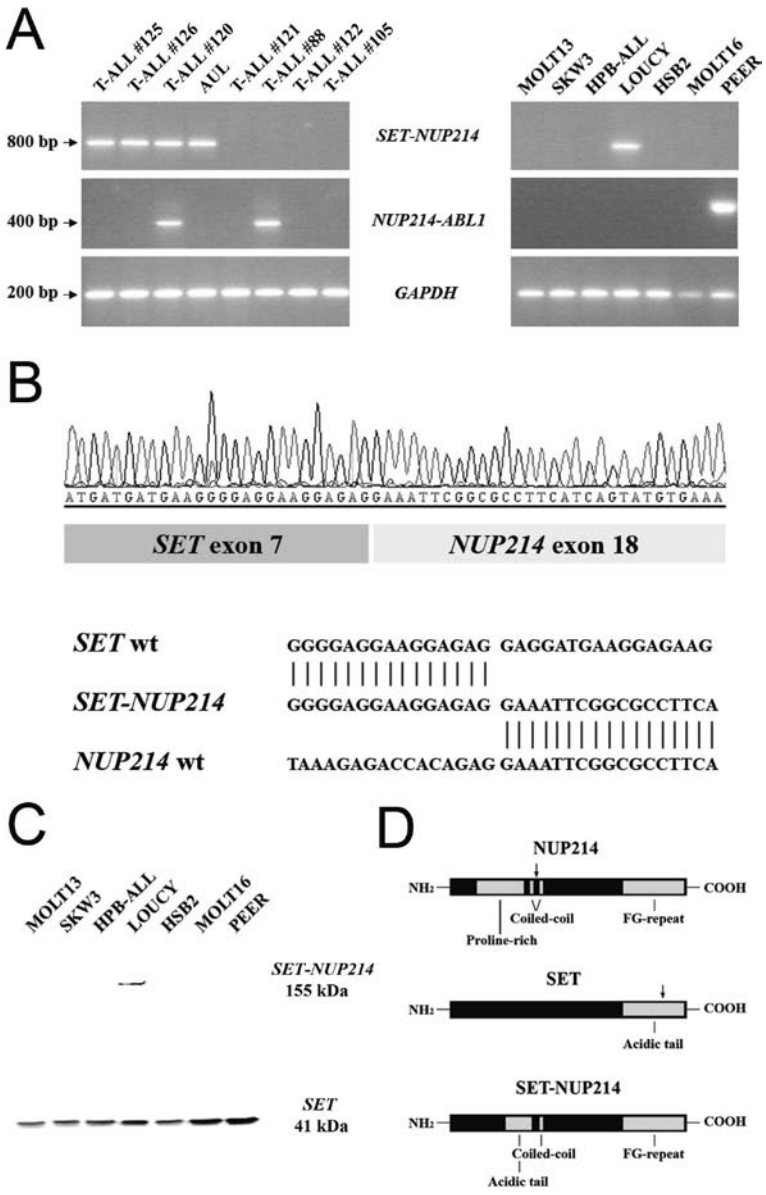

Figure 3. *SET-NUP214* fusion transcript in T-ALL.
(a) RT-PCR analysis using *SET* and *NUP214* specific primers and *GAPDH* primers as internal control, reveals a specific *SET-NUP214* fusion gene in T-ALL patients #125, #126, #120, the AUL patient and the T-ALL cell line LOUCY. *NUP214-ABL1* fusion was detected in patients #120, #88 and in the T-ALL cell line PEER **(b)** Sequence analysis confirmed an identical fusion between exon 7 of *SET* and exon 18 of *NUP214* in all *SET-NUP214* positive T-ALL patients, the AUL case and the LOUCY cell line, **(c)** Western blot analysis of T-ALL cell lines revealed a SET-NUP214 fusion in the cell line LOUCY. **(d)** At the protein level, the breakpoints are situated in the acidic tail of SET and the coiled-coil domain of NUP214.

Elevated *HOXA* levels in *SET-NUP214* positive patients

To confirm the clustering of these 3 del(9)(q34.11;q34.13) positive patients within the *HOXA* cluster based upon the most significant and differentially expressed probesets between the major T-ALL subgroups, we analyzed the expression of the *HOXA* gene cluster using RQ-PCR. As a control, we also determined the expression levels for these genes in various other patient samples representing other T-ALL subgroups. As described previously[8,10,18,19], *MLL* rearranged cases (n=2), *CALM-AF10* positive cases (n=4) and a patient with an inv(7)(p15q34) all highly expressed most genes from the *HOXA* cluster in contrast to *TAL1, LMO2, TLX3* or *TLX1* rearranged patients ($p<0.01$, Figure 4A-B, only results for *HOXA9* are shown). All 3 *SET-NUP214* positive T-ALL patients as well as the cell line LOUCY also highly expressed the *HOXA* cluster of genes. Other T-ALL cell lines including MOLT13, SKW3, HPB-ALL, HSB2 and PEER did not express the *HOXA* gene cluster. Although most *HOXA* genes

Table 1. Characteristics of 3 T-ALL cases and the T-ALL cell line LOUCY with the *SET-NUP214* fusion transcript.

ID	Sex	Age (yrs)	WBC	Perc blast	Immune Phenotype[a]	*CDKN2A*[b]	*NOTCH1* mutation	NUP214-ABL1	Other chromosomal abnormalities by array-CGH	Relapse CCR (#months)
126	F	15.3	213	98	Mature	+ / +	L1601Q	-	None	CCR, 83+
125	F	10.6	142	94	Mature	+ / +	L1601P	-	del(16)(p13.13) trisomy 21	CCR, 83+
120	F	17.1	15	93	Cortical	- / -	N1683D Q2460* (stop)	+	del(9)(p21.2) monosomy 21	CCR, 37+
LOUCY	F	38	NA	NA	Mature	+ / -	ND	-	del(5)(q14.3q31.1) del(5)(q33.1) del(6)(q16.4) del(9)(p21.2p21.3) del(12)(p13.1p13.3) dup(13)(q31.3) del(16)(p12.3)	NA

WBC, White blood cells (x 10^9 per l); [a]According to EGIL classification. [b]Status of the CDKN2A locus: +/+, no deletion; +/-, hemizygous deletion; -/-, homozygous deletion. CCR, continued complete remission; ND, none detected; NA, not available.

were highly expressed in LOUCY, in the AUL case and in the SET-NUP214 positive T-ALL patients, expression of *HOXA11* and *HOXA13* was virtually absent. In addition, the expression of the short *HOXA10* isoform, *HOXA10B*, which previously has been exclusively associated with inv(7)(p15q34) T-ALL patients[8,20], was also highly expressed in the *SET-NUP214* positive patients (Figure 4C).

From the expression microarray data, the most significant and differentially expressed probesets were calculated for the entire *HOXA* cluster. Twenty significant and differentially expressed probesets with a FDR rate lower than 5% were obtained for this cluster (Figure 4D). Various of these probesets encoding for *QKI, HOXA5, HOXA9* (2 probesets), *HOXA10* (2 probesets) and *HOXA11* were also previously found to be differentially expressed within *MLL*[19] or *CALM-AF10*[18] rearranged T-ALL patients or in T-ALL patients belonging to the *HOXA* subgroup[8].

SET-NUP214 activates *HOXA* expression, increases cellular proliferation and inhibits cellular differentiation

To study the role of the *SET-NUP214* fusion transcript in the pathogenesis of T-cell leukemia and its contribution to the activation of the *HOXA* gene cluster, *SET* and *SET-NUP214* expression were specifically downregulated in the cell line LOUCY by electroporation of *SET* specific siRNA's (Figure 5). Protein expression of *SET* and *SET-NUP214* was specifically reduced using a *SET* siRNA directed against exon 5, whereas *SET* but not *SET-NUP214* was downregulated using a *SET* siRNA directed against exon 8 (Figure 5A). *SET* and/or *SET-NUP214* mRNA expression levels were specifically targeted and this effect was sustained for over 7 days following transfection of *SET* siRNAs (Figure 5B). Specific downregulation of both *SET* and *SET-NUP214* resulted in significant reduction in the expression levels of the *HOXA* gene cluster while knockdown of *SET* but not *SET-NUP214* had any effect (Figure 5C). This confirms that *SET-NUP214* but not *SET* specifically upregulates the expression of *HOXA* genes. Knockdown of *SET-NUP214* also reduced cellular proliferation (Figure 5D, E). Cell cycle may be directly inhibited, as the percentage of apoptotic cells did not change over time following inhibition of *SET-NUP214* (Figure 5F). In addition, *SET-NUP214* downregulation resulted in the upregulation of both TCRγδ and membrane CD3 expression in LOUCY (Figure 5G), indicating that repression of *SET-NUP214* enforces differentiation.

SET-NUP214 directly activated *HOXA* expression by recruitment of DOT1L

Our siRNA mediated knockdown experiments indicated that SET-NUP214 regulates the transcription of the *HOXA* gene cluster. To investigate whether this activation was caused by direct interaction of SET-NUP214 with *HOXA* promoter sequences, chromatin immunoprecipitation (ChIP) analyses with the cell lines LOUCY and the

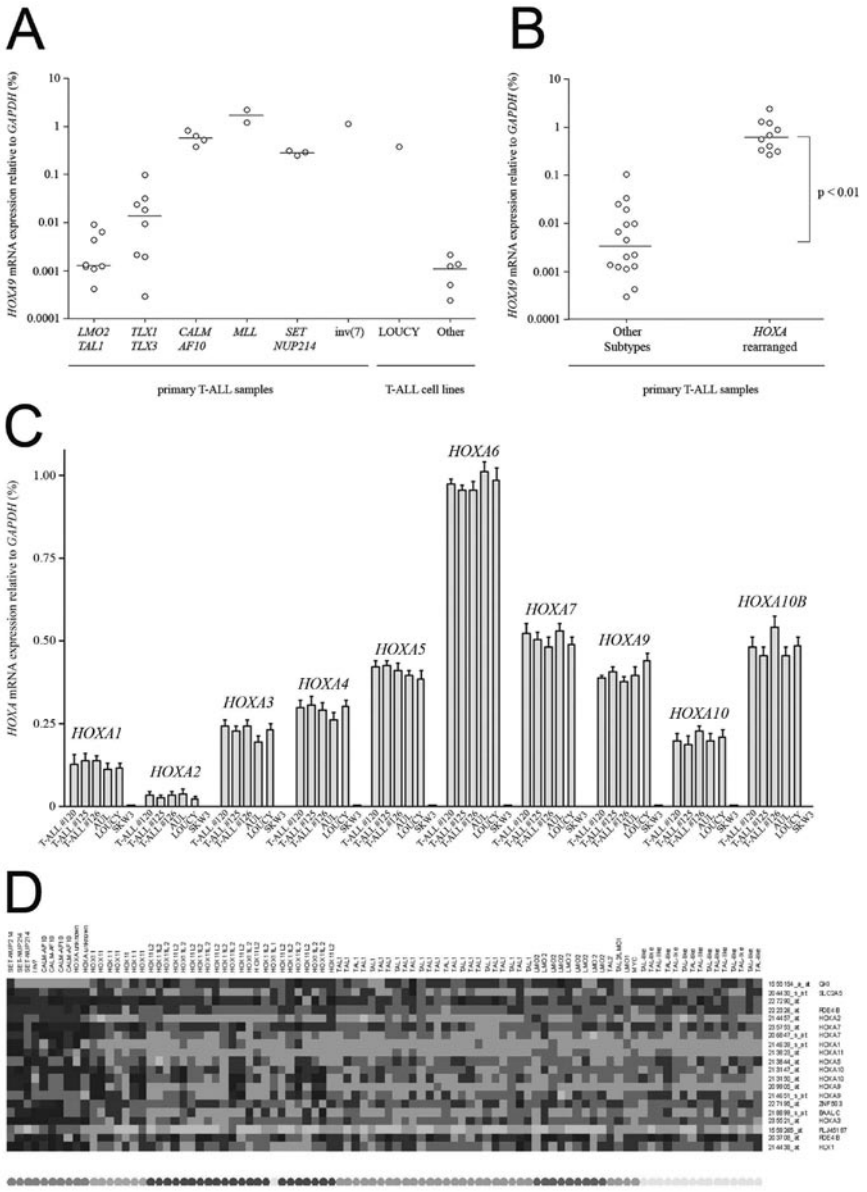

Figure 4. *HOXA* activation in *SET-NUP214* positive T-ALL.

(a) Relative *HOXA9* expression levels by RQ-PCR for *MLL* rearranged, *CALM-AF10* positive, inv(7)(p15q34), *TAL1*, *LMO2*, *TLX3* or *TLX1* rearranged patients and T-ALL cell lines including LOUCY, MOLT13, SKW3, HPB-ALL, HSB2 and PEER. **(b)** Comparison of *HOXA9* expression levels between the *HOXA* T-ALL subgroup (*MLL*, *CALM-AF10*, inv(7)(p15q34), SET-NUP214, n=10) and other T-ALL subgroups (*TAL1*, *LMO2*, *TLX3* or *TLX1*). **(c)** Relative expression levels of *HOXA* genes by RQ-PCR for the 3 *SET-NUP214* positive T-ALL patients, the LOUCY cell line, the AUL patient and SKW3. **(d)** Heatmap of the 20 significant and differentially expressed probesets with a FDR rate lower than 5% for the *HOXA* cluster compared to the other T-ALL cases.

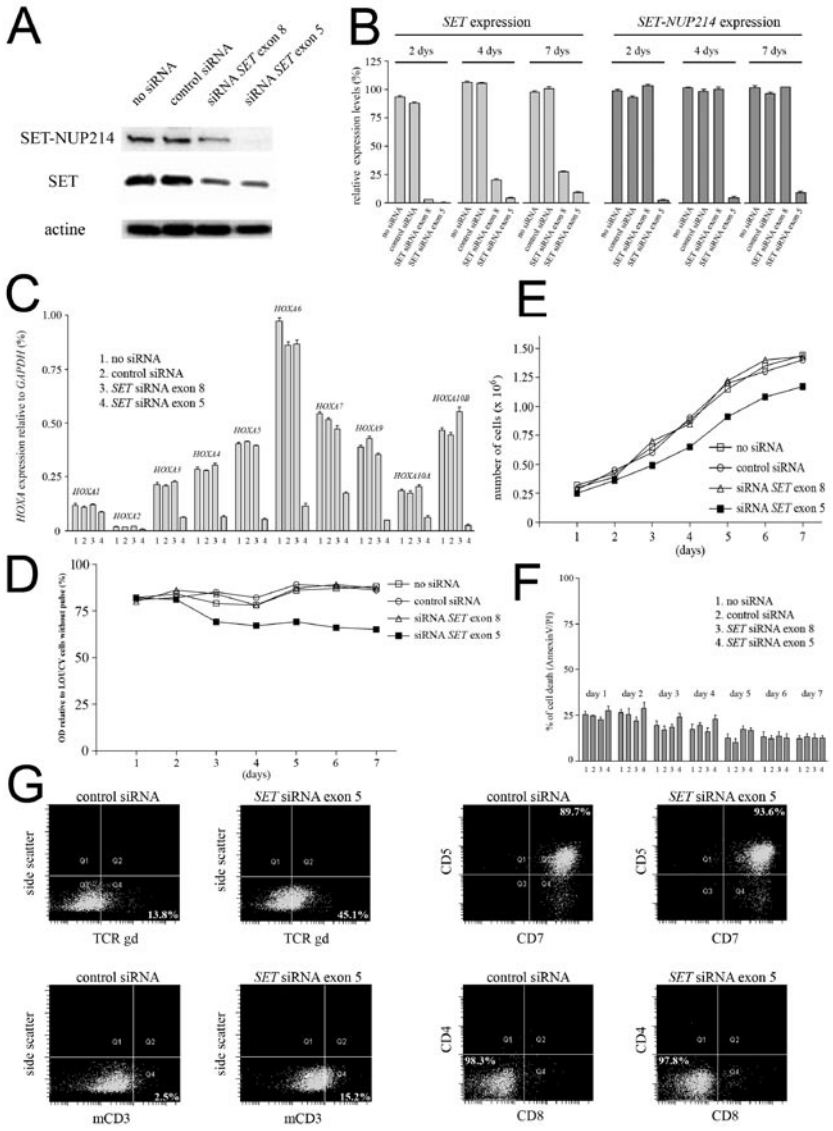

Figure 5. siRNA knockdown of SET and SET-NUP214 in T-ALL cell line LOUCY.
(a) SET expression using Western blot analysis 4 days after electroporation with the following conditions: no siRNA, control siRNA, siRNA *SET* exon 8 or siRNA *SET* exon 5. **(b)** Relative *SET* and *SET-NUP214* expression by RQ-PCR after 2, 4 and 7 days for conditions as mentioned in (a). **(c)** Relative expression of all members of the *HOXA* clusters by RQ-PCR (except for *HOXA11* and *HOXA13*) after 4 days for conditions as mentioned in (a). **(d)** OD values relative to control cells without pulse after 7 days for conditions as mentioned in (a). **(e)** Total cell numbers after 7 days for conditions as mentioned in (a). **(f)** Percentage of cell death relative to control cells without pulse after 7 days for conditions as mentioned in (a). **(g)** FACS analysis 6 days after electroporation with either no siRNA or siRNA *SET* exon 5, for TCRγδ, membrane CD3, CD4, CD5, CD7 and CD8 expression.

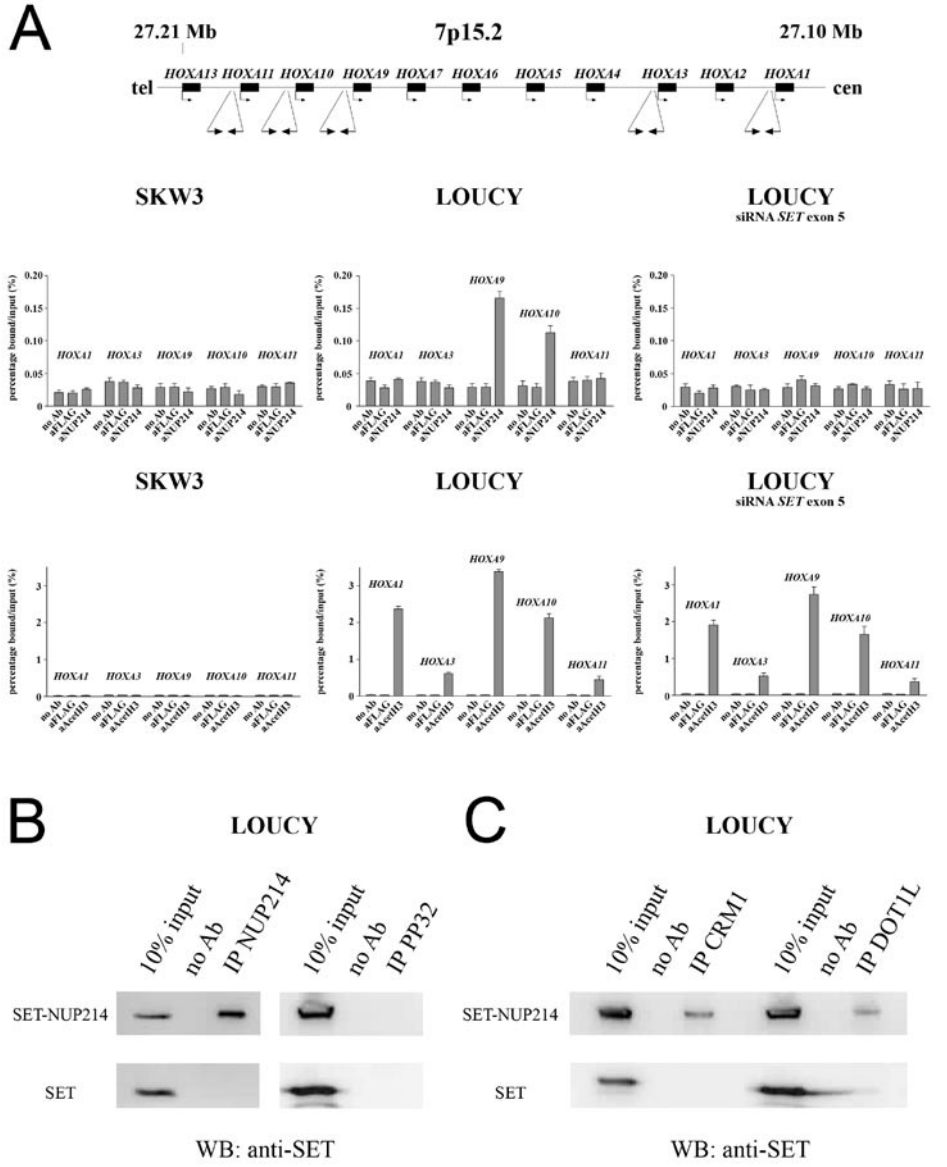

Figure 6. ChIP and coIP analysis of T-ALL cell lines LOUCY and SKW3.
(a) ChIP analysis of SKW3, LOUCY and LOUCY 4 days after electroporation with siRNA *SET* exon 5, for promoter sequences of *HOXA1*, *HOXA3*, *HOXA9*, *HOXA10* and *HOXA11*. The amount of bound DNA was calculated relative to the 5% input DNA in anti-NUP214 and anti-acetH3 immunoprecipitates, whereas no antibody and anti-FLAG immunoprecipitates were used as negative control. **(b)** Western blot analysis of NUP214 and PP32 immunoprecipitates of the cell line LOUCY using anti-SET. **(c)** Similar western blot analysis as in (b) for CRM1 and DOT1L immunoprecipitates in LOUCY.

negative control cell line SKW3 were performed. No enrichment of *HOXA* (*HOXA1, HOXA3, HOXA9, HOXA10* and *HOXA11*) promoter sequences was detected in NUP214 immunoprecipitates obtained for SKW3 control cells (Figure 6A). For LOUCY cells, *HOXA9* and *HOXA10* promoter sequences were enriched in NUP214 immunoprecipitates, but not *HOXA1*, *HOXA3* and *HOXA11* promoter sequences indicating that SET-NUP214 may only bind to specific members of the *HOXA* cluster (Figure 6A). Enrichment of *HOXA9* and *HOXA10* promoter sequences in the ChIP analysis could be completely reversed using SET siRNA molecules directed against exon 5.

Additional ChIP analysis using an anti-acetyl histone-H3 specific antibody revealed histone-H3 acetylation of *HOXA1, HOXA3, HOXA9, HOXA10* and *HOXA11* promoters in the cell line LOUCY, which was absent in SKW3 (Figure 6A). This further strengthens the idea that binding of SET-NUP214 as a specific transcriptional co-factor for some *HOXA* gene members may result in an open chromatine structure of the entire *HOXA* cluster. As SET normally associates with the *HOXA* gene cluster[30] and has an inhibitory role on gene transcription as part of the INHAT complex[31], we investigated whether SET-NUP214 may substitute for SET in this complex rendering this complex inactive. However, IP experiments failed to demonstrate a direct interaction between SET-NUP214 and components of the INHAT complex, i.e. SET and PP32 (Figure 6B).

CALM-AF10 and MLL-AF10 fusion proteins have been shown to recruit the methyltransferase DOT1L, leading to aberrant methylation of histone H3 thereby facilitating transcriptional activation of the HOXA gene cluster[32,33]. In this respect, we could demonstrate that SET-NUP214 also interacts with DOT1L in vivo (Figure 6C). Whether this reflects a direct interaction or requires the participation of additional proteins remains to be established. As shown by others[34], we could confirm an in vivo interaction between SET-NUP214 and CRM1 (Figure 6C), which normally binds to the FG-repeat of wildtype NUP214 as part of the nuclear pore complex.

DISCUSSION

Gene expression profiling studies in T-ALL have shown that patients with a *CALM-AF10* translocation, an *MLL* rearrangement and an inv(7)(p15q34) share a gene expression signature characterized by elevated expression levels of *HOXA* genes. Cluster analysis of 25 T-ALL cases lacking known cytogenetic abnormalities with 67 cytogenetically well-characterized cases led to the identification of 5 unknown cases that clustered with *HOXA* activated samples having *CALM-AF10* translocations or an inv(7)(p15q34).

Subsequent array-CGH analysis revealed an identical interstitial deletion, del(9)(q34.11q34.13), in 3 out of 5 cases as a novel chromosomal aberration in pediatric T-ALL that was also identified in the T-ALL cell line LOUCY. This deletion gives rise to a similar *SET-NUP214* fusion gene in all cases, that was also identical to a *SET-NUP214* fusion as described 15 years ago for a single acute undifferentiated leukemia patient with a reciprocal translocation t(9;9)(q34;q34)[29,35] and most recently for a single case of acute myeloid leukemia[36].

We studied the role of SET-NUP214 in the pathogenesis of T-ALL by siRNA-mediated knockdown of *SET-NUP214* expression in the T-ALL cell line LOUCY. Downregulation of SET-NUP214 reduced *HOXA* expression levels indicating that SET-NUP214 could function as a transcriptional regulator of the *HOXA* gene cluster. Our ChIP data in fact provide evidence that SET-NUP214 directly interacts with the promotor regions of specific *HOXA* members itself, and especially to *HOXA9* and *HOXA10,* and therefore may function as a transcriptional co-activator. SET-NUP214 does not bind to promotor sequences of *HOXA1*, *HOXA3*, *HOXA11* and possibly others despite their SET-NUP214 dependency for transcriptional activation in LOUCY. Binding of SET-NUP214 to *HOXA9* and *HOXA10* promotor regions may presumably lead to an open chromatin structure and transcriptional activation of the entire *HOXA* cluster. Enrichment of all *HOXA* promotor sequences in the ChIP analysis using an anti-acetylated histone H3 antibody may be in support of this notion.

For MLL-AF10 and CALM-AF10 fusion proteins, it has been demonstrated that the oncogenicity of these proteins depends on binding of DOT1L to the OM-LZ region of AF10[32,33]. MLL-AF10 and CALM-AF10 both bind to the promotor regions of the *HOXA* gene cluster, and it was shown that recruitment of DOT1L results in aberrant methylation of Lys79 in histone H3 and transcriptional activation of especially *HOXA9* for MLL-AF10[33] and *HOXA5* for CALM-AF10[32]. Our data suggest that *HOXA9* may also represent a bonafide target of the CALM-AF10 fusion protein, as *HOXA9* is highly expressed in CALM-AF10 positive T-ALL cells ([18] and this study). We propose a similar mechanism for SET-NUP214 in the activation of *HOXA* genes, and *HOXA9/HOXA10* in particular, as we could demonstrate binding of DOT1L to the SET-NUP214 fusion protein. An OM-LZ-like structure as present in AF10[33] seems lacking in SET-NUP214, and therefore other SET-NUP214 interacting proteins may facilitate recruitment of DOT1L. In this respect, we confirmed that CRM1 also binds to SET-NUP214[34], possibly to the FG-repeats as retained in this fusion protein.

SET-NUP214 is highly similar to the DEK-NUP214 fusion as previously identified in t(6;9)(p23;q34)-positive AML patients[37]. As DEK-NUP214 AML samples also have an activated *HOX*A gene signature (PJ Valk, personal communication), DEK-NUP214 may function in a similar fashion compared to SET-NUP214 by binding to

the promotor regions of specific HOXA gene members in t(6;9)(p23;q34)-positive AML patients.

SiRNA knockdown experiments in LOUCY led to complete absence of SET-NUP214 and down regulation of *HOXA* expression levels that sustained for over 7 days. Ablation of SET-NUP214 reduced cellular proliferation without inducing apparent apoptosis in this timeframe. In fact, inhibition of SET-NUP214 resulted in cellular differentiation and promoted mCD3 and TCRγδ expression. Our results are in agreement with previous data by others, in which overexpression of SET-NUP214 inhibits differentiation *in vitro*[38] as well as *in vivo*[39].

During normal T-cell development, *HOXA* expression (*HOXA7*, *HOXA9*, *HOXA10*) is restricted to the earliest stages of differentiation[40,41]. We therefore propose that SET-NUP214 will sustain *HOXA* gene expression and therefore impair T-cell differentiation. This differentiation arrest may encourage the acquisition of additional genetic hits, eventually leading towards the development of T-cell leukemia. In mouse studies, overexpression of *Hoxa10* inhibits both myeloid and lymphoid cell differentiation[42] whereas overexpression of *Hoxa9* results in defective T-cell development[43].

T-cell leukemia depends on multi-step pathogenic events[3-5]. Cooperative genetic abnormalities affecting cell cycle and proliferation, differentiation and survival initiate leukemic transformation of thymocytes. We identified a number of cooperative aberrations in the *SET-NUP214* positive T-ALL samples. *NOTCH1* mutations, generally present in about 50% of T-ALL[7], were found in all 3 *SET-NUP214* positive T-ALL samples. Besides the *SET-NUP214* fusion (differentiation arrest) and *NOTCH1* mutations, patient #120 also showed a homozygous *CDKN2A/CDKN2B* deletion (cell cycle defect) and an episomal *NUP214-ABL1* amplification (proliferation and survival), showing the multiple molecular pathways that are involved in the pathogenesis of T-ALL[4]. It is remarkable that in this case 2 different genetic rearrangements (*SET-NUP214* and *NUP214-ABL1*) target the same gene (*NUP214*) in a single leukemic cell. The SET-NUP214 fusion was present as a clonal genetic rearrangement present in all leukemic cells whereas NUP214-ABL was only present in a leukemic subclone. So SET-NUP214 probably acts as a primary oncogenic event, whereas NUP214-ABL1 rather functions as a further dedifferentiating event in T-ALL. In patient #125 and the LOUCY cell line, terminal deletions of chromosome 16 were identified (table 1). Because these 16p deletions were not previously identified as a recurrent abnormality in T-ALL[44], it is likely that they cooperate in *SET-NUP214* mediated leukemogenesis. Nevertheless, the target genes of this aberration remain to be identified.

In conclusion, we identified *SET-NUP214* as a novel recurrent fusion gene in T-cell leukemia. Our experiments show that *SET-NUP214* contributes to T-ALL pathogenesis by inhibition of T-cell maturation through the transcriptional activation of the *HOXA* genes.

ACKNOWLEDGEMENTS

P.V.V., J.T. and M.v.G designed and performed research and wrote the paper; C.L. collaborated on the array-CGH study and wrote the paper; E.v.W. and M.H. collected and made available patient samples; J.G performed and designed FISH analysis; P.J.S and A.S analyzed gene expression data; K.N. and M.F. provided antisera; J.C. and J.S designed research and wrote the paper; J.P.P.M, H.B.B and R.P. wrote grant, designed research and wrote the paper.

P.V.V. is financed by the Sophia Foundation for Medical Research (SSWO-440). This study was further supported by the Ter Meulen Fund, Royal Netherlands Academy of Arts and Sciences, and the Foundation "De Drie Lichten". MvG was financially supported by the Quality of Life and KOCR foundations. CL was supported in part by a National Cancer Institute grant (CA11560) and a Leukemia and Lymphoma Society Translational Grant (6161-05), and JT was supported by a German Research Foundation Fellowship Award (Tc-57/1-1).

REFERENCES

1. Pui CH, Relling MV, Downing JR. Acute lymphoblastic leukemia. N Engl J Med. 2004;350:1535-1548.
2. Clappier E, Cuccuini W, Kalota A, et al. The C-MYB locus is involved in chromosomal translocation and genomic duplications in human T-cell acute leukemia (T-ALL) - the translocation defining a new T-ALL subtype in very young children. Blood. 2007.
3. Armstrong SA, Look AT. Molecular genetics of acute lymphoblastic leukemia. J Clin Oncol. 2005;23:6306-6315.
4. De Keersmaecker K, Marynen P, Cools J. Genetic insights in the pathogenesis of T-cell acute lymphoblastic leukemia. Haematologica. 2005;90:1116-1127.
5. Grabher C, von Boehmer H, Look AT. Notch 1 activation in the molecular pathogenesis of T-cell acute lymphoblastic leukaemia. Nat Rev Cancer. 2006;6:347-359.
6. Graux C, Cools J, Melotte C, et al. Fusion of NUP214 to ABL1 on amplified episomes in T-cell acute lymphoblastic leukemia. Nat Genet. 2004;36:1084-1089.
7. Weng AP, Ferrando AA, Lee W, et al. Activating mutations of NOTCH1 in human T cell acute lymphoblastic leukemia. Science. 2004;306:269-271.
8. Soulier J, Clappier E, Cayuela JM, et al. HOXA genes are included in genetic and biologic networks defining human acute T-cell leukemia (T-ALL). Blood. 2005;106:274-286.
9. Lahortiga I, De Keersmaecker K, Van Vlierberghe P, et al. Duplication of the MYB oncogene in T cell acute lymphoblastic leukemia. Nat Genet. 2007;39:593-595.
10. Speleman F, Cauwelier B, Dastugue N, et al. A new recurrent inversion, inv(7)(p15q34), leads to transcriptional activation of HOXA10 and HOXA11 in a subset of T-cell acute lymphoblastic leukemias. Leukemia. 2005;19:358-366.
11. Graux C, Cools J, Michaux L, Vandenberghe P, Hagemeijer A. Cytogenetics and molecular genetics of T-cell acute lymphoblastic leukemia: from thymocyte to lymphoblast. Leukemia. 2006;20:1496-1510.
12. Van Vlierberghe P, van Grotel M, Beverloo HB, et al. The cryptic chromosomal deletion del(11)(p12p13) as a new activation mechanism of LMO2 in pediatric T-cell acute lymphoblastic leukemia. Blood. 2006;108:3520-3529.
13. Clappier E, Cuccuini W, Cayuela JM, et al. Cyclin D2 dysregulation by chromosomal translocations to TCR loci in T-cell acute lymphoblastic leukemias. Leukemia. 2006;20:82-86.
14. Sharma VM, Calvo JA, Draheim KM, et al. Notch1 contributes to mouse T-cell leukemia by directly inducing the expression of c-myc. Mol Cell Biol. 2006;26:8022-8031.
15. Weng AP, Millholland JM, Yashiro-Ohtani Y, et al. c-Myc is an important direct target of Notch1 in T-cell acute lymphoblastic leukemia/lymphoma. Genes Dev. 2006;20:2096-2109.
16. Palomero T, Lim WK, Odom DT, et al. NOTCH1 directly regulates c-MYC and activates a feed-forward-loop transcriptional network promoting leukemic cell growth. Proc Natl Acad Sci U S A. 2006;103:18261-18266.
17. Ferrando AA, Neuberg DS, Staunton J, et al. Gene expression signatures define novel oncogenic pathways in T cell acute lymphoblastic leukemia. Cancer Cell. 2002;1:75-87.
18. Dik WA, Brahim W, Braun C, et al. CALM-AF10+ T-ALL expression profiles are characterized by overexpression of HOXA and BMI1 oncogenes. Leukemia. 2005;19:1948-1957.

19. Ferrando AA, Armstrong SA, Neuberg DS, et al. Gene expression signatures in MLL-rearranged T-lineage and B-precursor acute leukemias: dominance of HOX dysregulation. Blood. 2003;102:262-268.

20. Cauwelier B, Cave H, Gervais C, et al. Clinical, cytogenetic and molecular characteristics of 14 T-ALL patients carrying the TCRbeta-HOXA rearrangement: a study of the Groupe Francophone de Cytogenetique Hematologique. Leukemia. 2007;21:121-128.

21. van Grotel M, Meijerink JP, Beverloo HB, et al. The outcome of molecular-cytogenetic subgroups in pediatric T-cell acute lymphoblastic leukemia: a retrospective study of patients treated according to DCOG or COALL protocols. Haematologica. 2006;91:1212-1221.

22. Huber W, von Heydebreck A, Sultmann H, Poustka A, Vingron M. Variance stabilization applied to microarray data calibration and to the quantification of differential expression. Bioinformatics. 2002;18 Suppl 1:S96-104.

23. Hochberg Y, Benjamini Y. More powerful procedures for multiple significance testing. Stat Med. 1990;9:811-818.

24. Barrett MT, Scheffer A, Ben-Dor A, et al. Comparative genomic hybridization using oligonucleotide microarrays and total genomic DNA. Proc Natl Acad Sci U S A. 2004;101:17765-17770.

25. Bernad R, van der Velde H, Fornerod M, Pickersgill H. Nup358/RanBP2 attaches to the nuclear pore complex via association with Nup88 and Nup214/CAN and plays a supporting role in CRM1-mediated nuclear protein export. Mol Cell Biol. 2004;24:2373-2384.

26. Bracken AP, Dietrich N, Pasini D, Hansen KH, Helin K. Genome-wide mapping of Polycomb target genes unravels their roles in cell fate transitions. Genes Dev. 2006;20:1123-1136.

27. Wadman IA, Osada H, Grutz GG, et al. The LIM-only protein Lmo2 is a bridging molecule assembling an erythroid, DNA-binding complex which includes the TAL1, E47, GATA-1 and Ldb1/NLI proteins. Embo J. 1997;16:3145-3157.

28. Ben-Bassat H, Shlomai Z, Kohn G, Prokocimer M. Establishment of a human T-acute lymphoblastic leukemia cell line with a (16;20) chromosome translocation. Cancer Genet Cytogenet. 1990;49:241-248.

29. von Lindern M, Breems D, van Baal S, Adriaansen H, Grosveld G. Characterization of the translocation breakpoint sequences of two DEK-CAN fusion genes present in t(6;9) acute myeloid leukemia and a SET-CAN fusion gene found in a case of acute undifferentiated leukemia. Genes Chromosomes Cancer. 1992;5:227-234.

30. Shimoyama T, Kato K, Miyaji-Yamaguchi M, Nagata K. Synergistic action of MLL, a TRX protein with template activating factor-I, a histone chaperone. FEBS Lett. 2005;579:757-762.

31. Seo SB, McNamara P, Heo S, Turner A, Lane WS, Chakravarti D. Regulation of histone acetylation and transcription by INHAT, a human cellular complex containing the set oncoprotein. Cell. 2001;104:119-130.

32. Okada Y, Jiang Q, Lemieux M, Jeannotte L, Su L, Zhang Y. Leukaemic transformation by CALM-AF10 involves upregulation of Hoxa5 by hDOT1L. Nat Cell Biol. 2006;8:1017-1024.

33. Okada Y, Feng Q, Lin Y, et al. hDOT1L links histone methylation to leukemogenesis. Cell. 2005;121:167-178.

34. Saito S, Miyaji-Yamaguchi M, Nagata K. Aberrant intracellular localization of SET-CAN fusion protein, associated with a leukemia, disorganizes nuclear export. Int J Cancer. 2004;111:501-507.

35. von Lindern M, Poustka A, Lerach H, Grosveld G. The (6;9) chromosome translocation, associated with a specific subtype of acute nonlymphocytic leukemia, leads to aberrant transcription of a target gene on 9q34. Mol Cell Biol. 1990;10:4016-4026.

36. Rosati R, La Starza R, Barba G, et al. Cryptic chromosome 9q34 deletion generates TAF-Ialpha/CAN and TAF-Ibeta/CAN fusion transcripts in acute myeloid leukemia. Haematologica. 2007;92:232-235.

37. von Lindern M, Fornerod M, van Baal S, et al. The translocation (6;9), associated with a specific subtype of acute myeloid leukemia, results in the fusion of two genes, dek and can, and the expression of a chimeric, leukemia-specific dek-can mRNA. Mol Cell Biol. 1992;12:1687-1697.

38. Kandilci A, Mientjes E, Grosveld G. Effects of SET and SET-CAN on the differentiation of the human promonocytic cell line U937. Leukemia. 2004;18:337-340.

39. Saito S, Nouno K, Shimizu R, Yamamoto M, Nagata K. Impairment of erythroid and megakaryocytic differentiation by a leukemia-associated and t(9;9)-derived fusion gene product, SET/TAF1b-CAN/NUP214. J Cell Physiol. 2007.

40. Taghon T, Stolz F, De Smedt M, et al. HOX-A10 regulates hematopoietic lineage commitment: evidence for a monocyte-specific transcription factor. Blood. 2002;99:1197-1204.

41. Taghon T, Thys K, De Smedt M, et al. Homeobox gene expression profile in human hematopoietic multipotent stem cells and T-cell progenitors: implications for human T-cell development. Leukemia. 2003;17:1157-1163.

42. Thorsteinsdottir U, Sauvageau G, Hough MR, et al. Overexpression of HOXA10 in murine hematopoietic cells perturbs both myeloid and lymphoid differentiation and leads to acute myeloid leukemia. Mol Cell Biol. 1997;17:495-505.

43. Kroon E, Krosl J, Thorsteinsdottir U, Baban S, Buchberg AM, Sauvageau G. Hoxa9 transforms primary bone marrow cells through specific collaboration with Meis1a but not Pbx1b. Embo J. 1998;17:3714-3725.

44. Mullighan CG, Goorha S, Radtke I, et al. Genome-wide analysis of genetic alterations in acute lymphoblastic leukaemia. Nature. 2007;446:758-764.

Chapter 6

Duplication of the *MYB* oncogene in T-cell acute lymphoblastic leukemia

Idoya Lahortiga[1,2,3], Kim De Keersmaecker[1,2], Pieter Van Vlierberghe[4], Carlos Graux[1,2,5], Barbara Cauwelier[6], Frederic Lambert[7], Nicole Mentens[1,2], H. Berna Beverloo[8], Rob Pieters[4], Frank Speleman[6], Maria D. Odero[3], Marijke Bauters[1,2], Guy Froyen[1,2],Peter Marynen[1,2], Peter Vandenberghe[2], Iwona Wlodarska[2], Jules P.P. Meijerink[4,9] and Jan Cools[1,2,9]

[1] Human Genome Laboratory, Department of Molecular and Developmental genetics, VIB, Leuven,Belgium;
[2] Human Genome Laboratory, Center for Human Genetics, K.U.Leuven, Leuven, Belgium;
[3] Division of Oncology, Center for Applied Medical Research (CIMA), University of Navarra, Pamplona,Spain;
[4] Department of Pediatric Oncology/Hematology, Erasmus Medical Center/Sophia Children's Hospital,Rotterdam, The Netherlands;
[5] Department of Hematology – Cliniques Universitaires UCL Mont-Godinne, Yvoir, Belgium;
[6] Center for Medical Genetics Ghent (CMGG), Ghent University Hospital, Gent, Belgium;
[7] Department of Human Genetics, Center for Biomedical Integrated Genoproteomics, University ofLiège, Belgium;
[8] Department of Clinical Genetics, Erasmus Medical Center Rotterdam, Rotterdam, The Netherlands;
[9] These authors can be considered as co-last authors

Nature Genetics 2007; 39(5):593-5

ABSTRACT

We identified a duplication of the *MYB* oncogene in 8.4 % of individuals with T-cell acute lymphoblastic leukemia (T-ALL) and in 5 T-ALL cell lines. The duplication is associated with a 3-fold increase in *MYB* expression, and knockdown of *MYB* expression initiates T-cell differentiation. Our results identify duplication of *MYB* as an oncogenic event and suggest that MYB could be a therapeutic target in human T-ALL.

INTRODUCTION

T-cell acute lymphoblastic leukemia (T-ALL) is an aggressive T-cell malignancy that is most common in children and adolescents[1]. Leukemic transformation of thymocytes is caused by the cooperation of mutations that affect proliferation, survival, cell cycle, and T-cell differentiation[2,3]. Molecular analyses have identified a large number of genetic alterations in T-ALL including deletion of *CDKN2A/CDKN2B*, ectopic expression of transcription factors, episomal amplification of *NUP214-ABL1*, and mutation of *NOTCH1*[2-5].

METHODS

Affected individuals

We retrospectively selected 27 individuals with T-ALL from the database of the Department of Human Genetics (Leuven) for the initial array-CGH screening. We later screened a set of 107 individuals with T-ALL from the Erasmus Medical Center/ Sophia Children's Hospital (Rotterdam) for the presence of the *MYB* duplication by Q-PCR. This study was approved by the Ethical Committee of the Medical Faculty of the University of Leuven and informed consent was obtained from all subjects.

Cytogenetics and Fluoresence in situ hybridization

We carried out cytogenetic studies on bone marrow or blood cells using direct or short-term cultures without mitogens and R banding. Fluorescence in situ hybridization was performed on stored fixed cell suspension originally used for karyotyping.

Array CGH

Array CGH was performed using Code Linked Slides (AP Biotech) containing the 3,527 BAC clones from the Wellcome Trust Sanger Institute 1 Mb Clone Set, a gift from N. P. Carter (The Wellcome Trust Sanger Institute, UK), as described before[5]. Additional clones covering all 90 protein tyrosine kinase genes were added to this set. The complete list of these clones, as well as the array slides are available upon request.

Real-Time Quantitation of DNA Copy Number

We used the comparative ddCt method (Sequence Detection System bulletin 2 (Applied Biosystems)) with SYBR-green. Primers were designed with PrimerExpress software (Applied Biosystems). We first validated whether the efficiency of amplification of the chosen primer sets was equal to that of the normalizer. A primer set for the

ABL1 and *TIE1* genes was used for normalization. The validation experiments were performed on fourfold dilutions of genomic DNA, starting with 100 ng in the first dilution. For relative quantitation, the reaction mixtures consisted of LightCycler 480 SYBR Green I Master (Roche) with 500 nM of each primer and 10 ng DNA in a total volume of 25 µl. After an initial denaturation step for 10 min at 95 °C, thermal cycling conditions were 15s at 95 °C and 1 min at 60 °C for 40 cycles. Finally, the dissociation curves for each reaction were determined. All samples were run in duplicate/tripiclate on a LightCycler 480 instrument (Roche). The primers used were: ABL1-F (5'GGTGTGAAGCCCAAACCAAA), ABL1-R (5'TGACTGGCGTGATGTAGTTGCT), TIE1-F (5'CGAGATCCAGCTGACATGGAA), TIE1-R (5'CTCCACAACGTACTTGGATATTGG), MYB-F (5'GAACACCACTCCACTCCATCTCT), MYB-R (5'GGCGAGGCGCTTTCTTC).

Gene expression array analysis and statistics

RNA integrity, processing and hybridization to the U133 plus 2.0 GeneChip oligonucleotide microarray (Affymetrix) was performed according to manufacturer's protocol. The expression of *MYB* was calculated relatively to the median expression of *GAPDH* (six probesets) for each patient sample. The difference in gene expression levels for patients with and without the *MYB* duplication was evaluated using the Mann–Whitney *U* test (MWU).

Cell culture

DND-41, HSB-2, RPMI-8402, ALL-SIL, MOLT-4, LOUCY, P12-ICHIKAWA, CCRF-CEM (DSMZ, Braunschweig, Germany) were cultured in RPMI-1640 supplemented with 20% fetal calf serum. The number of viable cells was counted with a Vi-cell XR cell viability analyzer (Beckman Coulter, Fullerton, CA). For differentiation experiments, cells were cultured during a period of 6 days and electroporated on the first day and again on the 4th day with 50 nM siRNA. *MYB* stealth select siRNAs were purchased from Invitrogen (Carlsbad, CA). MYB siRNA1 (MYB-HSS106819, sequence: 5'UAUAGUGUCUCUGAAUGGCUGCGGC) was found to be the most efficient siRNA and was used in the differentiation experiments. Electroporation with a stealth siRNA directed against *ERBB4* (Invitrogen, Carlsbad, CA), a gene not expressed in these cell lines, served as a control. FACS analysis with a FITC labeled siRNA (Invitrogen) indicated that transfection efficiencies were generally > 55 %.

For inhibition of NOTCH1, we treated the cell ines with 1 µM of Compound E (gamma-secretase inhibitor XXI, Calbiochem, San Diego, CA) or DMSO (control) for 2 days.

FACS analysis

Analysis of CD3, CD4 and CD8 expression and cell cycle analysis was performed on 0.3-1 x 10^6 cells 6 days after the first electroporation with siRNA. We used the TriTEST CD4 FITC/CD8 PE/CD3 PerCP Reagent kit (Becton Dickinson, San Jose, CA) and the CycleTEST™ PLUS DNA Reagent Kit (Becton Dickinson). After staining, the cells were detected on a FACSCanto Flow Cytometer (Becton Dickinson) and the data were analyzed with the BD FACSDiva software (Becton Dickinson). Unstained cells and cells treated with ERBB4 siRNA were used as controls.

RESULTS & DISCUSSION

In order to detect novel unbalanced genomic rearrangements in T-ALL, we have performed array comparative genomic hybridization (array CGH)[6] using an array

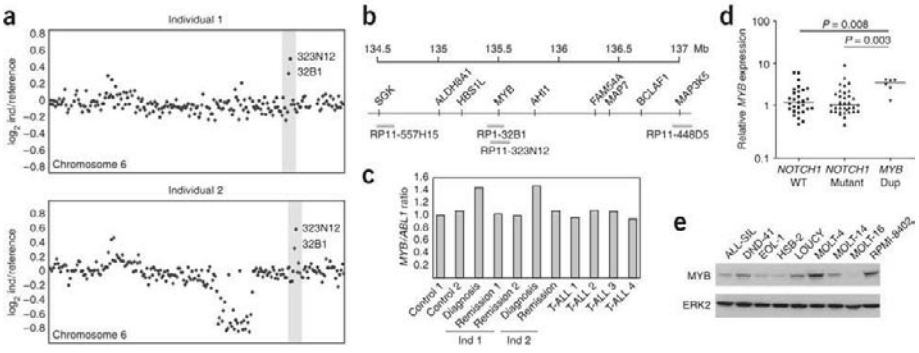

Figure 1 Molecular analysis of T-ALL cases with *MYB* duplication.
(a) Array CGH analysis of 2 individuals with T-ALL, revealing a duplication of the *MYB* locus. Each dot represents the log2 of the value for affected individuals versus a control sample, obtained for the different probes ordered based on their chromosomal location. The region between 131 and 141 Mb is shown as a shaded area. The location of the probes is shown in panel b. Individual 2 also has a large deletion on chromosome 6. The abnormalities were confirmed by dye swap experiments (not shown). (b) Schematic representation of the genomic region around the *MYB* locus. Probes that were on the array are indicated as grey bars. (c) Quantitative PCR documenting the presence of an extra copy of *MYB* in bone marrow cells from individuals 1 and 2 at time of diagnosis of T-ALL, and the absence of this extra copy in DNA extracted at time of remission. Control 1 and 2: normal individuals; T-ALL 1-4: T-ALL samples without *MYB* duplication detected by array CGH (d) Relative gene expression levels of *MYB* in T-ALL cases with *MYB* duplication (n=6), or without *MYB* duplication. Cases without *MYB* duplication are further divided in cases with *NOTCH1* mutation (n=35) or with wild type *NOTCH1* (n=29). (e) Western blot analysis of the expression of MYB in different T-ALL cell lines and 1 AML cell line (EOL-1). ALL-SIL, MOLT-4 and RPMI-8402 have the *MYB* duplication.

Table 1. Copy number of *MYB* and flanking genes in individuals and cell lines with *MYB* duplication

	Copy number as determined by quantitative PCR				
Individual	***SGK***	***HBS1L***	***MYB***	***AHI1***	***BCLAF1***
1	2	2	**3**	2	2
2	2	2	**3**	2	2
3	2	2	**3**	2	2
4	**3**	**3**	**3**	**3**	2
5	2	2	**3**	2	2
6	**4**	**4**	**4**	**4**	2
7	2	**3**	**3**	**3**	2
8	**3**	nd	**3**	nd	2
9	2	2	**3**	2	2
10	2	2	**3**	2	2
11	nd	nd	**3**	nd	nd
Cell line					
ALL-SIL	normal	dup	dup	dup	dup
RPMI-8402	normal	dup	dup	dup	normal
MOLT-4	normal	normal	dup	normal	normal
P12-ICHIKAWA	normal	dup	dup	dup	dup
CCRF-CEM	dup	dup	dup	dup	normal
MOLT-14	normal	normal	normal	normal	normal

nd, not determined; dup, duplicated.

with genomic BAC and PAC probes with an overall resolution of 1 Mb over the entire genome, but with additional probes around known and candidate oncogenes.

An initial screening of 27 T-ALL samples revealed an increased copy number of a small region (<2.5 Mb) at chromosome 6q23 in 2 individuals (Fig. 1a). The copy number change was detected with 2 probes covering the *MYB* (*c-MYB*) locus, whereas flanking probes on the array were unaffected (Fig. 1a,b). Quantitative PCR (Q-PCR) detected a duplication of *MYB* in these 2 individuals and confirmed a normal copy number for *MYB* in the other 25 individuals with T-ALL (Fig. 1c, data not shown). Copy number variations at the *MYB* locus have not been observed in the general population, based on data from the database of genomic variants[7,8]. In addition, Q-PCR analysis of DNA from diagnosis and remission samples showed the presence of the duplication in samples from diagnosis only, confirming that the duplication was an acquired event (Fig. 1c).

We next screened an independent set of 107 individuals with T-ALL and 12 T-ALL cell lines by Q-PCR. Duplication of *MYB* was detected in 9 of 107 (8.4 %) individuals

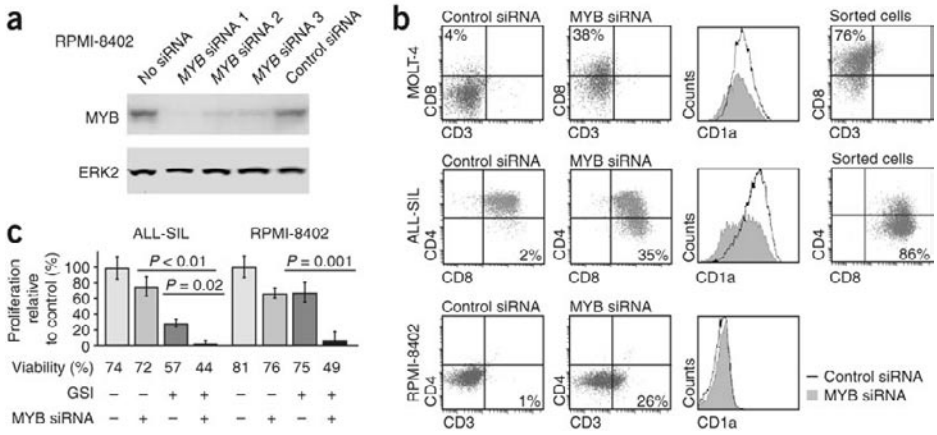

Figure 2 Effect of knock-down of *MYB* expression in T-ALL cell lines.
(a) Electroporation of 3 different MYB siRNA's in RPMI-8402 cells causes a decrease of *MYB* expression, compared to electroporation with no or control (*ERBB4*) siRNA. (b) Knock-down of *MYB* using MYB siRNA1 results in the differentiation of the ALL-SIL, RPMI-8402 and MOLT-4 cell lines, as observed by changes in expression of CD1a, CD3, CD4, or CD8 cell surface markers. Differentiated cells were separated from undifferentiated cells by flow sorting, and analysis of the sorted cells 10 days later indicates that the differentiation is irreversible. (c) Treatment of ALL-SIL and RPMI-8402 cells with gamma-secretase inhibitor (GSI), MYB siRNA or combination of both treatments indicates that knock-down of *MYB* expression in combination with GSI treatment blocks cell proliferation and affects cell survival. As control, cells were treated with DMSO or a control siRNA.

and in 5 cell lines (ALL-SIL, MOLT-4, P12-ICHIKAWA, CCRF-CEM and RPMI-8402). The flanking genes *HBS1L* and *AHI1* were duplicated in some patients, but the commonly duplicated region only covered the *MYB* gene (Table 1). Fluorescence *in situ* hybridization (FISH) revealed that the duplication of *MYB* was a local duplication with the extra copy of *MYB* located at chromosome 6q. Although the expression level of *MYB* was highly variable in T-ALL, likely to reflect the stage of T-cell differentiation[9] the mean expression level of *MYB* was found to be significantly elevated (3 fold) in T-ALL cases with *MYB* duplication compared to the other cases (Fig. 1d). In T-ALL cell lines, MYB protein expression was also variable, with MOLT-4 and RPMI-8402 (both with *MYB* duplication) showing high level MYB expression (Fig. 1e)[3].

The *MYB* gene encodes a nuclear transcription factor that is implicated in proliferation, survival and differentiation of hematopoietic progenitor cells[10]. Proper levels of MYB are important during hematopoietic cell development, and overexpression of *MYB* is implicated in murine leukemogenesis[9,11-14].

To determine a role for *MYB* duplication in the pathogenesis of human T-ALL, we downregulated *MYB* expression in T-ALL cell lines (Fig. 2a). Knock-down of *MYB* expression resulted in an irreversible differentiation of RPMI-8402, MOLT-4 and ALL-SIL cells, but not of cell lines without *MYB* duplication, as reported by changes in expression of the CD1a, CD3, CD4 or CD8 markers (Fig. 2b; data not

Table 2. Cytogenetic and molecular characteristics of individuals with T-ALL with *MYB* duplication

ind	karyotype	*NOTCH1* mutation	*CDKN2A*	other
1	46, XY[10]	Del P1583 Q2459*(stop)	+/+	ND
2	46, XY, del(9)(p13)[5]	F1593S	+/-	NA
3	46,XX,del(14)(q21q31)[4]	ND	+/+	NA
4	NA	InsS2468SRCHPRYSHP*(stop)	+/+	NA
5	46,XX[30]	NA	-/-	NA
6	NA	Del/InsFKRDA1607- 1611PSDLRLGGSDT	+/-	NA
7	46,XY,t(11,14)(p15,q11)[3]	Del/InsFK1607-1608RSE	-/-	*LMO1*$^{+}$ *TAL2*$^{+}$
8	NA	ND	+/-	NA
9	46,XY,t(10;14)(q2?4;q11)[2]; 46,idem,del(12)(p11)[10]; 46,idem,t(6;7)(p21;q34~35),del(12)(p11)[3]; 46,XY[9]	V1605G	-/-	*TLX1*$^{+}$
10	46,XY,del(6)(q15q21),del(14)(q11q32),der(14)inv(14); 46,idem,dup(1)?(q21q42)[2]; 46,idem,del(17)(p11)[4]	L1679P	+/+	NA
11	NA	V2286I	+/+	NA

Ind, individual; NA, not available; ND, none detected

shown). Downregulation of *MYB* expression had only a limited effect on the viability, proliferation and cell cycle (Fig 2c, data not shown). Since NOTCH1 was recently identified as a possible therapeutic target in TALL[4], and since 7 of 10 T-ALL cases and all 5 T-ALL cell lines with *MYB* duplication also harbored mutation of *NOTCH1* (Supplementary Table 2), we tested the effect of inhibition of NOTCH1 combined with MYB siRNA treatment. As previously shown, inhibition of NOTCH1 activation by treatment with a gamma-secretase inhibitor (GSI) led to inhibition of the proliferation of ALL-SIL and RPMI-8402[4].

Downregulation of *MYB* expression in combination with GSI treatment resulted in a strong synergistic effect on proliferation and viability (Fig. 2c). MOLT-4 is not sensitive to GSI treatment[4] and was not used for this analysis. Thus, while interference with MYB function mainly affects differentiation, a combined inhibition of MYB and NOTCH1 strongly affects proliferation and survival, establishing MYB as a novel target for therapy in T-ALL.

ACKNOWLEDGMENTS

This work was supported by grants from the Foundation against Cancer, foundation of public interest (J.C.), the 'Fonds voor Wetenschappelijk Onderzoek-Vlaanderen' (P.M., F.S.), the Interuniversity Attraction Poles (IAP) granted by the Federal Office for Scientific, Technical and Cultural Affairs, Belgium, a José Carreras fellowship from the European Hematology Association (J.C.), GOA grant 12051203 (F.S.), the Sophia Foundation for medical research (SSWO-404, P.V.V.), the Spanish Association against Cancer (I.L., M.D.O.), and a concerted action grant from the K.U.Leuven (J.C., P.V., I.W., P.M.). I.L. is a visiting postdoctoral researcher, K.D.K. an Aspirant, J.C. a postdoctoral researcher and P.V. a clinical investigator of the FWO-Vlaanderen. M.B. is funded by the IWT-Vlaanderen.

REFERENCES

1. Pui, C.H. *et al. N. Engl. J. Med.* **350**, 1535-1548 (2004).
2. Grabher, C. *et al. Nat. Rev. Cancer* **6**, 347-359 (2006).
3. De Keersmaecker, K. *et al. Haematologica* **90**, 1116-1127 (2005).
4. Weng, A.P. *et al. Science* **306**, 269-271 (2004).
5. Graux, C. *et al. Nat. Genet.* **36**, 1084-1089 (2004).
6. Speicher, M.R. & Carter,N.P. *Nat. Rev. Genet.* **6**, 782-792 (2005).
7. Iafrate, A.J. *et al. Nat. Genet.* **36**, 949-951 (2004).
8. Redon, R. *et al. Nature* **444**, 444-454 (2006).
9. Bender, T.P. *et al. Nat. Immunol.* **5**, 721-729 (2004).
10. Rothenberg, E.V. & Taghon,T. *Annu. Rev. Immunol.* **23**, 601-649 (2005).
11. Hess, J.L. *et al. Blood* **108**, 297-304 (2006).
12. Sakamoto, H. *et al. Blood* **108**, 896-903 (2006).
13. Lund, A.H. *et al. Nat. Genet.* **32**, 160-165 (2002).
14. Suzuki, T. *et al. Nat. Genet.* **32**, 166-174 (2002).

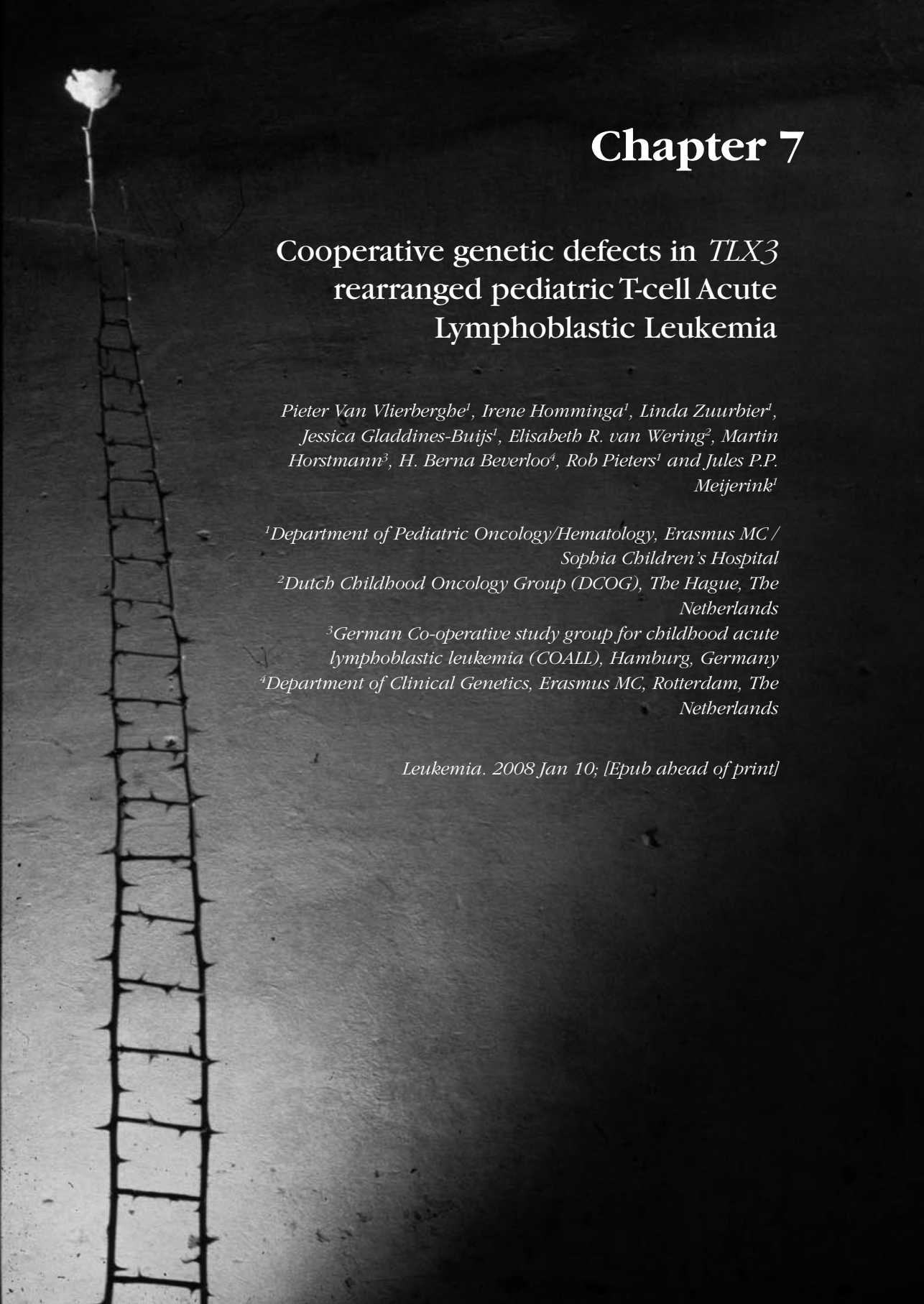

Chapter 7

Cooperative genetic defects in *TLX3* rearranged pediatric T-cell Acute Lymphoblastic Leukemia

Pieter Van Vlierberghe[1], Irene Homminga[1], Linda Zuurbier[1], Jessica Gladdines-Buijs[1], Elisabeth R. van Wering[2], Martin Horstmann[3], H. Berna Beverloo[4], Rob Pieters[1] and Jules P.P. Meijerink[1]

[1]Department of Pediatric Oncology/Hematology, Erasmus MC / Sophia Children's Hospital
[2]Dutch Childhood Oncology Group (DCOG), The Hague, The Netherlands
[3]German Co-operative study group for childhood acute lymphoblastic leukemia (COALL), Hamburg, Germany
[4]Department of Clinical Genetics, Erasmus MC, Rotterdam, The Netherlands

Leukemia. 2008 Jan 10; [Epub ahead of print]

ABSTRACT

T-ALL is an aggressive neoplastic disorder, in which multiple genetic abnormalities cooperate in the malignant transformation of thymocytes. About 20% of pediatric T-ALL cases are characterized by *TLX3* expression due to a cryptic translocation t(5;14)(q35;q32). Although a number of collaborating genetic events have been identified in *TLX3* rearranged T-ALL patients (*NOTCH1* mutations, *p15/p16* deletions, *NUP214-ABL1* amplifications), further elucidation of additional genetic lesions could provide a better understanding of the pathogenesis of this specific T-ALL subtype. In this study, we used array-CGH to screen *TLX3* rearranged T-ALL patients for new chromosomal imbalances. Array-CGH analysis revealed 5 recurrent genomic deletions in *TLX3* rearranged T-ALL, including del(1)(p36.31), del(5)(q35), del(13)(q14.3), del(16)(q22.1) and del(19)(p13.2). From these, the cryptic deletion, del(5)(q35), was exclusively identified in about 25% of *TLX3* rearranged T-ALL cases. In addition, 19 other genetic lesions were detected once in *TLX3* rearranged T-ALL cases, including a cryptic *WT1* deletion and a deletion covering the *FBXW7* gene, an U3-ubiquitin ligase that mediates the degradation of NOTCH1, MYC, JUN and Cyclin E. This study provides a genome wide overview of copy number changes in *TLX3* rearranged T-ALL and offers great new challenges for the identification of new target genes that may play a role in the pathogenesis of T-ALL.

INTRODUCTION

T-cell acute lymphoblastic leukemia (T-ALL) is an aggressive disorder of T-cells, and represents about 15% of pediatric ALL cases. T-ALL is characterized by a rapid progression of disease and shows a 30% relapse rate(1). Over the last decade, a large number of new genomic aberrations were identified in T-ALL, including chromosomal translocations (involving the genes *TAL1, LYL1, LMO1, LMO2, TLX1/HOX11, TLX3/HOX11L2, MYB, Cyclin D2)*, deletions (*SIL-TAL1*, del(6q), del(9)(p21), del(11)(p12p13)), amplifications (*NUP214-ABL1*), duplications (*MYB*) and mutations (*RAS*, *NOTCH1*)(2-11). Several of these abnormalities represent unique and mutually exclusive aberrations possibly delineating distinct T-ALL subgroups. Others occur in combination with various of these subgroups: for example, the del(9)(p21) that includes the *CDKN2A/p15* and *CDKN2B/p16* loci both deregulating the cell cycle(3, 12). Also *NOTCH1* activation mutations are present in more than half of all T-ALL cases of all subgroups(9). The genetic defects as identified in T-ALL so far target different cellular processes, including cell cycle regulation, T-cell differentiation, proliferation and survival. It is hypothesized that these genetic events cooperate in the leukemic transformation of thymocytes(13).

TLX3 is a homeobox gene that is not expressed in normal T-cell development. In T-ALL patients, it becomes aberrantly activated due to the cryptic translocation, t(5;14)(q35;q32), mostly juxtaposing *TLX3* to the *BCL11B* gene. *BCL11B* is normally expressed during T-cell maturation(14). Some alternative *TLX3* translocations have been described including the t(5;14)(q32;q11) juxtaposing *TLX3* to the *TCRα/δ* locus(15), and the t(5;7)(q35;q21) coupling *TLX3* to the *CDK6* gene(16). Although there is a clear relationship between the presence of *TLX3* translocations and *TLX3* expression levels(17), incidental *TLX3* expression has been described in the absence of chromosomal abnormalities(18, 19), suggesting that alternative mechanisms for *TLX3* activation exist in T-ALL. Conflicting data have been published about the relation between *TLX3* expression and treatment outcome. In some studies, *TLX3* rearranged T-ALL patients showed a poor prognosis, whereas in other studies *TLX3* translocations had no effect on outcome or was even associated with an improved outcome(17, 20, 21). These discrepancies have not been clarified thus far, but may be therapy dependent.

In this study, we used microarray-based comparative genome hybridization (array-CGH) to screen *TLX3* rearranged pediatric T-ALL patients for new chromosomal imbalances that could provide further insight in the development of *TLX3* mediated T-cell leukemia.

DESIGN & METHODS

Patients

Viably frozen diagnostic bone marrow or peripheral blood samples from 146 pediatric T-ALL patients were provided by the Dutch Childhood Oncology Group (DCOG) and the German Co-operative study group for childhood acute lymphoblastic leukemia (COALL)(17). The patients and patients' parents or their legal guardians provided informed consent to use leftover material for research purposes. Leukemic cells were isolated and enriched from these samples as previously described(8) and genomic DNA and total cellular RNA were isolated as described before(8).

Quantitative real-time RT-PCR (RQ-PCR)

cDNA synthesis and RQ-PCR in an ABI 7700 sequence detection system (Applied Biosystems, Foster City, CA, USA) was used to quantify the expression levels of *TLX3* transcripts relative to the endogenous housekeeping gene glyceraldehyde-3-phosphate dehydrogenase (*GAPDH*), as described previously(17). *NUP214-ABL1* fusions were determined as previously described(4).

Oligo array-CGH

Oligo array-CGH analysis was performed on the human genome CGH Microarray 44A (Agilent Technologies, Palo Alto, USA) according to the manufacturer's protocol, as previously described(8). Microarray images were analyzed using feature extraction software (version 8.1, Agilent) and the data were subsequently imported into array-CGH analytics software v3.1.28 (Agilent). For the detection of copy number abnormalities, we have used a Z-score cut-off value of 3. All copy number aberrations were compared to the database of genomic variants (http://projects.tcag.ca/variation) and all genomic regions previously linked to copy number variations(22) were not included in table 1.

FISH

Fluorescence in situ hybridization (FISH) was performed using a standard procedure, as described previously(17). *TLX3* translocations were determined using the *TLX3-U/TLX3-D* translocation probes (DakoCytomation, Glostrup, Denmark). BAC probes RP11-299P16 and RP11-98C11 (BACPAC resources, Oakland, CA, USA) were used to confirm the presence of *WT1* deletions, whereas RP11-300I24 and RP11-650G8 were used to confirm the *FBXW7* deletion. RP11-1072I20 (*RANBP17/TLX3*), RP11-10N18 (*RANBP17*) and RP11-117L6 (downstream of *TLX3*) as well as CTD-2243O22 (5qter) (Invitrogen, Breda, The Netherlands) were used to further characterize the deletion, del(5)(q35).

Real-Time Quantification of DNA Copy Number

Deletion analysis was performed using real-time quantitative PCR of the *NSD1* gene relative to the internal control gene, albumin, as previously described(23).

Mutation analysis

For the detection of *WT1* mutations, the purified DNA was subjected to 40 cycles of PCR of 15'' at 95ºC and 1' at 60ºC, using forward primer 5'-AAGCCTCCCTTC-CTCTTACTCT-3' and reverse primer 5'-TGGGTCCTTAGCAGTGTGAGA-3' for *WT1* exon 7. *FBXW7* mutation detection was performed using forward primer 5'-TTTTC-CAGTGTCTGAGAACAT-3' and reverse primer 5'-CCCAAATTCACCAATAATAGA-3' for exon 9, forward primer 5'- TAAACGTGGGTTTTTTTGTT-3' and reverse primer 5'- TCAGCAATTTGACAGTGATT-3' for exon 10 and forward primer 5'- GGACATG-GGTTTCTAAATATGTA-3' and reverse primer 5'- CTGCACCACTGAGAACAAG-3' for exon 12, using similar PCR conditions as described above. *NOTCH1* mutation screening in T-ALL was as previously described(24). PCR products were purified by standard methods and directly sequenced from both strands. The sequence data were analyzed using Seqscape V2.5 (Applied Biosystems).

RESULTS

Collaborating genetic events in *TLX3* rearranged T-ALL

In our previous study, we screened a large pediatric T-ALL cohort (n=146) for *TLX3* rearrangements using FISH and identified 29/146 (19%) rearranged cases(17), in line with previous studies(18, 19). All *TLX3* rearranged cases uniquely expressed *TLX3* whereas other T-ALL cases were negative(17). To identify additional genetic abnormalities that may cooperate with *TLX3* expression during T-cell leukemogenesis, we performed array-CGH analysis to detect genomic amplifications or deletions on those *TLX3* rearranged T-ALL cases for which material was available (n=21). All genomic deletions and/or amplifications as identified by array-CGH are summarized in table 1, except for known polymorphic copy number variations(22). Genomic deletions are more abundant compared to amplifications, as only 2 regions of genomic amplification in contrast to 22 regions of genomic deletion were identified in our *TLX3* rearranged patient cohort. To confirm if these additional aberrations are truly *TLX3* specific, we analyzed whether these additional abnormalities were also identified in a large-scale T-ALL array-CGH study (n=85, unpublished data) of non-*TLX3* rearranged T-ALL patients (table 1). Other known T-ALL specific genetic aberrations were determined using an RT-PCR or PCR and sequencing strategy or

Table 1. Novel genetic lesions in *TLX3* rearranged pediatric T-ALL

Chromosome Band	Gain Loss	Start (Mb)	End (Mb)	Size (Mb)	Case ID(s) (% of cases)	Gene(s) in region	*TLX3* WT*
1p36.31	Loss	5.95	7.21	1.26	2738, 2112, 2757, 585 (19)	18 genes including ***HES2/3, CAMTA*** and ***CHD5***	1
1p36.12-1p36.13	Loss	16.55	24.91	8.36	2757 (5)	> 50 genes	0
1p34.2-1p34.3	Loss	35.99	39.66	3.67	2757 (5)	> 30 genes	0
2p23.3-2p24.1	Loss	20.50	24.50	4.00	9012 (5)	12 genes including ***TP53I3*** and ***NCOA1***	1
2q37.1	Loss	233.30	234.45	1.15	2112 (5)	12 genes; non leukemia associated	1
3q13.32-3q21.2	Loss	119.90	126.40	6.50	585 (5)	> 50 genes, ***miR-198***	1
3q26.2-3q26.31	Loss	172.10	176.40	4.30	585 (5)	10 genes, ***miR-569***	2
4q31.3-4q32.1	Loss	153.08	155.51	2.43	2786 (5)	12 genes including ***FBXW7***	0
5q35.2-5q35.3	Loss	172.60	176.90	4.30	2112, 2640, 2650, 222, 9012 (24)	30 genes	0
6q25.1-6qter	Loss	149.94	170.80	20.86	222 (5)	> 100 genes	0
7q31.33-7q36.2	Loss	125.30	153.99	28.69	9012 (5)	> 100 genes, 11 microRNAs	1
8	Gain	0	146.25	146.25	2105 (5)	complete chromosome 8	7
9p24.1-9p24.2	Loss	2.71	5.12	2.41	2100 (5)	9 genes and *mIR-101-2*; breakpoint in ***JAK2***	0
9p21.3-9p21.3	Loss	21.70	22.10	0.40	16 cases** (76)	***CDKN2A/CDKN2B***	65
9q21.13-9q31.1	Loss	67.12	119.72	52.60	222 (5)	> 100 genes and 10 microRNAs	2
10p15.2-10p15.3	Loss	1.08	3.20	2.12	9858 (5)	*WDR37*, *ADARB2*, *PFKP* and *PITRM1*	0
10p11.23-10p12.1	Loss	27.99	30.05	2.06	9012 (5)	7 genes and *mIR-604*	0
11p13	Loss	32.00	33.50	1.50	2723 (5)	10 genes including ***WT1***	1
11q21-11q22.3	Loss	94.42	107.76	13.34	1179 (5)	> 20 genes, breakpoint in the ***ATM*** gene	1

Table 1. Novel genetic lesions in *TLX3* rearranged pediatric T-ALL							
12p13.1-12p13.2	Loss	12.50	13.10	0.60	9858 (5)	12 genes including ***CDKN1B***, *miR-613/614*	10
13q14.3	Loss	49.45	50.35	0.90	2112, 2723 (9)	*KCNRG*, ***miR-15/16a***, *DLEU7*	2
16q22.1	Loss	66.20	66.60	0.40	2100, 2112, 9012 (14)	12 genes including ***CTCF***	1
17q11.2	Loss	26.08	27.47	1.39	2780 (5)	11 genes including ***NF1,*** *mIR-193a / mIR-365-2*	2
19p13.2	loss	10.75	11.90	1.15	222, 378 (9)	33 genes, *miR-199a*	1
20p12.3-20pter	gain	0	5.94	5.94	9012 (5)	> 50 genes and *mIR-103-2*	1

*Number of non-*TLX3* rearranged T-ALL cases with a similar genetic aberration, identified in a large scale array-CGH study in T-ALL (n=85, unpublished data).

**Case ID(s) are shown in supplementary table 1.

using FISH, and included *NOTCH1* mutations(24), *NUP214-ABL1* amplifications(4) and *p15/p16* deletions.

The cryptic deletion, del(5)(q35), is associated with *TLX3* expression in T-ALL

The most frequent recurrent genetic abnormality identified in *TLX3* rearranged cases, was a heterozygous deletion at band 5q35, which was present in 5 out of 21 (24%) *TLX3* rearranged T-ALL cases. The deletional area differed in size among cases. In three cases (#2112, #2640 and #2650), the deletion started just downstream of the *TLX3* gene, as shown by the normal hybridization pattern of the *TLX3* probe, and loss of all 4 array-CGH probes covering the nucleophosmin (*NPM1*) gene located 80 kb telomeric of *TLX3* (Figure 1A,B). For these cases, FISH analysis using the *TLX3-U/TLX3-D* translocation probes confirmed the presence of this cryptic deletion (Figure 1C). In the other 2 cases (#9012 and #222), the deletion started upstream of *NKX2-5* (Figure 1D,E). However, gene expression array data revealed no *NKX2-5* expression in any of these 5 cases (data not shown). For cases #2112, #2640, #2650 and #9012, the deletion seemed to include the complete telomeric region (Figure 1E). For case #222, the terminal breakpoint was situated downstream of the *NSD1* gene. Therefore, the minimal deleted region at 5q35 for these 5 cases is about 4 Mb in size and contains 30 known genes including the *NSD1* gene. Gene expression array data revealed no difference in *NSD1* expression levels between del(5)(q35) positive and negative T-ALL patients (data not shown).

Quantitative PCR analysis of the *NSD1* gene, which is present in the minimal deleted region, on 26 *TLX3* rearranged T-ALL cases and 27 *TLX3* negative cases (including *TAL1* rearranged, *LMO2* rearranged, *TLX1* rearranged and *CALM-AF10* positive cases), confirmed a one-copy *NSD1* loss in all *TLX3* rearranged T-ALL cases having the cryptic del(5)(q35) deletion (Figure 1F). None of the non-*TLX3* rearranged cases showed loss of *NSD1*, indicating that none of these had a similar del(5)(q35).

Next, we studied whether the deletions that started just downstream of the *TLX3* gene (#2112, #2640 and #2650), truly represented cryptic 5q35 deletions, or rather corresponded to unbalanced *TLX3* translocations. Therefore, we performed FISH analysis using BAC clones covering the *RANBP17/TLX3* breakpoint region and the telomeric end of chromosome 5. For case 2650, FISH analysis using RP11-1072I20 and RP11-10N18, revealed 2 fusion signals indicating that both *TLX3* gene copies were normally present (data not shown). In addition, FISH analysis using RP11-1072I20, RP11-117L6 and CTD-2243O22, confirmed the presence of a del(5)(q35.1q35.3) (data not shown). In contrast, FISH analysis on case 2640 (data not shown) revealed an additional RP11-1072I20 (*RANBP17/TLX3*) hybridization signal, indicative for a cryptic unbalanced chromosomal rearrangement involving the *RANBP17/TLX3* loci. FISH analysis for the known translocation partners *TCR*α/δ, *TCR*β and *BCL11B* showed

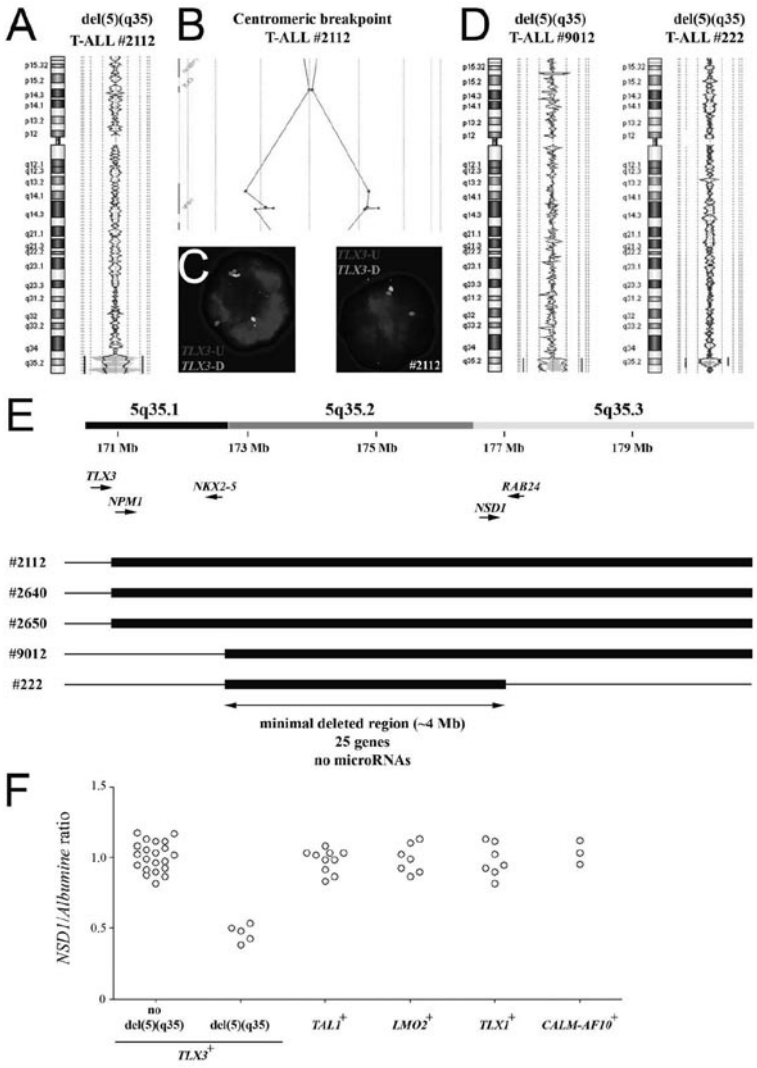

Figure 1. The recurrent cryptic deletion, del(5)(q35), in *TLX3* rearranged pediatric T-ALL. **(a)** Chromosome 5 ideogram and corresponding oligo array-CGH plot of case DNA:control DNA ratios (blue tracing) versus the dye-swap experiment (red tracing) for T-ALL cases 2112. Hybridization signals around the –2X or +2X lines represent loss of the corresponding region in the case DNA. **(b)** Detailed analysis of the centromeric breakpoint of the deletion in case 2112. **(c)** Dual-color FISH analysis on interphase cells of case 9858 (left panel) and case 2640 (right panel) using the *TLX3-U* (Red) and *TLX3-D* (Green) translocation probe set. Case 9858 showed a split signal, indicative for a *TLX3* translocation, whereas case 2640 showed loss of the *TLX3-D* (Green) signal. **(d)** Similar chromosome 5 ideograms as in **(a)** for T-ALL cases 9012 and 222. **(e)** Schematic overview of the minimal deleted region on chromosomal band 5q35 for the 5 TLX3 rearranged T-ALL cases showing a del(5)(q35). Depicted genome positions and gene locations are based on the UCSC Genome Browser at http://genome.ucsc.edu/. **(f)** quantitative PCR analysis of *NSD1*, present in the minimal deleted region, on 26 TLX3 rearranged T-ALL cases and 27 TLX3 negative cases.

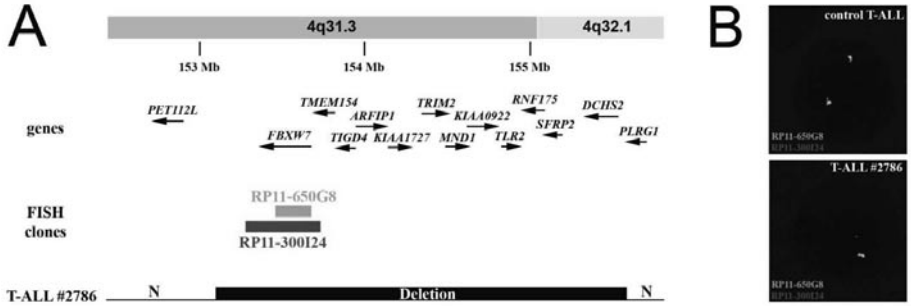

Figure 2. *FBXW7* deletion in pediatric T-ALL

(a) Schematic overview of the chromosomal deletion, del(4)(q31.3q32.1), as detected in case 2786. Genomic positions of genes situated in this chromosomal region and BAC clones used for FISH analysis are depicted. **(b)** FISH analysis using RP11-650G8 (green) and RP11-300I24 (red) confirms the presence of the del(4)(q31.3q32.1) in case 2786.

that these loci were not involved in this chromosomal rearrangement (data not shown), indicating that patient 2640 has a novel variant of *TLX3* rearrangement with subsequent loss of 5q35.1. For case 2112, no material was left to perform additional *TLX3* specific FISH analyses.

Other recurrent genomic deletions in TLX3 rearranged T-ALL

Besides the cryptic deletion, del(5)(q35), 4 other recurrent genetic abnormalities were identified in various *TLX3* rearranged T-ALL cases (table 1). At chromosome 1, an identical cryptic deletion of ~1 Mb was detected at chromosomal band 1p36 in three cases (#2738, #2112 and #585) (data not shown). This deletion area was also comprised in a larger deletion in case #2757 that in addition demonstrated multiple deletions on chromosome 1p (Table 1). The minimal deleted area on 1p36 for these 4 cases comprised 18 genes, including *HES2, HES3* and *CHD5* (data not shown). The centromeric breakpoints of the del(1)(p36.31) in cases #2738, #2112 and #585 all clustered in the *CAMTA1* gene (data not shown).

Cryptic deletions of chromosome 13q were identified in 2 *TLX3* rearranged T-ALL cases (#2112, #2723). These deletions differed in size and the minimal deleted region contained the microRNA cluster, *miR-15/miR-16a* (data not shown).

Three T-ALL cases showed cryptic deletions at chromosomal band 16q22.1 (#2100, #2112 and #9012) (table 1). This del(16)(q22.1) seemed identical in 2 cases (#2100 and #9012), but was smaller (~400 kb) in a third case (#2112). The minimal deleted area comprised 12 genes, and included the *CTCF* gene.

Finally, 2 other cases contained similar deletions at 19p13.2 (#222 and #378) covering a region of approximately 1.4 Mb (table 1) that covers 33 genes and the microRNA gene *miR-199a*.

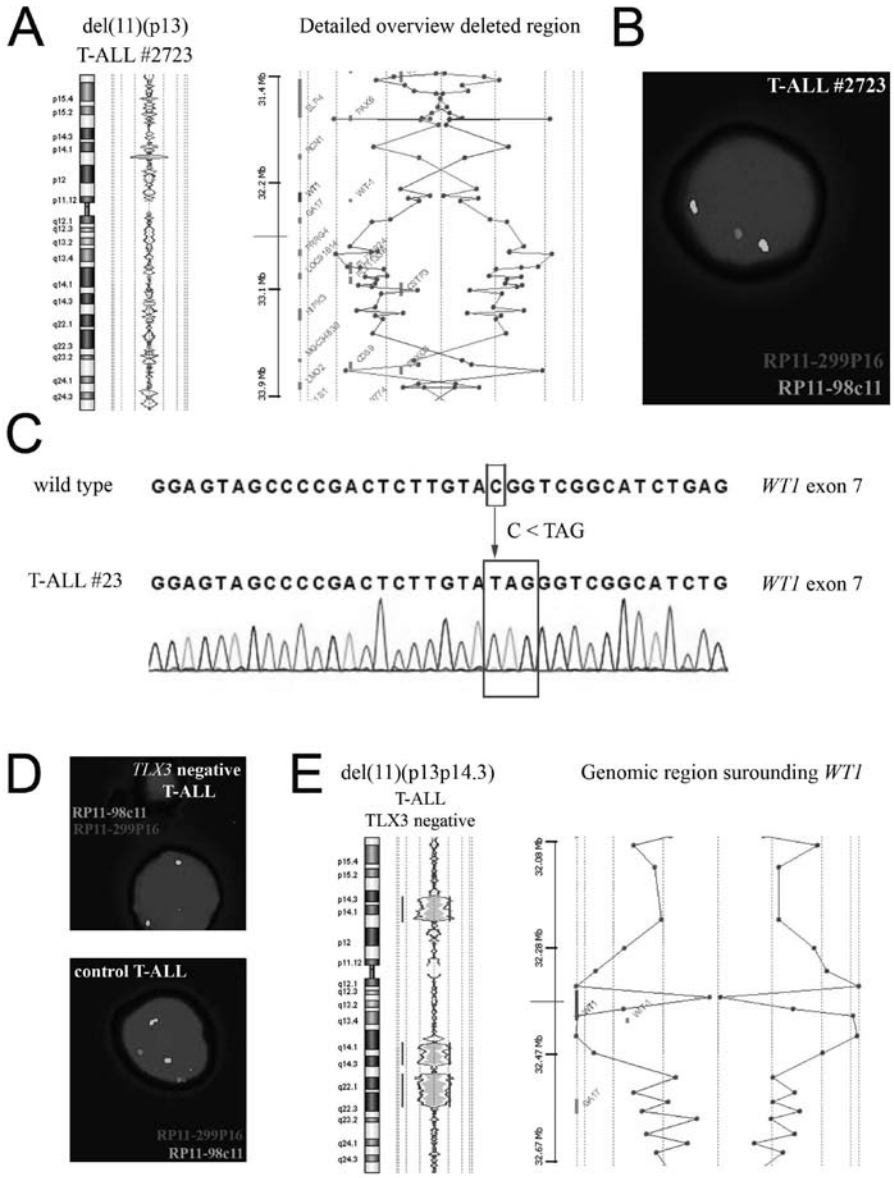

Figure 3. *WT1* inactivation in pediatric T-ALL

(a) Chromosome 11 ideogram and oligo array-CGH plot for the deletion, del(11)(p13), as detected in case 2723 (left panel). The right panel shows a detailed overview of the deleted region for this 11p13 deletion. **(b)** FISH analysis using RP11-98C11 (green) and RP11-299P16 (red, covering *WT1*) confirms the presence of the del(11)(p13) in case 2723. **(c)** Sequence analysis shows a truncating *WT1* exon 7 mutation on the remaining allele of case 2723. **(d)** Similar FISH analysis as in **(b)** on TLX3 wildtype T-ALL cases identified one additional case showing a biallelic *WT1* deletion. **(e)** Array-CGH analysis confirmed the presence of a large mono-allelic deletion, del(11)(p13p14.3), in combination with an additional loss of the genomic region surrounding the *WT1* gene on the other allele.

Genetic abnormalities identified in single TLX3 rearranged T-ALL cases

Apart from the recurrent abnormalities, other genetic abnormalities were observed in single cases (table 1) and occasionally contained known tumor suppressor genes (*FBWX7, WT1, ATM, p27KIP1, NF1*). None of these abnormalities have been reported as normal copy number variation in the healthy population(22).

One case (#2786) showed a cryptic deletion on the long arm of chromosome 4 of about 2.5 Mb in size, del(4)(q31.3q32.1), which contained amongst others the *FBXW7* gene (Figure 2). The loss of one *FBXW7* gene copy in this case was confirmed using FISH (Figure 2B). *FBXW7* mutations have recently been identified in 8-30% of primary T-ALL samples(25-28). Therefore, we screened case #2786 for the currently known *FBXW7* mutations. This analysis revealed no additional *FBXW7* mutation on the remaining allele of this case.

Other rearrangements identified in single *TLX3* rearranged cases included a cryptic deletion, del(12)(p13.1p13.2), including the *CDKN1B/p27/KIP1* gene (#9858) and a cryptic deletion, del(17)(q12), including the *NF1* gene (#2780) (29). In one case (#2100), the breakpoint of a cryptic deletion on chromosome 9, del(9)(p24.1p24.2), was situated in *JAK2*. In another case (#1179), the breakpoint of a cryptic deletion on chromosome 11, del(11)(q21q22.3), was located in the *ATM* gene.

WT1 inactivation in pediatric T-ALL

Another abnormality that was identified in a single *TLX3* rearranged case (#2723) was a cryptic deletion of about 1.5 Mb in size, del(11)(p13p13), and included the Wilms' tumor 1 (*WT1*) gene (Figure 3A). Because conflicting data have been reported on the role of WT1 as a tumor suppressor and/or oncogene in human leukemias(30), we wondered whether *WT1* was indeed the target gene of this genomic deletion. The telomeric breakpoint of this deletion was situated downstream of the *WT1* gene, whereas the centromeric breakpoint was located downstream of the *CD59* gene (Figure 3A). FISH analysis confirmed the one-copy loss of *WT1* in this case (Figure Figure 3B). In order to investigate *WT1* inactivation in this case, the remaining *WT1* allele was analyzed for the presence of inactivation mutations. A small frameshift mutation (delCinsTAG) was identified in exon 7, disrupting the *WT1* coding region (Figure 3C).

To investigate whether *WT1* inactivation is restricted to *TLX3* rearranged T-ALL cases, we performed additional *WT1* specific FISH analysis on 25 *TLX3* negative pediatric T-ALL cases. This revealed one additional case in which FISH analysis revealed a loss of both *WT1* gene copies (Figure 3D). Subsequent array-CGH analysis confirmed the presence of a large mono-allelic deletion on the short arm of chromosome 11, del(11)(p13p14.3), in combination with a loss of the genomic region surrounding the *WT1* gene on the other allele (Figure 3E). Gene expression array

data showed that *WT1* expression was virtually absent in this T-ALL case showing a homozygous *WT1* deletion (data not shown). For case #2723, *WT1* was equally expressed compared to *WT1* wildtype cases of all T-ALL subgroups (*TAL1, LMO2, TLX3, TLX1* and unknown) (data not shown).

DISCUSSION

In order to get more insight in new genetic defects that may cooperate with *TLX3* gene expression in the leukemic transformation of thymocytes, we performed array-CGH analysis on a *TLX3* rearranged T-ALL patient cohort.

About 25% of *TLX3* rearranged T-ALL cases showed a deletion at the terminal end of the long arm of chromosome 5. Interestingly, for a number of cases, the genomic breakpoint of this deletion was situated just downstream of the *TLX3* oncogene. The deletions in these cases differ from the previously described *TLX3* deletions that involved a genomic region upstream of the *TLX3* gene near the translocation breakpoint(16). Although most T-ALL cases that show *TLX3* expression harbor a cryptic translocation at this genomic locus, a number of studies have reported *TLX3* activation in the presence of a seemingly normal *TLX3* locus(18, 19). For case 2650, combined array-CGH and FISH analysis strongly suggest that the *TLX3* expression is associated with a interstitial del(5)(q35.1q35.3) in the absence of a *TLX3* translocation. It is therefore tempting to speculate that *TLX3* is normally under transcriptional control of a negative regulatory domain downstream of *TLX3*. Deletion of this negative regulatory element may lead to ectopic *TLX3* expression. In addition, a potential tumor suppressor gene could be present in the minimal deleted area at 5q35 that specifically cooperates with *TLX3* expression in the leukemogenesis of T-ALL. This hypothesis is strengthened by the fact that 2 cases have smaller 5q35 deletions with breakpoints near *NKX2-5*. A potential candidate gene in this 5q35 genomic region is *NSD1*. Mutations or deletions of the *NSD1* gene are the major cause of Sotos syndrome, a constitutional overgrowth disorder(31), and patients with this syndrome have a higher risk for the development of leukemia(32-34). In addition, *NSD1* is involved in a cryptic translocation, t(5;11)(q35;p15.5), generating a *NUP98-NSD1* fusion gene in AML(35). Although gene expression array data revealed no difference in *NSD1* gene expression between patients with and without the del(5)(q35), a future mutation screening of *NSD1* in *TLX3* rearranged T-ALL is mandatory to evaluate a potential role for *NSD1* inactivation in T-ALL.

Cryptic deletions on chromosome 1 were identified in 4 T-ALL cases with a commonly deleted region surrounding chromosomal band 1p36. Similar 1p36 deletions were previously identified in about 30% of human neuroblastomas(36),

25% of colorectal cancer cases(37), and a variety of hematological malignancies including AML(38), CML(39) and non-Hodgkin's lymphoma(40). In neuroblastoma and colorectal cancer, reduced expression levels of the CAMTA1 gene correlated with adverse outcome, suggesting that *CAMTA1* could act as the 1p36-specifc tumor suppressor gene in these malignancies(36, 37). Another interesting target gene in this genomic region is the chromodomain helicase DNA binding domain 5 (*CHD5*) gene, which has been shown to be a tumor suppressor that controls proliferation and apoptosis via the p19Arf/p53 pathway(41). Other potential target genes within this genomic region are *HES2* and *HES3*, both of which are highly similar to *HES1* that is a bHLH transcriptional repressor and known *NOTCH1* target gene(42). Also the *TNFRSF25* gene may represent a target gene of this deletion. *TNFRSF25* is a member of the TNF-receptor family which controls lymphocyte proliferation and regulates cell apoptosis(43).

The minimal deleted region of the cryptic deletions on chromosome 13 contained the microRNA cluster, *miR-15/miR-16a*. In CLL, deletion of this *miR-15/miR-16a* cluster leads to the activation of anti-apoptotic BCL2(44). For example in case #2723 (data not shown), activation of BCL2 could cooperate with a homozygous deletion of the *p15/p16* locus, a *NOTCH1* mutation and activated *TLX3* expression in the development of T-ALL.

Three *TLX3* rearranged T-ALL cases showed cryptic deletions on chromosomal band 16q22.1. In AML, this genomic region is recurrently targeted by cytogenetic abnormalities including an inversion, inv(16)(p13q22), a translocation, t(16;16)(p13q22) and a deletion, del(16)(q22)(40). The inv(16) and t(16;16) both result in a *CBFB-MYH11* fusion gene, which is associated with a more favorable prognosis(45). In contrast, the deletion del(16)(q22) does not provide a favorable outcome and it remains to be elucidated whether *CBFB* is targeted in the 16q deletions in AML(46). In the *TLX3* rearranged T-ALL cases, the minimal deleted region on 16q22.1 contained 21 genes but lacked the *CBFB* gene. One interesting candidate genes in this genomic region is *CTCF*, which is a conserved transcriptional repressor of the *MYC* oncogene(47). MYC has been described in T-ALL to become aberrantly activated due to a TCR-mediated translocation(48) and has been shown to represent an important downstream target of activated *NOTCH1*(49, 50). Therefore, inactivation of *CTCF* could represent an alternative mechanism for MYC activation in T-ALL.

The majority of novel regions of genomic amplification or deletion were only detected in single *TLX3* rearranged T-ALL cases (n=19). Given their low frequency, one could argue that their oncogenic role in T-ALL is negligible. However, *NOTCH1*, which was originally identified due to its involvement in a rare chromosomal translocation (<1%), was later identified as the most predominant mutational target in T-ALL (>50% of cases)(9). Similarly, the cryptic deletion, del(4)(q31.3q32.1), that

was detected in a single case, includes the *FBXW7* gene. FBXW7 is an F-box protein that binds specific substrates including CyclinE, NOTCH1, cMYC and cJUN in order to target these for ubiquitin-mediated proteolysis. Heterozygous missense mutations of the *FBXW7* gene are present in 8-30% of T-ALL cases(25-28), demonstrating the importance of this gene in T-ALL albeit inactivation through chromosomal deletions is rare. Mutant *FBXW7* has lost the potential to bind the PEST domain of NOTCH1-IC and target NOTCH1 for proteolytic degradation. This results in stabilized NOTCH1-IC in the nucleus, providing an alternative mechanism of NOTCH1 activation in T-ALL that is insensitive for gamma-secretase inhibition. The present study describes the first case of a heterozygous *FBXW7* deletion in human T-ALL. Haploinsufficiency of *FBXW7* may be sufficient for NOTCH1 stabilization as no *FBXW7* mutation could be identified in the remaining allele. *FBXW7* mutations can occur in combination with NOTCH1 heterodimerization (HD) mutations but not with PEST truncating mutations, and may complement the relatively weak transcriptional activity of HD mutant NOTCH1 molecules(28). In our del(4)(q31.3q32.1)-positive T-ALL case, an activating NOTCH1 mutation was identified in the HD domain.

Deletions on the short arm of chromosome 12 are frequently detected in a wide range of hematological malignancies. A recent genome-wide copy number analysis showed 12p deletions in about 25% of B-ALL cases and suggested the *TEL* gene as the main target of this genomic abnormality(51). However, the 12p deletion that we identified was about 600 kb in size and included the *CDKN1B/p27/KIP1* gene and the microRNA genes *miR-613* and *miR-614*, whereas it did not include the *TEL* gene. This indicates that the target gene(s) for 12p deletions probably differs between T-cell and B-cell ALL. The *CDKN1B/p27/KIP1* gene encodes a cell cycle regulator that, similar to p15/p16, inhibits cyclin-dependent kinases (CDK). Loss of these CDK inhibitors may result in uncontrolled cell cycle. The T-ALL case with this *CDKN1B* deletion (#9858) also contained a homozygous *p15/p16* deletion, indicating that different T-cell cycle defects can collaborate with a *NOTCH1* mutation and *TLX3* overexpression in the development of T-ALL (data not shown).

WT1, a transcription factor involved in normal cellular development and cell survival, was initially discovered as a tumor suppressor in Wilms' Tumor, a pediatric kidney malignancy(52). In acute leukemias, there is evidence that this gene can both act as an oncogene as well as a tumor suppressor gene(30). *WT1* mutations have been described in acute myeloid leukemia (AML), leading to a truncated WT1 protein(53, 54). In addition, specific AML subtypes show low levels of *WT1* expression(30). Both observations are consistent with a tumor suppressor role of WT1 in AML. In contrast, a variety of leukemias are characterized by activated *WT1* expression compared to normal bone marrow or normal progenitor cells(55, 56), that has been associated with poor outcome(57, 58). Our single T-ALL case with a deletion

of *WT1* combined with an inactivational mutation in the remaining *WT1* allele points towards a potential tumor suppressor role of *WT1* in T-ALL. *WT1* inactivation is not restricted to *TLX3* rearranged T-ALL cases, as bi-allelic WT1 deletions were also observed in a *TLX3* negative T-ALL case indicating that WT1 inactivation may be a more general collaborating genetic event in T-cell leukemia. Nevertheless, the *TLX3* rearranged T-ALL case showing *WT1* inactivation also harbored a *miR-15/miR-16a* deletion, further extending the range of different genetic defects that collaborate in T-ALL development.

In conclusion, we performed a genome wide copy number screening on *TLX3* rearranged T-ALL cases and identified the cryptic deletion, del(5)(q35), as a new and recurrent genetic aberration that is exclusively associated with *TLX3* expression in T-ALL. In addition, we identified a number of genetic events, including *FBXW7* and *WT1* inactivation that could collaborate with *TLX3* expression, *NOTCH1* activation and *p15/p16* deletion in the development of T-cell leukemia. As shown for *FBXW7*, the identification of new genomic deletions/amplifications, even at low frequency, can still highlight important target genes with a broader role in T-ALL. Therefore, it is likely that the current overview of genetic defects will be further helpful for a better understanding of the molecular pathways leading to T-cell leukemia.

REFERENCES

1. Pui CH, Relling MV, Downing JR. Acute lymphoblastic leukemia. *N Engl J Med* 2004 Apr 8; **350**(15)**:** 1535-1548.
2. Clappier E, Cuccuini W, Cayuela JM, Vecchione D, Baruchel A, Dombret H*, et al*. Cyclin D2 dysregulation by chromosomal translocations to TCR loci in T-cell acute lymphoblastic leukemias. *Leukemia* 2006 Jan; **20**(1)**:** 82-86.
3. De Keersmaecker K, Marynen P, Cools J. Genetic insights in the pathogenesis of T-cell acute lymphoblastic leukemia. *Haematologica* 2005 Aug; **90**(8)**:** 1116-1127.
4. Graux C, Cools J, Melotte C, Quentmeier H, Ferrando A, Levine R*, et al*. Fusion of NUP214 to ABL1 on amplified episomes in T-cell acute lymphoblastic leukemia. *Nat Genet* 2004 Oct; **36**(10)**:** 1084-1089.
5. Lahortiga I, De Keersmaecker K, Van Vlierberghe P, Graux C, Cauwelier B, Lambert F*, et al*. Duplication of the MYB oncogene in T cell acute lymphoblastic leukemia. *Nat Genet* 2007 May; **39**(5)**:** 593-595.
6. Soulier J, Clappier E, Cayuela JM, Regnault A, Garcia-Peydro M, Dombret H*, et al*. HOXA genes are included in genetic and biologic networks defining human acute T-cell leukemia (T-ALL). *Blood* 2005 Jul 1; **106**(1)**:** 274-286.
7. Speleman F, Cauwelier B, Dastugue N, Cools J, Verhasselt B, Poppe B*, et al*. A new recurrent inversion, inv(7)(p15q34), leads to transcriptional activation of HOXA10 and HOXA11 in a subset of T-cell acute lymphoblastic leukemias. *Leukemia* 2005 Mar; **19**(3)**:** 358-366.
8. Van Vlierberghe P, van Grotel M, Beverloo HB, Lee C, Helgason T, Buijs-Gladdines J*, et al*. The cryptic chromosomal deletion del(11)(p12p13) as a new activation mechanism of LMO2 in pediatric T-cell acute lymphoblastic leukemia. *Blood* 2006 Nov 15; **108**(10)**:** 3520-3529.
9. Weng AP, Ferrando AA, Lee W, Morris JPt, Silverman LB, Sanchez-Irizarry C*, et al*. Activating mutations of NOTCH1 in human T cell acute lymphoblastic leukemia. *Science* 2004 Oct 8; **306**(5694)**:** 269-271.
10. Clappier E, Cuccuini W, Kalota A, Crinquette A, Cayuela JM, Dik WA*, et al*. The C-MYB locus is involved in chromosomal translocation and genomic duplications in human T-cell acute leukemia (T-ALL), the translocation defining a new T-ALL subtype in very young children. *Blood* 2007 Aug 15; **110**(4)**:** 1251-1261.
11. Graux C, Cools J, Michaux L, Vandenberghe P, Hagemeijer A. Cytogenetics and molecular genetics of T-cell acute lymphoblastic leukemia: from thymocyte to lymphoblast. *Leukemia* 2006 Sep; **20**(9)**:** 1496-1510.
12. Armstrong SA, Look AT. Molecular genetics of acute lymphoblastic leukemia. *J Clin Oncol* 2005 Sep 10; **23**(26)**:** 6306-6315.
13. Grabher C, von Boehmer H, Look AT. Notch 1 activation in the molecular pathogenesis of T-cell acute lymphoblastic leukaemia. *Nat Rev Cancer* 2006 May; **6**(5)**:** 347-359.
14. Bernard OA, Busson-LeConiat M, Ballerini P, Mauchauffe M, Della Valle V, Monni R*, et al*. A new recurrent and specific cryptic translocation, t(5;14)(q35;q32), is associated with expression of the Hox11L2 gene in T acute lymphoblastic leukemia. *Leukemia* 2001 Oct; **15**(10)**:** 1495-1504.
15. Hansen-Hagge TE, Schafer M, Kiyoi H, Morris SW, Whitlock JA, Koch P*, et al*. Disruption of the RanBP17/Hox11L2 region by recombination with the TCRdelta locus in acute lymphoblastic leukemias with t(5;14)(q34;q11). *Leukemia* 2002 Nov; **16**(11)**:** 2205-2212.

16. Su XY, Busson M, Della Valle V, Ballerini P, Dastugue N, Talmant P, *et al.* Various types of rearrangements target TLX3 locus in T-cell acute lymphoblastic leukemia. *Genes Chromosomes Cancer* 2004 Nov; **41**(3)**:** 243-249.

17. van Grotel M, Meijerink JP, Beverloo HB, Langerak AW, Buys-Gladdines JG, Schneider P, *et al.* The outcome of molecular-cytogenetic subgroups in pediatric T-cell acute lymphoblastic leukemia: a retrospective study of patients treated according to DCOG or COALL protocols. *Haematologica* 2006 Sep; **91**(9)**:** 1212-1221.

18. Berger R, Dastugue N, Busson M, Van Den Akker J, Perot C, Ballerini P, *et al.* t(5;14)/HOX11L2-positive T-cell acute lymphoblastic leukemia. A collaborative study of the Groupe Francais de Cytogenetique Hematologique (GFCH). *Leukemia* 2003 Sep; **17**(9)**:** 1851-1857.

19. Mauvieux L, Leymarie V, Helias C, Perrusson N, Falkenrodt A, Lioure B, *et al.* High incidence of Hox11L2 expression in children with T-ALL. *Leukemia* 2002 Dec; **16**(12)**:** 2417-2422.

20. Ballerini P, Blaise A, Busson-Le Coniat M, Su XY, Zucman-Rossi J, Adam M, *et al.* HOX11L2 expression defines a clinical subtype of pediatric T-ALL associated with poor prognosis. *Blood* 2002 Aug 1; **100**(3)**:** 991-997.

21. Cave H, Suciu S, Preudhomme C, Poppe B, Robert A, Uyttebroeck A, *et al.* Clinical significance of HOX11L2 expression linked to t(5;14)(q35;q32), of HOX11 expression, and of SIL-TAL fusion in childhood T-cell malignancies: results of EORTC studies 58881 and 58951. *Blood* 2004 Jan 15; **103**(2)**:** 442-450.

22. Redon R, Ishikawa S, Fitch KR, Feuk L, Perry GH, Andrews TD, *et al.* Global variation in copy number in the human genome. *Nature* 2006 Nov 23; **444**(7118)**:** 444-454.

23. Waggoner DJ, Raca G, Welch K, Dempsey M, Anderes E, Ostrovnaya I, *et al.* NSD1 analysis for Sotos syndrome: insights and perspectives from the clinical laboratory. *Genet Med* 2005 Oct; **7**(8)**:** 524-533.

24. van Grotel M, Meijerink JP, van Wering ER, Langerak AW, Beverloo HB, Buijs-Gladdines JG, *et al.* Prognostic significance of molecular-cytogenetic abnormalities in pediatric T-ALL is not explained by immunophenotypic differences. *Leukemia* 2007 Oct 11 (advance online publication).

25. Malyukova A, Dohda T, von der Lehr N, Akhondi S, Corcoran M, Heyman M, *et al.* The tumor suppressor gene hCDC4 is frequently mutated in human T-cell acute lymphoblastic leukemia with functional consequences for Notch signaling. *Cancer Res* 2007 Jun 15; **67**(12)**:** 5611-5616.

26. Maser RS, Choudhury B, Campbell PJ, Feng B, Wong KK, Protopopov A, *et al.* Chromosomally unstable mouse tumours have genomic alterations similar to diverse human cancers. *Nature* 2007 Jun 21; **447**(7147)**:** 966-971.

27. O'Neil J, Grim J, Strack P, Rao S, Tibbitts D, Winter C, *et al.* FBW7 mutations in leukemic cells mediate NOTCH pathway activation and resistance to gamma-secretase inhibitors. *J Exp Med* 2007 Aug 6; **204**(8)**:** 1813-1824.

28. Thompson BJ, Buonamici S, Sulis ML, Palomero T, Vilimas T, Basso G, *et al.* The SCFFBW7 ubiquitin ligase complex as a tumor suppressor in T cell leukemia. *J Exp Med* 2007 Aug 6; **204**(8)**:** 1825-1835.

29. Balgobind B, Van Vlierberghe P, van den Ouweland A, Beverloo HB, Terlouw-Kromosoeto J, van Wering ER, *et al.* Leukemia associated NF1 inactivation in pediatric T-ALL and AML patients lacking evidence for neurofibromatosis. *Blood* 2007 (in press).

30. Yang L, Han Y, Suarez Saiz F, Minden MD. A tumor suppressor and oncogene: the WT1 story. *Leukemia* 2007 May; **21**(5)**:** 868-876.

31. Kurotaki N, Imaizumi K, Harada N, Masuno M, Kondoh T, Nagai T, *et al.* Haploinsufficiency of NSD1 causes Sotos syndrome. *Nature genetics* 2002 Apr; **30**(4)**:** 365-366.

32. Al-Mulla N, Belgaumi AF, Teebi A. Cancer in Sotos syndrome: report of a patient with acute myelocytic leukemia and review of the literature. *J Pediatr Hematol Oncol* 2004 Mar; **26**(3)**:** 204-208.

33. Martinez-Glez V, Lapunzina P. Sotos syndrome is associated with leukemia/lymphoma. *Am J Med Genet A* 2007 Jun 1; **143**(11)**:** 1244-1245.

34. Ziino O, Rondelli R, Micalizzi C, Luciani M, Conter V, Arico M. Acute lymphoblastic leukemia in children with associated genetic conditions other than Down's syndrome. The AIEOP experience. *Haematologica* 2006 Jan; **91**(1)**:** 139-140.

35. Brown J, Jawad M, Twigg SR, Saracoglu K, Sauerbrey A, Thomas AE, *et al.* A cryptic t(5;11)(q35;p15.5) in 2 children with acute myeloid leukemia with apparently normal karyotypes, identified by a multiplex fluorescence in situ hybridization telomere assay. *Blood* 2002 Apr 1; **99**(7)**:** 2526-2531.

36. Henrich KO, Fischer M, Mertens D, Benner A, Wiedemeyer R, Brors B, *et al.* Reduced expression of CAMTA1 correlates with adverse outcome in neuroblastoma patients. *Clin Cancer Res* 2006 Jan 1; **12**(1)**:** 131-138.

37. Kim MY, Yim SH, Kwon MS, Kim TM, Shin SH, Kang HM, *et al.* Recurrent genomic alterations with impact on survival in colorectal cancer identified by genome-wide array comparative genomic hybridization. *Gastroenterology* 2006 Dec; **131**(6)**:** 1913-1924.

38. Mori N, Morosetti R, Mizoguchi H, Koeffler HP. Progression of myelodysplastic syndrome: allelic loss on chromosomal arm 1p. *Br J Haematol* 2003 Jul; **122**(2)**:** 226-230.

39. Mori N, Morosetti R, Spira S, Lee S, Ben-Yehuda D, Schiller G, *et al.* Chromosome band 1p36 contains a putative tumor suppressor gene important in the evolution of chronic myelocytic leukemia. *Blood* 1998 Nov 1; **92**(9)**:** 3405-3409.

40. Melendez B, Cuadros M, Robledo M, Rivas C, Fernandez-Piqueras J, Martinez-Delgado B, *et al.* Coincidental LOH regions in mouse and humans: evidence for novel tumor suppressor loci at 9q22-q34 in non-Hodgkin's lymphomas. *Leuk Res* 2003 Jul; **27**(7)**:** 627-633.

41. Bagchi A, Papazoglu C, Wu Y, Capurso D, Brodt M, Francis D, *et al.* CHD5 is a tumor suppressor at human 1p36. *Cell* 2007 Feb 9; **128**(3)**:** 459-475.

42. Fischer A, Gessler M. Delta-Notch--and then? Protein interactions and proposed modes of repression by Hes and Hey bHLH factors. *Nucleic Acids Res* 2007; **35**(14)**:** 4583-4596.

43. Chinnaiyan AM, O'Rourke K, Yu GL, Lyons RH, Garg M, Duan DR, *et al.* Signal transduction by DR3, a death domain-containing receptor related to TNFR-1 and CD95. *Science (New York, NY* 1996 Nov 8; **274**(5289)**:** 990-992.

44. Cimmino A, Calin GA, Fabbri M, Iorio MV, Ferracin M, Shimizu M, *et al.* miR-15 and miR-16 induce apoptosis by targeting BCL2. *Proc Natl Acad Sci U S A* 2005 Sep 27; **102**(39)**:** 13944-13949.

45. Plantier I, Lai JL, Wattel E, Bauters F, Fenaux P. Inv(16) may be one of the only 'favorable' factors in acute myeloid leukemia: a report on 19 cases with prolonged follow-up. *Leuk Res* 1994 Dec; **18**(12)**:** 885-888.

46. Betts DR, Ammann RA, Hirt A, Hengartner H, Beck-Popovic M, Kuhne T, *et al.* The prognostic significance of cytogenetic aberrations in childhood acute myeloid leukaemia. A study of the Swiss Paediatric Oncology Group (SPOG). *Eur J Haematol* 2007 Jun; **78**(6)**:** 468-476.

47. Filippova GN, Fagerlie S, Klenova EM, Myers C, Dehner Y, Goodwin G, *et al.* An exceptionally conserved transcriptional repressor, CTCF, employs different combinations of zinc fingers

to bind diverged promoter sequences of avian and mammalian c-myc oncogenes. *Mol Cell Biol* 1996 Jun; **16**(6)**:** 2802-2813.

48. Inaba T, Murakami S, Oku N, Itoh K, Ura Y, Nakanishi S*, et al*. Translocation between chromosomes 8q24 and 14q11 in T-cell acute lymphoblastic leukemia. *Cancer Genet Cytogenet* 1990 Oct 1; **49**(1)**:** 69-74.

49. Palomero T, Lim WK, Odom DT, Sulis ML, Real PJ, Margolin A*, et al*. NOTCH1 directly regulates c-MYC and activates a feed-forward-loop transcriptional network promoting leukemic cell growth. *Proc Natl Acad Sci U S A* 2006 Nov 28; **103**(48)**:** 18261-18266.

50. Weng AP, Millholland JM, Yashiro-Ohtani Y, Arcangeli ML, Lau A, Wai C*, et al*. c-Myc is an important direct target of Notch1 in T-cell acute lymphoblastic leukemia/lymphoma. *Genes Dev* 2006 Aug 1; **20**(15)**:** 2096-2109.

51. Mullighan CG, Goorha S, Radtke I, Miller CB, Coustan-Smith E, Dalton JD*, et al*. Genome-wide analysis of genetic alterations in acute lymphoblastic leukaemia. *Nature* 2007 Apr 12; **446**(7137)**:** 758-764.

52. Little M, Wells C. A clinical overview of WT1 gene mutations. *Hum Mutat* 1997; **9**(3)**:** 209-225.

53. King-Underwood L, Pritchard-Jones K. Wilms' tumor (WT1) gene mutations occur mainly in acute myeloid leukemia and may confer drug resistance. *Blood* 1998 Apr 15; **91**(8)**:** 2961-2968.

54. King-Underwood L, Renshaw J, Pritchard-Jones K. Mutations in the Wilms' tumor gene WT1 in leukemias. *Blood* 1996 Mar 15; **87**(6)**:** 2171-2179.

55. Miwa H, Beran M, Saunders GF. Expression of the Wilms' tumor gene (WT1) in human leukemias. *Leukemia* 1992 May; **6**(5)**:** 405-409.

56. Miyagi T, Ahuja H, Kubota T, Kubonishi I, Koeffler HP, Miyoshi I. Expression of the candidate Wilm's tumor gene, WT1, in human leukemia cells. *Leukemia* 1993 Jul; **7**(7)**:** 970-977.

57. Barragan E, Cervera J, Bolufer P, Ballester S, Martin G, Fernandez P*, et al*. Prognostic implications of Wilms' tumor gene (WT1) expression in patients with de novo acute myeloid leukemia. *Haematologica* 2004 Aug; **89**(8)**:** 926-933.

58. Chiusa L, Francia di Celle P, Campisi P, Ceretto C, Marmont F, Pich A. Prognostic value of quantitative analysis of WT1 gene transcripts in adult acute lymphoblastic leukemia. *Haematologica* 2006 Feb; **91**(2)**:** 270-271.

Chapter 8

Leukemia associated *NF1* inactivation in pediatric T-ALL and AML patients lacking evidence for neurofibromatosis

Brian V. Balgobind[1*], Pieter Van Vlierberghe[1*], Ans M.W. van den Ouweland[2], H. Berna Beverloo[2], Joan N.R. Terlouw-Kromosoeto[2], Elisabeth R. van Wering[3], Dirk Reinhardt[4], Martin Horstmann[5], Gertjan J.L. Kaspers[6], C. Michel Zwaan[1], Rob Pieters[1], Marry M. Van den Heuvel-Eibrink[1,7] and Jules P.P. Meijerink[1,7]

**These authors contributed equally to this study*

[1]Department of Pediatric Oncology/Hematology, Erasmus MC / Sophia Children's Hospital, Rotterdam, The Netherlands
[2]Department of Clinical Genetics, Erasmus MC, Rotterdam, The Netherlands
[3]Dutch Childhood Oncology Group (DCOG), The Hague, The Netherlands
[4]AML-BFM Study Group, Hannover, Germany
[5]German Co-operative study group for childhood acute lymphoblastic leukemia (COALL), Hamburg, Germany
[6]Department of Pediatric Oncology/Hematology, VU University Medical Center, Amsterdam, The Netherlands
[7]These authors can be considered equally as last authors

Blood. 2008 Jan 5; [Epub ahead of print]

ABSTRACT

Neurofibromatosis type 1 (NF1) is an autosomal dominant genetic disorder caused by mutations in the *NF1* gene. NF1 patients have a higher risk to develop juvenile myelomonocytic leukemia (JMML) with a possible progression towards acute myeloid leukemia (AML). In an oligo array-comparative genomic hybridization based screening of 103 pediatric T-cell acute lymphoblastic leukemia (T-ALL) and 71 *MLL* rearranged AML patients, a recurrent cryptic deletion, del(17)(q11.2), was identified in 3 T-ALL and 2 *MLL* rearranged AML patients. This deletion has previously been described as a microdeletion of the *NF1* region in patients with NF1. However, our patients lacked clinical NF1 symptoms. Mutation analysis in 4 of these del(17)(q11.2)-positive patients revealed that mutations in the remaining *NF1* allele were present in 3 patients, confirming its role as a tumor-suppressor gene in cancer. In addition, *NF1* inactivation was confirmed at the RNA expression level in 3 patients tested. Since the NF1 protein is a negative regulator of the RAS pathway (RAS-GTPase activating protein), homozygous *NF1* inactivation represent a novel type-I mutation in pediatric *MLL* rearranged AML and T-ALL with a predicted frequency that is less than 10%. *NF1* inactivation may provide an additional proliferative signal towards the development of leukemia.

INTRODUCTION

Neurofibromatosis type 1 (NF1) is an autosomal genetic disorder that is clinically characterized by cafe-au-lait spots and frequent fibromatous tumors of the skin and tumors of the central nervous system. The NF1 disorder is caused by genetic heterozygous mutations in the *NF1* gene on chromosome 17q11.2. The majority of *NF1* mutations is intragenic and has been found over the complete gene. They comprise a diversity of mutation types, where splicing mutations are particularly prevalent given the number of exons. This result into truncation for a large percentage of cases, thereby inactivating the encoded protein neurofibromin[1]. Another genetic aberration includes microdeletions affecting the entire *NF1* locus. Patients with these *NF1* microdeletions display a more severe NF1 phenotype, characterized by mental retardation, facial dysmorphism, and increased risk for developing malignant tumors including leukemias[2,3]. To this end, NF1 has also been associated with juvenile myelomonocytic leukemia (JMML), with a risk of progression towards acute myeloid leukemia (AML). These malignancies are associated with loss of the wild-type allele, either through deletions or the acquisition of point mutations. In JMML, it has also frequently been reported that the wild-type allele is replaced by the mutant allele as an effect of recombinational events leading to uniparental disomy (UPD)[4-6]. Previously, it was shown that bi-allelic inactivation of *NF1* are found as somatic abnormalities in JMML patients that lack clinical evidence of NF1[7]. Somatic inactivation of Nf1 in hematopoietic cells results in a progressive myeloproliferative disorder in mice[8], confirming that *NF1* acts as a tumor suppressor gene[5]. The NF1 gene protein product, neurofibromin, is a GTPase-activating protein (GAP) which inhibits RAS signaling by hydrolysis of active RAS-GTP into inactive RAS-GDP[1,9]. Therefore NF1 deficiencies act as functional equivalents of activational mutations in *RAS*. Indeed, *NF1* inactivation and *RAS* mutations have been found in a mutually exclusive manner in JMML[7].

AML is a heterogeneous disease, in which early treatment response and cytogenetic abnormalities are the most important prognostic factors. In AML, genetic aberrations can be classified as type-I or type-II mutations. One hypothesis about the development of AML is the co-existence of both type I and type II mutations which confer proliferative signals (type I mutations affecting the *FLT3, C-KIT, NRAS, KRAS* or *PTPN11* genes) in combination with type II differentiation impairing mutations (such as *PML-RARα*, *AML-ETO*, *CBFB-MYH11* or *MLL* rearrangements)[10].

MLL rearrangements account for 8-20% of all cytogenetic abnormalities in pediatric AML[11,12]. *HOX*-genes are the prime targets of MLL fusion products and regulate cellular differentiation in normal hematopoietic development. However Eguchi et al point to another role of MLL fusion products in *MLL* rearranged leukemias through

the alteration of cell cycle arrest and apoptosis[13]. Most of these *MLL*-positive AML samples are morphologically classified as FAB-M4 and FAB-M5 and it has been suggested that *MLL* rearrangements in pediatric AML are associated with a poor outcome. Interestingly, in some studies the t(9;11) subgroup has been associated with a higher sensitivity to different classes of drugs and a better prognosis[14-16]. In addition, many of these *MLL* rearranged AML patients lack mutations in *FLT3*, *C-KIT*, *NRAS*, *KRAS* and *PTPN11*, indicating that the type I mutations remains to be elucidated. High-resolution genomic screening of MLL rearranged AML patients could provide us with further insight into novel genetic aberrations with prognostic significance or new type-I mutations in MLL rearranged AML.

T-ALL represents about 15% of pediatric ALL cases and is characterized by a rapid progression of disease and a 30% relapse rate within the first 2 years after diagnosis[17]. Over the last decade, a large number of new genomic aberrations were identified in T-ALL, including chromosomal translocations, deletions, amplifications and mutations[18-20]. All these genetic defects target different cellular processes, including the cell-cycle, T-cell differentiation, proliferation and survival. Cooperation of these genetic events initiates leukemic transformation of thymocytes[18]. *RAS* mutations have been found in less than 5 percent of T-ALL patients showing that proliferative hits affecting the RAS pathway remain rare[18]. On the other hand, more than 50 percent of the T-ALL cases are characterized by activating mutations in the NOTCH1 pathway including the *NOTCH1* gene itself[21,22], or the NOTCH1 regulating U3-ubiquitin ligase *FBXW7*[23,24].

In this study, we used oligo array-comparative genomic hybridization (array-CGH) and identified somatic NF1 microdeletions as a cryptic genetic abnormality in pediatric T-ALL and MLL rearranged AML patients that lack symptoms of neurofibromatosis. We present further evidence for the role of *NF1* inactivation as a functional equivalent to activated RAS signalling, and suggest that this can be considered as a new type I mutation in MLL rearranged AML and a proliferative hit in T-ALL.

MATERIAL AND METHODS

Patients

Viably frozen diagnostic bone marrow or peripheral blood samples from 103 pediatric T-ALL patients and 71 pediatric *MLL* rearranged AML patients were provided by the Dutch Childhood Oncology Group (DCOG), the German Co-operative study group for childhood acute lymphoblastic leukemia (COALL) and the 'Berlin-Frankfurt-Münster' AML Study Group (AML-BFM-SG). Informed consent was obtained according to local law and regulations. Leukemic cells were isolated and enriched

from these samples as previously described[25]. All resulting samples contained ≥90% leukemic cells, as determined morphologically by May-Grünwald-Giemsa (Merck, Darmstadt, Germany)-stained cytospins. These leukemic cells were used for DNA and RNA extraction, and a minimum of 5×10^6 leukemic cells were lysed in Trizol reagent (Gibco BRL, Life Technologies, Breda, The Netherlands) and stored at -80°C. Genomic DNA and total cellular RNA were isolated as described before[25]. From the patients with a deletion of NF1, remission and relapse material was only available for patient #2736.

Oligo array-CGH

Oligo array-CGH analysis was performed on the human genome CGH Microarray 44k-A (Agilent Technologies, Palo Alto, USA) according to the manufacturer's protocol using a dye-swap experimental design to minimize false positive results, as previously described[25,26].

Multiplex ligation-dependent probe amplification (MLPA)

MLPA analysis was performed using the SALSA P081/082 MLPA assay (MRC Holland, Amsterdam, The Netherlands) SALSA P081/082 consists of two reaction mixes containing probes for all constitutive NF1 exons except for exons 5, 7, 17, 19A, 45, and 47. The exact localization of the MLPA probes can be downloaded from the MRC Holland Web site (www.mrc-holland.com). The two reactions contain 15 and 13 control probes in other regions of the genome, respectively. The patients' samples were analyzed with MLPA according to the manufacturer's protocol[27,28]. Data were analyzed using GeneMarker v1.5 (Softgenetics, State College, USA).

Mutation analysis

For the detection of NF1 mutations, DNA was subjected to 40 cycles of polymerase chain reaction (PCR) of 15" at 95ºC and 1' at 60ºC, using specific primers for all *NF1* exons, which are being used in NF1 diagnostics (Department of Clinical Genetics, Erasmus MC, Rotterdam, The Netherlands, manuscript in preparation, primers are available on request at a.vandenouweland@erasmusmc.nl). *RAS, PTPN11* and *C-KIT* mutation screening was performed as described in supplementary table 1. *NOTCH1* and *FLT3* mutational screening were done as previously described[21,29,30]. PCR products were purified by standard methods and directly sequenced from both strands. The sequence data were analysed using Seqscape V2.5 (Applied Biosystems, Foster City, USA).

NF1 expression analysis

NF1 expression was calculated based upon non-normalized gene expression array data, performed on the human genome U133 Plus 2.0 array (Affymetrix, Santa Clara, USA), as previously described[31], which were available for 3 del(17)(q11.2)-positive and 7 del(17)(q11.2)-negative leukemia patients. For the *NF1* probe-sets, the expression was normalized to the median expression of *GAPDH* (6 probesets) for each patient sample. The difference in relative gene expression levels between patients with and without the del(17)(q11.2) was evaluated using the Mann-Whitney-U test.

RESULTS

High resolution genomic screening of a selected subgroup of 103 pediatric T-ALL and 71 *MLL* rearranged AML patients using a 44K oligo array-CGH platform led to the identification of a cryptic deletion, del(17)(q11.2). This deletion was recurrently observed in 3 T-ALL and 2 AML cases (Figure 1a,b; Table 1). These deletions were about 1.2 Mb in size and covered the *NF1* gene. For all patients, the telomeric breakpoints were situated in the *JJAZ1* gene, whereas the centromeric breakpoints clustered in its pseudogene *JJAZ1P* (Figure 1c,d). The deletion area in these samples was equivalent to those observed in patients with NF1. Genetic and clinical patient characteristics for all del(17)(q11.2)-positive leukemia patients are summarized in table 1. One of the 3 T-ALL and at least one of the two AML patients relapsed.

To further confirm the deletion breakpoints, four out of five del(17)(q11.2)-positive leukemia patients and 15 del(17)(q11.2)-negative controls (7 T-ALL and 8 AML) were analyzed using an *NF1* locus specific MLPA assay[27,28]. No residual material was available for patient #6421. These analyses confirmed that one copy of the *NF1* locus was lost in all these 4 cases (Figure 2, only T-ALL 2736 is shown), whereas all control patients retained both copies of the *NF1* gene (only AML control 3339 is shown).

In order to investigate complete *NF1* inactivation in our patients, we performed mutation analysis on all exons and exon/intron boundaries of the *NF1* gene in the 4 del(17)(q11.2)-positive leukemia patients, and in an additional group of 39 patients without a deletion involving chromosomal band 17q11.2 (including 21 *MLL* rearranged AMLs and 18 T-ALLs). Small frameshift mutations disrupting the *NF1* coding region were only detected in 3 out of 4 del(17)(q11.2)-positive patients (table 1, figure 3), leading to bi-allelic inactivation of NF1 in these patients. One T-ALL patient and two *MLL* rearranged AML patients without a del(17)(q11.2) had a mono-allelic mutation in non-functional domains, possibly reflecting rare polymorphisms. Furthermore, *NF1* expression in the del(17)(q11.2)-positive T-ALL and *MLL* rearranged

AML leukemias was significantly lower in 3 patients tested, as compared to 7 cases of T-ALL and AML patient samples which are wild-type for *NF1* (Figure 4).

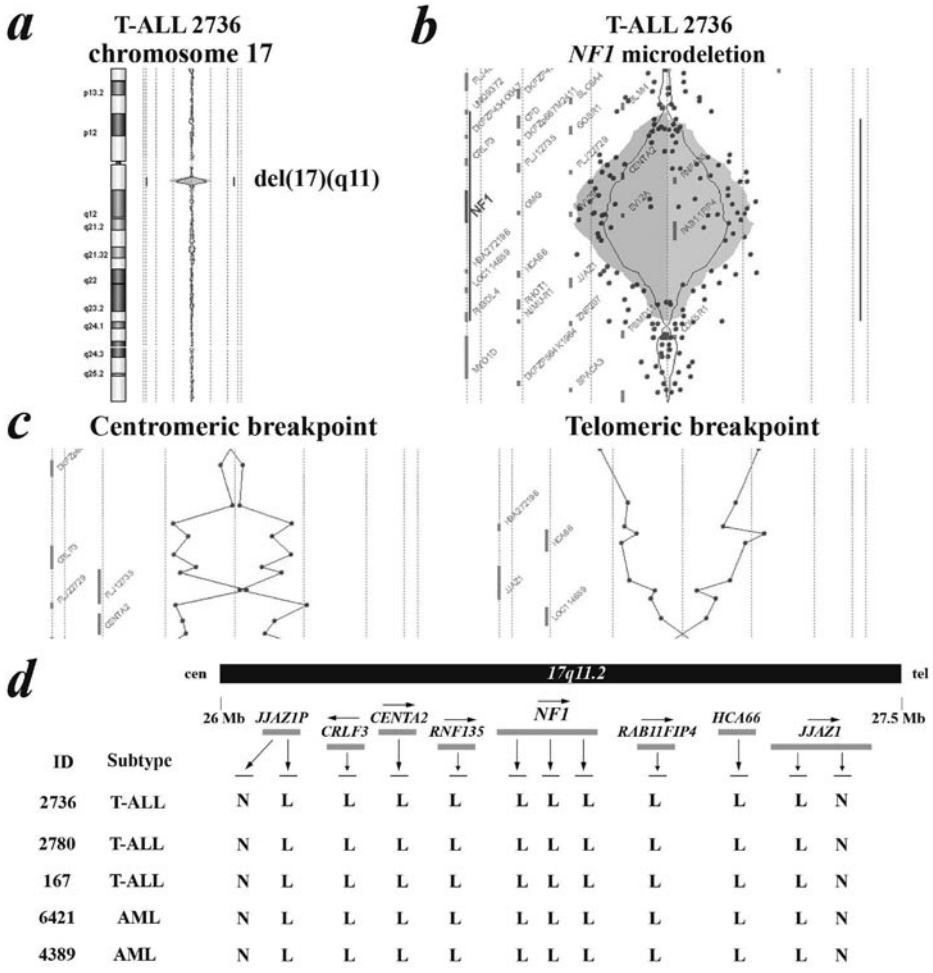

Figure 1. *NF1* microdeletions in pediatric acute leukemias.

(a) Chromosome 17 ideogram and corresponding oligo array-CGH plot of patient DNA/control DNA ratios (blue tracing) versus the dye-swap experiment (red tracing) for T-ALL patient #2736.

(b) Detailed visualization of the *NF1* microdeletion at chromosomal band 17q11 in T-ALL patient #2736. Hybridization signals around the –2X or +2X lines represent loss of the corresponding region in the patient DNA.

(c) Detailed analysis of the centromeric (left panel) and telomeric (right panel) breakpoint of the *NF1* microdeletion in patient #2736.

(d) Overview of oligo array-CGH results in the chromosomal region 17q11.2 for 3 T-ALL and 2 AML patients with del(17)(q11.2). The 60-mer oligos present on the DNA array and located in this genomic area, as well as the specific genes located in this region with their transcription direction, are shown. Arrows above the indicated genes represent the direction of transcription

Abbreviations: N; normal, L; loss, cen: centromere, tel: telomere.

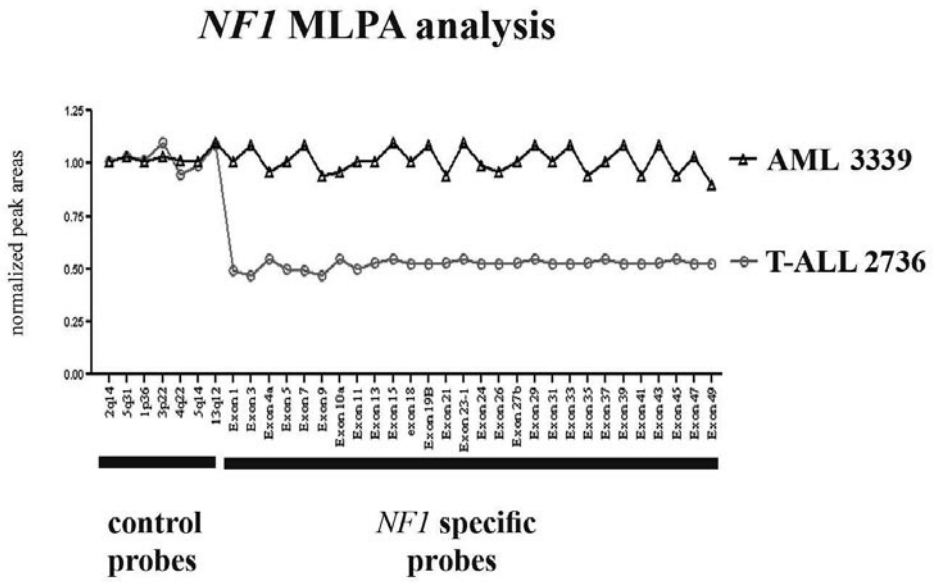

Figure 2. MLPA analysis of *NF1* in selected cases.
MLPA analysis of the *NF1* locus in T-ALL patient #2736 and AML patient #3339. Normalized peak areas around 0.5 represent monoallelic loss of the corresponding genomic region.

To further verify a somatic rather than a genetic origin of *NF1* inactivation, we screened relapse and remission material of T-ALL patient #2736, for whom material was available. At relapse the *NF1* microdeletion and *NF1* mutation on the other allele were present, while in the remission sample both mutations remained undetected.

Since *NF1* deficiency could act as a novel type 1 mutation, we screened all del(17)(q11.2)-positive leukemia patients for activational mutations in *RAS*. Although *N-RAS* or *K-RAS* mutations have been described in *MLL* rearranged AML and T-ALL, no somatic *N-RAS* or *K-RAS* mutations were found in our 5 del(17)(q11.2)-positive leukemia patients. In addition, both *MLL* rearranged AML patients with a NF1 deletion lacked other type I mutations in *FLT3*, *C-KIT* or *PTPN11* in their leukemic cells. The frequency of these mutations in the 71 *MLL* rearranged AML samples was low, as expected. Only 35% had one of these mutations, and all these mutations were mutually exclusive. Furthermore, the del(17)(q11.2)-positive T-ALL patients were screened for rearrangements at the *TAL1*, *HOX11L2*, *HOX11*, *CALM-AF10*, *MLL* and *cMYC* loci or the presence of *NOTCH1* mutations. One patient (#167) lacked rearrangements of any of the loci mentioned above, whereas a *HOX11L2* translocation (#2780) and a *CALM-AF10* fusion gene (#2736) were detected in 2 other cases. *NOTCH1* mutations were identified in patients #2780 (heterodimerization domain; L1601P) and #167 (PEST domain; 2445insLL).

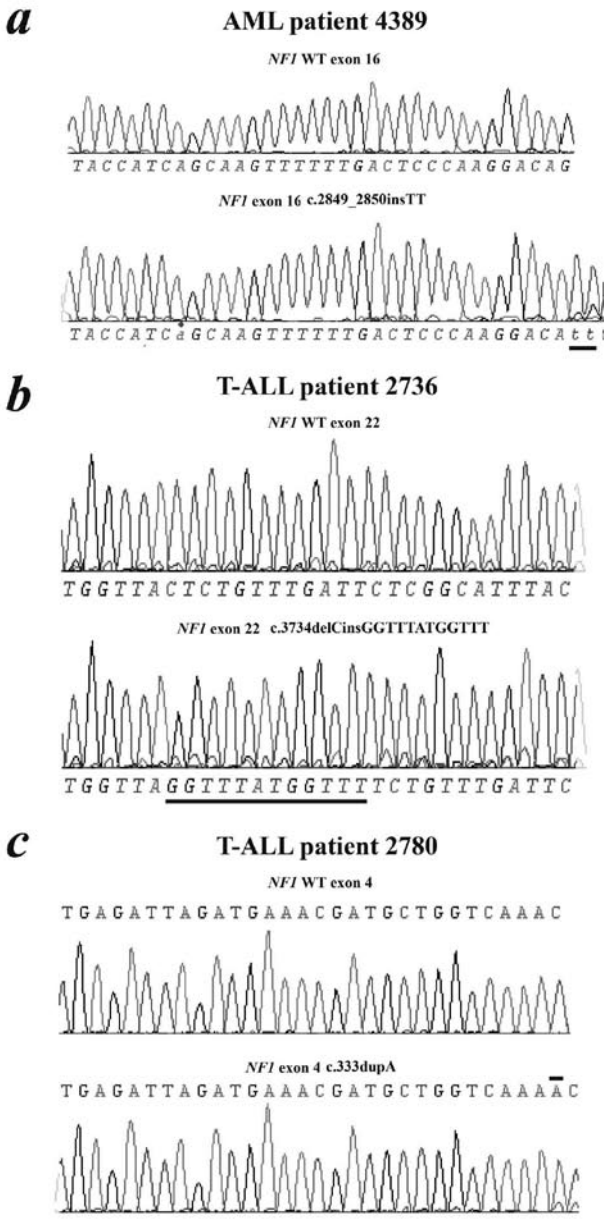

Figure 3. Truncating *NF1* mutations in pediatric T-ALL and AML.

(a) Sequence analysis of patient #4389 (AML) showing a *c.2849_2850insTT* mutation in the remaining *NF1* allele

(b) Sequence analysis of patient #2736 (T-ALL) showing a *c.3734delCinsGGTTTATGGTTT* mutation in the remaining *NF1* allele

(c) Sequence analysis of patient #2780 (T-ALL) showing a *c.333dupA* mutation in the remaining *NF1* allele

Table 1. Patient characteristics and truncating *NF1* mutations in pediatric T-ALL and AML

ID	Subtype	Sex	Age (yrs)	WBC (x 10^9 / l)	Relapse CCR, (# months)	Genetic Subtype	Karyotype	*NF1* del	*NF1* Mutation analysis		Additional mutation analysis			
									Nucleotide level		*FLT3*	*C-KIT*	*RAS*	*PTPN11*
									exon	mutation				
2736	T-ALL	M	10.1	13	Relapse, 15	*CALM-AF10*	46,XY,t(2;9)(q21;q34),?t(8,8)(?q22;q?24)	yes	22	c.3734delCinsGGTTTATGGTTT	WT	WT	WT	WT
2736 Remission							46,XY	no		WT	WT	WT	WT	WT
2736 Relapse							46,XY,t(2;9)(q21;q34),?t(8,8)(?q22;q?24)	yes	22	c.3734delCinsGGTTTATGGTTT	WT	WT	WT	WT
2780	T-ALL	F	5	140	CCR, 50+	*TLX3*	46,XX	yes	4	c.333dupA	WT	WT	WT	WT
167	T-ALL	M	16.4	170.9	CCR, 56+	Unknown	NA	yes	WT		WT	WT	WT	WT
4389	AML	F	18.8	41.7	NA	*MLL-AF9*	46,XX,t(9;11)(p22;q23)[4]/46,XX [7]	yes	16	c.2849_2850insTT	WT	WT	WT	WT
6421	AML	F	6.5	NA	Relapse, 68	*MLL-AF10*	47,XX,t(10;11)(p13;q23),+19	yes	ND		WT	WT	WT	WT

WBC: White blood cell count; CCR: continued complete remission; WT: Wildtype; ND: Not determined; NA: Not available

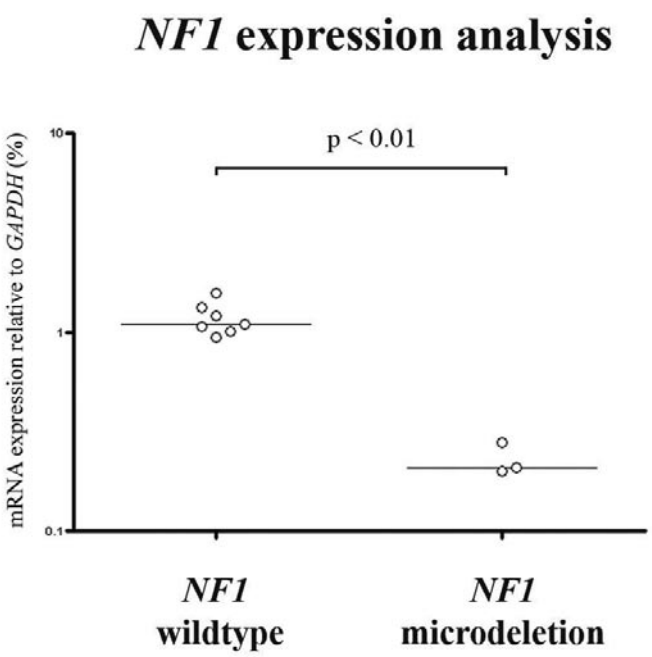

Figure 4. *NF1* expression analysis in pediatric T-ALL and *MLL*-rearranged AML.
NF1 mRNA expression data relative to *GAPDH* (%), based upon gene expression array data, which were available for 3 del(17)(q11.2)-positive (patient #2736, #2780 and #167) and 7 del(17)(q11.2)-negative leukemia patients.

DISCUSSION

Genetic events that lead to leukemogenesis by activating uncontrolled cell proliferation remain to be elucidated in most pediatric T-ALL and *MLL* rearranged AML cases. We used oligo array-CGH to identify new abnormalities and found somatic *NF1* microdeletions as a cryptic genetic abnormality in patients lacking clinical symptoms of neurofibromatosis. This array-CGH study is currently expanded to other subtypes of leukemias. Recent SNP array analysis of pediatric ALL by investigators from St Jude Children's Research Hospital showed that this microdeletion in *NF1* may be present at low frequencies in other types of acute leukemia as well.[32]

NF1 microdeletions are observed in about 5-20% of NF1 patients[1]. The majority of these NF1 patients have a 1.4 Mb *NF1* microdeletion due to interchromosomal homologous recombination between the low-copy repeats of the *WI-12393* gene flanking *NF1* and sequences with homology to chromosome 19 during meiosis[33]. A second type of *NF1* microdeletions of about 1.2 Mb in size is due to a mitotic intrachromosomal recombination between the *JJAZ1* and the homologous *JJAZ1P* pseudogene[34,35]. The *NF1* microdeletions in our leukemia patients seemed identical

to this 1.2Mb microdeletion type[33]. However, in contrast to NF1 patients with similar *NF1* deletions, our leukemia patients did not meet the clinical criteria for NF1, lacking cafe-au-lait spots, mental retardation and/or facial dysmorphism. This suggests that the *NF1* deletion in our patients is somatic and leukemia specific, rather than of constitutional genetic origin, although molecular diagnostics for NF1 was not performed in these patients.

Deletion of one allele of *NF1* and further inactivation of the other *NF1* allele in 3 patients through the acquisition of point mutations further confirms the role of *NF1* as a tumor-suppressor gene in the pathogenesis of both pediatric *MLL* rearranged AML and T-ALL. This point was further strengthened by the finding of clonal stability in one of the del(17)(q11.2) patients, where the deletion of *NF1* on one allele and the point-mutation in the other *NF1* allele were both present at diagnosis and relapse while absent in the remission sample. Therefore, the *NF1* abnormalities were of somatic origin in at least patient #2736 and were only present in the leukemic cells. Similar findings have been described for JMML patients[7], explaining why these patients did not have any clinical symptoms of neurofibromatosis.

Since *NF1* deficiency leads to the activation of the RAS signaling pathway[9], and none of the del(17)-positive leukemia patients had mutations in *NRAS* or *KRAS*, *NF1* microdeletions presumably provide an alternative mechanism for RAS activation in both *MLL* rearranged myeloid and T-lymphoid leukemias, thereby representing a novel type I abnormality. These leukemia patients may potentially benefit from additional treatment with RAS inhibitors like farnesylthiosalicylic acid[36] or downstream inhibitors.

Both del(17)-positive AML patients were further screened for any of the other currently known type I mutations in AML. As expected, no other type I mutations were detected, indicating that *NF1* microdeletions could act as a novel type I mutation which cooperate with the *MLL* translocation (type II mutation) in the pathogenesis of AML.

The idea of a multi-step pathogenesis in T-cell leukemia is widely accepted[18-20,37]. Cooperative genetic events affect cell-cycle, T-cell differentiation, proliferation and survival. We identified a number of cooperative aberrations in the del(17)(p11.2)-positive T-ALL samples. *NOTCH1* mutations, generally present in about 50% of T-ALL[21], were identified in 2 out of 3 del(17)(p11.2)-positive T-ALL samples. In addition, genetic aberrations that induce a T-cell differentiation arrest were identified in patient #2780 (*HOX11L2* translocation) and patient #2736 (*CALM-AF10* translocation). These data further suggests that loss of *NF1* can be involved in the development of T-ALL, as one of the genetic hits in multistep oncogenesis.

In this study, we identified 3 patients whith a deletion of *NF1* and an inactivational mutation on the remaining allele. We could not identify homozygous somatic *NF1*

mutations in 21 *MLL* rearranged AML and 18 T-ALL patients without a microdeletion. This suggests that the frequency of bi-allelic inactivation, until now the only mechanism described for oncogenesis, is less than 10% in these groups.

Other mechanisms of NF1 inactivation, such as inactivation through the duplication of the mutated (UPD) *NF1* allele at the expense of the remaining wild-type allele, as observed in NF1 patients with JMML, may have been missed[6]. Of interest, recent SNP array analysis of pediatric ALL, and JMML without underlying NF1, showed that there was no UPD involved in the *NF1* region[6,32]. In addition, in adult AML ~20% have large regions of UPD, but none of them involves the *NF1* locus[38,39]. Hence, UPD of the NF1 locus may be a rare event in leukemias of somatic origin compared to leukemias which originate from patients with clinical evidence of NF1. Therefore, the frequency of bi-allelic *NF1* inactivation in pediatric *MLL* rearranged AML and T-ALL as we reported here may be underestimated. Future studies should be extended by sequencing the *NF1* locus, including the promoter region and the 3' untranslated region (UTR) and look for abnormalities in NF1 protein expression.

In conclusion, we report the identification of *NF1* microdeletions in pediatric T-ALL and *MLL* rearranged AML cases without clinical evidence of NF1. We confirmed *NF1* inactivation by reduced *NF1* expression levels, and bi-allelic *NF1* mutations in 3 out of 5 patients, confirming the role of *NF1* as a tumor suppressor gene in cancer. *NF1* inactivation is a novel type I mutation in *MLL* rearranged AML and a new proliferative hit in T-ALL.

AUTHORSHIP SECTION

B.V.B. and P.V.V. designed and performed research and wrote the paper; G.J.L. collaborated on the *MLL*-AML study; E.V.W., D.R. and M.H. made this research possible by collecting patient samples and characteristics in there own study groups and providing additional information; A.M.W.O. and J.N.R.T. performed and designed *NF1* analysis; J.P.P.M, M.M.H., H.B.B, C.M.Z. and R.P. designed research and wrote the paper.

REFERENCES

1. Theos A, Korf BR. Pathophysiology of neurofibromatosis type 1. Ann Intern Med. 2006;144:842-849.
2. Jenne DE, Tinschert S, Stegmann E, et al. A common set of at least 11 functional genes is lost in the majority of NF1 patients with gross deletions. Genomics. 2000;66:93-97.
3. Jenne DE, Tinschert S, Reimann H, et al. Molecular characterization and gene content of breakpoint boundaries in patients with neurofibromatosis type 1 with 17q11.2 microdeletions. Am J Hum Genet. 2001;69:516-527.
4. Kai S, Sumita H, Fujioka K, et al. Loss of heterozygosity of NF1 gene in juvenile chronic myelogenous leukemia with neurofibromatosis type 1. Int J Hematol. 1998;68:53-60.
5. Side L, Taylor B, Cayouette M, et al. Homozygous inactivation of the NF1 gene in bone marrow cells from children with neurofibromatosis type 1 and malignant myeloid disorders. N Engl J Med. 1997;336:1713-1720.
6. Flotho C, Steinemann D, Mullighan CG, et al. Genome-wide single-nucleotide polymorphism analysis in juvenile myelomonocytic leukemia identifies uniparental disomy surrounding the NF1 locus in cases associated with neurofibromatosis but not in cases with mutant RAS or PTPN11. Oncogene. 2007.
7. Side LE, Emanuel PD, Taylor B, et al. Mutations of the NF1 gene in children with juvenile myelomonocytic leukemia without clinical evidence of neurofibromatosis, type 1. Blood. 1998;92:267-272.
8. Le DT, Kong N, Zhu Y, et al. Somatic inactivation of Nf1 in hematopoietic cells results in a progressive myeloproliferative disorder. Blood. 2004;103:4243-4250.
9. McCormick F. Ras signaling and NF1. Curr Opin Genet Dev. 1995;5:51-55.
10. Gilliland DG, Griffin JD. The roles of FLT3 in hematopoiesis and leukemia. Blood. 2002;100:1532-1542.
11. Grimwade D, Walker H, Oliver F, et al. The importance of diagnostic cytogenetics on outcome in AML: analysis of 1,612 patients entered into the MRC AML 10 trial. The Medical Research Council Adult and Children's Leukaemia Working Parties. Blood. 1998;92:2322-2333.
12. Raimondi SC, Chang MN, Ravindranath Y, et al. Chromosomal abnormalities in 478 children with acute myeloid leukemia: clinical characteristics and treatment outcome in a cooperative pediatric oncology group study-POG 8821. Blood. 1999;94:3707-3716.
13. Eguchi M, Eguchi-Ishimae M, Knight D, Kearney L, Slany R, Greaves M. MLL chimeric protein activation renders cells vulnerable to chromosomal damage: an explanation for the very short latency of infant leukemia. Genes Chromosomes Cancer. 2006;45:754-760.
14. Rubnitz JE, Raimondi SC, Tong X, et al. Favorable impact of the t(9;11) in childhood acute myeloid leukemia. J Clin Oncol. 2002;20:2302-2309.
15. Lie SO, Abrahamsson J, Clausen N, et al. Treatment stratification based on initial in vivo response in acute myeloid leukaemia in children without Down's syndrome: results of NOPHO-AML trials. Br J Haematol. 2003;122:217-225.
16. Palle J, Frost BM, Forestier E, et al. Cellular drug sensitivity in MLL-rearranged childhood acute leukaemia is correlated to partner genes and cell lineage. Br J Haematol. 2005;129:189-198.
17. Pui CH, Relling MV, Downing JR. Acute lymphoblastic leukemia. N Engl J Med. 2004;350:1535-1548.

18. De Keersmaecker K, Marynen P, Cools J. Genetic insights in the pathogenesis of T-cell acute lymphoblastic leukemia. Haematologica. 2005;90:1116-1127.

19. Armstrong SA, Look AT. Molecular genetics of acute lymphoblastic leukemia. J Clin Oncol. 2005;23:6306-6315.

20. Grabher C, von Boehmer H, Look AT. Notch 1 activation in the molecular pathogenesis of T-cell acute lymphoblastic leukaemia. Nat Rev Cancer. 2006;6:347-359.

21. Weng AP, Ferrando AA, Lee W, et al. Activating mutations of NOTCH1 in human T-cell acute lymphoblastic leukemia. Science. 2004;306:269-271.

22. Breit S, Stanulla M, Flohr T, et al. Activating NOTCH1 mutations predict favorable early treatment response and long-term outcome in childhood precursor T-cell lymphoblastic leukemia. Blood. 2006;108:1151-1157.

23. Thompson BJ, Buonamici S, Sulis ML, et al. The SCFFBW7 ubiquitin ligase complex as a tumor suppressor in T-cell leukemia. J Exp Med. 2007;204:1825-1835.

24. O'Neil J, Grim J, Strack P, et al. FBW7 mutations in leukemic cells mediate NOTCH pathway activation and resistance to gamma-secretase inhibitors. J Exp Med. 2007;204:1813-1824.

25. Van Vlierberghe P, van Grotel M, Beverloo HB, et al. The cryptic chromosomal deletion del(11)(p12p13) as a new activation mechanism of LMO2 in pediatric T-cell acute lymphoblastic leukemia. Blood. 2006;108:3520-3529.

26. Barrett MT, Scheffer A, Ben-Dor A, et al. Comparative genomic hybridization using oligonucleotide microarrays and total genomic DNA. Proc Natl Acad Sci U S A. 2004;101:17765-17770.

27. Schouten JP, McElgunn CJ, Waaijer R, Zwijnenburg D, Diepvens F, Pals G. Relative quantification of 40 nucleic acid sequences by multiplex ligation-dependent probe amplification. Nucleic Acids Res. 2002;30:e57.

28. Wimmer K, Yao S, Claes K, et al. Spectrum of single- and multiexon NF1 copy number changes in a cohort of 1,100 unselected NF1 patients. Genes Chromosomes Cancer. 2006;45:265-276.

29. Yamamoto Y, Kiyoi H, Nakano Y, et al. Activating mutation of D835 within the activation loop of FLT3 in human hematologic malignancies. Blood. 2001;97:2434-2439.

30. Kiyoi H, Naoe T, Yokota S, et al. Internal tandem duplication of FLT3 associated with leukocytosis in acute promyelocytic leukemia. Leukemia Study Group of the Ministry of Health and Welfare (Kohseisho). Leukemia. 1997;11:1447-1452.

31. Holleman A, Cheok MH, den Boer ML, et al. Gene-expression patterns in drug-resistant acute lymphoblastic leukemia cells and response to treatment. N Engl J Med. 2004;351:533-542.

32. Mullighan CG, Goorha S, Radtke I, et al. Genome-wide analysis of genetic alterations in acute lymphoblastic leukaemia. Nature. 2007;446:758-764.

33. Kehrer-Sawatzki H, Kluwe L, Sandig C, et al. High frequency of mosaicism among patients with neurofibromatosis type 1 (NF1) with microdeletions caused by somatic recombination of the JJAZ1 gene. Am J Hum Genet. 2004;75:410-423.

34. Petek E, Jenne DE, Smolle J, et al. Mitotic recombination mediated by the JJAZF1 (KIAA0160) gene causing somatic mosaicism and a new type of constitutional NF1 microdeletion in two children of a mosaic female with only few manifestations. J Med Genet. 2003;40:520-525.

35. Raedt TD, Stephens M, Heyns I, et al. Conservation of hotspots for recombination in low-copy repeats associated with the NF1 microdeletion. Nat Genet. 2006;38:1419-1423.

36. Barkan B, Starinsky S, Friedman E, Stein R, Kloog Y. The Ras inhibitor farnesylthiosalicylic acid as a potential therapy for neurofibromatosis type 1. Clin Cancer Res. 2006;12:5533-5542.

37. Graux C, Cools J, Michaux L, Vandenberghe P, Hagemeijer A. Cytogenetics and molecular genetics of T-cell acute lymphoblastic leukemia: from thymocyte to lymphoblast. Leukemia. 2006.

38. Fitzgibbon J, Smith LL, Raghavan M, et al. Association between acquired uniparental disomy and homozygous gene mutation in acute myeloid leukemias. Cancer Res. 2005;65:9152-9154.

39. Raghavan M, Lillington DM, Skoulakis S, et al. Genome-wide single nucleotide polymorphism analysis reveals frequent partial uniparental disomy due to somatic recombination in acute myeloid leukemias. Cancer Res. 2005;65:375-378.

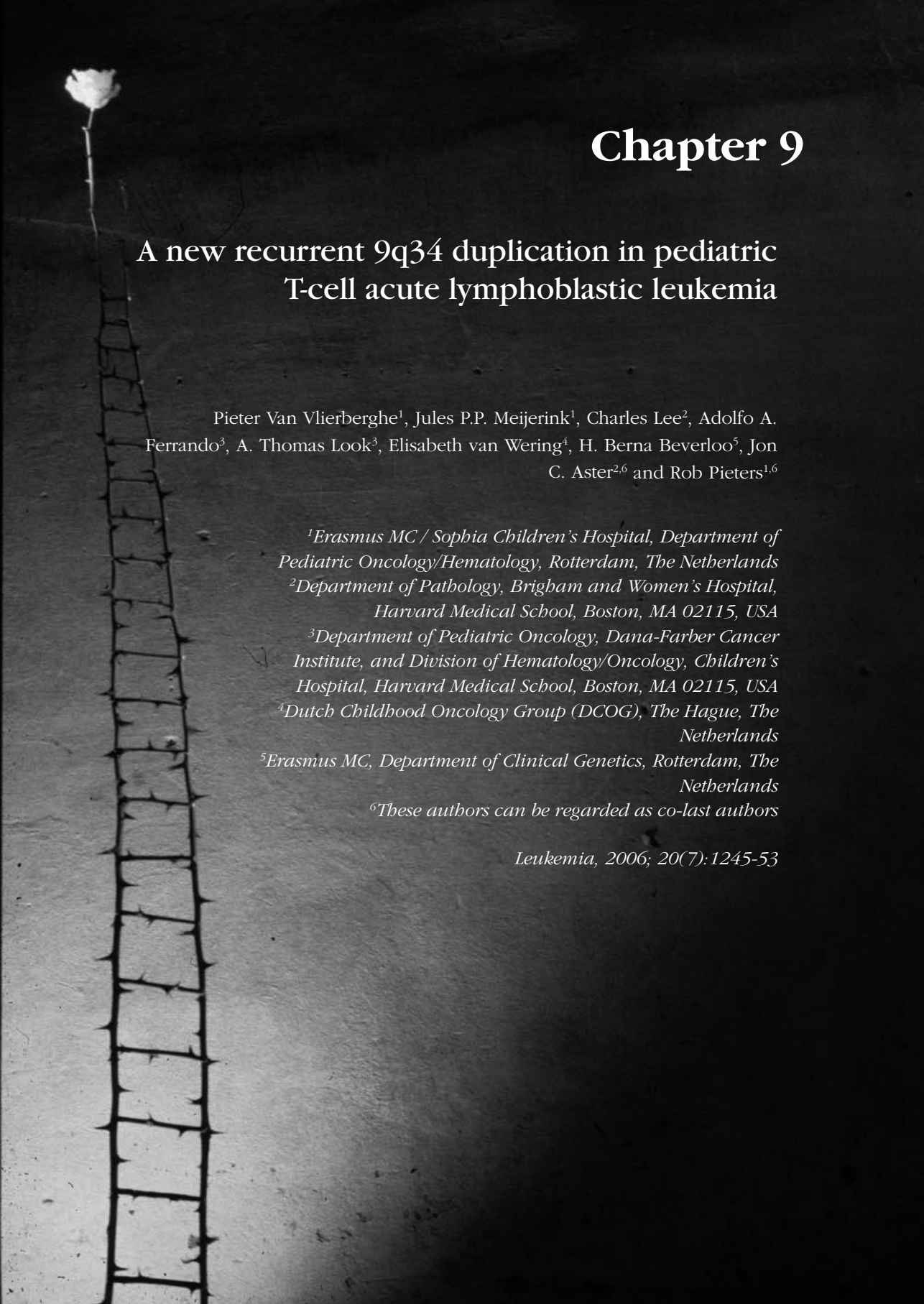

Chapter 9

A new recurrent 9q34 duplication in pediatric T-cell acute lymphoblastic leukemia

Pieter Van Vlierberghe[1], Jules P.P. Meijerink[1], Charles Lee[2], Adolfo A. Ferrando[3], A. Thomas Look[3], Elisabeth van Wering[4], H. Berna Beverloo[5], Jon C. Aster[2,6] and Rob Pieters[1,6]

[1]Erasmus MC / Sophia Children's Hospital, Department of Pediatric Oncology/Hematology, Rotterdam, The Netherlands
[2]Department of Pathology, Brigham and Women's Hospital, Harvard Medical School, Boston, MA 02115, USA
[3]Department of Pediatric Oncology, Dana-Farber Cancer Institute, and Division of Hematology/Oncology, Children's Hospital, Harvard Medical School, Boston, MA 02115, USA
[4]Dutch Childhood Oncology Group (DCOG), The Hague, The Netherlands
[5]Erasmus MC, Department of Clinical Genetics, Rotterdam, The Netherlands
[6]These authors can be regarded as co-last authors

Leukemia, 2006; 20(7):1245-53

ABSTRACT

Over the last decade, genetic characterization of T-cell acute lymphoblastic leukemia (T-ALL) has led to the identification of a variety of chromosomal abnormalities. In this study, we used array-comparative genome hybridization (array-CGH) and identified a novel recurrent 9q34 amplification in 33% (12/36) of pediatric T-ALL samples, which is therefore one of the most frequent cytogenetic abnormalities observed in T-ALL thus far. The exact size of the amplified region differed among patients, but the critical region encloses 4 Mb and includes *NOTCH1*. The 9q34 amplification may lead to elevated expression of various genes, and *MRLP41, SSNA1* and *PHPT1* were found significantly expressed at higher levels. Fluorescence in situ hybridization (FISH) analysis revealed that this 9q34 amplification was in fact a 9q34 duplication on one chromosome and could be identified in 17–39 percent of leukemic cells at diagnosis. Although this leukemic subclone did not predict for poor outcome, leukemic cells carrying this duplication were still present at relapse, indicating that these cells survived chemotherapeutic treatment. Episomal *NUP214-ABL1* amplification and activating mutations in *NOTCH1*, two other recently identified 9q34 abnormalities in T-ALL, were also detected in our patient cohort. We showed that both of these genetic abnormalities occur independently from this newly identified 9q34 duplication.

INTRODUCTION

Pediatric T cell acute lymphoblastic leukemia (T-ALL) accounts for about 10-15% of pediatric ALL cases. Current intensive treatment schedules have improved outcome, as the 5 year relapse-free survival rate nearly reaches 75%. Further improvement of this survival rate will be expected by a better understanding of the pathogenesis of T-ALL and the mechanism of cellular resistance against chemotherapy, providing new rationales for therapeutic intervention[1]. Genetic analyses of this malignancy have elucidated an enormous heterogeneity in genetic aberrations including chromosomal translocations, deletions and amplifications. Most of these abnormalities cause aberrant expression of a specific set of helix-loop-helix transcription factors, e.g. *TAL1/SCL*, *TAL2*, *LYL1*, *LMO1*, and *LMO2*; deregulate the expression of homeobox genes like *TLX1*, *HOXA10/HOXA11* and *TLX3*; or lead to the generation of fusion genes like *CALM-AF10*[2-11]. Some of these genetic defects are cryptic aberrations and for that reason remain undetected by conventional cytogenetics. New high-resolution cytogenetic techniques may therefore lead to the identification of novel abnormalities in pediatric T-ALL. One such technique is the array comparative genome hybridization (array-CGH) technique enabling genome-wide high-resolution screening to detect new chromosomal regions of deletion or amplification[12-14]. It has mainly been used thus far for genomic screening of solid tumors[15-18] and its application in the genomic analysis of hematological malignancies is limited to a few studies[19,20].

Episomal *NUP214-ABL1* amplifications were recently detected in pediatric T-ALL, leading to an aberrant activation of the protein tyrosine kinase activity of *ABL1*[21]. For this, the genomic region from *ABL1* to *NUP214* is circularized to form a *NUP214-ABL1* fusion gene. This phenomenon results in the formation of a variable number of episomes, not previously detected by conventional cytogenetics, and accounts for a novel genetic mechanism leading to the activation of a tyrosine kinase in cancer. The *NUP214-ABL1* amplification, which is observed in about 5% of the T-ALL samples, is suggested to be associated with poor outcome, and patients may therefore benefit from additional treatment with imatinib, a tyrosine kinase inhibitor[21]. Recently, another *ABL1* fusion was identified in a T-ALL patient with a cryptic t(9;14)(q34;q32). In that case, the constitutive activation of the *ABL1* tyrosine kinase activity was established by the formation of an EML1-ABL1 fusion product[22].

Another abnormality also involving the 9q34 region in T-ALL were the recently identified mutations in the *NOTCH1* gene[23-33]. A specific role for *NOTCH1* in human T-ALL was previously postulated due to its involvement in the rare chromosomal translocation t(7;9)(q34;q34.3), coupling *NOTCH1* to the T cell receptor-β locus[24]. The identification of activating *NOTCH1* mutations in more than 50% of human T-ALL samples[23], suggests a much broader role for this gene in human T cell

leukemogenesis[25]. NOTCH1 has a major role in normal hematopoiesis as early transcription factor to commit lymphoid progenitor cells towards T cell development. It encodes for a dimer of the extracellular subunit (NEC) non-covalently bound to the transmembrane (NTM) subunit. Two specific dimerization regions (HD-N, HD-C) regulate the stable association between these subunits. NOTCH1 activation is initiated by ligand binding to NEC, leading to the release of intracellular NOTCH after successive proteolytic cleavages. Intracellular NOTCH translocates to the nucleus where it forms a complex that activates the transcription of various target genes, including *HES-1*, *PRE-Tα*, *DELTEX-1* and *P21*[26-27]. So far *NOTCH1* mutations appear to be restricted to 3 hotspot domains: the HD-N, the HD-C and the PEST domain. It has been suggested that these mutations lead to ligand independent activation of this transmembrane receptor[23].

In the present study, we used array-CGH to identify a novel duplication involving the 9q34 region in 33% of pediatric T-ALL samples, which is one of the most frequent cytogenetic abnormalities observed in T-ALL thus far. The relevance of this new and recurrent abnormality in relation to other newly discovered abnormalities in the 9q34 genomic region, like *NUP214-ABL1* amplification or activating mutations in *NOTCH1,* has been investigated.

MATERIALS AND METHODS

Patient samples

Viable frozen leukemic cell suspensions obtained from either bone marrow and/or peripheral blood samples at diagnosis from untreated children with T-ALL were collected from the Sophia Children's Hospital/Erasmus MC and the Dutch Childhood Oncology Group (DCOG). At diagnosis, informed consent of the patients and/or parents was obtained to use left-over material for research purposes. Leukemic cells were isolated and enriched from these samples as previously described[28]. All samples contained ≥90% leukemic cells, as determined morphologically by May-Grünwald-Giemsa (Merck, Darmstadt, Germany)-stained cytospins. Thawed cells were used for several procedures. For DNA and RNA extraction, a minimum of 5×10^6 leukemic cells were lysed in Trizol reagent (Gibco BRL, Life Technologies, Breda, The Netherlands) and stored at -80°C. A total of 25×10^3 leukemic cells was used for cytospin preparations for fluorescence in situ hybridization (FISH) which were stored at -20°C. For the preparation of metaphase slides a minimum of 5×10^6 leukemic cells were cultured for 72 hr in serum free medium (JRH Biosciences, Kansas, USA) in the presence of IL7 (10 ng/ml) and IL2 (10 ng/ml), and harvested according to standard cytogenetic techniques.

Genomic DNA isolation, RNA extraction and cDNA synthesis

Genomic DNA and total cellular RNA were isolated according to the manufacturers' protocol, with minor modifications. An additional phenol-chloroform extraction was performed and the DNA was precipitated with isopropanol along with 1 µl (20 µg/ml) glycogen (Roche, Almere, The Netherlands). After precipitation, RNA pellets were dissolved in 20µl RNAse-free TE-buffer (10mM Tris-HCl, 1mM EDTA, pH=8.0). The RNA concentration was quantified spectrophotometrically. Following a denaturation step of 5 min at 70°C, 1µg of RNA was reverse transcribed to single-stranded cDNA using a mix of random hexamers (2.5 µM) and oligo dT primers (20 nM). The RT reaction was performed in a total volume of 25 µl containing 0.2 mM of each dNTP (Amersham Pharmacia BioTech, Piscataway, NJ, USA), 200 U Moloney murine leukemia virus reverse transcriptase (M-MLV RT) (Promega, Madison, WI, USA) and 25 U RNAsin (Promega). Conditions for the reaction were 37°C for 30 minutes, 42°C for 15 minutes, and 94°C for 5 minutes. The obtained cDNA was diluted to a final concentration of 8 ng/µl and stored at -80°C.

Array-CGH

Array-CGH analysis was performed in duplicate for each patient, using a dye-swap experimental design to minimize false positive results. Patient genomic DNA (2 µg) and male/female reference DNA (2 µg) (Promega) were fragmented by sonification (VibraCell Model VC130, Sonics & Materials, Newtown, CT), size-verified by agarose gel electrophoresis and labeled with Cy5 and Cy3 dyes according to standard random priming protocols (Bioprime Labeling Kit, Invitrogen, Carlsbad, CA, USA). The DNAs were combined, denatured, and applied to two separate 1 Mb GenomeChip™ V1.2 Human BAC arrays (2,632 BAC clones spotted on a single array; Spectral Genomics, Houston, TX, USA) according to the manufacturer's protocol. DNA hybridization and washes were performed as recommended, and the slides were scanned on a GenePix 4000B Microarray Scanner (Axon Instruments, Union City, CA, USA). Cy3 and Cy5 fluorescent intensities at each DNA spot were quantified by GenePix Pro 4.0 Microarray Image Analysis Software and the data were subsequently imported into SpectralWare software (Spectral Genomics). Background intensities were subtracted and initial fluorescent ratios were log2 transformed. Data points greater than 2 standard deviations away from the population mean ratio were identified as "outliers" and removed. This procedure was repeated until the data points were all within the 2 standard deviations-established threshold[29]. Regression was performed against a ratio value of 1. Using such strict normalization procedures, including the requirement that the deviation occurs for both components of the dye-swap experiment[29], some significant data points might be eliminated (i.e. false negatives), but increased confidence in defining abnormal data points is obtained. The ratios for each clone

were subsequently plotted into chromosome-specific profiles. At this stage, known large-scale copy number polymorphisms were not considered disease-related[29]. The cut-off fluorescence ratios used for detection of genomic gain or loss were 0.8 and 1.2. In addition, the aberration needed to be present in both dye-swapped experiments.

FISH validation experiments

BACs were obtained from BAC/PAC Resource Center (Children's Hospital, Oakland, USA). BAC DNAs were isolated using DNA MiniPrep plasmid kit (Promega) and labeled by nick translation with Spectrum Orange-dUTP (Vysis, Ill, USA). ABL1 amplification was detected using the LSI BCR-ABL ES (Vysis) translocation probe. HOX11L2 translocations were identified with the TLX3 split signal probe (Dakocytomation, Glostrup, Denmark). The BAC clones RP11-408N14 (9p21.3) and RP11-91o4 (11q21) were used to identify del(9)(p21.3p23) and del(11)(q14.1q22.3) in T-ALL patient 1179, respectively. The BAC clones RP11-707o3 (NOTCH1) and RP11-576c12 (9q32) were used to identify the 9q34 duplication. The cases without 9q34 abnormalities were used to calculate the cut-off value for this probe combination for use in interphase nuclei. The cut-off value was defined as the mean plus three times the standard deviation. The cut-off value for the presence of 3 RP11-707o3 signals was 3%. FISH analysis was performed on interphase and metaphase preparations from methanol/acetic acid cell suspensions stored at –20°C. Cytospins and metaphase preparations were stored at -20°C. Before use, they were thawed on ice for 60 min and fixated in methanol/acetic acid (3:1). Afterwards, the slides were pre-treated with RNAse and pepsin, and post-fixed with formaldehyde, before being denatured for 2 min 15 sec in 70% formamide/2x SSC at 72°C. FISH probes were denatured for 8 min at 72°C and hybridized overnight at 37°C in a moist chamber. Slides were washed in 50% formamide/2x SSC and 2x SSC at 50°C, 4 min each. After dehydration through an ethanol series (70%, 85%, and 96%), they were mounted with antifade containing 4'6-diamino-2-phenyl indol (DAPI) as counterstain. For each sample a minimum of 100 interphase cells were scored, as well as 10-25 metaphases if present. Images were captured using an epifluorescence microscope (Zeiss Axioplan 2, Sliedrecht, the Netherlands) using MacProbe software (version 4.3, Applied Imaging, Newcastle upon Tyne, UK).

Mutational screening of *NOTCH1*

Mutational screening of *NOTCH1* was performed as previously described[23]. Briefly, exon 26, encoding the N terminal region of the HD domain of NOTCH1, was divided in 2 amplicons. Exon 27, encoding the C terminal region of the HD domain of NOTCH1, was amplified as 1 amplicon and exon 34, encoding the PEST domain of

NOTCH1, was divided in three amplicons. Direct sequencing was performed on all of the generated PCR products.

Quantitative real-time RT-PCR (Taqman)

The mRNA expression levels of *NOTCH1* and an endogenous housekeeping gene encoding for glyceraldehydes-3-phosphate dehydrogenase (GAPDH) as a reference were quantified using real-time polymerase chain reaction (PCR) analysis (TaqMan chemistry) as previously described[28]. The relative *NOTCH1* mRNA expression level in each patient was calculated using the comparative cycle time (C_t) method, as previously described[30]. Briefly, the target PCR C_t values (ie, the cycle number at which emitted fluorescence exceeds 10 × the standard deviation (SD) of baseline emissions as measured from cycles 3 to 15) is normalized to the GAPDH PCR C_t value by subtracting the GAPDH C_t value from the target PCR C_t value, which gives the ΔC_t value. From this, the relative mRNA expression to GAPDH for each target PCR can be calculated using the following equation:

relative mRNA expression = $2^{-(\text{Ct target} - \text{Ct GAPDH})} \times 100\%$

Gene expression array analysis and statistics

Total cellular RNA was extracted from a minimum of $5x10^6$ leukemic cells using Trizol reagent (GIBCO BRL) according to the manufacturer's protocol with minor modifications that included an additional RNA purification step with phenol–chloroform–isoamylalcohol (25:24:1) as previously described[31]. RNA integrity, processing and hybridization to the U133 plus 2.0 GeneChip oligonucleotide microarray (Affymetrix) was performed as described before[31]. Probe sets located in the 9q33-34 regions with raw fluorescent intensities that were 3 fold higher than the arbitrary background level of 50 were selected (78 probesets, reflecting 53 genes). For these probe-sets, the expression was calculated relatively to the median expression of *GAPDH* (6 probesets) for each patient sample. The difference in gene expression levels for patients with and without the 9q34 duplication was evaluated using the Mann-Whitney-U test.

RESULTS

New recurrent aberration in pediatric T-ALL

To find new chromosomal imbalances in pediatric T-ALL possibly related to outcome or leukemogenesis, array-CGH analysis was performed on a selected cohort of 36 clinically and karyotypically well-characterized diagnostic patient samples (Table 1). Array-CGH analysis led to the identification of all numerical chromosomal

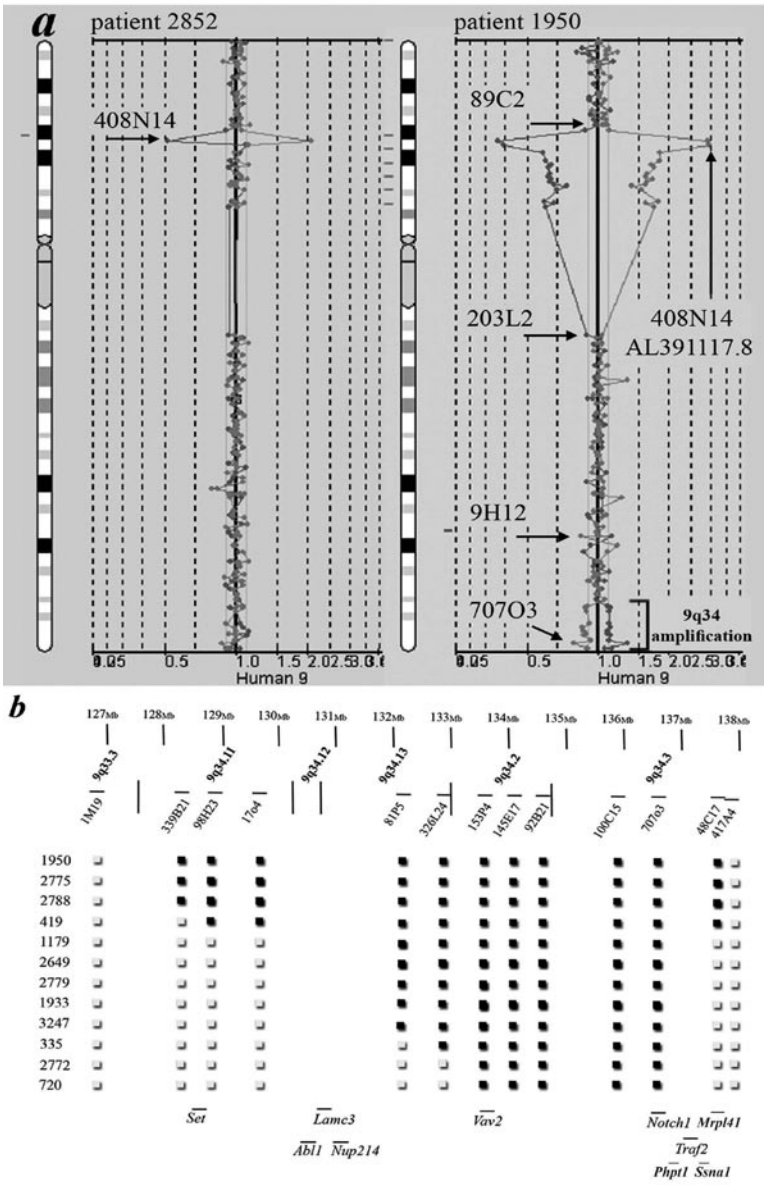

Figure 1. Subclonal 9q34 amplification in pediatric T-ALL

(a) Chromosome 9 ideogram and corresponding array-CGH plot of test DNA:control DNA ratios (blue tracing), and the dye-swapped control DNA:test DNA ratios (red tracing), for T-ALL patients 2852 (left panel) and 1950 (middle panel). **(b)** Overview of array-CGH results for the 9q34 region for each of the 12 pediatric T-ALL patients with the 9q34 duplication. The BAC clones present on the DNA array and located on chromosome bands 9q33.3-q34.3 are shown. The BAC clones within the region of genomic gain are shown as black boxes, clones giving a 1:1 ratio are shown as white boxes. Specific genes located in this region that regulate important cellular processes or that were previously linked to leukemogenesis, are indicated below. Depicted genome positions are based on the UCSC Genome Browser.[35]

aberrations, amplifications and deletions that matched previous karyotypic data, confirming the reliability of this genome-wide screening-technique. As depicted in Figure 1a for example, analysis of the array-CGH plot for chromosome 9 of patient 1950 showed a heterozygous deletion at 9p22-q21 also partly observed by conventional karyotyping (Table 1). Unlike conventional karyotyping, array-CGH allows a more precise determination of the size of the amplified or deleted regions. For example, the heterozygous deletion at 9p22-q21 in patient 1950 could be specified to the region between 9p21.3-p22 (BAC 89C2) and 9q21.11 (BAC 203L2; Figure 1a). Within this area, the region covered by the BAC clones 408N14 and AL391117.8 was homozygous deleted, including the *p15INK4B-p16INK4A* loci that are frequently deleted in pediatric T-ALL[32].

In addition to the aberrations previously detected by conventional cytogenetics, a gain of genomic material was present at 9q34 in 33% (12/36) of our pediatric T-ALL cases (Figure 1a). The exact size of the amplified region varied among patients (Figure 1b). The largest region of amplification was flanked by the BAC clones 1M19 (9q33.3) and 417A4 (9q34.3), whereas the smallest region ranged from BAC clone 326L24 (9q34.13) to 48C17 (9q34.3). The common region of genomic gain therefore includes clones 153P4, 145E17, 92B21, 100C15 and 707O3, which are all located distally from the *ABL1* and *NUP214* genes at 9q34.12-q34.13 (Figure 1b).

The relative difference in hybridization in the array-CGH analysis between the patient and the control DNA was lower than expected for a single copy gain in all leukemic cells of the patient. We therefore postulated that this amplification is only present in a sub-fraction of the total leukemic population. To determine the percentage of cells carrying the 9q34 amplification, interphase cells were analyzed by FISH using the probes RP11-707o3 (*NOTCH1*) located in the common region of genomic gain, and RP11-576c12 (9q32), situated outside the amplified region. Samples with the 9q34 amplification showed an additional 9q34.3-specific (RP11-707o3) hybridization signal in a minority of leukemic cells (Figure 2a,b). Additional FISH analysis on metaphase cells (Figure 2) using the same 9q34.3 specific probe showed that patients with the 9q34 amplification had a duplication of the 9q34 region. The percentage of cells with a 9q34 duplication ranged from 17 to 39 percent of the leukemic population at diagnosis (Table 2).

Clinical relevance of the 9q34 duplication in pediatric T-ALL

The 9q34 duplication was observed in 12 out of 36 patients (Table 2), of which 6 patients relapsed (Table 1). Relapse material was available for four of these patients (patients 335, 1179, 1933, 3247; Table 2). FISH analysis on the relapse samples using the same 9q34 specific BAC-probe (707O3) showed 9q34 duplication in about 20%-25% of the leukemic cells for all four specimens (Table 2). Array-CGH analysis

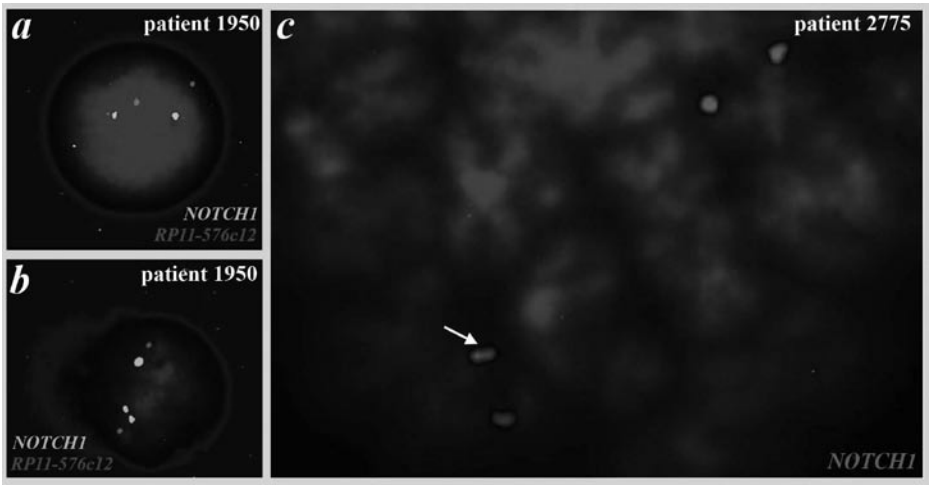

Figure 2. FISH analysis showing subclonal 9q34 duplication in T-ALL patients 1950 and 2775.

(a) FISH analysis on interphase cells of patient 1950, using RP11-707o3 (*NOTCH1*) in green and RP11-576c12 (9q32) in red. Example of an interphase cell showing a normal hybridization pattern. **(b)** Amplification of RP11-707o3 (*NOTCH1*) is identified in a minority (32%) of the leukemic cell population. **(c)** Single-color FISH analysis on metaphase spreads of patient 2775, showing an enlarged hybridization signal on one of the chromosomes 9 (white arrow), indicating duplication of 9q34 in one of the chromosomes 9.

on the relapse material from these 4 patients confirmed the presence of the 9q34 duplication in a subpopulation of cells in all 4 relapse samples (Figure 3a).

The episomal amplification of *NUP214-ABL1* and the 9q34 duplication are independent genetic events in pediatric T-ALL

We then investigated the relationship between this 9q34 duplication and the recently identified *NUP214-ABL1* amplification also involving the 9q34 region. We failed to detect the *NUP214-ABL1* amplification in our array-CGH analysis because no BAC clone covering this genomic region was present at the DNA chips. Therefore, the incidence of the episomal *NUP214-ABL1* amplification in our patient cohort was determined by FISH analysis using the LSI *BCR-ABL* ES translocation probe. We identified the episomal *ABL1* amplification in 2 out of 36 samples (5.6%; Table 2). This genetic abnormality was present in a very low percentage of cells (5% and 3%) at diagnosis (patients 1179, 2775; Table 2; Figure 3b). Both patients also carried the 9q34 duplication in a subclone of the leukemic cells (Table 2). Notably, both patients relapsed but relapse material was only available for patient 1179. Interestingly, in this patient, the episomal amplification of *NUP214-ABL1* was detected in 81% of the leukemic population at relapse (Figure 3c). The 9q34 duplication was present in only 22% of the leukemic cells (Table 2), suggesting that none of the leukemic cells

Table 1. Clinical and cytogenetic patient characteristics

ID	Sex	Age*	WBC (x 10^9 / l)	Relapse CCR, (#months)	Karyotype
335_D	M	13.9	533	Relapse, 14	46,XY[26]
335_R					46,XY[20]
419	M	10.3	149	CCR, 36+	46,XY,t(10;14)(q2?4;q11)[2]/46,idem,del(12)(p11)[10]/
					46,idem,t(6;7)(p21;q34~35),del(12)(p11)[3] / 46,XY[9]
720	M	13.2	417	CCR, 33+	46,XY,t(7;9)(p1?3;p2?2)[30]/46,XY[4]
1179_D	M	5.9	276	Relapse, 13	46,XY,del(11)(q2?1q2?4)[21]/
1179_R	M		17,9		46,XY,der(6)t(6;8)(q26;q24),del(8)(q24),
					del(9)(p21p21),der(9)del(9)(p21p21)add(9)(q11),
					del(11)(q21q23)[6]/46,idem,der(3;9)(p10;q10),
					der(6)t(3;6)(q29;p25),+del(9)[8]/46,XY[11]
1933_D	M	12.6	305	Relapse, 12	47,XY,+mar1[9]/48,idem,+mar2[7]/46,XY[8]
1933_R	M		29		46,XY,del(6)(q16q24)[17]/47,XY,+ mar1[5]
1950	F	9.3	900	Relapse, 5	46,XX,del(9)(p13p23)[10]/46,idem,del(13)(q14q22)[5]/
					46,idem,del(6)(q13q23)[8] / 46,idem,del(6),del(13)[2]
2649	F	16.6	86	CCR, 22+	46,XX,del(6)(q13q21),t(8;14)(q24;q11),del(9)(p22)[20]
2772	M	5.1	80	CCR, 40+	46,XY[30]
2775	M	15.9	136	Relapse, 6	46,XY,del(6)(q2?q2?)[15]/
					46,idem,del(10)(q2?)[2]
2779	F	2.8	57	CCR, 119+	46,XX,del(6)(q?)[8]
2788	M	9.3	310	CCR, 75+	46,XY,t(1;14)(p32;q11),inc[2]
3247_D	M	4.6	232	Relapse, 12	46,XY[25]
3247_R	M		32		46,XY[30]
531	F	8	132	CCR, 35+	46,XX,?add(9)(p1?)[6]/46,XX[30]
1946	M	4.5	405	Relapse, 10	46,XY[10]
1953	M	8.5	130	CCR, 116+	47,XY,+8[15]
2036_D	M	8.1	271	Relapse, 19	45,XY,der(7;9)(q10;q10), t(11;14)(p13;q11)[4]/
					45,idem,t(11;14)(p13;q11)[21]/46,XY[8]
2036_R	M		102		ND
2101	M	6.2	167	Relapse, 4	47,XY,+?6[4]/48,idem,+mar[2]/46,XY[30]
2105_D	M	5	140	Relapse, 12	46,XY[30]
2105_R	M		25		46,XY[25]
2640	M	6.2	68	Relapse, 9	46,XY[10]
2720	M	15.4	200	Relapse, 13	46,XY,t(1;14)(p32;q11)[20]/47,idem,+mar[5]
2721	M	2	580	Relapse, 12	ND

Table 1 continued

ID	Sex	Age*	WBC (x 10^9 / l)	Relapse CCR, (#months)	Karyotype
2722	M	11.3	192	CCR, 87+	46,XY,t(1;7)(p31;q32)[13]/46,XY[12]
2723	F	6.4	98	Relapse, 6	45,XX,dic(7;8)(p12;p12)[7]
2735	F	4.7	212	Relapse, 7	46,XX[32]
2736	M	10.1	13	Relapse, 15	46,XY,t(2;9)(q21;q34),?t(8,8)(?q22;q?24)[18]
2737	M	11.2	53	Relapse, 36	46,XY,t(10;14)(q24;q11)[24]
2738	F	12.3	34	CCR, 11+	46,XX,del(9)(p2?1)[9]/46,XX,add(9)(p12)[6]
2748	M	1.3	177	Relapse, 7	46,XY[31]
2759	M	3.3	590	CCR, 56+	46,XY[30]
2773	M	5.3	31	CCR, 41+	46,XY[32]
2792	M	7.5	56	CCR, 62	47,XY,+del(9)(p1?1)[11]
2846	M	2.3	124	CCR, 51+	46,XY[20]
2852	M	13.8	128	Relapse, 10	46,XY,t(8;14)(q24;q11)[14]
2854	M	6.4	188	CCR, 54+	46,XY[30]
3244_D	M	3.7	13,9	Relapse, 16	47,XY,+X[7]/47,idem,del(6)(q21)[35]
3244_R	M		4,3		47,XY,+X,del(6)(q21)[13]
3246_D	M	12.2	292	Relapse, 72	46,XY[10]/47,XY,+mar[10]
3246_R	M		45		47,XY,+8,t(11;14)(p13;q11)[29] / 46,XY[3]

CCR, continue complete remission; WBC, white blood cell count; _D, diagnosis; _R, relapse; *, years at diagnosis

carried both genetic abnormalities simultaneously. FISH analysis on diagnosis and relapse material of patient 1179 using the *ABL1*- and a *NOTCH1* probes simultaneously confirmed that the *ABL1* amplification and the 9q34 duplication were present in separate leukemic cells (data not shown). Analysis using array-CGH (Figure 3a) and FISH (not shown) on the relapse material of patient 1179 further confirmed that *NUP214-ABL1* amplification and 9q34 duplication occur in independent leukemic subclones.

Identification of novel *NOTCH1* mutations in pediatric T-ALL

We then screened part of our pediatric T-ALL cohort (30/36) for the presence of mutations in the three hot spot regions of *NOTCH1* involving exon 26 (HD-N), exon 27 (HD-C) and exon 34 (PEST). Seventeen *NOTCH1* mutations were identified in 16 out of 30 T-ALL samples (53%; Table 2). The majority of mutations were located in exon 26. Only 1 patient had a mutated exon 27 and 4 patients showed a mutation in exon 34. Ten out of 17 mutations were novel mutations, whereas 7 were identical to mutations previously described[23,33]. Leucine to proline conversions were observed most frequently (5/17 mutations (29%)) at residues 1586, 1594, 1601 and 1679. Deletion of (GTG) at residue 1579 was observed in 2 patient samples. One patient showed two *NOTCH1* mutations, both in the HD-N and PEST domains

Table 2. Array-CGH, FISH and *NOTCH1* mutation/relative expression analysis on 36 pediatric T-ALL patients.

	Array-CGH	FISH results		Mutational data *NOTCH1*				Expression
Patient ID	9q34 duplication	*NOTCH1* duplication Nuclei (%)[a]	*ABL1* amplification Nuclei (%)[b]	Exon	Nucleotide level	Protein level	Previously described[c]	*NOTCH1*[d]
335_D	yes	23	N	WT				0.094
335_R	yes	20	N	ND				ND
419	yes	27	N	26	GTG to GGG	V1605G	no	0.255
720	yes	17	N	26	del (CCG))	del P (1583	no	0.572
1179_D	yes	35	5	WT				0.583
1179_R	yes	22	81	ND				ND
1933_D	yes	18	N	ND				ND
1933_R	yes	25	N	ND				ND
1950	yes	32	N	WT				1.038
2649	yes	33	N	WT				0.605
2772	yes	ND	ND	26	del(GTG)	del V (1579)	yes	2.356
2775	yes	39	3	26	del(GTG)	del V (1579)	yes	0.048
2779	yes	35	N	WT				0.180
2788	yes	24	N	26	CTG to CCG	L1601P	yes	0.443
3247_D	yes	26	N	ND				ND
3247_R	yes	20	N	ND				ND
531	no	N	N	WT				0.054
1946	no	N	N	WT				1.755
1953	no	N	N	26	CTG to CAG	L1586Q	no	2.704
2036_D	no	N	N	ND				ND
2036_R	no	N	N	ND				ND
2101	no	N	N	WT				0.949
2105_D	no	N	N	ND				ND
2105_R	no	N	N	ND				ND
2640	no	N	N	26	CTG to CCG	L1594P	yes	0.457

Patient ID	Array-CGH	FISH results		Mutational data *NOTCH1*				Expression
	9q34 duplication	*NOTCH1* duplication Nuclei (%)[a]	*ABL1* amplification Nuclei (%)[b]	Exon	Nucleotide level	Protein level	Previously described[c]	*NOTCH1*[d]
2720	no	N	N	26	CTG to CCG	L1586P	yes	1.214
2721	no	N	N	WT				ND
2722	no	N	N	34	insertion	stop (2418)	no	2.026
2723	no	N	N	27	CTG to CCG	L1679P	yes	0.401
2735	no	N	N	34	insertion	stop (2467)	no	1.231
2736	no	N	N	WT				6.090
2737	no	N	N	26	GTG to GAG	V1579E	no	0.723
2738	no	N	N	26	insertion	GVG (1601)	no	2.995
				34	ACG to ATG	T2484M	no	ND
2748	no	N	N	26	CTG to CCG	L1586P	yes	1.256
2759	no	N	N	WT				0.145
2773		N	N	26	GTG to GAG	V1605E	no	0.511
2792	no	N	N	WT				1.458
2846	no	N	N	WT				0.431
2852	no	N	N	WT				0.345
2854	no	N	N	34	insertion	stop (2437)	no	0.070
3244_D	no	N	N	ND				ND
3244_R	no	N	N	ND				ND
3246_D	no	N	N	ND				ND
3246_R	no	N	N	ND				ND

[a]Percentage of interphase nuclei showing the signal pattern specific for duplication of *NOTCH1* (Figure 2). [b]Percentage of interphase nuclei showing *NUP214-ABL1* amplification. [c]References 23, 33 [d]Relative mRNA expression of *NOTCH1* to *GAPDH* (%). WT, wildtype; ND, not done; N, normal; _D, diagnosis; _R, relapse.

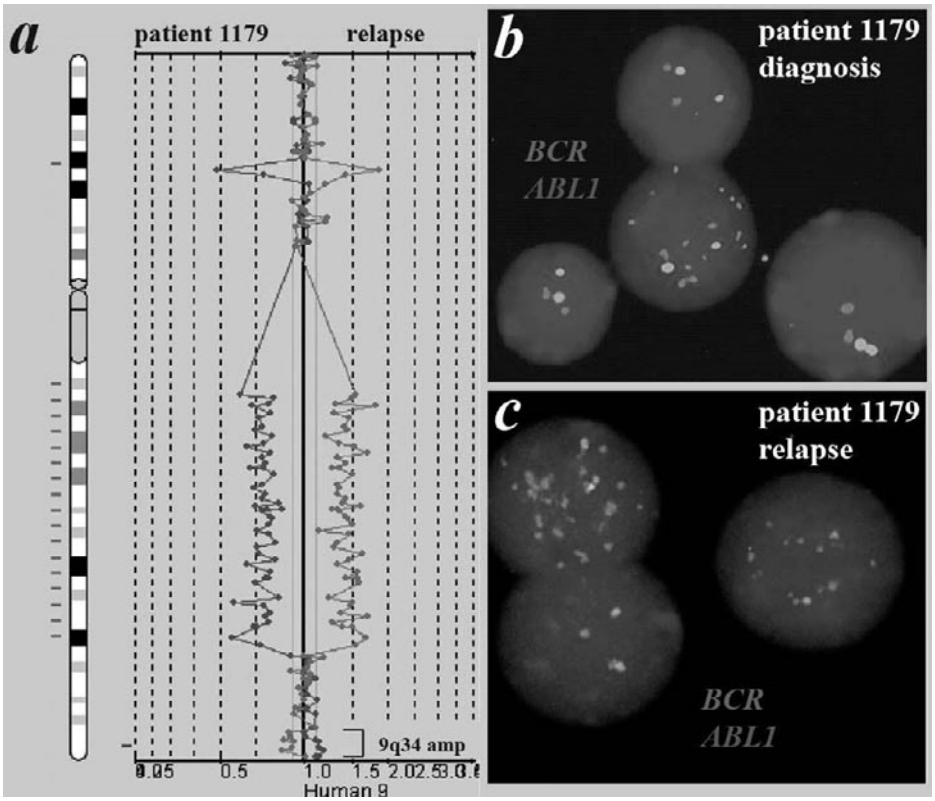

Figure 3. Episomal *NUP214-ABL1* amplification and 9q34 duplication.
(a) Chromosome ideogram and corresponding array-CGH plot of chromosome 9, as described in the legend of figure 1, for patient 1179 at relapse. The 9q34 duplication remains subclonal at relapse. The del(9)(p12q33) (12P15 to 451E16) is only detected in the relapse material. Interphase dual-color FISH analysis on **(b)** diagnostic material and **(c)** relapse material using the LSI BCR-ABL ES probes showing episomal *ABL1* amplification at diagnosis and relapse, respectively.

(patient 2738). Unfortunately, lack of patient material hampered confirmation whether both mutations occurred in *cis*. Since only 5 out of 10 T-ALL samples with evidence for the 9q34 duplication, carried mutations in the *NOTCH1* gene (Table 2), no significant correlation between *NOTCH1* mutations and the presence of a 9q34 duplicated subclone could be proven. Patients with or without a *NOTCH1* mutation had comparable relapse rates (44% vs. 53%, respectively).

Quantitative real-time PCR was used to measure the mRNA expression levels of *NOTCH1* in pediatric T-ALL samples (Table 2). No evidence for altered *NOTCH1* expression levels in 9q34 duplicated patient samples were obtained (Table 2). Based upon raw fluorescent intensities from micro-array data, we then tested whether other genes located in the 9q34 region were deregulated as consequence of the 9q34 duplication. For 21 pediatric T-ALLs, including 7 patients with a subclonal

9q34 duplication, the expression levels for 78 probesets reflecting 53 genes located in the 9q33-34 region were calculated relative to the median *GAPDH* expression level. Three genes were identified, all located in the common region of duplication, that significantly expressed higher levels (less than 2-fold) in patients with a 9q34-duplication, i.e. *MRPL41* (Mann-Whitney; p=0.004), *SSNA1* (Mann-Whitney; p=0.009) and *PHPT1* (Mann-Whitney; p=0.01).

DISCUSSION

Pediatric T-ALL is characterized by a high diversity of chromosomal abnormalities involving helix-loop-helix proteins, *HOX*-genes or other genes involved in various cellular processes. Most of these abnormalities seem to affect the complete leukemic cell population. However, new abnormalities like the *NUP214-ABL1* episomal amplification, affect only a minor leukemic subpopulation probably as consequence of clonal evolution.

In the present study, 36 pediatric T-ALL samples were screened by array-CGH analysis. The most frequently abnormality detected was a 9q34 duplication, present in a subpopulation of the leukemic cells in 33% of our patients. A recent polymorphism study[29] used the same array-CGH slides as our study, and hybridized against the same reference DNA. In that study, the 9q34 duplication was never observed in over 200 healthy individuals (Personal communication, Dr. Charles Lee, Dr, John Iafrate), excluding the fact that this 9q34 duplication could be constitutional.

The high incidence makes this chromosomal aberration one of the most frequent cytogenetic abnormalities in pediatric T-ALL. The critical genomic region covers several genes previously linked to leukemogenesis, i.e. *NOTCH1*, *VAV2* and *TRAF2*. As a consequence of the duplication, some or all of these genes are potentially subject to deregulation of gene expression.

The *NOTCH1* gene has previously been implicated with human T-ALL, due to its involvement in a rare translocation coupling *NOTCH1* to the *TCR*-β locus[24]. Recently a broader role for *NOTCH1* was suggested as 50 percent of T-ALL cases carry an activating mutation in any of the three hot-spots[23]. This is confirmed in our independent cohort of T-ALL patients of whom 53% had *NOTCH1* mutations. Ten of the observed mutations were not previously described[23,33]. Two *NOTCH1* mutations (in exon 26 and exon 34) were simultaneously present in one patient (2738). This is of particular interest because mutations in cis may lead to an enhanced *NOTCH1* activity 20- to 40-fold[23]. Patients, harboring *NOTCH1* mutations, were randomly distributed throughout our pediatric T-ALL cohort, showing no specific relationship with the

other abnormalities at the 9q34 region. No enhanced expression level of *NOTCH1* could be measured by real-time PCR in the 9q34 duplicated cases.

In our cohort, the presence of a leukemic subclone containing the 9q34 duplication did not seem to affect clinical outcome. On the other hand, of the 6 patients that carried this 9q34 duplication and had relapsed, 4 patients showed the presence of leukemic cells at relapse that retained this duplication. This suggests that this leukemic subclone present at diagnosis, had actually survived intensive chemotherapeutic treatment, and may be associated with resistance to chemotherapeutic agents. Since leukemic cells with the 9q34 duplication reflected a leukemic subclone at relapse in all 4 patients analyzed, it obviously does not provide a survival and/or proliferation advantage, or only provides a limited survival advantage but the subclone was just being overgrown by another subclone with a stronger survival/proliferation advantage as may be the case for patient 1179.

We also investigated a possible relationship with the newly identified *NUP214-ABL1* episomal amplification and our 9q34 duplication. In two patients with the 9q34 duplication who relapsed, evidence was found for the presence of an episomal *NUP214-ABL1* amplification at diagnosis in a low percentage of leukemic cells as well. In patient 1179, the leukemic subclone having the episomal *ABL1* amplification had increased its representation in the total leukemic cell population from 5% to ~80%, implying that the episomal *NUP214-ABL1* amplification may indeed be a poor prognostic marker as previously suggested[21].

Molecular cytogenetic analysis of material from patient 1179 demonstrates the presence of a *HOX11L2* translocation, t(5;14)(q35;q32), as well as deletions involving chromosome 11 (del(11)(q14.1q22.3)) and 9 (add(9)(p21) next to an add(9)(q11); Table 1). In this patient, *HOX11L2*, del(11)(q14.1q22.3) and loss of *p15INK4B* and *p16INK4A*, presumably represent early genetic events during leukemogenesis, as they are present in the leukemic cells at diagnosis as well as at relapse (Table 3). This ancestral leukemic clone initially represented about 60% of the total leukemic population, from which two independent subclones evolved bearing additional genetic aberrations, one having an episomal *NUP214-ABL1* amplification (5%) and the other having a 9q34 duplication (35%). Following treatment, both of these subclones survived, with the *NUP214-ABL1* bearing clone having increased representation in the total leukemic cell population at relapse. The genetic abnormalities, as detected for patient 1179, suggests that T-ALL is a genetically unstable disease that readily forms complex subclones as a consequence of clonal evolution.

The subclonal 9q34 duplication seems not associated with mutations in *NOTCH1*, elevated *NOTCH1* expression or episomal *NUP214-ABL1* amplification. Analysis of microarray data for expressed genes located in the 9q33-34 region revealed significant overexpression of *MRLP41*, *SSNA1* and *PHPT1* in 9q34 duplicated T-ALL cases.

All three genes are situated in the common region of amplification. *SSNA1* encodes a nuclear autoantigen which is detected in patients with the Sjogren's syndrome, a chronic autoimmune disorder[34]. *PHPT1* encodes a phosphohistidine phosphatase, whereas *MRLP41* is translated into a mitochondrial ribosomal protein. None of these genes have been implicated in leukemogenesis before. Since the 9q34 duplication represent a minor leukemic clone, it is technical almost impossible to prove activation of specific genes located in the common duplicated region. It is therefore at present unclear whether these 3 genes are specifically activated or that also other genes in this region like *VAV2* or *TRAF2* are activated as well.

In conclusion, we report the identification of a novel recurrent 9q34 duplication in 33 percent of pediatric T-ALL The exact size of the amplified region differed slightly among patients, but the critical region encloses *VAV2*, *TRAF2* and *NOTCH1*. This duplication appears to be an independent genetic event from both the episomal *NUP214-ABL1* amplification[21] and the *NOTCH1* mutations[23], but leads to the activation of at least *MRLP41*, *SSNA1* and *PHPT1*. The 9q34 duplicated leukemic subclone was still present at relapse in four patients analyzed, indicating that the 9q34 may provide cellular resistance towards chemotherapy.

REFERENCES

1. Pui CH, Relling MV, Downing JR. Acute lymphoblastic leukemia. N Engl J Med 2004;350(15):1535-48.
2. Asnafi V, Radford-Weiss I, Dastugue N, Bayle C, Leboeuf D, Charrin C, et al. CALM-AF10 is a common fusion transcript in T-ALL and is specific to the TCRgammadelta lineage. Blood 2003;102(3):1000-6.
3. Bernard OA, Busson-LeConiat M, Ballerini P, Mauchauffe M, Della Valle V, Monni R, et al. A new recurrent and specific cryptic translocation, t(5;14)(q35;q32), is associated with expression of the Hox11L2 gene in T acute lymphoblastic leukemia. Leukemia 2001;15(10):1495-504.
4. Dube ID, Kamel-Reid S, Yuan CC, Lu M, Wu X, Corpus G, et al. A novel human homeobox gene lies at the chromosome 10 breakpoint in lymphoid neoplasias with chromosomal translocation t(10;14). Blood 1991;78(11):2996-3003.
5. Ferrando AA, Neuberg DS, Staunton J, Loh ML, Huard C, Raimondi SC, et al. Gene expression signatures define novel oncogenic pathways in T cell acute lymphoblastic leukemia. Cancer Cell 2002;1(1):75-87.
6. Fitzgerald TJ, Neale GA, Raimondi SC, Goorha RM. c-tal, a helix-loop-helix protein, is juxtaposed to the T-cell receptor-beta chain gene by a reciprocal chromosomal translocation: t(1;7)(p32;q35). Blood 1991;78(10):2686-95.
7. McGuire EA, Hockett RD, Pollock KM, Bartholdi MF, O'Brien SJ, Korsmeyer SJ. The t(11;14)(p15;q11) in a T-cell acute lymphoblastic leukemia cell line activates multiple transcripts, including Ttg-1, a gene encoding a potential zinc finger protein. Mol Cell Biol 1989;9(5):2124-32.
8. Mellentin JD, Smith SD, Cleary ML. lyl-1, a novel gene altered by chromosomal translocation in T cell leukemia, codes for a protein with a helix-loop-helix DNA binding motif. Cell 1989;58(1):77-83.
9. Royer-Pokora B, Loos U, Ludwig WD. TTG-2, a new gene encoding a cysteine-rich protein with the LIM motif, is overexpressed in acute T-cell leukaemia with the t(11;14)(p13;q11). Oncogene 1991;6(10):1887-93.
10. Speleman F, Cauwelier B, Dastugue N, Cools J, Verhasselt B, Poppe B, et al. A new recurrent inversion, inv(7)(p15q34), leads to transcriptional activation of HOXA10 and HOXA11 in a subset of T-cell acute lymphoblastic leukemias. Leukemia 2005;19(3):358-66.
11. Xia Y, Brown L, Yang CY, Tsan JT, Siciliano MJ, Espinosa R, III, et al. TAL2, a helix-loop-helix gene activated by the (7;9)(q34;q32) translocation in human T-cell leukemia. Proc Natl Acad Sci U S A 1991;88(24):11416-20.
12. Pinkel D, Segraves R, Sudar D, Clark S, Poole I, Kowbel D, et al. High resolution analysis of DNA copy number variation using comparative genomic hybridization to microarrays. Nat Genet 1998;20(2):207-11.
13. Albertson DG, Pinkel D. Genomic microarrays in human genetic disease and cancer. Hum Mol Genet 2003;12 Spec No 2:R145-52.
14. Mantripragada KK, Buckley PG, de Stahl TD, Dumanski JP. Genomic microarrays in the spotlight. Trends Genet 2004;20(2):87-94.
15. Veltman JA, Fridlyand J, Pejavar S, Olshen AB, Korkola JE, DeVries S, et al. Array-based comparative genomic hybridization for genome-wide screening of DNA copy number in bladder tumors. Cancer Res 2003;63(11):2872-80.

16. Hurst CD, Fiegler H, Carr P, Williams S, Carter NP, Knowles MA. High-resolution analysis of genomic copy number alterations in bladder cancer by microarray-based comparative genomic hybridization. Oncogene 2004;23(12):2250-63.

17. Snijders AM, Nowee ME, Fridlyand J, Piek JM, Dorsman JC, Jain AN, et al. Genome-wide-array-based comparative genomic hybridization reveals genetic homogeneity and frequent copy number increases encompassing CCNE1 in fallopian tube carcinoma. Oncogene 2003;22(27):4281-6.

18. Wilhelm M, Veltman JA, Olshen AB, Jain AN, Moore DH, Presti JC, Jr., et al. Array-based comparative genomic hybridization for the differential diagnosis of renal cell cancer. Cancer Res 2002;62(4):957-60.

19. Baldus CD, Liyanarachchi S, Mrozek K, Auer H, Tanner SM, Guimond M, et al. Acute myeloid leukemia with complex karyotypes and abnormal chromosome 21: Amplification discloses overexpression of APP, ETS2, and ERG genes. Proc Natl Acad Sci U S A 2004;101(11):3915-20.

20. Schwaenen C, Nessling M, Wessendorf S, Salvi T, Wrobel G, Radlwimmer B, et al. Automated array-based genomic profiling in chronic lymphocytic leukemia: development of a clinical tool and discovery of recurrent genomic alterations. Proc Natl Acad Sci U S A 2004;101(4):1039-44.

21. Graux C, Cools J, Melotte C, Quentmeier H, Ferrando A, Levine R, et al. Fusion of NUP214 to ABL1 on amplified episomes in T-cell acute lymphoblastic leukemia. Nat Genet 2004;36(10):1084-9.

22. De Keersmaecker K, Graux C, Odero MD, Mentens N, Somers R, Maertens J, et al. Fusion of EML1 to ABL1 in T-cell acute lymphoblastic leukemia with cryptic t(9;14)(q34;q32). Blood 2005.

23. Weng AP, Ferrando AA, Lee W, Morris JPt, Silverman LB, Sanchez-Irizarry C, et al. Activating mutations of NOTCH1 in human T cell acute lymphoblastic leukemia. Science 2004;306(5694):269-71.

24. Ellisen LW, Bird J, West DC, Soreng AL, Reynolds TC, Smith SD, et al. TAN-1, the human homolog of the Drosophila notch gene, is broken by chromosomal translocations in T lymphoblastic neoplasms. Cell 1991;66(4):649-61.

25. Pear WS, Aster JC. T cell acute lymphoblastic leukemia/lymphoma: a human cancer commonly associated with aberrant NOTCH1 signaling. Curr Opin Hematol 2004;11(6):426-433.

26. Radtke F, Wilson A, Mancini SJ, MacDonald HR. Notch regulation of lymphocyte development and function. Nat Immunol 2004;5(3):247-53.

27. Harper JA, Yuan JS, Tan JB, Visan I, Guidos CJ. Notch signaling in development and disease. Clin Genet 2003;64(6):461-72.

28. Stam RW, den Boer ML, Meijerink JP, Ebus ME, Peters GJ, Noordhuis P, et al. Differential mRNA expression of Ara-C-metabolizing enzymes explains Ara-C sensitivity in MLL gene-rearranged infant acute lymphoblastic leukemia. Blood 2003;101(4):1270-6.

29. Iafrate AJ, Feuk L, Rivera MN, Listewnik ML, Donahoe PK, Qi Y, et al. Detection of large-scale variation in the human genome. Nat Genet 2004;36(9):949-51.

30. Meijerink J, Mandigers C, van de Locht L, Tonnissen E, Goodsaid F, Raemaekers J. A novel method to compensate for different amplification efficiencies between patient DNA samples in quantitative real-time PCR. J Mol Diagn 2001;3(2):55-61.

31. Holleman A, Cheok MH, den Boer ML, Yang W, Veerman AJ, Kazemier KM, et al. Gene-expression patterns in drug-resistant acute lymphoblastic leukemia cells and response to treatment. N Engl J Med 2004;351(6):533-42.

32. Quesnel B, Preudhomme C, Fenaux P. p16ink4a gene and hematologicalmalignancies. Leuk Lymphoma 1996;22(1-2):11-24.

33. Lee SY, Kumano K, Masuda S, Hangaishi A, Takita J, Nakazaki K, et al. Mutations of the Notch1 gene in T-cell acute lymphoblastic leukemia: analysis in adults and children. Leukemia 2005;19(10):1841-3.

34. Fox RI. Sjogren's syndrome. Lancet 2005;366(9482):321-31.

35. UCSC Genome Browser. http://genome.ucsc.edu. Build March 2004

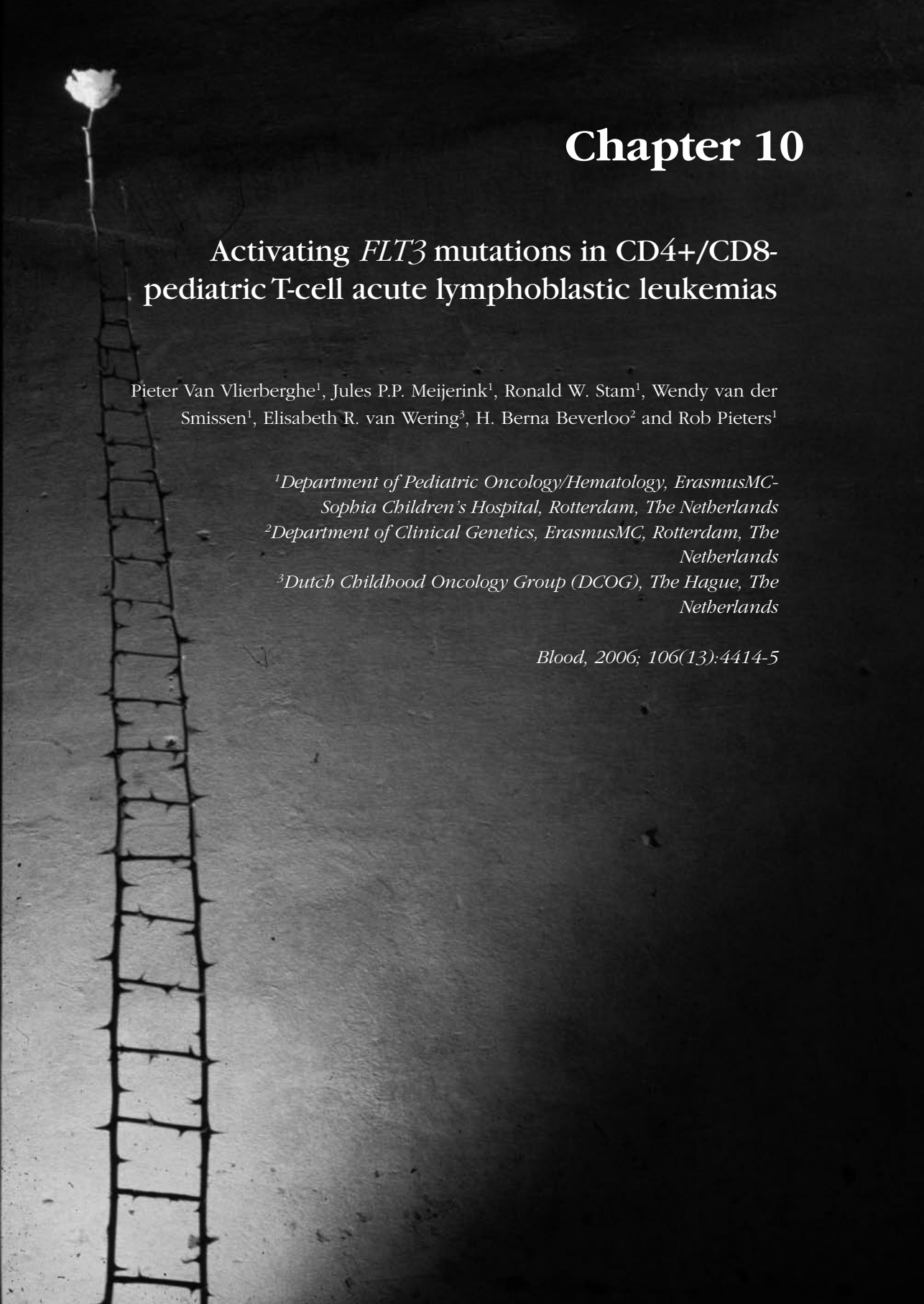

Chapter 10

Activating *FLT3* mutations in CD4+/CD8- pediatric T-cell acute lymphoblastic leukemias

Pieter Van Vlierberghe[1], Jules P.P. Meijerink[1], Ronald W. Stam[1], Wendy van der Smissen[1], Elisabeth R. van Wering[3], H. Berna Beverloo[2] and Rob Pieters[1]

[1]Department of Pediatric Oncology/Hematology, ErasmusMC-Sophia Children's Hospital, Rotterdam, The Netherlands
[2]Department of Clinical Genetics, ErasmusMC, Rotterdam, The Netherlands
[3]Dutch Childhood Oncology Group (DCOG), The Hague, The Netherlands

Blood, 2006; 106(13):4414-5

TO THE EDITOR

Activating mutations in the *FMS-like tyrosine kinase 3* gene (*FLT3*) including internal tandem duplications (ITD) in the juxtamembrane (JM) domain or point mutations (PM) in the activation loop are the most common genetic aberration in acute myeloid leukemia (AML).[1] Recently, Paietta *et al* investigated the presence of *FLT3* mutations in 69 adult T-ALL patients.[2] Three positive cases (2 ITDs and 1 PM) were identified sharing a similar early pro-thymocytic T-cell developmental state exclusively expressing cKIT/CD117, and a trial to test the efficacy of FLT3 inhibitors for this T-ALL subset was suggested.

To validate the incidence of *FLT3* mutations and to investigate a relation to outcome and other parameters, we screened 72 diagnostic pediatric T-ALL samples for *FLT3* mutations, as previously described.[3,4] We identified *FLT3*/ITD mutations in 2 pediatric T-ALL (Figure 1a), whereas no point mutations in the kinase domain were detected. Sequence analysis confirmed a 51 base pair insertion in patient 2112 and a 57 base pair insertion in patient 1179 (Figure 1b). Moreover, no wild-type *FLT3* was identified in patient 2112, suggesting loss of the wild-type allele.[1]

Immunophenotypic analyses revealed a similar profile for both *FLT3* mutated patient samples, i.e. TdT^+, $CD2^+$, $CD5^+$, $CD7^+$, $CD4^+/CD8^-$, cytoplasmic $CD3^+$, surface $CD3^-$ and $CD10^-$. CD34 expression was detected in 24% and 21% of the leukemic blasts in patient 2112 and 1179, respectively. Only patient 2112 weakly expressed CD13 (24%) but not CD33. Although representing early T-cell differentiation stages for both patient samples, the maturation stage seems more advanced compared to the *FLT3* mutated adult T-ALL cases ($CD34^+$, $CD4^-/CD8^-$).[2] Since no additional patient material was left for flowcytometry, *cKIT/CD117* expression was determined by RQ-PCR on isolated blasts[5] (>90% leukemic cells) from all pediatric T-ALL samples (figure 1d). Whereas only the 3 *FLT3*-mutated adult T-ALL patients highly expressed cKIT[2], most pediatric T-ALL samples expressed *cKIT* mRNA to some extend. Patient 2112 highly expressed *cKIT*, whereas patient 1179 showed a weak *cKIT* expression that was about 26 fold lower. Since various non-*FLT3* mutated T-ALL samples highly expressed *cKIT/CD117* at levels comparable to patient 2112, we conclude that *cKIT/CD117* expression is not exclusively associated with *FLT3* mutations. Nevertheless, transcript levels do not necessarily correlate with protein expression levels[2]. In line with previous observations[2], leukemic blasts of *FLT3* mutated samples highly expressed *LYL1* and *LMO2*. Both pediatric samples carried a *HOX11L2* translocation in contrast to the *FLT3* mutated adult T-ALL cases [2].

Patient 1179 relapsed 13 months after initial diagnosis, whereas patient 2112 is in continued complete remission (CCR, 61^+). Interestingly, patient 1179 showed no *FLT3*/ITD mutation at relapse (Figure 1c), possibly due to loss of the mutated allele

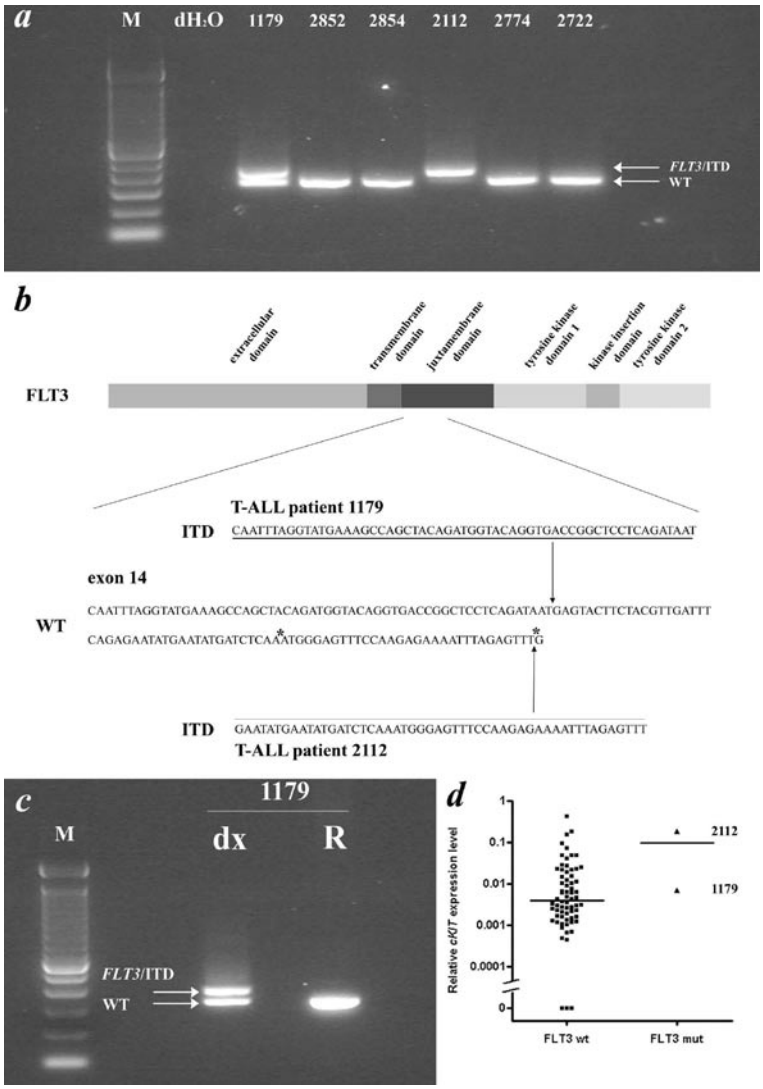

Figure 1. Activating *FLT3* mutations in pediatric T-ALL.

(a) Genomic PCR analysis for the *FLT3* gene. PCR results for 6 pediatric T-ALL patient samples are shown. T-ALL patient 1179 shows a heterozygous FLT3/ITD mutation. No wild-type *FLT3* is detected in T-ALL patient 2112, probably due to loss of heterozygosity of the wild-type allele. **(b)** Overview of the functional domains in the FLT3 tyrosine kinase receptor. Genomic position of the FLT3/ITD mutations detected in patients 1179 and 2112 are shown. Mutation position annotation is based on the FLT3 reference sequence NM_004119. **(c)** *FLT3* mutation analysis of diagnosis and relapse material of T-ALL patient 1179. The FLT3/ITD mutation was present at diagnosis, but absent at relapse. **(d)** Relative *cKIT/CD117* mRNA expression indicated as percentage of GAPDH expression for the investigated pediatric T-ALL cohort (*FLT3* wt vs. *FLT3* mut). For both groups the median *FLT3* mRNA expression is shown.

WT; wild-type; mut; mutated; dx; at diagnosis; R; at relapse; *, genomic position of the recently identified FLT3/ITD mutations in adult T-ALLs[2].

during therapy, or alternatively, the *FLT3*/ITD positive clone was eliminated during chemotherapy with a subsequent relapse from a non-*FLT3*-mutated parental clone.

In conclusion, we confirm the presence of *FLT3* mutations in pediatric T-ALL (2/72, 2.7%). Although both immature, the immunophenotypes of the *FLT3* mutated pediatric and adult[2] T-ALL cases differed. In addition, a link between mRNA expression of *cKIT/CD117* and *FLT3* mutations could not be demonstrated. Since patient 2112 is in CCR and relapse material of patient 1179 did not show evidence for *FLT3* mutation, the *FLT3* mutated T-ALL subclone seem to be effectively eradicated by current chemotherapy. This suggests that the application of FLT3 inhibitors for *FLT3*-mutated T-ALL, as suggested by Paietta[2], may not further improve treatment outcome in pediatric T-ALL.

REFERENCES

1. Levis M, Small D. FLT3: ITDoes matter in leukemia. Leukemia. 2003;17:1738-1752.
2. Paietta E, Ferrando AA, Neuberg D, et al. Activating FLT3 mutations in CD117/KIT(+) T-cell acute lymphoblastic leukemias. Blood. 2004;104:558-560.
3. Kiyoi H, Naoe T, Yokota S, et al. Internal tandem duplication of FLT3 associated with leukocytosis in acute promyelocytic leukemia. Leukemia Study Group of the Ministry of Health and Welfare (Kohseisho). Leukemia. 1997;11:1447-1452.
4. Yamamoto Y, Kiyoi H, Nakano Y, et al. Activating mutation of D835 within the activation loop of FLT3 in human hematologic malignancies. Blood. 2001;97:2434-2439.
5. Stam RW, den Boer ML, Schneider P, et al. Targeting FLT3 in primary MLL gene rearranged infant acute lymphoblastic leukemia. Blood. 2005.

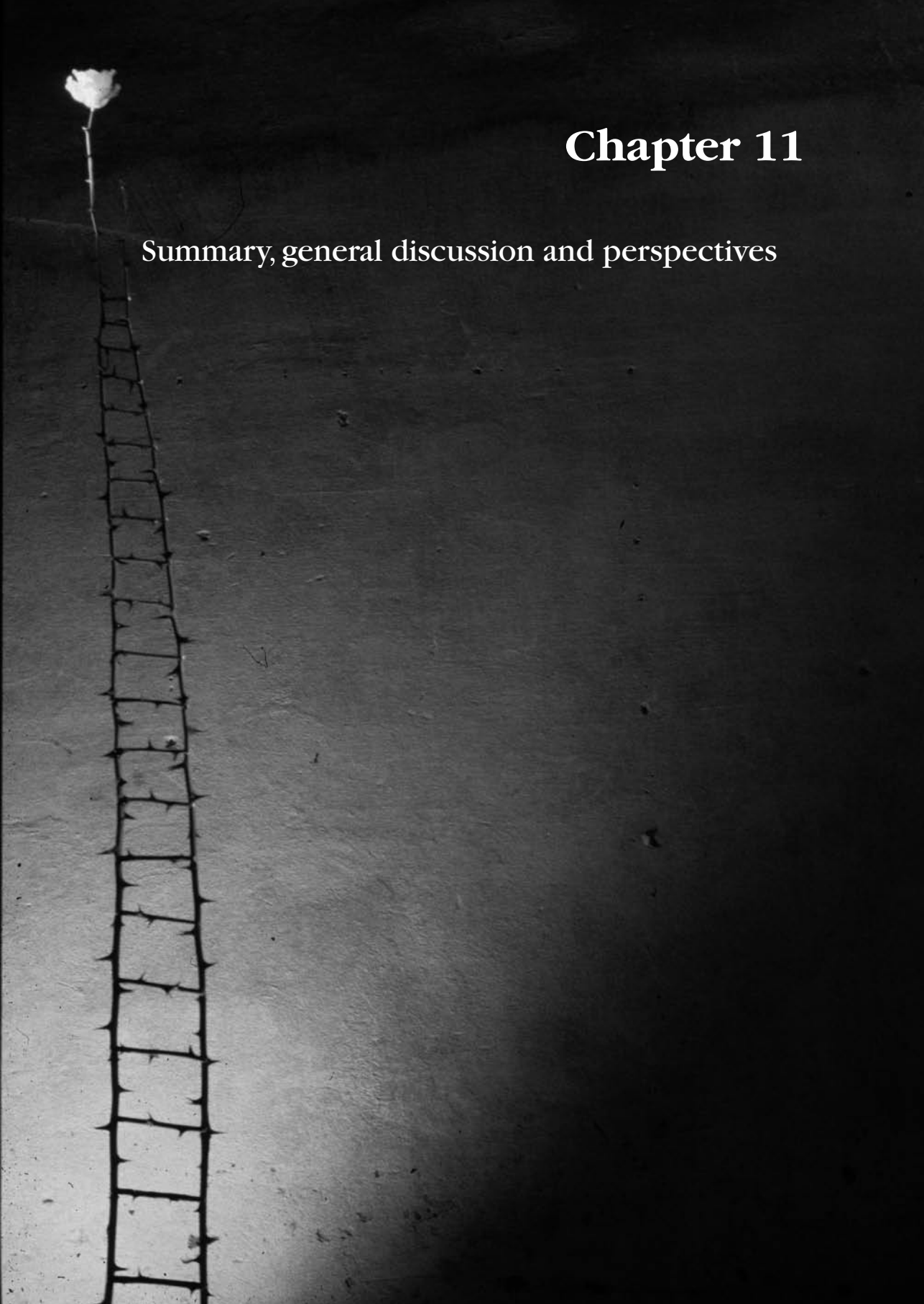

Chapter 11

Summary, general discussion and perspectives

Pediatric T-cell ALL is an aggressive malignancy of thymocytes that accounts for about 15 percent of ALL cases and for which treatment outcome remains inferior compared to B-lineage acute leukemias. About 30 percent of childhood T-ALL patients relapse within 4 years after diagnosis and ultimately die[1]. Despite its complexity on the genetic level, genetic abnormalities are clinically not used for therapy stratification. Further improvement of treatment in this high-risk disease will require the development of drugs that target specific pathways involved in the pathogenesis and maintenance of the malignant cells. Therefore, studies focusing on the molecular and genetic characterization of pediatric T-ALL are crucial to improve T-ALL treatment schedules and eventually switch towards treatment stratification based upon genetic T-ALL subtypes.

In T-ALL, leukemic transformation of maturating thymocytes is caused by a multistep pathogenesis involving numerous genetic abnormalities that drive normal T-cells into uncontrolled cell growth and clonal expansion[2-5]. A wide variety of genetic events affecting various cellular processes like the cell cycle, differentiation and survival have thus far been identified. In general, specific aberrations can be subdivided into type A and type B abnormalities. Type A abnormalities occur in a mutually exclusive manner and mainly function by facilitating differentiation arrest at specific stages of T-cell development. These type A mutations may delineate distinct molecular-cytogenetic T-ALL subgroups. Type B abnormalities are found in all major T-ALL subgroups and may synergize with type A mutations during T-cell pathogenesis. Various micro-array studies performed over the last years[6,7] indeed confirmed that specific expression profiles for various T-ALL subgroups are characterized by the presence of the type A mutations. Since some of these type A mutations affect genes that function in similar cellular processes, a number of type A abnormalities share similar gene expression profiles and can be recognized as one single T-ALL subgroup. Currently, we distinguish 5 different genetic subgroups in T-ALL: *TAL/LMO, TLX1, TLX3, HOXA* and *MYB*. The current knowledge on the genetics of T-ALL is extensively reviewed in chapter 2.

LMO2 is a well known oncogene in T-ALL due to its involvement in the translocations t(11;14)(p13;q11) and t(7;11)(q35;p13), in which the *TCR-LMO2* fusion results in a constitutive activation of the *LMO2* gene[8]. High *LMO2* expression levels have also been reported in the absence of translocations, suggesting that alternative mechanisms may exist in T-ALL resulting in the activation of *LMO2*. In chapter 3, we identified such a new *LMO2* activation mechanism, ie. the cryptic deletion, del(11)(p12p13)[9]. A FISH-based screening revealed the presence of this deletion in 6 out of 138 pediatric T-ALL patients (4%). In most patients, this deletion resulted in the loss of a negative regulatory element located just upstream of the *LMO2* oncogene. Loss of this domain results in the aberrant activation of an otherwise silent promoter

region that is present in intron 3 of the *LMO2* gene. Since the protein coding domain of *LMO2* starts in exon 4, this deletion results in aberrant activation of wildtype LMO2 in most of the del(11)(p12p13) positive patients. *LMO2* rearrangements, including this del(11)(p12p13), t(11;14)(p13;q11) and t(7;11)(q35;p13), were found in the absence of other recurrent cytogenetic abnormalities involving *TLX3*, *TLX1, CALM-AF10*, *TAL1*, *MLL* or *MYC*. This study showed that *LMO2* abnormalities (translocations and cryptic deletions), which represented about 9% of pediatric T-ALL, are more frequent than appreciated up till now, and represent a distinct cytogenetic T-ALL subgroup.

Our initial screening for cryptic *LMO2* deletions using FISH on 138 childhood T-ALL cases may have been unsuccessful to detect relatively small deletions upstream of *LMO2*. For this reason, we developed a Multiplex Ligation Probe Amplification (MLPA) assay with multiple probes located in or just flanking the negative regulatory region to detect such smaller deletions upstream of *LMO2*. Using this approach, we identified one additional T-ALL case with an *LMO2* deletion that had remained undetected in our previous FISH analysis (chapter 4). This deletion, del(11)(p13p13), was about 400 kb in size and included the genes *CAPRIN1, NAT10* and *ABTB2*. Therefore, smaller deletions, del(11)(p13p13), compared to the del(11)(p12p13) deletions, as described in chapter 3, occur in pediatric T-ALL.

LMO2 is highly expressed in the most immature stages of normal T cell development and is down regulated upon further T cell maturation in the thymus[10,11]. Therefore, most immature T-ALL samples display high *LMO2* expression levels, possibly reflecting their cell of origin rather than pointing to a genomic defect at the *LMO2* locus. Our combined FISH and MLPA analysis (chapter 3 and 4) provided us with an overview of all genomic *LMO2* rearrangements (translocations and deletions) in pediatric T-ALL. Because bi-allelic *LMO2* expression has been suggested as an alternative mechanism for oncogene activation in T-ALL[10], we investigated if biallelic *LMO2* expression could act as an oncogenic event in our pediatric T-ALL cohort. All *LMO2* rearranged cases (translocations and deletions) had mono-allelic expression of *LMO2*. In addition, all patients who showed high *LMO2* gene levels (comparable to *LMO2* rearranged cases) in combination with biallelic *LMO2* expression had an immature phenotype and were frequently characterized by other type A abnormalities, including an *MLL-AF6* or a *CALM-AF10* translocation. These data support our hypothesis that biallelic activation of *LMO2* in immature T-ALL cases reflects their early T-cell development stage rather than representing a true oncogenic mechanism.

Our gene expression profiling study in T-ALL (chapter 5) showed that del(11)(p12p13) positive and *LMO2* translocated T-ALL patients have highly similar gene expression signatures, indicating that *LMO2* rearranged T-ALL patients trigger common oncogenic mechanisms. In addition, these *LMO2* rearranged T-ALL patients were part of a larger cluster of T-ALL cases with a uniform expression profile which

also included samples with *TAL1*, *TAL2* and *LMO1* rearrangements. This is likely due to the fact that these genes encode for proteins that normally participate in the same transcriptional complex[11,12]. Therefore, *TAL*- or *LMO*-like abnormalities seem to trigger a common pathogenic mechanism in T-ALL. In total, this *TAL/LMO* cluster of patients included about half of all pediatric T-ALL samples. Future identification of a common target within this *TAL/LMO* gene expression signature could open the way towards targeted therapy within this specific T-ALL subtype comprising a large proportion (~50%) of pediatric T-ALL patients.

Another genetic subgroup consists of T-ALL patients who share an expression profile characterized by the activation of the *HOXA* cluster of genes. This subgroup consists of *CALM-AF10* translocations, *MLL*-rearrangements or inversions of chromosome 7, i.e. the inv(7)(p15q35)[7]. A previous microarray study[7] identified patients with such a *HOXA* expression signature that lacked all genetic lesions mentioned above, indicating that alternative *HOXA* activation mechanisms exist in T-ALL. A potential strategy to identify such novel *HOXA* activation mechanisms is the combined analyses of gene expression profiling, in which patients lacking known genetic abnormalities, cluster together with genetically characterized samples, and genomic profiling by array-CGH (chapter 5). Using such an approach, we identified an identical interstitial deletion, del(9)(q34.11q34.13), in 3 out of 5 cases that clustered together with *HOXA* activated samples having *CALM-AF10* translocations or an inv(7)(p15q34)[13]. This deletion gave rise to a *SET-NUP214* fusion gene, identical to the *SET-NUP214* fusion described 15 years ago for a single acute undifferentiated leukemia patient with a reciprocal t(9;9)(q34;q34)[14] and most recently for a single case of acute myeloid leukemia[15]. The *SET-NUP214* gene fusion was also identified in the T-ALL cell line LOUCY, providing an opportunity to functionally test the role of SET-NUP214. We discovered that SET-NUP214 binds in the promoter regions of specific *HOXA* genes, i.e. *HOXA9* and *HOXA10*. Here, it interacts with 2 proteins, CRM1 and DOT1L. The interaction with DOT1L, a histone H3 methyltransferase, supports a role for local epigenetic regulation of gene expression through the modification of the histone backbone. We demonstrated that the histones that interact with the promoter regions of various *HOXA* gene members were acetylated on histone H4, representing a local "open genomic state" of the *HOXA* gene cluster. Methylation and acetylation of histones on specific amino acid residues may open the chromosomal structure enabling the binding of transcription factors to the promoter regions of genes in that region. This way, recruitment of DOT1L by SET-NUP214 may enable activation of all *HOXA* gene members. Targeted inhibition of SET-NUP214 by siRNA in LOUCY cells abolished expression of *HOXA* genes further confirming the direct link between *SET-NUP214* and *HOXA* activation. In addition, SET-NUP214 knockdown induced differentiation in the T-ALL cell line LOUCY, whereas this effect could not be demonstrated in

SET-NUP214 negative T-ALL lines. From this study, we concluded that SET-NUP214 contributes to the pathogenesis of T-ALL by enforcing T-cell differentiation arrest through induction of *HOXA* gene expression. It is likely that other *HOXA* activating mechanisms await identification in T-ALL, since additional T-ALL cases with a *HOXA* gene signature lacked any of the *HOXA* related rearrangements mentioned above.

From a therapeutical point of view, the recruitment of DOT1L by SET-NUP214 is of particular interest since this methyltransferase has previously been implicated in *HOXA* activation by CALM-AF10[16], MLL-ENL[17] and MLL-AF10[18] mediated leukemias. Since DOT1L seems to be the common factor in the leukemogenic *HOXA* activation for these different fusion genes, further research could focus on a potential role of DOT1L as a therapeutic target in the treatment of SET-NUP214, MLL-AF10, MLL-ENL and CALM-AF10 mediated leukemias. The oncogenic potential of SET-NUP214 could further be investigated by studying the proliferation kinetics of hematopoietic progenitor cells infected with a retrovirus encoding SET-NUP214, and compare these data with the oncogenic potential of other *HOXA* activating fusion genes including CALM-AF10 or MLL-ENL. In addition, the in vivo leukemogenic potential of SET-NUP214 could be investigated by injection of these retrovirally infected murine progenitor cells into recipient mice. Furthermore, the domains of SET-NUP214 that are specifically required for *HOXA* gene activation could be identified using *SET-NUP214* deletion/mutation constructs. For the identification of additional *SET-NUP214* downstream targets (besides *HOXA*), gene expression profiles before and after siRNA mediated SET-NUP214 knockdown could be combined with a ChIP-on-ChIP analysis of SET-NUP214 in the cell line LOUCY.

The *MYB* gene encodes a nuclear transcription factor that is critically required during T-cell development. Until recently, overexpression of *MYB* had only been implicated in murine leukemogenesis. No recurrent rearrangements involving the *MYB* locus had thus far been reported in human leukemia. Using an array-CGH platform with an overall resolution of 1 Mb, and with additional probes covering candidate oncogenes, we identified copy number changes in the chromosomal region covering the *MYB* locus (6q23) in both T-ALL cell lines and primary patient samples[19] (chapter 6, collaboration with Prof. J. Cools and Dr. I. Lahortiga, Leuven, Belgium). Approximately at the same time, others identified the translocation, t(6;7)(q23;q34), as a novel recurrent abnormality in T-ALL resulting in the activation of *MYB* through rearrangement with the *TCR*β locus[20]. The *MYB* duplication was associated with a 3-fold increase in *MYB* expression, and siRNA-mediated knockdown of *MYB* expression initiated T-cell differentiation in a T-ALL cell line model without affecting cell survival. These results identified the *MYB* duplication as an oncogenic event in T-ALL and suggest that *MYB* activation contributes to the pathogenesis of T-ALL by enforcing T-cell differentiation arrest. Synergistic effects on cell proliferation

and survival were identified in T-ALL cell lines by combined inhibition of *MYB* and *NOTCH1*, suggesting that *MYB* could act as a novel target for therapy in T-ALL. For *NOTCH1* mutated T-ALL cell lines that are resistant to γ-secretase inhibitors, combined inhibition of MYB and the PI3K-AKT pathway could possibly lead to similar synergistic effects. To further explore the therapeutic potential of MYB inhibition, additional studies should focus on mechanisms that could interfere with the function of the *MYB* oncogene in T-ALL.

About 20% of pediatric T-ALL cases are characterized by *TLX3* expression due to a cryptic translocation t(5;14)(q35;q32). Although a number of collaborating genetic events have been identified in *TLX3* rearranged T-ALL patients (*NOTCH1* mutations, *CDKN2A/CDKN2B* deletions, *NUP214-ABL1* amplifications), further elucidation of additional genetic lesions could provide a better understanding of the pathogenesis of this specific T-ALL subtype. Therefore, we performed array-CGH analysis on a *TLX3* rearranged T-ALL patient cohort and identified new genetic defects that may cooperate with *TLX3* gene expression in the leukemic transformation of thymocytes (chapter 7). The recurrent genomic deletions included a del(1)(p36.31), del(5)(q35), del(13)(q14.3), del(16)(q22.1) and del(19)(p13.2). From these, the cryptic deletion del(5)(q35) was exclusively identified in about 25% of *TLX3* rearranged T-ALL cases. Since these 5q35 deletions differed in size, a potential tumor suppressor gene could be present in the minimal deleted area at 5q35 specifically cooperating with *TLX3* expression in the leukemogenesis of T-ALL. A potential candidate gene in this 5q35 genomic region is *NSD1*. Mutations or deletions of the NSD1 gene are the major cause of Sotos syndrome, a constitutional overgrowth disorder[21], and patients with this syndrome have a higher risk for the development of leukemia[22-24]. Therefore, a future mutation screening of *NSD1* in *TLX3* rearranged T-ALL is mandatory to evaluate a potential role for *NSD1* inactivation in T-ALL. Nevertheless, about 30 other genes are also present in the minimal deleted 5q35 region and further expression and/or mutational analysis will be required to identify other potential target genes in this chromosomal region. Some of the other recurrent deletions identified in this study were previously identified in other cancer malignancies and could point to interesting genes with potential involvement in T-ALL pathogenesis. The *CHD5* gene (1p36) has been shown to be a tumor suppressor that controls proliferation and apoptosis via the p19Arf/p53 pathway[25] and similar 1p36.31 deletions have been identified in neuroblastoma, colorectal cancer and a variety of hematological malignancies[26-28]. Deletion of the *miR-15/miR-16a* cluster (13q14) could lead to the activation of anti-apoptotic BCL2, and has been detected in CLL and B-ALL patients[29,30]. Inactivation of the *CTCF* gene (16q22.1), which is a conserved transcriptional repressor of the *MYC* oncogene[31], could represent an alternative mechanism for *MYC* activation in T-ALL. Therefore, these data provide a rationale for a future mutational/FISH/protein

screening study of *CHD5*, *miR-15/miR-16a* and *CTCF* in order to evaluate their potential role in T-ALL. A number of other genetic lesions were detected in single *TLX3* rearranged T-ALL cases and could also point towards interesting candidate genes in T-ALL. In this respect, *FBXW7* (4q31) and *WT1* (11p13) were identified as potential tumor suppressor genes in T-ALL.

Neurofibromatosis type 1 (NF1) is an autosomal dominant genetic disorder caused by mutations in the *NF1* gene[32]. NF1 patients have a higher risk to develop juvenile myelomonocytic leukemia[33] (JMML) and AML[34]. In NF patients, these malignancies are associated with loss of the wild-type allele, either through *NF1* deletions or the acquisition of *NF1* point mutations. Previously, it was shown that bi-allelic inactivation of *NF1* is also found as a somatic abnormality in JMML patients that lack clinical evidence of NF1[35]. In our array-CGH based screening of pediatric T-ALL, we identified a recurrent cryptic deletion, del(17)(q11.2q11.2), in 3 T-ALL patients that did not have any clinical evidence of NF1 (chapter 8). This same deletion was previously described as a microdeletion of the *NF1* region in congenital NF1 patients[32]. Subsequent mutation analysis of these T-ALL cases revealed that mutations in the remaining *NF1* allele were present, confirming the role of *NF1* as a bona fide tumor-suppressor gene in cancer. In addition, *NF1* inactivation was confirmed at the RNA expression level in the patients tested. Since the NF1 protein is a negative regulator of the RAS pathway[32], *NF1* inactivation could represent a new proliferative hit in the development of T-cell leukemia. Cooperative aberrations detected in these *NF1*-inactivated T-ALL samples included *NOTCH1* mutations, a *TLX3* translocation and *CALM-AF10* translocation. Simultaneous array-CGH screening studies on other leukemia subtypes in our laboratory reported similar *NF1* microdeletions in both B-lineage ALL and *MLL*-rearranged AML patients, indicating that *RAS* activation through *NF1* inactivation probably reflects a general oncogenic mechanism in both myeloid and lymphoid leukemias. These leukemia patients could potentially benefit from additional treatment with RAS inhibitors like farnesylthiosalicylic acid[36] or downstream inhibitors.

In T-ALL, a number of genetic defects are only detected in a limited percentage of leukemic cells, indicating that they probably reflect a progression marker, rather than an initiating leukemogenic event, in the development of T-cell leukemia. For example, we identified a new and recurrent 9q34 duplication in 33 percent of pediatric T-ALL samples[37] (chapter 9). This duplication was identified in 17–39 percent of leukemic cells at diagnosis and cells carrying this duplication were still present at relapse. The minimal amplified region of these 9q34 duplications contained *NOTCH1*, the main mutational target in T-ALL[38]. Although no clear relationship between the presence of *NOTCH1* mutations and this 9q34 abnormality could be determined, duplication of

this genomic region could induce subtle changes in *NOTCH1* gene expression levels and contribute to global *NOTCH1* activation in T-ALL.

FLT3 mutations are another example of a progression marker in T-ALL. Previously, *FLT3* mutations were identified in adult T-ALL patients[39]. We identified *FLT3/ITD* mutations in 2/72 pediatric T-ALLs (2.7%), whereas 0/72 showed point mutations in the kinase domain[40] (chapter 10). Immunophenotypic analysis revealed a similar profile for both pediatric *FLT3* mutated patient samples, i.e. $CD4^+/CD8^-$. Although representing early T-cell differentiation stages for both patient samples, the immunophenotype was more maturated than the *FLT3* mutated adult T-ALL cases, previously described ($CD34^+$, $CD4^-/CD8^-$)[39]. Both pediatric *FLT3* mutated T-ALL patients showed high levels of *LYL1* and *LMO2* expression and contained a *TLX3* translocation, which was not present in the *FLT3* mutated adult T-ALL cases. The first *FLT3* mutated patient had a relapse 13 months after initial diagnosis. Interestingly, the relapse material showed no *FLT3/ITD* mutation, indicating that the *FLT3* mutated T-ALL subclone seems to be effectively eradicated by current chemotherapy. The other patient was still in continued complete remission 5 years after diagnosis and can be considered cured. We therefore conclude that the application of *FLT3* inhibitors for *FLT3* mutated T-ALL, as suggested by Paietta et al.[39], may not further improve treatment outcome in pediatric T-ALL.

In conclusion, this thesis on molecular-cytogenetic insights in T-ALL confirms that T-cell leukemia is not a single disease entity, but rather reflects a genetically diverse malignancy. In addition, our work shows that genome wide copy number screening using array-CGH is a valuable tool for the identification of new chromosomal imbalances in T-ALL and provides further insight in the pathogenesis of T-cell leukemia. One of the main shortcomings of our array-CGH analysis compared to copy number screening studies using SNP arrays, is that array-CGH is unable to detect uniparental disomy (chapter 1) as an alternative mechanism for gene (in)activation. For example, *NF1* inactivation (chapter 8) could also result from duplication of the mutated *NF1* allele at the expense of the remaining wild-type allele. Therefore, it is possible that we are currently underestimating the incidence of such genetic defects in T-ALL. Our complete overview of new copy number changes in T-ALL (chapter 2) offers great new challenges for the identification of new target genes that may play a role in the pathogenesis of T-ALL. Even the genetic defects that only occurred at low frequency could reveal new and important genes with a broader role in T-ALL, as illustrated for *FBXW7* and *PTEN* (chapter 2 and 7). Therefore, a large number of genetic abnormalities, as described in this thesis, are probably still hiding genes that could help us further understand the biology of this disease. Future analysis on the mutational status, epigenetics and protein level of all these genes of interest will probably guide us to new candidate genes involved in T-ALL pathogenesis.

Hopefully, these future research efforts will further improve our knowledge on the molecular genetic characteristics of this aggressive malignancy, and will eventually lead to better treatment results and/or target therapy that could partially replace or diminish the use of aggressive chemotherapeutics.

REFERENCES

1. Pui CH, Evans WE. Treatment of acute lymphoblastic leukemia. The New England journal of medicine. 2006;354:166-178.
2. Armstrong SA, Look AT. Molecular genetics of acute lymphoblastic leukemia. J Clin Oncol. 2005;23:6306-6315.
3. De Keersmaecker K, Marynen P, Cools J. Genetic insights in the pathogenesis of T-cell acute lymphoblastic leukemia. Haematologica. 2005;90:1116-1127.
4. Grabher C, von Boehmer H, Look AT. Notch 1 activation in the molecular pathogenesis of T-cell acute lymphoblastic leukaemia. Nat Rev Cancer. 2006;6:347-359.
5. Graux C, Cools J, Michaux L, Vandenberghe P, Hagemeijer A. Cytogenetics and molecular genetics of T-cell acute lymphoblastic leukemia: from thymocyte to lymphoblast. Leukemia. 2006;20:1496-1510.
6. Ferrando AA, Neuberg DS, Staunton J, et al. Gene expression signatures define novel oncogenic pathways in T cell acute lymphoblastic leukemia. Cancer Cell. 2002;1:75-87.
7. Soulier J, Clappier E, Cayuela JM, et al. HOXA genes are included in genetic and biologic networks defining human acute T-cell leukemia (T-ALL). Blood. 2005;106:274-286.
8. Sanchez-Garcia I, Rabbitts TH. LIM domain proteins in leukaemia and development. Semin Cancer Biol. 1993;4:349-358.
9. Van Vlierberghe P, van Grotel M, Beverloo HB, et al. The cryptic chromosomal deletion del(11)(p12p13) as a new activation mechanism of LMO2 in pediatric T-cell acute lymphoblastic leukemia. Blood. 2006;108:3520-3529.
10. Ferrando AA, Herblot S, Palomero T, et al. Biallelic transcriptional activation of oncogenic transcription factors in T-cell acute lymphoblastic leukemia. Blood. 2004;103:1909-1911.
11. Herblot S, Steff AM, Hugo P, Aplan PD, Hoang T. SCL and LMO1 alter thymocyte differentiation: inhibition of E2A-HEB function and pre-T alpha chain expression. Nat Immunol. 2000;1:138-144.
12. Chervinsky DS, Zhao XF, Lam DH, Ellsworth M, Gross KW, Aplan PD. Disordered T-cell development and T-cell malignancies in SCL LMO1 double-transgenic mice: parallels with E2A-deficient mice. Mol Cell Biol. 1999;19:5025-5035.
13. Van Vlierberghe P, Tchinda J, van Grotel M, et al. The recurrent SET-NUP214 fusion as a new HOXA activation mechanism in pediatric T-cell acute lymphoblastic leukemia. PLoS Medicine. 2007.
14. von Lindern M, Breems D, van Baal S, Adriaansen H, Grosveld G. Characterization of the translocation breakpoint sequences of two DEK-CAN fusion genes present in t(6;9) acute myeloid leukemia and a SET-CAN fusion gene found in a case of acute undifferentiated leukemia. Genes, chromosomes & cancer. 1992;5:227-234.
15. Rosati R, La Starza R, Barba G, et al. Cryptic chromosome 9q34 deletion generates TAF-Ialpha/CAN and TAF-Ibeta/CAN fusion transcripts in acute myeloid leukemia. Haematologica. 2007;92:232-235.
16. Okada Y, Jiang Q, Lemieux M, Jeannotte L, Su L, Zhang Y. Leukaemic transformation by CALM-AF10 involves upregulation of Hoxa5 by hDOT1L. Nat Cell Biol. 2006;8:1017-1024.
17. Mueller D, Bach C, Zeisig D, et al. A role for the MLL fusion partner ENL in transcriptional elongation and chromatin modification. 2007.

18. Okada Y, Feng Q, Lin Y, et al. hDOT1L links histone methylation to leukemogenesis. Cell. 2005;121:167-178.

19. Lahortiga I, De Keersmaecker K, Van Vlierberghe P, et al. Duplication of the MYB oncogene in T cell acute lymphoblastic leukemia. Nature genetics. 2007;39:593-595.

20. Clappier E, Cuccuini W, Kalota A, et al. The C-MYB locus is involved in chromosomal translocation and genomic duplications in human T-cell acute leukemia (T-ALL) - the translocation defining a new T-ALL subtype in very young children. Blood. 2007.

21. Kurotaki N, Imaizumi K, Harada N, et al. Haploinsufficiency of NSD1 causes Sotos syndrome. Nature genetics. 2002;30:365-366.

22. Al-Mulla N, Belgaumi AF, Teebi A. Cancer in Sotos syndrome: report of a patient with acute myelocytic leukemia and review of the literature. Journal of pediatric hematology/oncology. 2004;26:204-208.

23. Martinez-Glez V, Lapunzina P. Sotos syndrome is associated with leukemia/lymphoma. American journal of medical genetics. 2007;143:1244-1245.

24. Ziino O, Rondelli R, Micalizzi C, Luciani M, Conter V, Arico M. Acute lymphoblastic leukemia in children with associated genetic conditions other than Down's syndrome. The AIEOP experience. Haematologica. 2006;91:139-140.

25. Bagchi A, Papazoglu C, Wu Y, et al. CHD5 is a tumor suppressor at human 1p36. Cell. 2007;128:459-475.

26. Kim MY, Yim SH, Kwon MS, et al. Recurrent genomic alterations with impact on survival in colorectal cancer identified by genome-wide array comparative genomic hybridization. Gastroenterology. 2006;131:1913-1924.

27. Mori N, Morosetti R, Mizoguchi H, Koeffler HP. Progression of myelodysplastic syndrome: allelic loss on chromosomal arm 1p. British journal of haematology. 2003;122:226-230.

28. Mori N, Morosetti R, Spira S, et al. Chromosome band 1p36 contains a putative tumor suppressor gene important in the evolution of chronic myelocytic leukemia. Blood. 1998;92:3405-3409.

29. Cimmino A, Calin GA, Fabbri M, et al. miR-15 and miR-16 induce apoptosis by targeting BCL2. Proc Natl Acad Sci U S A. 2005;102:13944-13949.

30. Mullighan CG, Goorha S, Radtke I, et al. Genome-wide analysis of genetic alterations in acute lymphoblastic leukaemia. Nature. 2007;446:758-764.

31. Filippova GN, Fagerlie S, Klenova EM, et al. An exceptionally conserved transcriptional repressor, CTCF, employs different combinations of zinc fingers to bind diverged promoter sequences of avian and mammalian c-myc oncogenes. Molecular and cellular biology. 1996;16:2802-2813.

32. Theos A, Korf BR. Pathophysiology of neurofibromatosis type 1. Annals of internal medicine. 2006;144:842-849.

33. Kai S, Sumita H, Fujioka K, et al. Loss of heterozygosity of NF1 gene in juvenile chronic myelogenous leukemia with neurofibromatosis type 1. International journal of hematology. 1998;68:53-60.

34. Side L, Taylor B, Cayouette M, et al. Homozygous inactivation of the NF1 gene in bone marrow cells from children with neurofibromatosis type 1 and malignant myeloid disorders. The New England journal of medicine. 1997;336:1713-1720.

35. Side LE, Emanuel PD, Taylor B, et al. Mutations of the NF1 gene in children with juvenile myelomonocytic leukemia without clinical evidence of neurofibromatosis, type 1. Blood. 1998;92:267-272.

36. Barkan B, Starinsky S, Friedman E, Stein R, Kloog Y. The Ras inhibitor farnesylthiosalicylic acid as a potential therapy for neurofibromatosis type 1. Clinical cancer research. 2006;12:5533-5542.

37. van Vlierberghe P, Meijerink JP, Lee C, et al. A new recurrent 9q34 duplication in pediatric T-cell acute lymphoblastic leukemia. Leukemia. 2006;20:1245-1253.

38. Weng AP, Ferrando AA, Lee W, et al. Activating mutations of NOTCH1 in human T cell acute lymphoblastic leukemia. Science (New York, NY. 2004;306:269-271.

39. Paietta E, Ferrando AA, Neuberg D, et al. Activating FLT3 mutations in CD117/KIT(+) T-cell acute lymphoblastic leukemias. Blood. 2004;104:558-560.

40. Van Vlierberghe P, Meijerink JP, Stam RW, et al. Activating FLT3 mutations in CD4+/CD8- pediatric T-cell acute lymphoblastic leukemias. Blood. 2005;106:4414-4415.

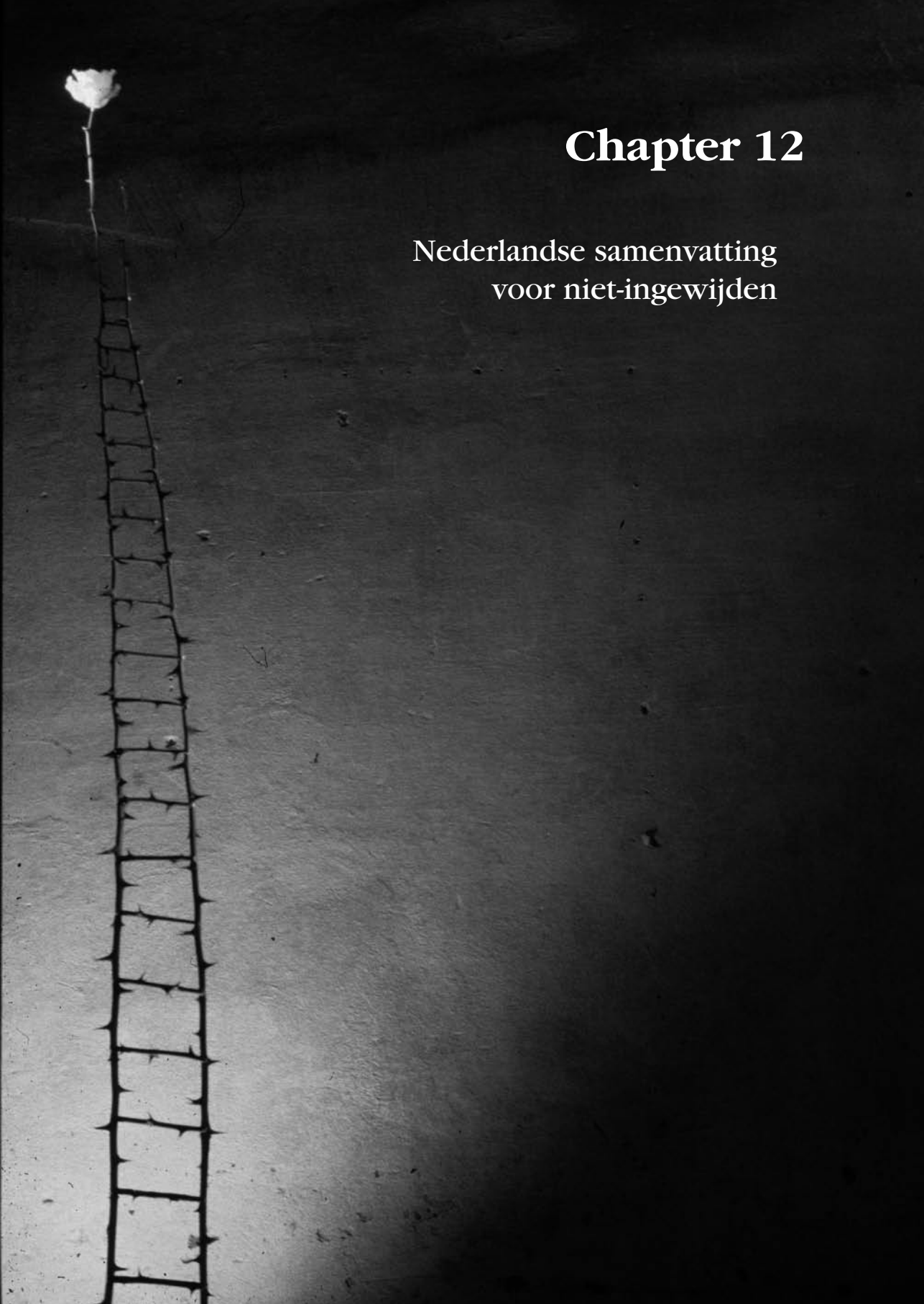

Chapter 12

Nederlandse samenvatting voor niet-ingewijden

DE GENETISCHE CODE VAN DE MENS

Elke cel van het menselijk lichaam bevat een genetische code die de specifieke functie van elke lichaamscel bepaald. Deze genetische informatie is opgeslagen in het desoxyribonucleïnezuur van elke cel, kortweg het DNA. Het DNA is onderverdeeld in genen die ieder zorgen voor de aanmaak van één specifiek eiwit. Complexe regulatie mechanismen zorgen er vervolgens voor dat vanuit dit DNA op het juiste ogenblik specifieke eiwitten worden aangemaakt die in een bepaalde fase van het cellulaire leven noodzakelijk zijn. Chemische eigenschappen zorgen ervoor dat het DNA als twee strengen in een dubbele helix structuur samengehouden wordt. Het DNA en de menselijke genen zijn op hun beurt opgeslagen in 23 chromosoomparen. Hiervan zijn er 22 genummerd, min of meer in volgorde van grootte, en bepaald het laatste chromosoompaar het geslacht (twee X-chromosomen bij de vrouw; een X- en een Y-chromosoom bij de man).

BLOED

Het bloed kan beschouwd worden als een vloeibaar orgaan in het menselijk lichaam en is opgebouwd uit verschillende soorten bloedcellen (rode en witte bloedcellen, bloedplaatjes) die door een geelachtige vloeistof (het bloedplasma) doorheen het lichaam getransporteerd worden. Het bloed dankt zijn rode kleur aan de aanwezigheid van hemoglobine in de rode bloedcellen. De verschillende types bloedcellen hebben maar een beperkte levensduur en dienen daarom voortdurend opnieuw aangemaakt te worden. Vorming van nieuwe bloedcellen (hematopoëse) gebeurt in een sponsachtige, rode substantie (beenmerg) die zich bevindt in het binnenste van onze beenderen. In het beenmerg bevinden zich hematopoëtische stamcellen die de mogelijkheid in zich dragen om uit te groeien tot elk van de verschillende bloedcellen. Via complexe uitrijpingsprocessen zorgen deze hematopoëtische stamcellen voor de aanmaak van functionele rode bloedcellen (zuurstof transport), witte bloedcellen (afweer tegen ziekte) en bloedplaatjes (bloedstolling) en handhaven zodoende het gezonde evenwicht tussen de verschillende bloedcelsoorten. De witte bloedcellen worden nog verder onderverdeeld in lymfatische cellen (B- en T-lymfocyten) en niet-lymfatische (of myeloïde) cellen (monocyten en granulocyten).

LEUKEMIE

Leukemie of bloedkanker wordt gekenmerkt door het ongecontroleerd vermenigvuldigen van onrijpe witte bloedcellen. Deze niet-functionele witte bloedcellen (leukemiecellen) stapelen zich op in het beenmerg en verdringen de functionele bloedcellen uit het bloedbeeld. Wanneer de leukemiecellen vervolgens ook de aanmaak van nieuwe gezonde bloedcellen verhinderen, ontstaat er bloedarmoede (tekort aan gezonde rode bloedcellen), verhoogde kans op infecties (tekort aan gezonde witte bloedcellen) en bloedingen (tekort aan gezonde bloedplaatjes). Wanneer de leukemiecellen ten slotte infiltreren in de bloedsomloop kunnen ook andere organen, zoals milt, lever en nieren, aangetast worden. Zonder behandeling is leukemie een dodelijke ziekte.

Leukemieën worden op basis van het type witte bloedcel, dat in het beenmerg is beginnen woekeren, onderverdeeld in lymfatische en myeloïde leukemieën. Binnen de lymfatische leukemieën wordt nog een onderscheid gemaakt tussen B- en T-cel leukemie, en ook myeloïde leukemieën worden nog verder onderverdeeld afhankelijk van de myeloïde cel van oorsprong. Tot slot worden zowel de lymfatische als de myeloïde leukemieën nog verder onderverdeeld in acute en chronische leukemieën. Acute leukemieën worden gekenmerkt door een snel en agressief ziekteverloop, terwijl chronische leukemieën een tragere ziekteontwikkeling vertonen.

LEUKEMIE BIJ KINDEREN

Leukemie omvat ongeveer 30% van alle kanker diagnoses bij kinderen en is daarmee de meest voorkomende vorm van kanker en de belangrijkste doodsoorzaak bij kinderen. De meest voorkomende variant van leukemie bij kinderen is acute lymfatische leukemie (ALL), die wordt gediagnosticeerd in 80-85% van alle kinderen met leukemie. De prognose voor kinderen met ALL is gedurende de afgelopen decennia sterk verbeterd en de huidige behandelingsprotocollen, die vooral zijn opgebouwd uit combinaties van verschillende chemotherapeutica, zorgen voor een overlevingskans van ongeveer 80%. Hoewel de genezingskans voor kinderen met ALL met de huidige behandelingsprotocollen dus relatief gunstig is, treden er nog vaak complicaties op vanwege de neveneffecten van de chemotherapie. Ook wordt het langzaam duidelijk dat een chemotherapie behandeling op kinderleeftijd op lange termijn belangrijke implicaties kan hebben. Naast de zoektocht naar nieuwe behandelingsmogelijkheden voor patiënten die ziekteherval vertonen, moet het wetenschappelijk onderzoek zich dan ook toespitsen op de ontwikkeling van alternatieven voor chemotherapie in de behandeling van ALL. In Nederland wordt jaarlijks

bij ongeveer 150 kinderen leukemie geconstateerd, van wie de meeste kinderen tussen drie en vijf jaar oud zijn.

T-CEL ACUTE LYMFATISCHE LEUKEMIE (T-ALL)

T-ALL bij kinderen komt voor in ongeveer 15% van ALL patiënten en ontstaat door ongeremde groei van een uitrijpende T-cel. Deze T-cellen ontwikkelen zich echter, in tegenstelling tot andere bloedcellen, niet in het beenmerg maar in de thymus (zwezerik). In dit orgaan, dat zich tussen het borstbeen en de luchtpijp bevindt, worden onrijpe T-cellen als het ware opgeleid om lichaamsvreemde stoffen (zoals virussen of bacteriën) te herkennen. Tijdens dit proces wordt een groot deel van de ontwikkelende T-cellen vernietigd, bijvoorbeeld vanwege reactiviteit tegen lichaamseigen stoffen. Een minderheid van cellen slaagt er echter toch in om zich te ontwikkelen tot een functionele T-cel die via een unieke T-cel receptor op zijn celoppervlak kan interageren met één specifiek lichaamsvreemd antigeen. Deze opgeleide T-cellen zullen vervolgens de thymus verlaten en een functie vervullen als afweercel in het lichaam.

Om te zorgen voor de enorme diversiteit aan T-cel receptoren die nodig is om de grote variatie aan lichaamsvreemde stoffen te kunnen herkennen, treden er tijdens de T-cel ontwikkeling herschikkingen op van de T-cel receptor genen. Deze genherschikkingen, die ervoor zorgen dat miljarden verschillende T-cellen kunnen gevormd worden, zijn echter erg gevoelig voor recombinatie fouten, waardoor T-cel receptor gemedieerde translocaties kunnen ontstaan. Het is dan ook niet verwonderlijk dat T-cel receptor genen vaak betrokken zijn bij genetische afwijkingen die geïdentificeerd worden in de leukemische cellen van T-ALL patiënten. Deze translocaties zorgen ervoor dat bepaalde T-cel specifieke proto-oncogenen onder de regulatie komen van actieve DNA elementen van de T-cel receptor genen. T-cel receptor gemedieerde translocaties komen voor in ongeveer 35% van T-ALL patiënten.

Intensief wetenschappelijk onderzoek heeft gedurende de laatste jaren ook nog geleid tot de identificatie van een hele reeks nieuwe, niet-T-cel receptor gemedieerde, genetische afwijkingen in T-ALL, waaronder chromosomale translocaties, inversies, deleties, duplicaties, amplificaties en mutaties. Het *NOTCH1* gen vormt het belangrijkste doelwit voor mutaties in T-ALL, dewelke voorkomen in meer dan 50% van de T-ALL patiënten.

TYPE A EN TYPE B GENETISCHE AFWIJKINGEN IN T-ALL

In T-ALL zorgen verschillende genetische afwijkingen er samen voor dat een normale T-cel zal transformeren tot een acute leukemie door ontspoorde celgroei en ongecontroleerde celdeling. In dit uit meerdere stappen bestaande proces werken genetische afwijkingen samen die ingrijpen op verschillende cellulaire processen zoals de celcyclus, T-cel differentiatie en celoverleving. Een ontwikkelde T-cel zal bijvoorbeeld een genetisch defect oplopen waardoor de onrijpe T-cel niet verder kan differentiëren. Dit arrest in de T-cel ontwikkeling maakt die specifieke cel vatbaar voor het oplopen van additionele gendefecten die uiteindelijk zullen zorgen voor de ontwikkeling van de leukemie. In **Hoofdstuk 2** geven we een overzicht van de verschillende genetische afwijkingen en hun potentiële doelwit genen die op dit moment geassocieerd worden met de ontwikkeling van T-ALL. Verder maken we een onderscheid tussen twee klassen van genetische abnormaliteiten in T-ALL. Type A afwijkingen zijn mutueel exclusief en bepalen het onderscheid tussen verschillende genetische T-ALL subgroepen. Andere genetische afwijkingen komen voor in alle genetische T-ALL subgroepen en worden type B afwijkingen genoemd. Op dit moment onderscheiden we 5 verschillende genetische subgroepen in T-ALL op basis van de genherschikkingen die in deze patiënten teruggevonden worden: *TAL/LMO, TLX1, TLX3, HOXA* en *MYB*.

ALTERNATIEVE *LMO2* ACTIVATIE IN T-ALL

LMO2 is een bekend oncogen in T-ALL omdat bepaalde T-ALL patiënten een T-cel receptor gemedieerde translocatie vertonen die zorgt voor constitutieve activatie van het *LMO2* gen. Verhoogde expressie van het *LMO2* gen, gelegen op chromosoom 11, is echter ook beschreven in afwezigheid van bovengenoemde translocatie, zodat er in T-ALL waarschijnlijk alternatieve *LMO2* activatie mechanismen bestaan. In **Hoofdstuk 3** beschrijven we een nieuwe deletie op chromosoom 11 die voorkomt in ongeveer 4% van T-ALL patiënten. Het genetisch materiaal van chromosoom 11 dat in deze patiënten verloren is gegaan ligt vlakbij het *LMO2* gen en zorgt er normaal voor dat de expressie van het *LMO2* gen onderdrukt wordt. Door het verlies van dit kleine stukje chromosoom 11 wordt in deze T-ALL patiënten de *LMO2* expressie echter continu geactiveerd. Deze cryptische chromosoom 11 deleties vormen dan ook een nieuw *LMO2* activatie mechanisme in de ontwikkeling van T-ALL. In **Hoofdstuk 4** hebben we met een hogere resolutie gekeken of het mogelijk is dat er in T-ALL nog kleinere deleties optreden in de buurt van het *LMO2* gen op chromosoom 11. Door deze analyses hebben we nog 1 additionele T-ALL patiënt geïdentificeerd bij wie de

chromosoom 11 deletie ongeveer 6 keer kleiner was dan de deleties die in hoofdstuk 3 werden beschreven. Naast *LMO2* translocaties vormen de *LMO2* deleties, dewelke in grootte kunnen verschillen tussen patiënten, dus een nieuw mechanisme voor *LMO2* genactivatie in T-ALL. Hoewel het *LMO2* gen zowel door een translocatie als door een deletie geactiveerd kan worden, hoeft een verhoogde *LMO2* expressie niet per definitie een oncogene rol te hebben in de ontwikkeling van T-ALL. *LMO2* komt immers tot hoge expressie gedurende de vroegste ontwikkelingsstadia van de normale T-cel ontwikkeling, waarna de expressie afneemt bij het verder uitrijpen van de T cellen in de thymus. Wanneer een T-cel leukemie zich ontwikkelt vanuit een heel onrijpe T-cel, reflecteert een verhoogde *LMO2* expressie waarschijnlijk eerder de cel van oorsprong dan dat er daadwerkelijk een genetisch defect ten grondslag ligt aan de *LMO2* gen activatie.

Gen expressieprofilering is een relatief recente technologie waarbij in één analyse de expressie van een groot aantal genen in kaart kan worden gebracht. Onze gen expressieprofileringstudie in T-ALL (**Hoofdstuk 5**) toont aan dat T-ALL patiënten met een *LMO2* translocatie of een *LMO2* deletie een zeer gelijkend patroon van gen expressie vertonen. *LMO2* herschikte T-ALL patiënten blijken dus gemeenschappelijke oncogene signaalpaden te activeren. Bovendien vormen deze *LMO2* herschikte T-ALL patiënten een onderdeel van een nog grotere reeks patiënten met een gelijkaardig expressieprofiel die afwijkingen vertoonden aan het *TAL1*, *TAL2* en *LMO1* gen. Dit zou mogelijk verklaard kunnen worden door het feit dat deze genen normaal participeren in eenzelfde transcriptiecomplex en dus gelijklopende functies vervullen. Blijkbaar is er dus een belangrijke overlap tussen de leukemie ontwikkeling in *TAL*- en *LMO*-gemedieerde T-ALL patiënten. De patiënten binnen dit *TAL/LMO* gen expressiecluster vertegenwoordigen ongeveer de helft van alle kinderen met T-ALL. De identificatie van een gemeenschappelijk doelwit gen in dit *TAL/LMO* gen expressieprofiel zou daarom de weg kunnen effenen naar een doelgerichte therapie die geïmplementeerd zou kunnen worden in een groot gedeelte (~50%) van kinderen met T-ALL.

HET *SET-NUP214* FUSIEGEN IN T-ALL

In de genetica van leukemieën komen een hele reeks verschillende fusiegenen voor. Dit zijn "nieuwe" genen die specifiek in de leukemische cel van een patiënt voorkomen en gecreëerd worden door een bepaalde genetische afwijking die ervoor zorgt dat 2 verschillende genen aan elkaar gekoppeld worden en een nieuw samengesteld gen vormen. Zulk fusiegen zorgt dan voor de aanmaak van een fusie eiwit dat bijdraagt tot de ontwikkeling van de leukemie.

Een andere genetische subgroep in T-ALL bestaat uit patiënten die gekarakteriseerd worden door activatie van de *HOXA* genen. Deze activatie kan gebeuren via een chromosoom 7 inversie of translocatie waarin de *HOXA* genen direct betrokken zijn, alsook indirect via de fusiegenen *MLL-ENL* of *CALM-AF10*. In een voorgaande gen expressie studie werd echter aangetoond dat bepaalde T-ALL patiënten ook een geactiveerd *HOXA* gen expressieprofiel kunnen vertonen in afwezigheid van bovengenoemde genetische herschikkingen.

In **Hoofdstuk 5** beschrijven we 5 T-ALL patiënten bij wie het op genetisch niveau onduidelijk is waarom ze een geactiveerde *HOXA* genexpressie vertonen. Verdere analyses tonen aan dat in de leukemische cellen van drie van deze patiënten eenzelfde stuk genetisch materiaal op chromosoom 9 verloren is gegaan. Op de respectievelijke uiteinden van het verdwenen stuk DNA liggen de genen *SET* en *NUP214*. Verdere moleculaire analyses tonen aan dat het *SET* en *NUP214* gen door deze chromosoom 9 deletie aan elkaar gezet worden waardoor een nieuw *SET-NUP214* fusiegen ontstaat wat mogelijk bijdraagt tot de ontwikkeling van de T-cel leukemie. Wanneer het SET-NUP214 fusie eiwit geïnactiveerd wordt, neemt de expressie van de *HOXA* genen af, wat de link tussen de aanwezigheid van SET-NUP214 en *HOXA* genactivatie bevestigt. Verder bleek dat bij SET-NUP214 inactivatie de leukemiecellen langzaam opnieuw gingen uitrijpen. Het is dus aannemelijk dat SET-NUP214 bijdraagt tot de pathogenese van T-ALL door ervoor te zorgen dat een ontwikkelende T-cel wordt gearresteerd in een bepaald stadium van zijn ontwikkeling. Ook in onze studie bleven er nog twee patiënten over voor wie het *HOXA* expressie signatuur niet verklaard kon worden. Er blijven dus nog alternatieve *HOXA* activatie mechanismen in T-ALL die nog dienen geïdentificeerd te worden.

MYB, EEN NIEUW ONCOGEN IN T-ALL

Hoewel MYB een belangrijke rol speelt in het T-cel ontwikkelingsproces, was er tot dusver slechts in muismodellen een verband aangetoond tussen *MYB* overexpressie en leukemie ontwikkeling. Vooralsnog waren er geen voorbeelden van *MYB* genherschikkingen in de leukemische cellen van T-ALL patiënten. In **Hoofdstuk 6** (samenwerking met Prof. J. Cools en Dr. I. Lahortiga, Leuven, België) tonen we echter aan dat zowel primaire T-ALL patiënten als T-ALL cellijnen vaak extra chromosoom 6 materiaal vertonen corresponderend met de genetische regio waar het *MYB* gen gelegen is. Deze *MYB* duplicaties zijn geassocieerd met een verhoogde *MYB* expressie. Ongeveer gelijktijdig werd in een andere studie aangetoond dat bepaalde T-ALL patiënten ook T-cel receptor gemedieerde translocaties vertonen waarbij het *MYB* gen verhoogd tot expressie wordt gebracht. Wanneer in een T-ALL cellijn model het

MYB gen wordt uitgeschakeld, gaan de leukemische cellen opnieuw differentiëren. Deze resultaten wijzen erop dat *MYB* duplicaties een nieuwe oncogene hit vormen in T-ALL en dat verhoogde *MYB* expressie bijdraagt tot de ontwikkeling van T-ALL door het initiëren van een T-cel differentiatie arrest.

GENETISCHE DEFECTEN IN *TLX3* POSITIEVE T-ALL

Een volgende genetische T-ALL subgroep, die bestaat uit ongeveer 20% van kinderen met T-ALL, wordt gekarakteriseerd door de expressie van het *TLX3* gen. Gedurende de normale T-cel ontwikkeling komt *TLX3* niet tot expressie, maar in de leukemische cellen van deze patiënten zorgt een niet-T-cel receptor gemedieerde translocatie voor de activatie van dit oncogen. In **Hoofdstuk 7** kijken we specifiek in deze T-ALL subgroep naar nieuwe deleties die mogelijk kunnen samenwerken met *TLX3* overexpressie in de ontwikkeling van T-cel leukemie. Op de chromosomen 1, 5, 13, 16 en 19 blijken regio's te liggen die in meerdere *TLX3* positieve T-ALL patiënten verloren zijn gegaan. Daarnaast worden nog een hele reeks andere deleties geïdentificeerd die slechts in de leukemische cellen van één enkele patiënt teruggevonden werden. Omdat voor de recurrente afwijkingen de hoeveelheid DNA materiaal die per patiënt verloren is gegaan sterk verschilt, is het aannemelijk dat de minimaal gedeleteerde gebieden van deze chromosomale regio's één of meerdere genen bevatten die als tumor supressor kunnen fungeren. Tumor supressor genen zorgen er in niet maligne cellen voor dat de tumorontwikkeling onderdrukt wordt. Wanneer de functie van deze genen echter verloren gaat, door mutatie en/of deletie, kan dit mogelijk bijdragen tot de ontwikkeling van een welbepaald kankertype. Sommige deleties die in deze studie opgepikt werden, zijn vroeger reeds geassocieerd met bepaalde kankertypes. Het *CHD5* gen, dat gelegen is op chromosoom 1 in één van de recurrent gedeleteerde gebieden, is bijvoorbeeld voorheen reeds beschreven als tumor supressor gen in neuroblastoom en darm kanker. Analoog worden in dit hoofdstuk het *CTCF* gen (chromosom 16), het *FBXW7* gen (chromosoom 4) en het *WT1* gen (chromosoom 11) naar voren geschoven als potentiële tumor supressor genen in T-ALL.

NF1 INACTIVATIE IN T-ALL

Neurofibromatose (NF1) is een erfelijke aandoening die vooral de huid en het zenuwstelsel aantast. Deze ziekte wordt veroorzaakt door mutaties in het *NF1* gen, gelegen op chromosoom 17. Bij NF1 patiënten is in alle cellen van het lichaam

1 kopie van het *NF1* gen geïnactiveerd door mutatie. Afhankelijk van het celtype waarin ook de andere kopie van het *NF1* gen geïnactiveerd wordt, zullen bepaalde NF1 geassocieerde symptomen optreden. Café-au-lait vlekken op de huid zijn bijvoorbeeld een kenmerkend NF1 symptoom. In de huidcellen die deze specifieke vlekken veroorzaken zijn beide *NF1* genen aangetast, terwijl de omliggende huidcellen slechts inactivatie van één NF1 gen vertonen. NF1 patiënten vertonen eveneens een verhoogde kans op het ontwikkelen van bepaalde types leukemie. Hierbij vertonen de leukemiecellen, analoog aan de huidcellen, verlies van het 2de *NF1* gen door mutatie of deletie. Omdat het NF1 eiwit een negatieve regulator is van RAS, een bekend leukemogeen eiwit, zorgt het verlies van beide *NF1* kopieën voor leukemie geassocieerde RAS activatie. In **Hoofdstuk 8** tonen we aan dat in de leukemiecellen van bepaalde T-ALL patiënten, die geen specifieke klinische NF1 symptomen vertonen, een verlies van de *NF1* gen regio op chromosoom 17 kan optreden. Verdere genetische analyse toont inderdaad aan dat in de niet-leukemische bloedcellen van deze patiënten geen *NF1* gen inactivatie voorkomt. Specifieke mutatie analyse van deze patiënten toont echter wel aan dat het overgebleven *NF1* gen in de leukemische cellen daadwerkelijk geïnactiveerd is door een mutatie. Specifiek in de leukemische cellen is het *NF1* gen dus compleet uitgeschakeld, wat, analoog als bij NF1 patiënten die secundair een leukemie ontwikkelen, uiteindelijk zal leiden tot een leukemie geassocieerde RAS activatie. Simultane analyses in andere types leukemie tonen echter aan dat dit fenomeen niet enkel voorkomt in T-ALL patiënten maar eerder een algemeen leukemogeen mechanisme is in zowel lymfoïde als myeloïde leukemieën. Een aanvullende behandeling met RAS inhibitoren kan in deze leukemie patiënten mogelijk leiden tot een verbeterde therapie.

PROGRESSIE MERKERS IN T-ALL

In T-ALL worden bepaalde genetische defecten slechts teruggevonden in een beperkt percentage van de leukemische cellen. Waarschijnlijk treden deze genetische afwijkingen dan ook op als een progressie merker tijdens het ziekteverloop van de leukemie en hebben ze slechts een beperkte rol in de initiële ontwikkeling van de T-cel leukemie. In **Hoofdstuk 9** identificeren we bijvoorbeeld een nieuwe duplicatie van een klein deel van chromosoom 9 die voorkomt in 33% van de kinderen met T-ALL. Deze duplicatie komt echter slechts voor in 17-39% van de leukemische cellen bij diagnose. Het *NOTCH1* gen is gelegen in de minimaal geamplificeerde regio van dit genetisch defect, zodat deze duplicatie zou kunnen leiden tot subtiele verschillen in *NOTCH1* expressie en zodoende bijdragen aan de algemene NOTCH1 activatie in T-ALL.

Mutaties in het *FLT3* gen zijn een ander voorbeeld van een progressie merker in T-ALL die voordien reeds in volwassenen met T-ALL geïdentificeerd werd. In **hoofdstuk 10** hebben we de frequentie van *FLT3* mutaties bij kinderen met T-ALL nagekeken. In een cohort van 72 kinderen met T-ALL werden slechts 2 patiënten gevonden waarin de leukemische cellen een *FLT3* mutatie vertoonden. Beide *FLT3* positieve patiënten werden gekarakteriseerd door een hoge *LMO2* expressie, maar dit was mogelijk te wijten aan de erg onrijpe T-cellen waaruit deze leukemieën ontstonden. De eerste *FLT3* gemuteerde patiënt vertoonde ziekte herval 13 maanden na initiële diagnose. Het leukemisch materiaal van deze patiënt ten tijde van herval vertoonde echter geen *FLT3* mutatie meer. De *FLT3* gemuteerde leukemische subpopulatie bleek dus efficiënt verwijderd te zijn door de chemotherapie behandeling. De tweede *FLT3* gemuteerde patiënt vertoonde 5 jaar na initiële diagnose nog steeds geen herval en kan als genezen beschouwd worden. Op therapeutisch gebied kunnen we daarom concluderen dat het gebruik van specifieke *FLT3* inhibitoren naar alle waarschijnlijkheid de overlevingskansen van kinderen met T-ALL niet zal verhogen.

CONCLUSIES EN PERSPECTIEVEN

T-cel ALL is een agressieve maligniteit die voorkomt in ongeveer 15% van kinderen met ALL en die in vergelijking met B-cel leukemieën een duidelijk slechtere prognose heeft. Ongeveer 30% van de kinderen met T-ALL vertonen herval van ziekte binnen 4 jaar na initiële diagnose, waarna de meeste overlijden. Ondanks de genetische complexiteit van deze ziekte, worden in de kliniek genetische afwijkingen op dit moment niet gebruikt voor therapie stratificatie. Verder werd gedurende de laatste jaren slechts een beperkte vooruitgang geboekt met op chemotherapie gebaseerde behandelingen. Dit alles toont aan dat voor de verdere verbetering van de behandeling van dit ziektebeeld, nieuwe geneesmiddelen ontwikkeld zullen moeten worden die specifiek ingrijpen op de signaalwegen die betrokken zijn in de pathogenese van de leukemie. Daarom zijn studies die zich bezig houden met de genetische en moleculaire karakterisering van T-ALL van cruciaal belang om T-ALL behandelingsprotocollen verder te optimaliseren en uiteindelijk over te schakelen naar behandeling stratificatie gebaseerd op genetische T-ALL subtypes.

Dit proefschrift bevestigt dat T-ALL niet kan gezien worden als één uniform ziektebeeld, maar dat het eerder een verzamelnaam is van genetisch erg diverse aandoeningen die ontstaan uit eenzelfde type voorlopercel. Verder biedt het compleet overzicht van nieuwe deleties en amplificaties in T-ALL (**Hoofdstuk 2**) nieuwe uitdagingen voor de identificatie van doelwit genen die mogelijk een rol kunnen

spelen in de ontwikkeling van T-ALL. Zelfs wanneer deze genetische defecten slechts in een beperkt aantal patiënten geïdentificeerd konden worden, leiden ze ons toch naar nieuwe en belangrijke genen die mogelijk een bredere rol vervullen in de T-cel leukemogenese, zoals aangetoond voor *FBXW7* en *PTEN* (**Hoofdstuk 2 en 7**). Daarom is het erg waarschijnlijk dat een groot aantal van de genetische afwijkingen die in dit proefschrift beschreven worden nog belangrijke genen verbergen die ons verder kunnen helpen in het ontrafelen van de biologie van T-ALL. Verdere analyses naar de mutatiestatus en de eiwit expressie van deze mogelijke doelwit genen zijn dan ook van cruciaal belang om de rol van deze genen in de ontwikkeling van T-ALL verder te karakteriseren. Hopelijk zullen deze toekomstige onderzoeksinitiatieven onze kennis van de moleculair genetische karakteristieken van deze agressieve ziekte verder verbeteren, wat uiteindelijk zal leiden tot een verbeterde prognose en/of nieuwe doelwit gerichte therapieën die gedeeltelijk het gebruik van agressieve chemotherapie zouden kunnen vervangen of verminderen.

About the author

LIST OF PUBLICATIONS

(Authored and co-authored by Pieter Van Vlierberghe)

Van Vlierberghe P, Meijerink JP, Stam RW, van der Smissen W, van Wering ER, Beverloo HB, Pieters R. Activating *FLT3* mutations in CD4+/CD8- pediatric T-cell acute lymphoblastic leukemias. ***Blood***. 2005 Dec 15;106(13):4414-5.

Van Vlierberghe P, Meijerink JP, Lee C, Ferrando AA, Look AT, van Wering ER, Beverloo HB, Aster JC, Pieters R.A new recurrent 9q34 duplication in pediatric T-cell acute lymphoblastic leukemia. ***Leukemia***. 2006 Jul;20(7):1245-53.

Van Vlierberghe P, van Grotel M, Beverloo HB, Lee C, Helgason T, Buijs-Gladdines J, Passier M, van Wering ER, Veerman AJ, Kamps WA, Meijerink JP, Pieters R. The cryptic chromosomal deletion del(11)(p12p13) as a new activation mechanism of *LMO2* in pediatric T-cell acute lymphoblastic leukemia. ***Blood***. 2006 Nov 15;108(10):3520-9.

Lahortiga I, De Keersmaecker K, **Van Vlierberghe P**, Graux C, Cauwelier B, Lambert F, Mentens N, Beverloo HB, Pieters R, Speleman F, Odero MD, Bauters M, Froyen G, Marynen P, Vandenberghe P, Wlodarska I, Meijerink JP, Cools J. Duplication of the *MYB* oncogene in T cell acute lymphoblastic leukemia. ***Nature Genetics***. 2007 May;39(5):593-5.

Van Vlierberghe P, Beverloo HB, Gladdines-Buijs J, van Wering ER, Horstmann M, Pieters R, Meijerink JPP. Mono- or biallelic *LMO2* expression in relation to genomic *LMO2* rearrangements and T-cell maturation arrest in pediatric T-ALL. ***Leukemia***. 2007 Dec 13; [Epub ahead of print].

Balgobind, B*, **Van Vlierberghe, P***, van den Ouweland AM, Beverloo HB, Terlouw-Kromosoeto JN, van Wering ER, Reinhardt D, Horstmann M, Kaspers GJ, Pieters R, Zwaan CM, Van den Heuvel-Eibrink MM, Meijerink JP. Leukemia associated *NF1* inactivation in pediatric T-ALL and AML patients lacking evidence for neurofibromatosis. ***Blood***. 2008 Jan 2; [Epub ahead of print].
*both authors contributed equally to this study and can be regarded as co-first authors.

Van Vlierberghe P, Beverloo HB, Gladdines-Buijs J, Zuurbier L, van Wering ER, Horstmann M, Pieters R and Meijerink JPP. Cooperative genetic defects in *TLX3* rearranged pediatric T-ALL. ***Leukemia***. 2008 Jan 10; [Epub ahead of print].

Van Vlierberghe P, van Grotel M, Tchinda J, Lee C, Beverloo HB, van der Spek PJ, Stubbs A, Cools J, Nagata K, Fornerod M, Gladdines-Buijs J, Horstmann M, van Wering ER, Soulier J, Pieters R and Meijerink. The recurrent SET-NUP214 fusion as a new *HOXA* activation mechanism in pediatric T-cell acute lymphoblastic leukemia. ***Blood***. 2008 Feb 22 [Epub ahead of print].

Van Vlierberghe P, Beverloo HB, Pieters R and Meijerink JPP. Molecular-genetic insights in pediatric TALL. Submitted for publication.

CURRICULUM VITAE

Pieter Van Vlierberghe werd geboren op 26 april 1980 te Antwerpen. Van 1992–1998 liep hij school op het Sint-Lievenscollege in Antwerpen, alwaar hij in 1998 afstudeerde in de richting Wiskunde-Wetenschappen. Aansluitend startte hij de opleiding Toegepaste Biologische Wetenschappen (Bio-Ingenieur) waarvan hij de kandidatuursjaren (1999-2000) voltooide aan het Rijksuniversitair Centrum Antwerpen (RUCA) om vervolgens de ingenieursjaren (2001-2003) af te leggen aan de Katholieke Universiteit Leuven (KU Leuven). In 2003 ontving hij zijn diploma Bio-Ingenieur in de Cel- en Genbiotechnologie.

Op 1 september 2003 werd hij werkzaam als Assistant In Opleiding (AIO) op de afdeling kinderoncologie/hematologie aan het Erasmus MC/Sophia Kinderziekenhuis te Rotterdam op het promotieonderzoek dat uiteindelijk resulteerde in dit proefschrift. Onder begeleiding van Dr. Jules Meijerink, Dr. Berna Beverloo en Prof. dr. Rob Pieters verrichtte hij als promovendus onderzoek naar nieuwe genetische afwijkingen in T-cel leukemie bij kinderen. In 2004 liep hij in het kader van dit promotieonderzoek gedurende enkele maanden stage aan het Brigham and Women's Hospital in Boston onder begeleiding van Prof. Charles Lee.

Sinds 1 september 2007 is hij als wetenschappelijk onderzoeker verbonden aan het Centrum voor Medische Genetica (CMG) van het Universitair Ziekenhuis Gent (UZ Gent), alwaar hij onder de supervisie van Prof. dr. Frank Speleman en Prof. dr. Yves Benoit, zijn onderzoek omtrend de genetische karakterisatie van acute leukemieën zal continueren.

Dankwoord

Juni 2003. Vanop een zolderkamer in de Maria-theresia straat te Leuven surf ik naar de website van de afdeling kinderoncologie/hematologie van het Erasmus Medisch Centrum in Rotterdam. Een zekere Dr. Jules Meijerink zoekt een promovendus voor een project rond T-cel leukemieën bij kinderen. Ik besluit te solliciteren, wordt uitgenodigd voor een gesprek en krijg de baan. Ondanks de "gaat gij dan elke dag naar Rotterdam rijden?" en de "zijn er nu echt geen jobs dichterbij te vinden?", besluit ik toch om nergens anders meer te sollicteren en per 1 september in Rotterdam aan de slag te gaan. De duistere kracht die me op dat moment deze ogenschijnlijk vreemde beslissing heeft doen nemen, ben ik eeuwig dankbaar, want het zijn 4 FANTASTISCHE jaren geworden. Iedereen die, in wel opzicht dan ook, heeft bijgedragen tot deze leuke tijd, zou ik graag van harte willen bedanken.

Wanneer je besluit om te gaan promoveren zijn er een aantal mensen die zich engageren om je hierbij te helpen, begeleiden en, zowel in goede als in slechte tijden, de nodige steun te bieden; je promotor en copromotoren. Ook al heb je niet te kiezen wie deze mensen zullen zijn, ze bepalen naar mijn mening wel of je promotie enige kans van slagen heeft. Ik heb geluk gehad! Het triumviraat dat ik kreeg toegewezen (Dr. J. Meijerink, Dr. B. Beverloo en Prof. R. Pieters) was van uitstekende kwaliteit!!!

Nochtanes was het even schrikken toen op mijn eerste werkdag (1 september 2003) een promovendus uit de T-ALL onderzoeksgroep van Dr. Meijerink doodleuk kwam vertellen dat ze per direct stopte met haar baan. "Oeioei", bedacht ik, "als dat maar goed komt met die Meijerink". En of het goed kwam…

Jules, als copromotor, maar vooral als mijn "vaste" begeleider doorheen dit promotietraject heb jij de grootste bijdrage geleverd aan het tot stand komen van dit boekje en aan de jonge onderzoeker die ik gedurende de afgelopen jaren geworden ben. Al snel wist je me te besmetten met jou passie en enthousiasme voor het project waar ik de komende 4 jaar aan moest gaan werken. Ook al hadden we een wekelijks overlegmoment op maandag, we liepen continue ideeën uit te wisselen waardoor we vaak tijdens de lunch een "zijn jullie nu weeral over het werk (T-ALL) bezig" om de oren kregen van één van de collega's. Net iets te vaak zag ik interessante pistes opduiken in het project waardoor ik enkele tientallen deelprojectjes wel "snel even zou gaan afwerken". Gelukkig had jij de gave om het groter geheel niet uit het oog te verliezen en enige focus te leggen in dit kluwen van onderzoeksideeën. Ook al hield je er een intensieve vorm van begeleiding op na, het zegt genoeg dat onze enige ruzie in de afgelopen jaren een lachwekkende discussie betrof over enkele uitroeptekens in een gecorrigereerde versie van een manuscript... Met de glimlach

denk ik eveneens terug aan onze ASH trilogie Atlanta, Orlando, Atlanta, waar we het fanatiek bezoeken van een wetenschappelijk congres combineerde met avondlijk/nachtelijk vertier. Liesbeth vindt het nog steeds onbegrijpelijk dat ik al die tijd een kamer deelde met mijn "baas", maar ik vond het geweldig!

Jules, ik hoop dat je stelling 11 van dit proefschrift aandachtig hebt gelezen en wil je fantastisch bedanken voor alles wat je voor me gedaan hebt de afgelopen jaren. Ook al blijven mijn pogingen om jou naar België te halen vooralsnog steeds maar weer mislukken, ik hoop van harte dat ons T-ALL onderzoeksenthousiasme ooit nog eens opnieuw verenigd zal worden! Bedankt voor alles!!!

Berna, als mede copromotor vervulde je vanop de 8ste verdieping een cruciale rol in het verloop van mijn promotie. Eerst en vooral zou mijn onderzoeksproject überhaupt nooit van start zijn gegaan als jij Jules niet had warm gemaakt voor de introductie van nieuwe cytogenetische technieken in het kinderleukemie onderzoek. Verder zette ik op jullie afdeling mijn eerste stappen in het chromosoom onderzoek (uitknippen en juistleggen) en kreeg ik gedurende de eerste jaren van mijn promotie met Ellen van Drunen een fantastische personal coach voor de FISH en SKY experimenten (Bedankt Ellen!!). Ook vormde de 8ste verdieping voor mij een ideaal plekje om even rustig langs te lopen als de zaken wat te hectisch werden op de 15de voor een research update of een gezellige babbel (of een product dat op was…). Ook zal ik ons gegniffel missen wanneer we op de maandagochtend vergadering weer eens moesten horen hoe een bepaalde gen expressie clustering ook al weer tot stand was gekomen (niet persoonlijk nemen, Jules). Berna, hartelijk bedankt voor al je werk en input gedurende de afgelopen 4 jaar, maar vooral voor je prettige manier waarop je met mensen weet om te gaan. Zoals jij lopen er geen 5 rond in heel die witte ErasmusMC toren! Bedankt!!!

Rob, wat jij de afgelopen 10 jaar hebt opgebouwd in Rotterdam op gebied van wetenschappelijk onderzoek is fenomenaal. Bedankt dat ik er gedurende de afgelopen jaren een onderdeeltje van heb mogen uitmaken. Tijdens onze overlegmomenten viel me telkens weer op dat jij het werk van enkele (soms vele) maanden in een handomdraai kon herleiden tot zijn essentie en er vrijwel meteen de pijnpunten uit kon destilleren. Die eigenschap heeft volgens mij de afronding van mijn proefschrift in belangrijke mate bespoedigd. Naar het einde van mijn promotietraject heb ik jou persoonlijk advies inzake mijn toekomstplannen, "Ga toch Spele Man!", erg weten te appreciëren!!

During my PhD project, I had the privilege of spending a couple of months at the Cytogenetic Research Laboratory of Prof. Charles Lee from the Brigham and Woman's Hospital, Harvard Medical School in Boston, Massachusetts, USA. Dear Charles, thanks for introducing me to the fascinating world of array-CGH analysis and for our nice collaboration on several chapters of this thesis. I would also like to thank both you and your former co-workers (Harvey Greisman, John Iafrate, Marc Listewnik, Abha Aggarwal, Amanda Smith and Joelle Tchinda) for the warm welcome you gave both Liesbeth and me during our research stay at your laboratory.

Verder zou ik graag alle andere "werkgroepleiders" van het lab kinderoncologie/ hematologie willen bedanken voor hun interesse in mijn onderzoek. Marry, Erna, Max, Michel, Monique en Ronald, alle succes in de verdere uitbouw van jullie respectievelijke onderzoeksgroepen.

Ronald, ook al sta je hierboven al vermeld tussen de "werkgroepleiders" (plots draagt hij een net jasje), toch wou ik je graag nog even persoonlijk bedanken voor de nochtans moeilijk te definiëren rol die je tijdens mijn promotie hebt vervuld. Ik hou het bij een soort van grote broer waarbij ik steeds terecht kon om de meest uiteenlopende dingen te bespreken (en voor de nodige hulp bij de laatste promotie beslommeringen). Bedankt om naast wetenschappelijk raadgever ook geregeld op te treden als mijn zangpartner tijdens het pipetteren. Onze "Bont en Blauw" versie van Bram Vermeulen mag er best wezen! Alle succes en geluk (al doet het gerucht de ronde dat jou geluk nu zo ongeveer wel opgebruikt moet zijn) in het MLL onderzoek en wie weet zien we elkaar binnekort terug aan de oostkust van de Verenigde Staten! Naar het schijnt heeft Mike Stern daar ergens zijn stamcafé....

Dan komen we bij het kloppend hart van ons laboratorium: de analisten! Karin, Jessica, Monique, Mathilde, Pauline, Susan, Wilco en Pieter, jullie moeten dringend opslag vragen (al zal Karin die dan waarschijnlijk niet meer krijgen)! Niet alleen zorgen jullie ervoor dat het leukemie patiëntenmateriaal nauwkeurig opgewerkt en geïnventariseerd wordt, jullie slagen er vervolgens ook nog in om het experimenteel werk van zo goed als alle promovendi te ondersteunen. Voor deze dubelle dagtaak zou heel ons laboratorium jullie elke dag van het jaar dankbaar moeten zijn! Jullie zijn fantastisch!!

Jessica, gedurende de afgelopen jaren heb ik het geluk gehad om (heel) veel met je samen te mogen werken. Ontelbare keren heb ik je gevraagd of je mij "even" met iets zou kunnen helpen en steeds vond je met de glimlach nog wel ergens een moment om me uit de nood te helpen. Je hebt dan ook een gigantische bijdrage

geleverd aan het voltooien van dit proefschrift (eigenlijk zou jij moeten promoveren). Zelfs tijdens de laatste maanden belde ik je nog (al te) vaak vanuit Gent voor een kleinigheid en zelfs dan wist je nog iets voor mij te regelen... Blijkbaar kan ik er maar moeilijk aan wennen dat met het voltooien van dit proefschrift ook onze leuke samenwerking teneinde zal zijn. Gelukkig hebben Liesbeth, Luna en ik, jou en Paul gedurende de afgelopen tijd ook leren kennen als goeie vrienden, zodat we in de toekomst nog geregeld zullen afspreken. Bedankt voor alles!!!

Ook de ondertussen sterk uitgebreide groep van AIO's zou ik graag willen bedanken voor de leuke en gezellige tijd op het lab. Irene, Linda, Martine, Brian, Judith, Iris, Diane, Dominique en Jill, heel veel succes in jullie onderzoek en het afronden van jullie proefschriften. Ook wil ik onze postdocs Esther, Marjon en Mirjam het allerbeste toewensen in hun verdere wetenschappelijke loopbaan.

Martine, omdat we in ons onderzoek hetzelfde patiënten cohort bestudeerden hebben we veel van onze data onderling kunnen uitwisselen, hetgeen volgens mij onze beide projecten een duidelijke meerwaarde heeft gegeven. Bedankt voor al je input in de genetische karakterisatie van onze patiënten, het data management en de uitwerking van de gen expressieanalyses! Succes met je eindsprint!!!

Brian (Brain, Train?), enkele jaren geleden werd ik aangeduid om jou in je eerste weken als AIO de array-CGH techniek aan te leren. Na het vakkundig verknoeien van één van mijn samples bij ServiceXS en enkele amusante treinritjes naar Leiden bleek dat we het erg goed met elkaar konden vinden. Niet alleen slopen we weg uit het Lab om tijdens het EK voetbal met een biertje bij Engels de middagwedstrijden te volgen, maar we schreven samen ook gewoon doodleuk een volledig hoofdstuk in dit proefschrift! Fantastisch bedankt voor deze leuke tijd en je doorzettingsvermogen bij onze NF1 publicatie!!!

Linda en Irene, de 2 nieuwe T-ALL meiden van Jules. Ik zie dat ook jullie reeds gebeten zijn door de T-ALL onderzoeksmicrobe en wens jullie respectievelijk (naast een fantastische promotie, maar dat komt wel in orde), veel plezier in Washington (Linda) en een prachtig kindje (Irene)!!

I also would like to thank both Pietro and Marcello Chiarenza for their great interest in my PhD thesis and for their valuable discussion concerning the cover of my thesis. The cover visualizes an art work of Marcello Chiarenza that provides a link to the content of this thesis by representing the revival of a patient after intensive chemotherapy treatment. Also in between the different chapters, another art work of

Marcello Chiarenza further illustrates the tough recovery from a terrible disease like leukemia. Marcello, thanks a lot for providing me with your work!!

Mijn ouders zou ik graag willen bedanken voor hun onvoorwaardelijke steun (en bezorgdheid hé mère) die ze me altijd hebben gegeven. Ook al leidde dit soms tot fiasco's (0 op 20 op "fysiologie van de huisdieren" na een wonderpilletje van de ouderlijke tandem), toch is het een fantastisch gevoel om te weten dat Ella, Luna, Liesbeth en ik altijd (en op allerlei gebied) op jullie kunnen terugvallen.

Liefste Frieda, tenslotte wil ik jou bedanken voor alles wat je ondertussen al 13 jaar voor mij betekent. Zonder jou begrip ("sorry, het zal een trein later worden"), hulp en steun was er van dit boekje helemaal niks terecht gekomen! Ik kijk enorm uit naar de geboorte van onze tweede dochter en hou zielsveel van jou en Luna.

Pieter

Color figures

CHAPTER 2

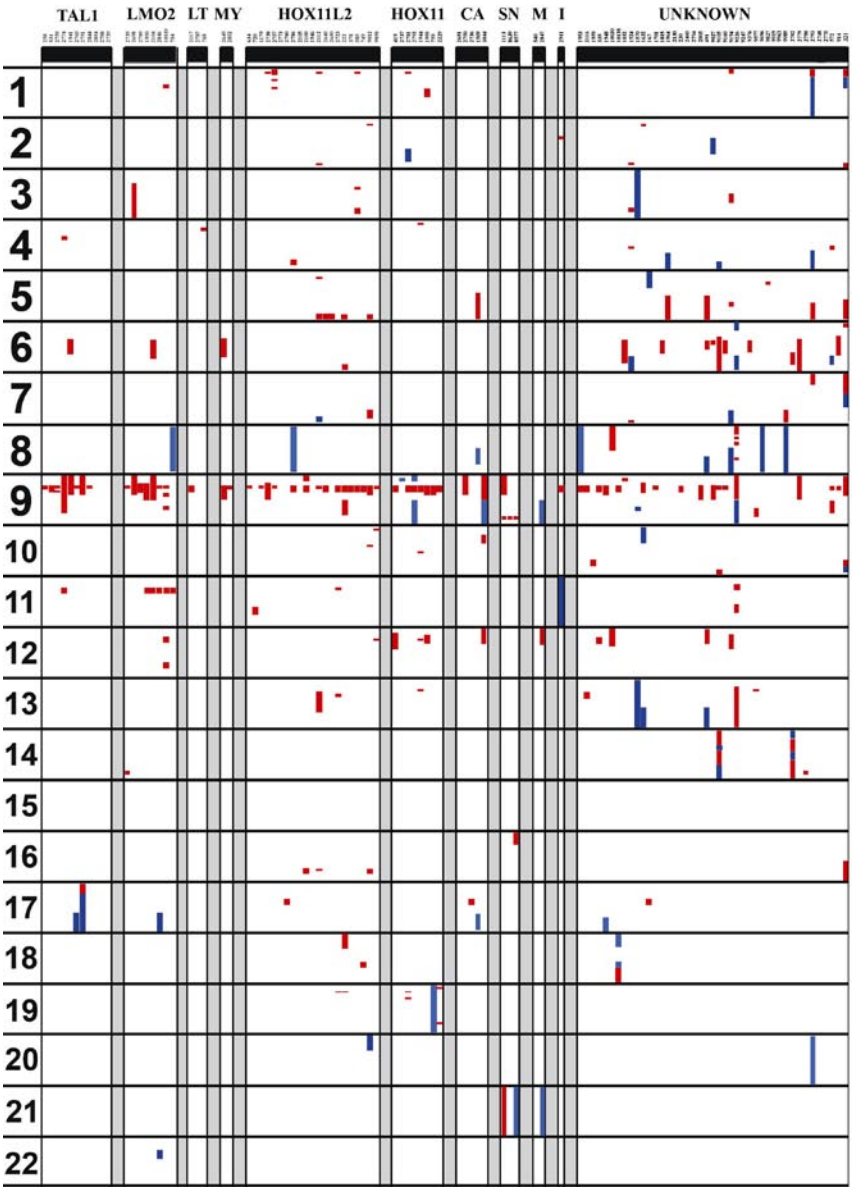

Figure 4. Genome-wide copy number analysis of 107 pediatric T-ALL patients in relation to T-ALL subgroups.

Overview of array-CGH data on 107 genetically well-characterized T-ALL patients including *TAL1* (n=11), *LMO2* (n=8), *LMO1/TAL2* (n=3), *MYC* (n=2), *TLX3* (n=21), *TLX1* (n=8), *CALM-AF10* (n=5), *SET-NUP214* (n=3), *MLL* (n=2), inv(7) (n=1) and unknown (=43) cases. Deletions are visualized in red, whereas amplifications are shown in blue.

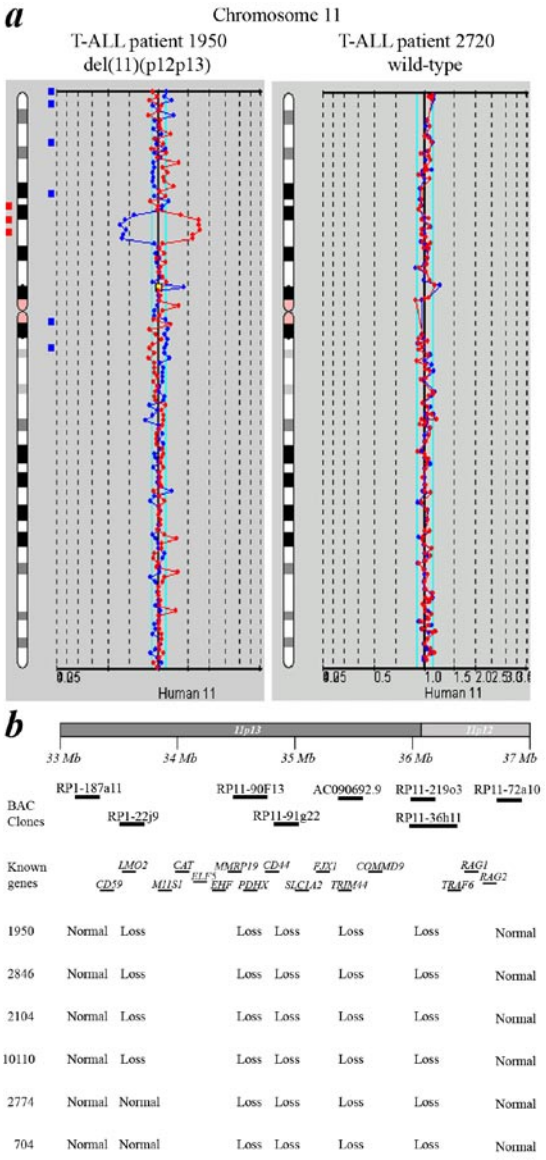

Figure 1. New recurrent deletion, del(11)(p12p13), in pediatric T-ALL.
(a) Chromosome 11 ideogram and corresponding BAC array-CGH plot of test DNA:control DNA ratios (blue tracing) versus the dye-swap experiment (red tracing) for T-ALL patients 1950 (left panel) and 2720 (right panel). **(b)** Overview of BAC array-CGH results for the 11p12-11p13 region for the 4 DCOG and the 2 COALL T-ALL patients with del(11)(p12p13). The BAC clones present on the DNA array and located on chromosome bands 11p12-11p13 are shown. Specific genes located in this region are indicated. Depicted genome positions are based on the UCSC Genome Browser at http://genome.ucsc.edu/.

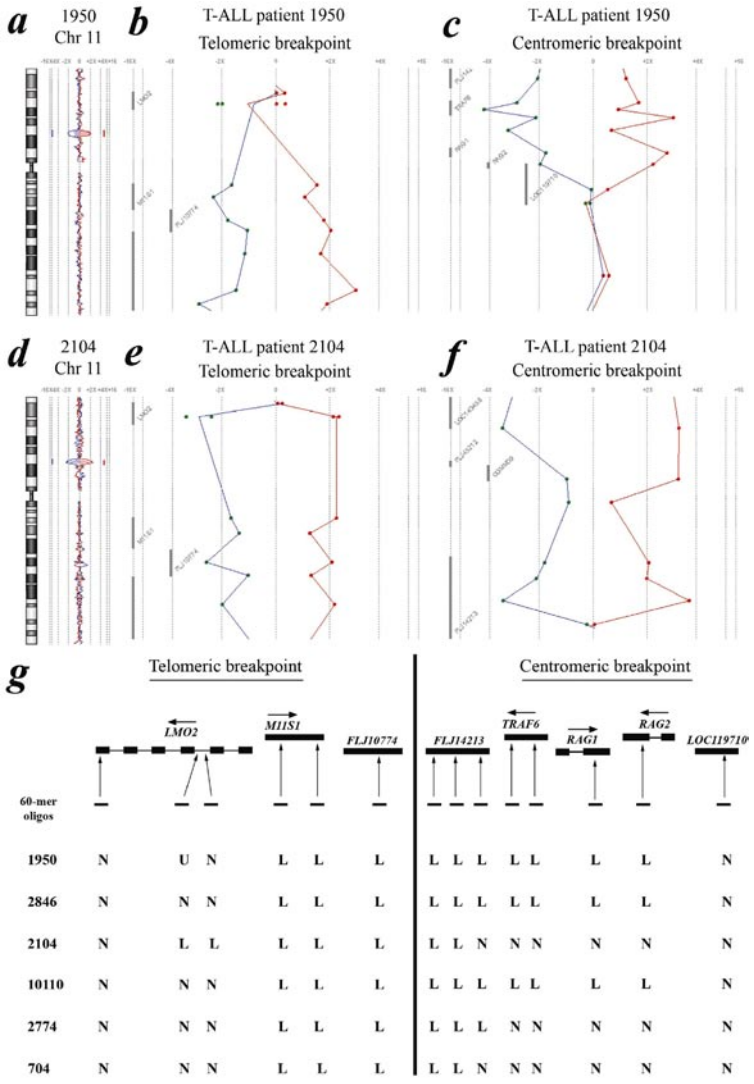

Figure 2. Molecular characterization of deletion, del(11)(p12p13), in 6 pediatric T-ALL patients.

Chromosome 11 ideogram and corresponding oligo array-CGH plot of test DNA:control DNA ratios (blue tracing) versus the dye-swap experiment (red tracing) for T-ALL patient 1950 **(a)** and patient 2104 **(d)**. Hybridization signals in the absence of amplifications or deletions scatter around the "zero"line, indicating equal hybridization for patient and reference DNA. Hybridization signals around the –2X or +2X lines represent loss of the corresponding region in the patient DNA. Detailed analysis of the telomeric breakpoints in patients 1950 **(b)** and 2104 **(e)** and the centromeric breakpoints in patients 1950 **(c)** and 2104 **(f)** of the deletion, del(11)(p12p13). **(g)** Overview of oligo array-CGH results in the potential breakpoint regions for 4 DCOG and the 2 COALL T-ALL patients with del(11)(p12p13). The 60-mer oligos present on the DNA array and located in the telomeric and centromeric breakpoint regions, as well as the specific genes located in this region with their transcription direction, are shown. Abbreviations: N; normal, L; loss, U; non-informative.

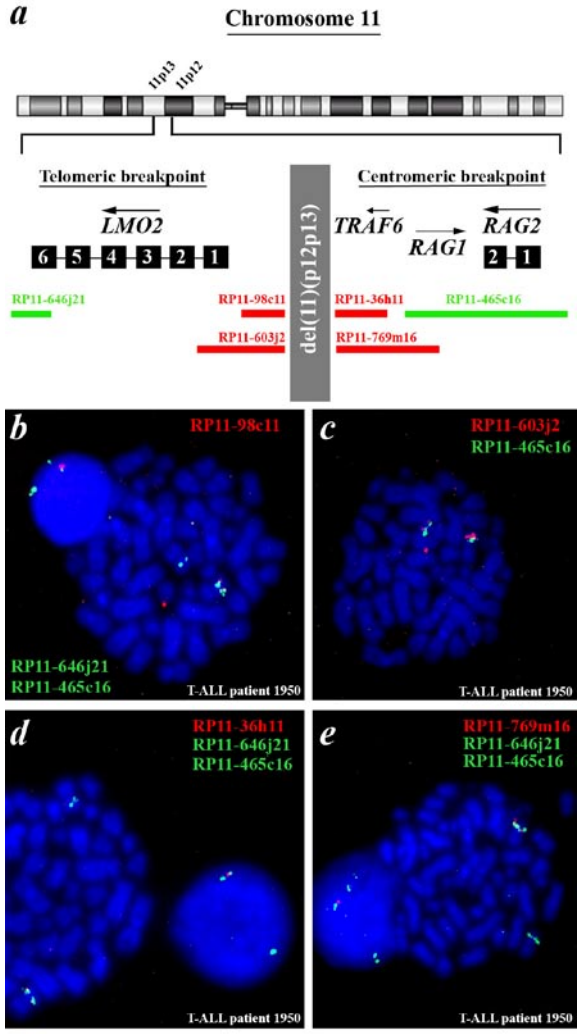

Figure 3. FISH analysis confirms the presence of del(11)(p12p13) in T-ALL patient 1950.
(a) Chromosome ideogram and overview of the genomic position of the BAC clones used for FISH analysis, located in the telomeric and centromeric breakpoint regions. **(b)** Dual-color FISH analysis on metaphase spreads of patient 1950 using RP11-465C16 (Green), RP11-646J21 (Green) and RP11-98C11 (Red). The wild-type allele of chromosome 11 shows 2 green and 1 red signal, whereas on the mutated allele the red signal is lost and both green signals fuse. The extrachromosomal red signal represents background. **(c)** Dual-color FISH analysis on metaphase spreads of the same patient using RP11-465C16 (Green) and RP11-603J2 (Red). The intensity of the red signal is lower compared to the wild-type allele of chromosome 11, suggesting that only part of RP11-603J2 is deleted. **(d)** Dual-color FISH analysis on metaphase spreads using RP11-465C16 (Green), RP11-646J21 (Green) and RP11-36H11 (Red). The wild-type allele of chromosome 11 shows 2 green and 1 red signal, whereas on the mutated allele the red signal is lost and both green signals fuse. **(e)** Dual-color FISH analysis on metaphase spreads using RP11-465C16 (Green), RP11-646J21 (Green) and RP11-769M16 (Red). The wild-type allele of chromosome 11 shows 2 green and 1 red signal, whereas on the mutated allele the red signal is lost and both green signals fuse.

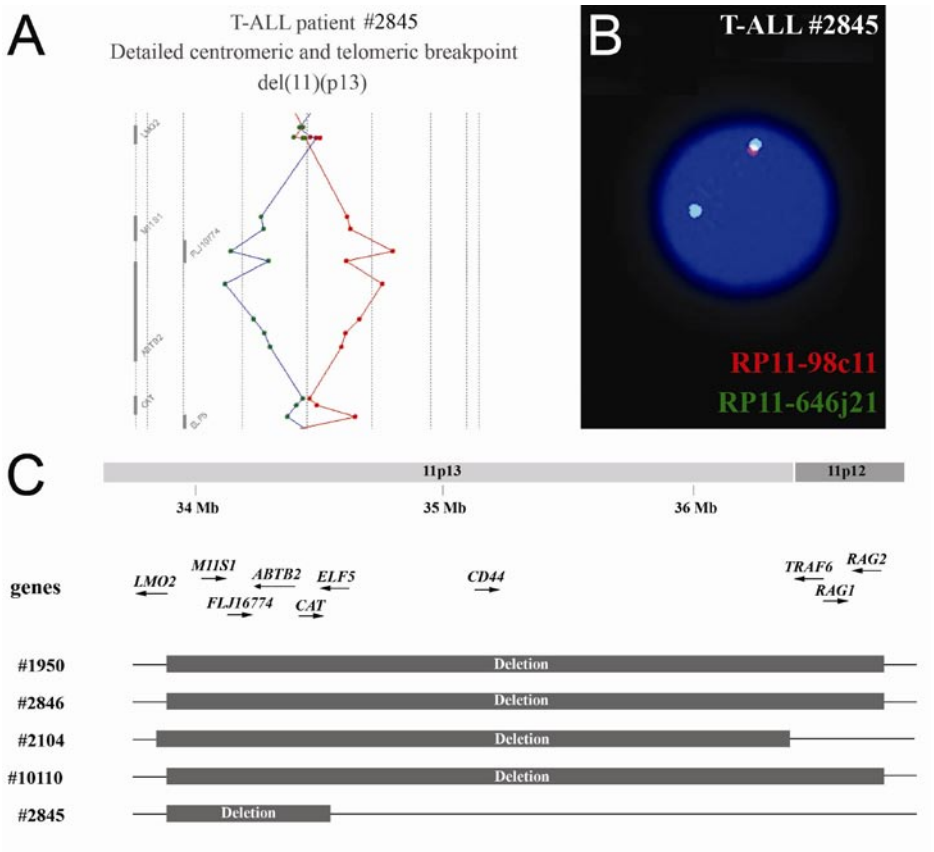

Figure 2. A novel cryptic deletion, del(11)(p13p13), targeting *LMO2* in T-ALL.
(a) Detailed overview of the centromeric and telomeric breakpoints of the del(11)(p13p13) deletion based upon oligo array-CGH micro-array results (44K oligo array, Agilent) for T-ALL case #2845. Patient DNA versus control DNA ratios are indicated in Blue whereas the reciprocal experiment is shown in red. Hybridization signals around the –2X or +2X lines represent loss of the corresponding region in the patient DNA. **(b)** FISH analysis using a BAC clone situated just upstream (RP11-98C11, Red) and downstream (RP11-646J21, Green) of *LMO2* confirming loss of a genomic region upstream of *LMO2* in case 2845. **(c)** Overview of the deletion areas for del(11)(p12p13) positive cases as previously described[3] as well as the del(11)(p13p13) of case #2845 characterized by the activation of the *LMO2* gene. RP11-98C11 is situated just upstream of *LMO2*, whereas RP11-646J21 is positioned telomeric of *LMO2*.

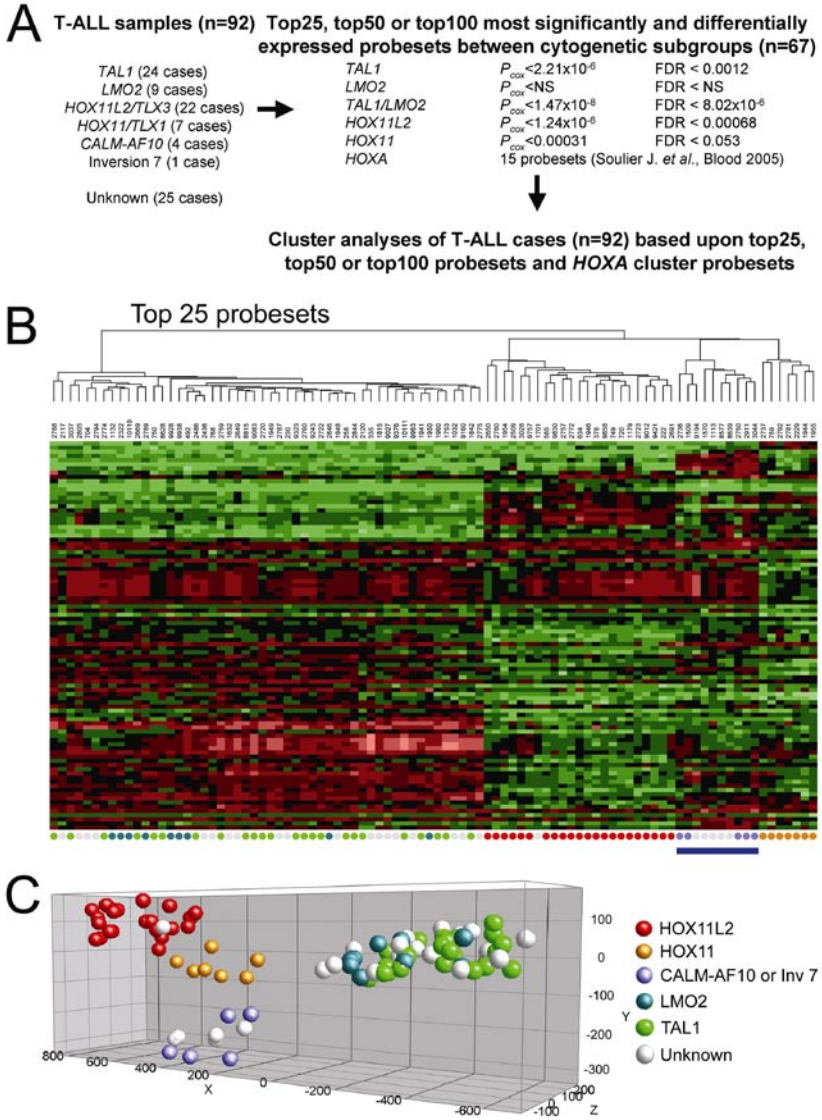

Figure 1. Gene expression profiles of 92 T-ALL patients.
(a) Differentially expressed genes among the major molecular cytogenetic T-ALL subgroups (*TAL1*, *LMO2*, *HOXA*, *TLX1*, and *TLX3, n=67*). The significance level (Wilcoxon *p*-value) and FDR corrected *p*-value for the top100 gene in each T-ALL subgroup is indicated. *TAL1*, *TLX1* and *TLX3* subgroups show significant differentially expressed probesets. (b) Cluster analysis of 92 T-ALL patients (67 known, 25 unknown) based upon the top25 most significant probesets for the *TAL1*, *TAL1/LMO2*, *TLX1* and *TLX3* subgroups combined with 15 *HOXA* probesets as previously described[8]. (c) Principal component analyses shows clustering of the unknown T-ALL cases along the molecular cytogenetic known cases: 1 *TLX3*-like, 19 *TAL1/LMO2*-like and 5 *HOXA*-like patients.

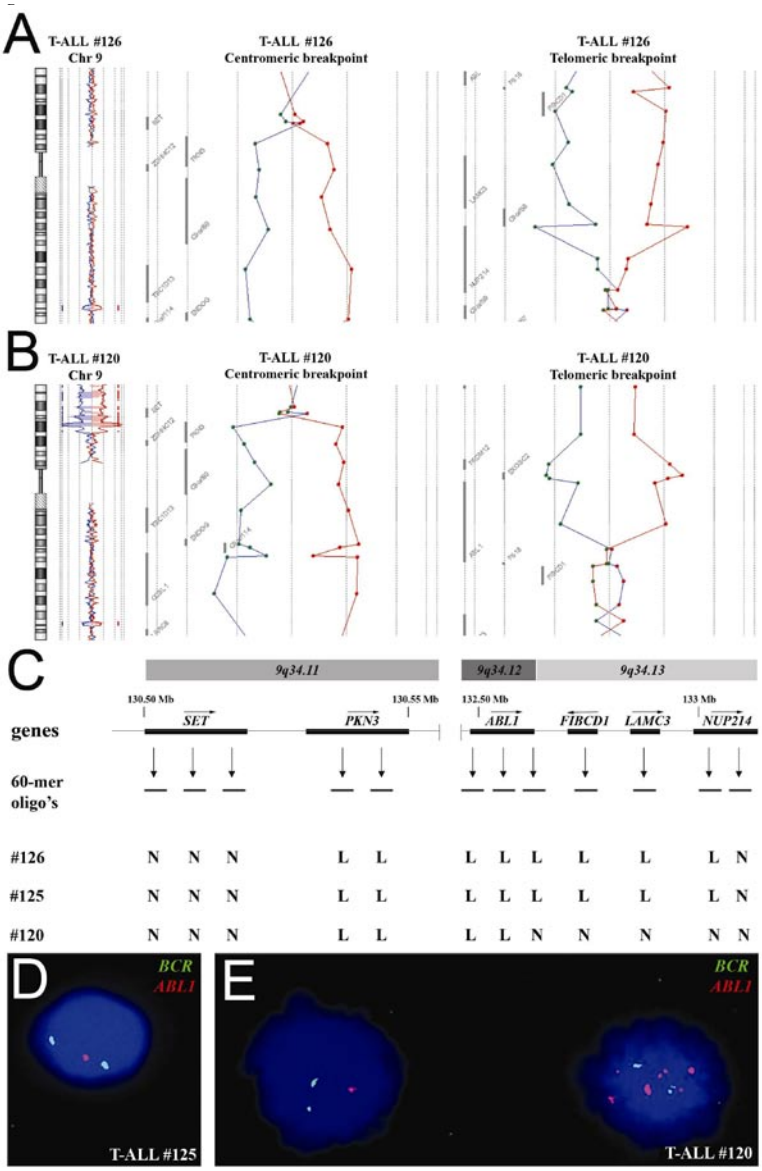

Figure 2. Submicroscopic del(9)(q34.11q34.13) in T-ALL.
(a) Chromosome 9 ideogram and corresponding oligo array-CGH plots of test DNA:control DNA ratios (blue tracing) versus the dye-swap experiment (red tracing) for patient #126. Detailed analyses of the centromeric and telomeric breakpoints show involvement of *SET* and *NUP214*. **(b)** Similar array-CGH plot for patient #120. Centromeric and telomeric breakpoints show involvement of *SET* and *ABL1*. **(c)** Overview of oligo array-CGH results in the potential breakpoint regions for 3 T-ALL patients with del(9)(q34.11q34.13). The 60-mer oligonucleotide probes present on the array-CGH slide and located in the telomeric and centromeric breakpoint regions, as well as the specific genes located in this region with their transcription direction, are shown. Dual-color FISH analysis of patient #125 **(d)** and #120 **(e)** using the LSI *BCR-ABL* ES translocation probe.

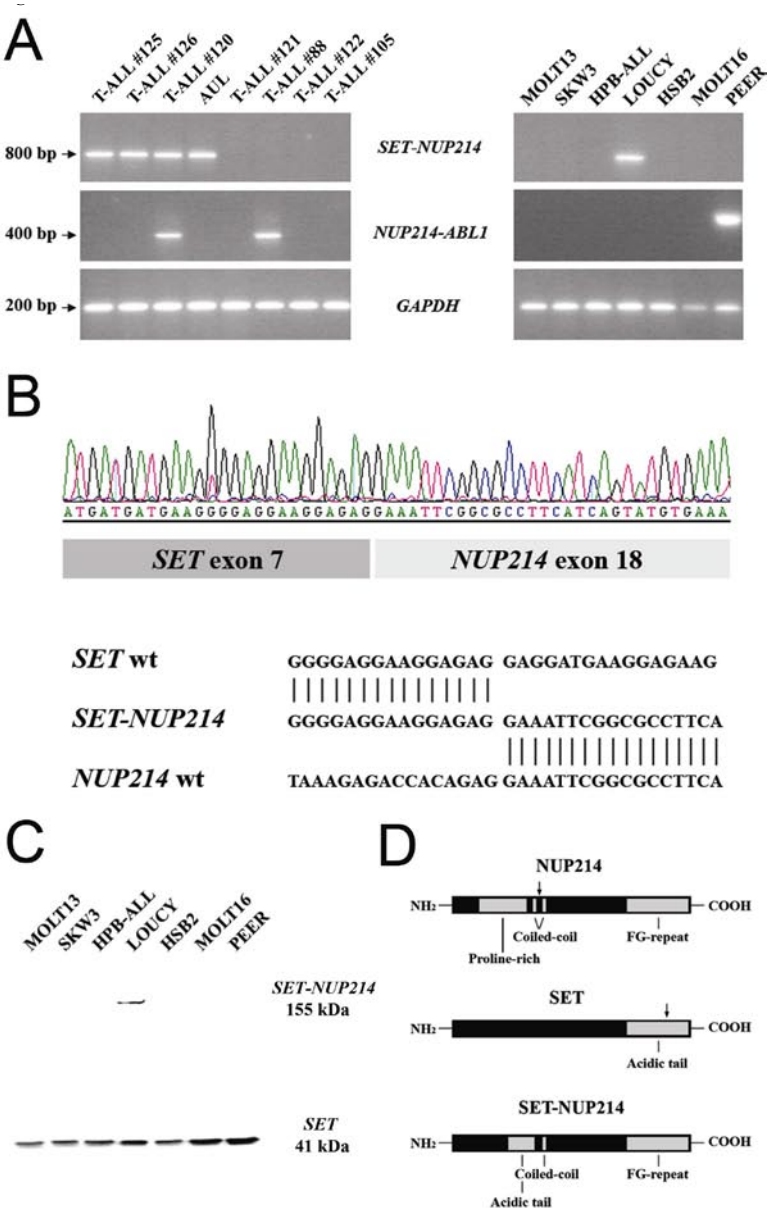

Figure 3. *SET-NUP214* fusion transcript in T-ALL.
(a) RT-PCR analysis using *SET* and *NUP214* specific primers and *GAPDH* primers as internal control, reveals a specific *SET-NUP214* fusion gene in T-ALL patients #125, #126, #120, the AUL patient and the T-ALL cell line LOUCY. *NUP214-ABL1* fusion was detected in patients #120, #88 and in the T-ALL cell line PEER **(b)** Sequence analysis confirmed an identical fusion between exon 7 of *SET* and exon 18 of *NUP214* in all *SET-NUP214* positive T-ALL patients, the AUL case and the LOUCY cell line, **(c)** Western blot analysis of T-ALL cell lines revealed a SET-NUP214 fusion in the cell line LOUCY. **(d)** At the protein level, the breakpoints are situated in the acidic tail of SET and the coiled-coil domain of NUP214.

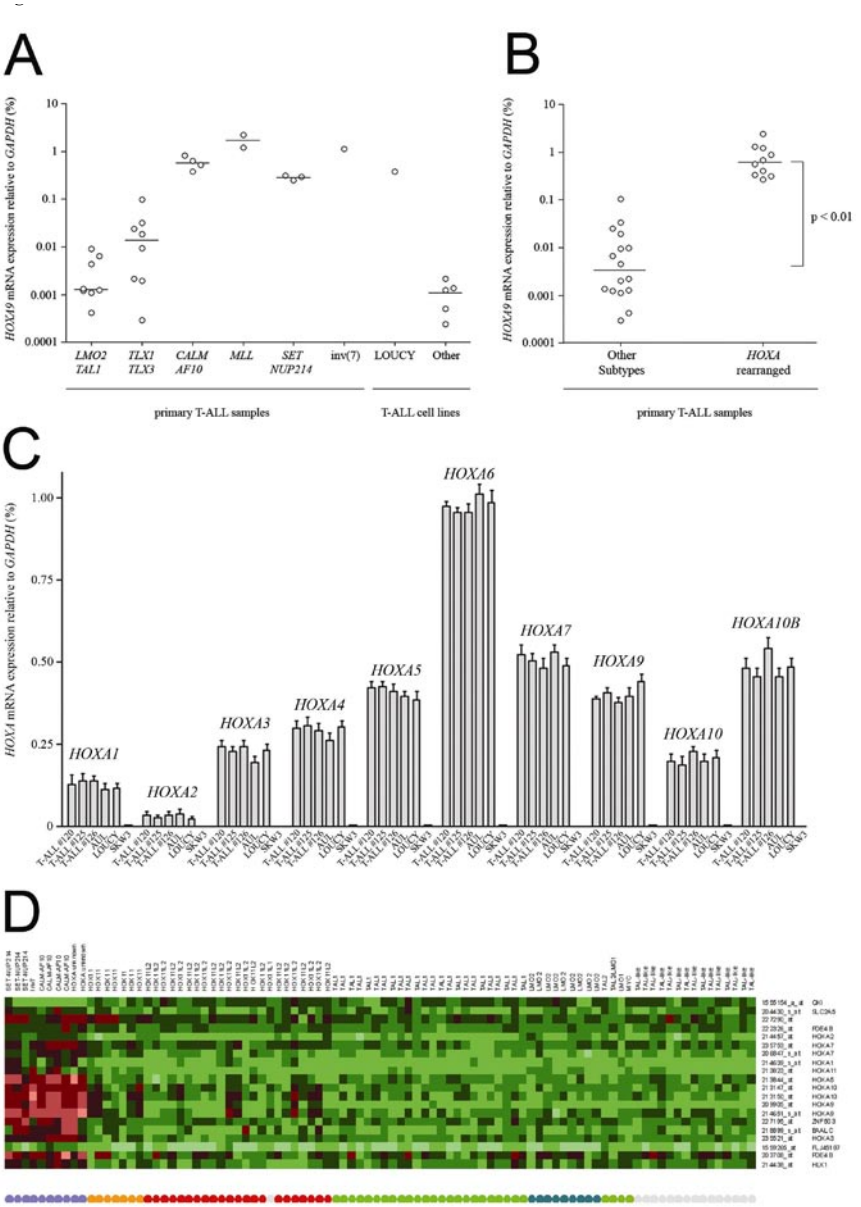

Figure 4. *HOXA* activation in *SET-NUP214* positive T-ALL.
(a) Relative *HOXA9* expression levels by RQ-PCR for *MLL* rearranged, *CALM-AF10* positive, inv(7)(p15q34), *TAL1*, *LMO2*, *TLX3* or *TLX1* rearranged patients and T-ALL cell lines including LOUCY, MOLT13, SKW3, HPB-ALL, HSB2 and PEER. **(b)** Comparison of *HOXA9* expression levels between the *HOXA* T-ALL subgroup (*MLL*, *CALM-AF10*, inv(7)(p15q34), SET-NUP214, n=10) and other T-ALL subgroups (*TAL1*, *LMO2*, *TLX3* or *TLX1*). **(c)** Relative expression levels of *HOXA* genes by RQ-PCR for the 3 *SET-NUP214* positive T-ALL patients, the LOUCY cell line, the AUL patient and SKW3. **(d)** Heatmap of the 20 significant and differentially expressed probesets with a FDR rate lower than 5% for the *HOXA* cluster compared to the other T-ALL cases.

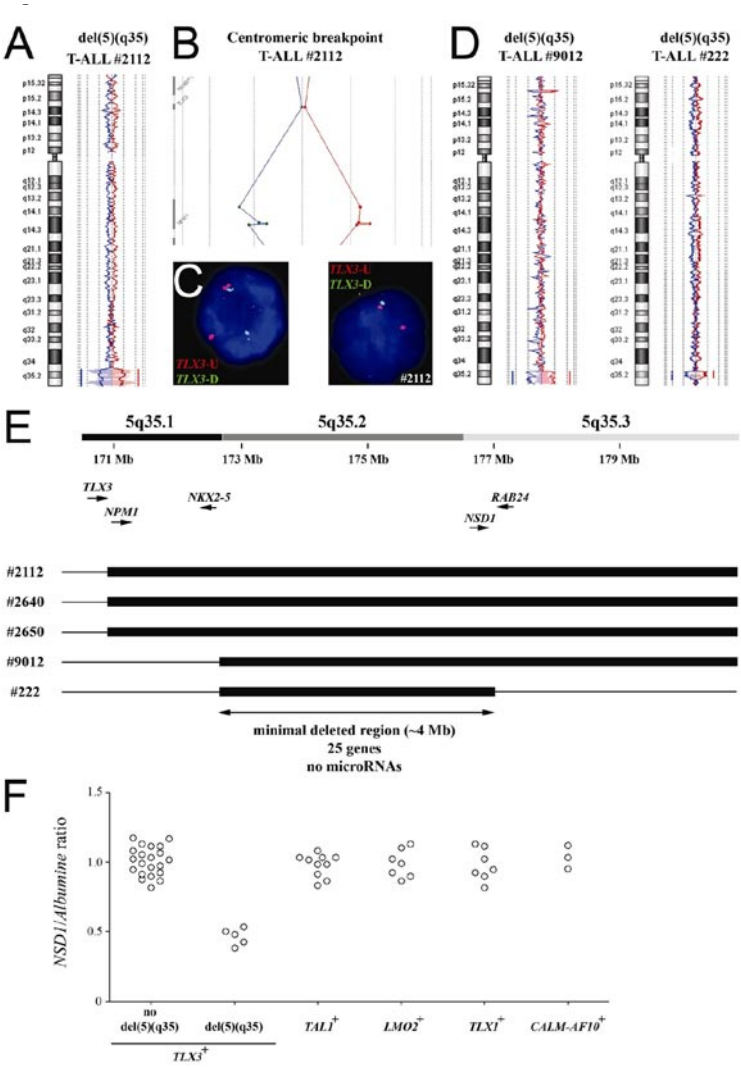

Figure 1. The recurrent cryptic deletion, del(5)(q35), in *TLX3* rearranged pediatric T-ALL. **(a) Chromosome** 5 ideogram and corresponding oligo array-CGH plot of case DNA:control DNA ratios (blue tracing) versus the dye-swap experiment (red tracing) for T-ALL cases 2112. Hybridization signals around the –2X or +2X lines represent loss of the corresponding region in the case DNA. **(b)** Detailed analysis of the centromeric breakpoint of the deletion in case 2112. **(c)** Dual-color FISH analysis on interphase cells of case 9858 (left panel) and case 2640 (right panel) using the *TLX3-U* (Red) and *TLX3-D* (Green) translocation probe set. Case 9858 showed a split signal, indicative for a *TLX3* translocation, whereas case 2640 showed loss of the *TLX3-D* (Green) signal. **(d)** Similar chromosome 5 ideograms as in **(a)** for T-ALL cases 9012 and 222. **(e)** Schematic overview of the minimal deleted region on chromosomal band 5q35 for the 5 TLX3 rearranged T-ALL cases showing a del(5)(q35). Depicted genome positions and gene locations are based on the UCSC Genome Browser at http://genome.ucsc.edu/. **(f)** quantitative PCR analysis of *NSD1*, present in the minimal deleted region, on 26 TLX3 rearranged T-ALL cases and 27 TLX3 negative cases.

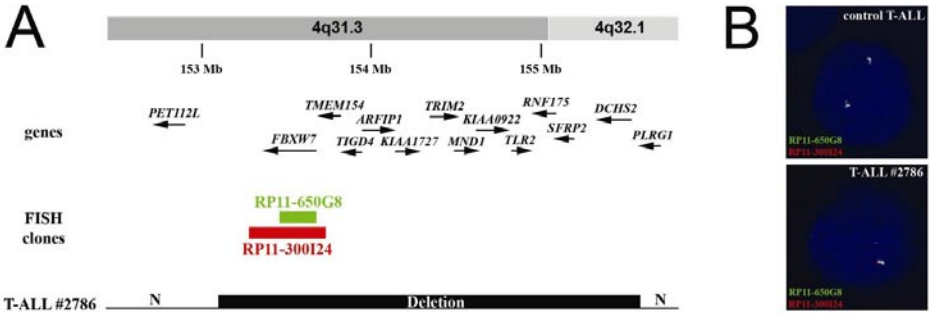

Figure 2. *FBXW7* deletion in pediatric T-ALL
(a) Schematic overview of the chromosomal deletion, del(4)(q31.3q32.1), as detected in case 2786. Genomic positions of genes situated in this chromosomal region and BAC clones used for FISH analysis are depicted. **(b)** FISH analysis using RP11-650G8 (green) and RP11-300I24 (red) confirms the presence of the del(4)(q31.3q32.1) in case 2786.

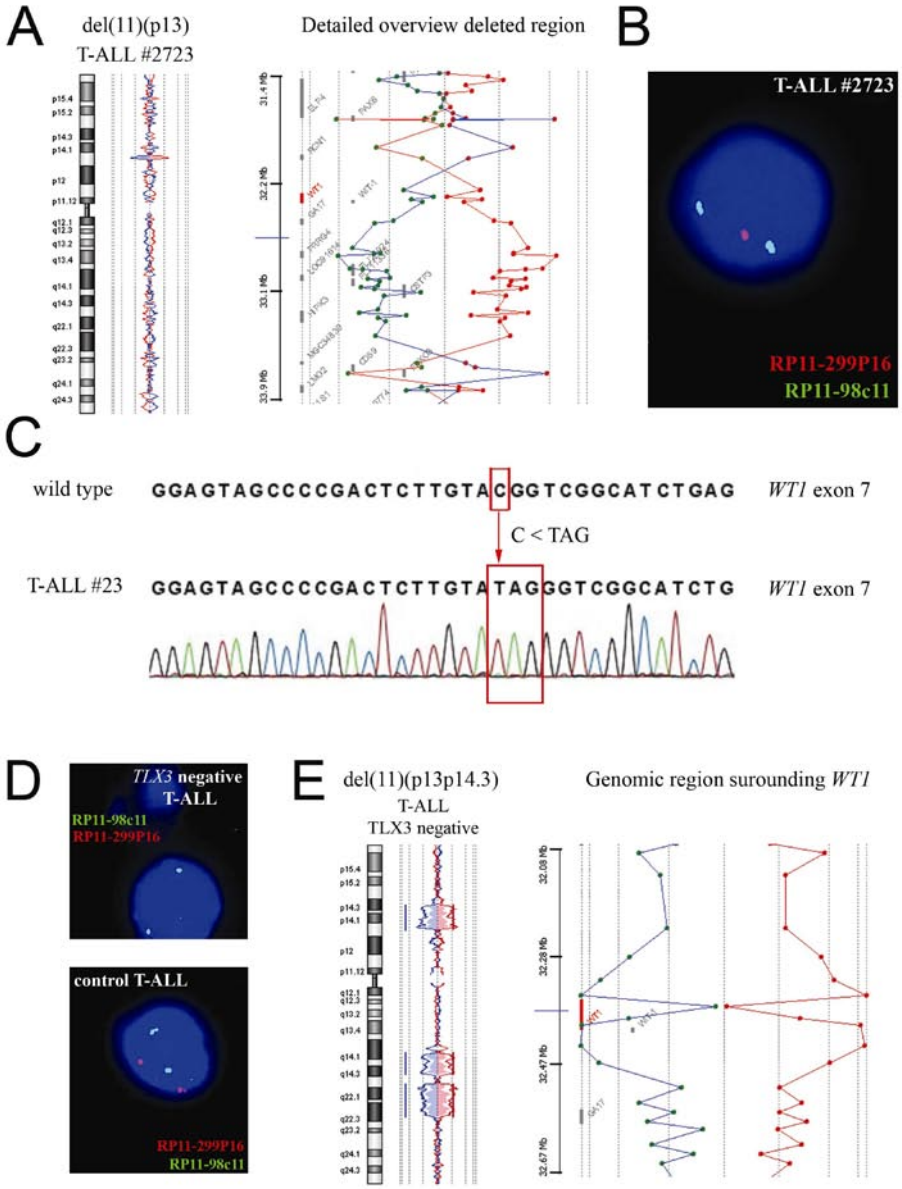

Figure 3. *WT1* inactivation in pediatric T-ALL

(a) Chromosome 11 ideogram and oligo array-CGH plot for the deletion, del(11)(p13), as detected in case 2723 (left panel). The right panel shows a detailed overview of the deleted region for this 11p13 deletion. **(b)** FISH analysis using RP11-98C11 (green) and RP11-299P16 (red, covering *WT1*) confirms the presence of the del(11)(p13) in case 2723. **(c)** Sequence analysis shows a truncating *WT1* exon 7 mutation on the remaining allele of case 2723. **(d)** Similar FISH analysis as in **(b)** on TLX3 wildtype T-ALL cases identified one additional case showing a biallelic *WT1* deletion. **(e)** Array-CGH analysis confirmed the presence of a large mono-allelic deletion, del(11)(p13p14.3), in combination with an additional loss of the genomic region surrounding the *WT1* gene on the other allele.

CHAPTER 8

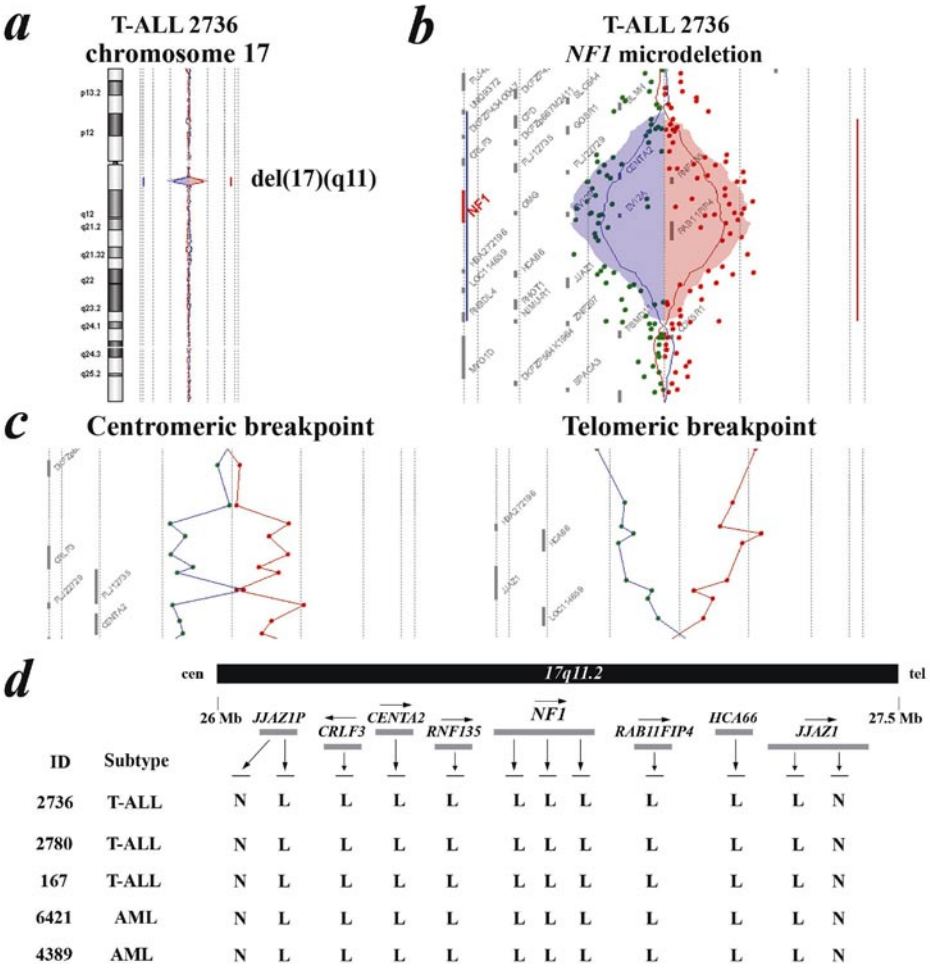

Figure 1. *NF1* microdeletions in pediatric acute leukemias.
(a) Chromosome 17 ideogram and corresponding oligo array-CGH plot of patient DNA/control DNA ratios (blue tracing) versus the dye-swap experiment (red tracing) for T-ALL patient #2736.
(b) Detailed visualization of the *NF1* microdeletion at chromosomal band 17q11 in T-ALL patient #2736. Hybridization signals around the –2X or +2X lines represent loss of the corresponding region in the patient DNA.
(c) Detailed analysis of the centromeric (left panel) and telomeric (right panel) breakpoint of the *NF1* microdeletion in patient #2736.
(d) Overview of oligo array-CGH results in the chromosomal region 17q11.2 for 3 T-ALL and 2 AML patients with del(17)(q11.2). The 60-mer oligos present on the DNA array and located in this genomic area, as well as the specific genes located in this region with their transcription direction, are shown. Arrows above the indicated genes represent the direction of transcription
Abbreviations: N; normal, L; loss, cen: centromere, tel: telomere.

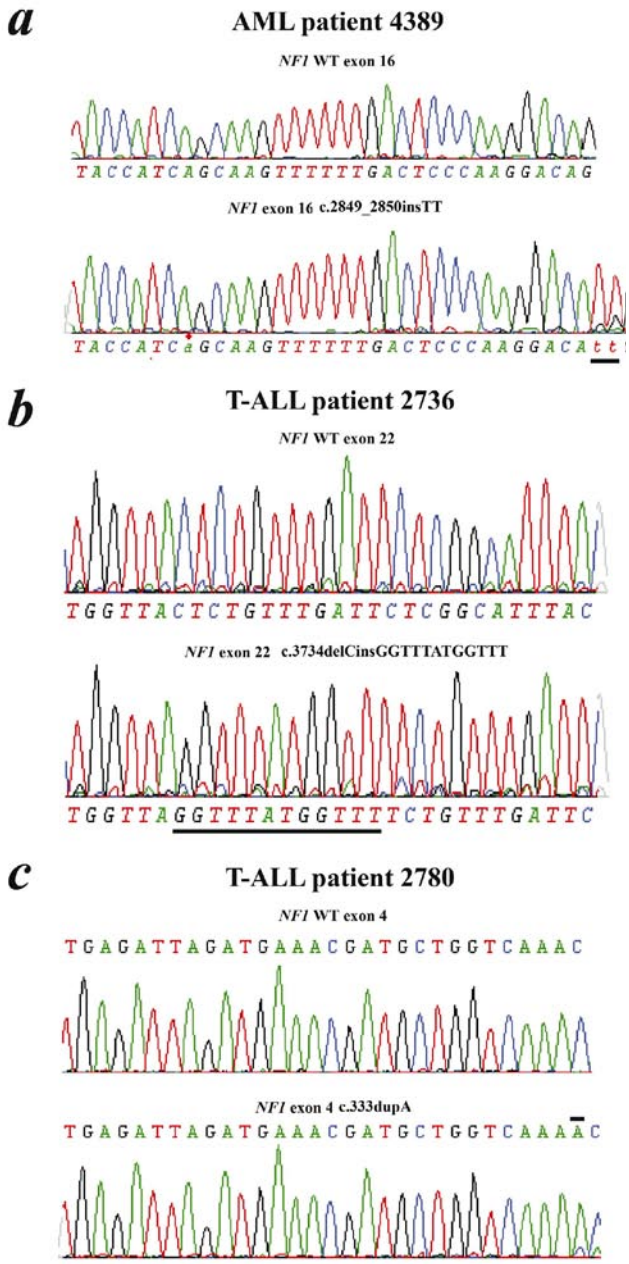

Figure 3. Truncating *NF1* mutations in pediatric T-ALL and AML.
(a) Sequence analysis of patient #4389 (AML) showing a *c.2849_2850insTT* mutation in the remaining *NF1* allele
(b) Sequence analysis of patient #2736 (T-ALL) showing a *c.3734delCinsGGTTTATGGTTT* mutation in the remaining *NF1* allele
(c) Sequence analysis of patient #2780 (T-ALL) showing a *c.333dupA* mutation in the remaining *NF1* allele

CHAPTER 9

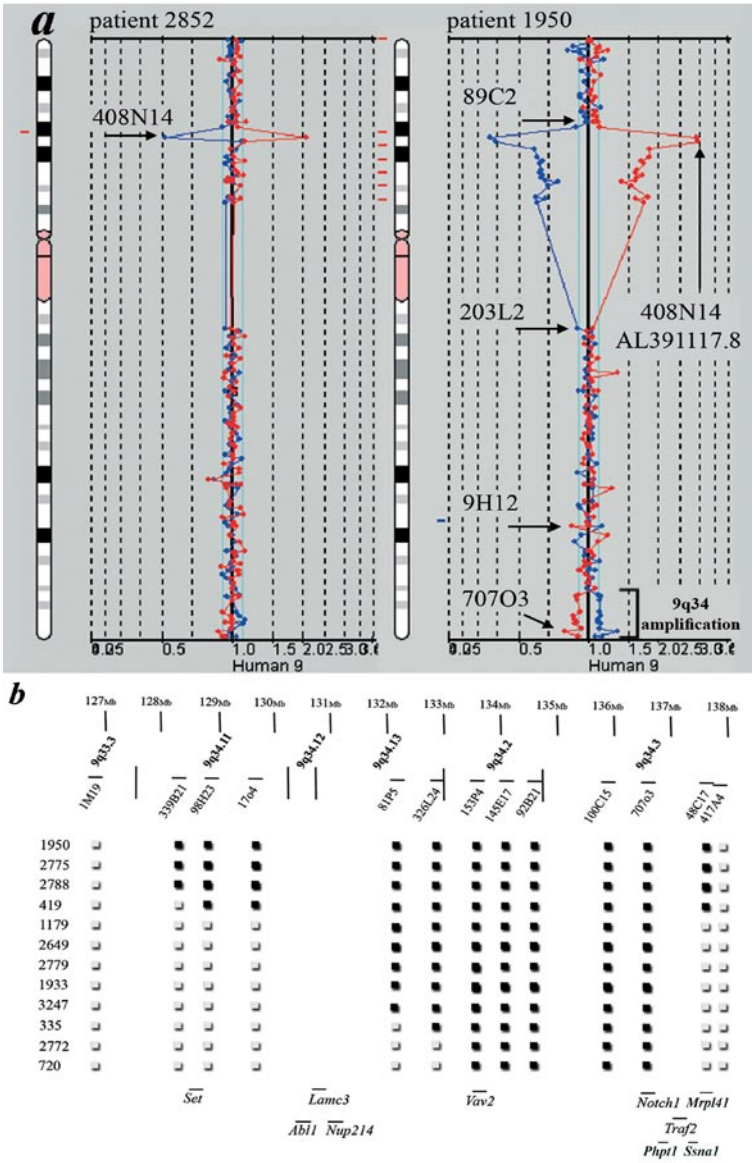

Figure 1. Subclonal 9q34 amplification in pediatric T-ALL
(a) Chromosome 9 ideogram and corresponding array-CGH plot of test DNA:control DNA ratios (blue tracing), and the dye-swapped control DNA:test DNA ratios (red tracing), for T-ALL patients 2852 (left panel) and 1950 (middle panel). **(b)** Overview of array-CGH results for the 9q34 region for each of the 12 pediatric T-ALL patients with the 9q34 duplication. The BAC clones present on the DNA array and located on chromosome bands 9q33.3-q34.3 are shown. The BAC clones within the region of genomic gain are shown as black boxes, clones giving a 1:1 ratio are shown as white boxes. Specific genes located in this region that regulate important cellular processes or that were previously linked to leukemogenesis, are indicated below. Depicted genome positions are based on the UCSC Genome Browser.[35]

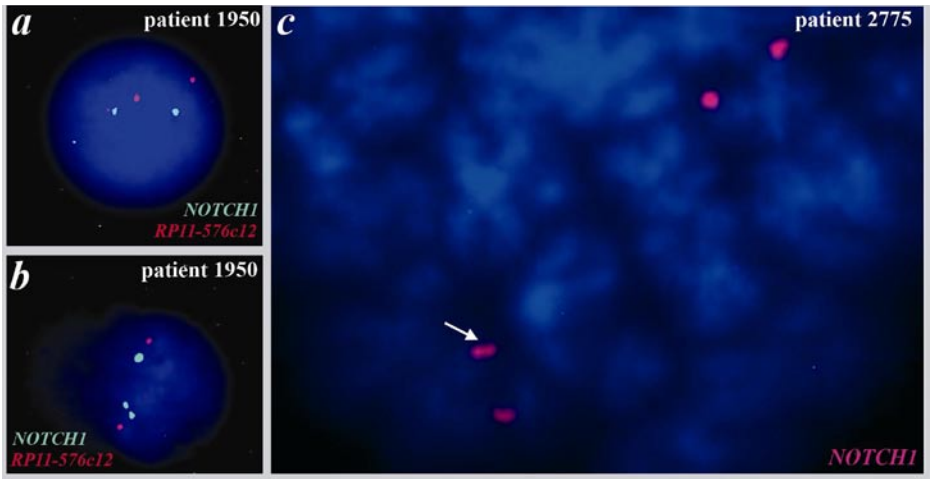

Figure 2. FISH analysis showing subclonal 9q34 duplication in T-ALL patients 1950 and 2775. (a) FISH analysis on interphase cells of patient 1950, using RP11-707o3 (*NOTCH1*) in green and RP11-576c12 (9q32) in red. Example of an interphase cell showing a normal hybridization pattern. **(b)** Amplification of RP11-707o3 (*NOTCH1*) is identified in a minority (32%) of the leukemic cell population. **(c)** Single-color FISH analysis on metaphase spreads of patient 2775, showing an enlarged hybridization signal on one of the chromosomes 9 (white arrow), indicating duplication of 9q34 in one of the chromosomes 9.

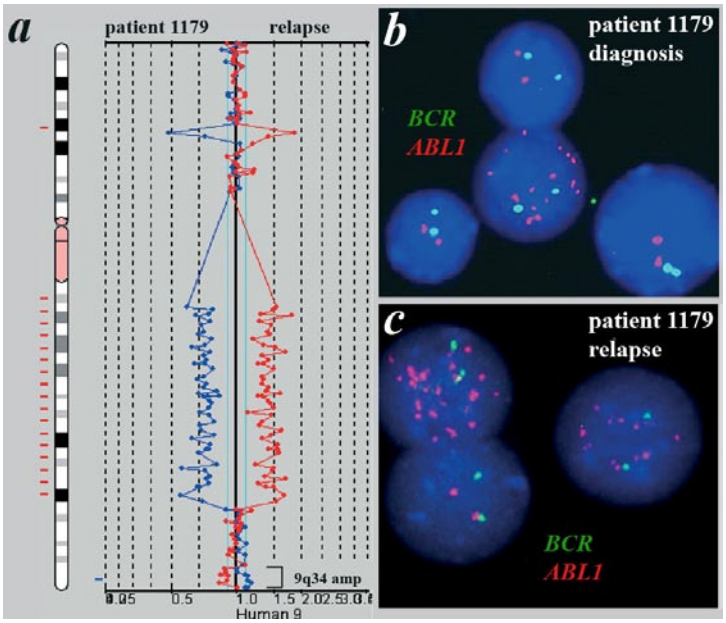

Figure 3. Episomal *NUP214-ABL1* amplification and 9q34 duplication.
(a) Chromosome ideogram and corresponding array-CGH plot of chromosome 9, as described in the legend of figure 1, for patient 1179 at relapse. The 9q34 duplication remains subclonal at relapse. The del(9)(p12q33) (12P15 to 451E16) is only detected in the relapse material. Interphase dual-color FISH analysis on **(b)** diagnostic material and **(c)** relapse material using the LSI BCR-ABL ES probes showing episomal *ABL1* amplification at diagnosis and relapse, respectively.